In silico studies targeting G-protein coupled receptors for drug research against Parkinson's disease

Agostinho Lemos[a,b], Rita Melo[c,d], Antonio J. Preto[c], Jose G. Almeida[c], Irina S. Moreira[*c,e], M. Natália D. S. Cordeiro*[a]

[a]*LAQV/REQUIMTE, Department of Chemistry and Biochemistry, Faculty of Sciences, University of Porto, Rua do Campo Alegre s/n, 4169-007 Porto, Portugal;* [b]*GIGA Cyclotron Research Centre In Vivo Imaging, University of Liège, 4000 Liège, Belgium;* [c]*CNC - Center for Neuroscience and Cell Biology, Faculty of Medicine, University of Coimbra, Rua Larga, 3004-517 Coimbra, Portugal;* [d]*Centro de Ciências e Tecnologias Nucleares, Instituto Superior Técnico, Universidade de Lisboa, Estrada Nacional 10 (ao km 139,7), 2695-066 Bobadela LRS, Portugal;* [e]*Bijvoet Center for Biomolecular Research, Faculty of Science - Chemistry, Utrecht University, Utrecht, 3584CH, The Netherlands*

* Address correspondence to these authors at: (MNDSC) LAQV@REQUIMTE/Department of Chemistry and Biochemistry, University of Porto, 4169-007 Porto, Portugal; Fax: +351 220402659; E-mail: ncordeir@fc.up.pt**;** (ISM) CNC - Center for Neuroscience and Cell Biology, Faculty of Medicine, University of Coimbra, Rua Larga, 3004-517 Coimbra, Portugal; Fax: +351 304502930; E-mail: irina.moreira@cnc.uc.pt

This is a post-peer-review, pre-copyedit version of an article published in Current Neuropharmacology. The final authenticated version is available online at: http://dx.doi.org/10.2174/1570159X16666180308161642

Abstract

Parkinson's Disease (PD) is a long-term neurodegenative brain disorder that mainly affects the motor system. The causes are still unknown, and even though currently there is no cure, several therapeutic options are available to manage its symptoms. The development of novel anti-parkinsonian agents and an understanding of their proper and optimal use are, indeed, highly demanding. For the last decades, L-3,4-DihydrOxyPhenylAlanine or levodopa (L-DOPA) has been the gold-standard therapy for the symptomatic treatment of motor dysfunctions associated to PD. However, the development of dyskinesias and motor fluctuations (*wearing-off* and *on-off* phenomena) associated to long-term L-DOPA replacement therapy have limited its antiparkinsonian efficacy. The investigation for non-dopaminergic therapies has been largely explored as an attempt to counteract the motor side effects associated to dopamine replacement therapy. Being one of the largest cell membrane protein families, G-Protein-Coupled Receptors (GPCRs) have become a

relevant target for drug discovery focused in a wide range of therapeutic areas, including Central Nervous System (CNS) diseases. The modulation of specific GPCRs potentially implicated in PD, excluding dopamine receptors, may provide promising non-dopaminergic therapeutic alternatives for symptomatic treatment of PD. In this review, we focused on the impact of specific GPCR subclasses, including dopamine receptors, adenosine receptors, muscarinic acetylcholine receptors, metabotropic glutamate receptors, and 5-hydroxytryptamine receptors, on the pathophysiology of PD and the importance of structure- and ligand-based *in silico* approaches for the development of small molecules to target these receptors.

Keywords: Parkinson's disease; G-protein-coupled receptors; drug design; ligand-docking; quantitative structure-activity relationships; pharmacophore.

1. INTRODUCTION

Parkinson's Disease (PD) was originally described by James Parkinson, in 1817, as a neurological disturbance consisting of resting tremor and a distinctive form of progressive motor disorder, designated as *shaking palsy* or *paralysis agitans* in his monograph entitled *An Essay On the Shaking Palsy* [1]. Currently, it is considered the second most common neurodegenerative disorder after Alzheimer's Disease (AD), affecting approximately 1% of population worldwide over 55 years old. PD has been defined as a progressive, irreversible, and chronic neurological disorder characterized by increasingly disabling motor symptoms that are associated to impaired coordinated movements including bradykinesia (slowness of initiation of voluntary movements), resting tremor, cogwheel rigidity, postural instability, and gait disorders [2-4]. In addition, the majority of PD patients do not suffer from motor disabilities alone and numerous nonmotor symptoms may lead to a decrease quality of life of patients: cognitive impairment, hallucinations, psychosis, anxiety, and depression [5,6]. Another frequent anomaly related to autonomic (gastrointestinal and cardiovascular), sensory and Rapid Eye Movement (REM) sleep behaviour dysfunctions are also clinically manifested in PD patients. Despite decades of comprehensive study and knowledge concerning the etiology and pathogenesis of PD, much has yet to be discovered in order to understand the pathophysiological mechanisms that contribute to the neuronal cell death (neurodegeneration) in PD. Although normal aging represents the most important risk factor, a combination of environmental (e.g. exposure to pesticides and herbicides, toxins, and organic solvents) and genetic factors may contribute to the

onset of PD [7]. Two distinctive pathological manifestations have been associated to the clinical diagnosis of PD in *post mortem* patients, including the selective and progressive degeneration of dopaminergic neuromelanin-containing neurons from the Substantia Nigra pars compacta (SNc) of the midbrain and stratium of the brain and the presence of Lewy bodies, intraneuronal inclusions of presynaptic protein α-synuclein in brain neurons [2-6].

The reduction of dopamine levels and the loss of SNc dopaminergic neurons have shown to influence directly the appearance of motor dysfunctions associated to PD in 6-HydroxyDopamine (6-OHDA)- and 1-Methyl-4-Phenyl-1,2,3,6-TetrahydroPyridine (MPTP)-treated animals. Since the degree of SNc dopaminergic neurodegeneration correlates positively with the severity of PD, dopamine replacement therapies have become the most effective therapeutic alternative to ameliorate daily function, quality of life, and survival in PD patients. However, the therapeutic strategy of direct administration of dopamine itself is not feasible, due to their inability to cross the Blood-Brain Barrier (BBB) [8]. An alternative BBB-permeable dopamine precursor, L-3,4-DihydrOxyPhenylAlanine or levodopa (L-DOPA), was conceived to effectively enhance dopamine concentration in the Central Nervous System (CNS). The antiparkinsionian effects of L-DOPA were first described by Carlsson and co-workers in reserpine-treated animals [9] and, later, in human PD patients after intravenous [10] and oral administration of low doses of L-DOPA [11]. Currently, L-DOPA is considered the most effective medication for correcting dopamine deficiency in PD, significantly attenuating the motor symptoms in human patients. Upon administration into systemic circulation, L-DOPA is converted to dopamine through a decarboxylation catalyzed by the natural occurring enzyme Aromatic L-Amino acid DeCarboxylase (AADCs; EC 4.1.1.28) in both CNS and Peripheral Nervous System (PNS). An excessive production of dopamine in the periphery can contribute to severe side effects that impair dopamine replacement therapy for PD patients. The administration of L-DOPA with AADC inhibitors as well as inhibitors of dopamine-metabolizing enzymes, including MonoAmine Oxidase-B (MAO-B; EC 1.4.3.4) and peripheral Catechol-*O*-MethylTransferase (COMT; EC 2.1.1.6) constitutes an alternative therapeutic approach to selectively increase dopamine levels in CNS [12-14].

Despite the effectiveness of dopamine replacement therapies in symptomatic PD treatment, their clinical efficacy often decreases, particularly after chronic administration of L-DOPA, leading to the *wearing-off* [15,16] and *on-off* phenomena [17,18] due to oscillations of L-DOPA/drug levels, and the development of long-term motor complications, such as the troublesome dyskinesias (involuntary muscle movements) [18,19]. In addition,

dopaminergic therapies focused on targeting dopamine receptors (DRs) with agonists have displayed favorable outcomes in early stages of PD, exhibiting antiparkinsonian effects with the lower risk of occurrence of problematic dyskinesias. DR agonists have also been used in combination with L-DOPA to delay the development of motor complications in late stages of the disease. Nevertheless, the use of DR agonists may result in non-motor complications (psychiatric disorders, nausea, vomiting, orthostatic hypotension, increased somnolence and sleep attacks, fatigue, and ankle edema) more severe than L-DOPA. Therefore, the occurrence of motor and nonmotor complications associated to all types of dopamine replacement therapy have suggested that the symptomatic treatment of PD focused on the re-establishment of dopaminergic neurotransmission may possess restricted therapeutic benefits for patients. Apart from dopaminergic therapies, the modulation of non-dopaminergic neurotransmission systems, including noradrenergic, cholinergic, adenosinergic, glutamatergic, and serotonergic, have been explored as therapeutic alternatives for symptomatic monotherapy and in combination with dopaminergic therapies. Interestingly, numerous studies have emphasized the relevance of pharmacological modulation of specific G-protein coupled receptors (GPCRs) for PD symptomatic therapy in preclinical PD animal models and clinical studies with PD patients. The present review highlights the impact of specific GPCR subclasses in the pathophysiology of PD, the structure-, and the ligand-based *in silico* approaches widely used in the identification of small-molecule modulators of these particular receptors.

2. G-protein-coupled receptors as therapeutic targets for Parkinson's disease

With the increasing number of new cases per year of PD, there has been a considerable increase in the look for new therapeutic alternatives. While the research and development of promising drugs are demanding for all emerging therapeutic areas, the discovery of new therapeutic agents acting on PD and other CNS diseases has been particularly demanding and is associated to a very high attrition rate [20]. GPCRs-targeted agents represent approximately ~30-40% of current marketed drugs for human therapeutics and these receptors have been subjected to a substantial number of computational studies [21] including as PD targets. GPCRs, also called seven TransMembrane (TM)-spanning receptors, represent the largest family of cell surface receptors of human genome and are characterized by a single polypeptide chain with a variable length that crosses the phospholipidic bilayer seven times adopting the typical structure of seven TM α-helices connected by three ExtraCellular (ECL) and three IntraCellular Loops (ICL) [22]. To date, over 800 human GPCRs have been identified and placed into five major families according to their amino acid sequence homology and

phylogenetic analysis: *Glutamate* (Class C, 22 members), *Rhodopsin* (Class A, 672 members), *Adhesion* (33 members), *Frizzled/Taste2* (Class F, 36 members), and *Secretin* (Class B, 15 members) [22]. Their members share >20% sequence identity in their TM domains and they mediate several downstream signaling pathways of physiological significance by responding to a plethora of structurally diverse ligands, particularly endogenous (biogenic amines, nucleotides, peptides, hormones, neurotransmitters, lipids, glycoproteins, and ions) and exogenous (therapeutic agents, photons, tastants, and odorants) ligands [23,24]. The complexity of GPCR-mediated responses is determined by association of the activated receptors to specific heterotrimeric Guanine nucleotide-binding-proteins (G-proteins). Heterotrimeric G-proteins are composed of two functional units, a Guanine-binding α-subunit (G_α) and a dimer consisting of the β- and γ- subunits ($G_{\beta\gamma}$). In the absence of a GPCR agonist, G_α is bound to Guanosine DiPhoshate (GDP) and associated with $G_{\beta\gamma}$. Agonist-mediated GPCR activation promotes conformational changes in GPCRs, contributing to the stabilization of active conformation of the receptor, and to the coupling and activation of heterotrimeric G-proteins. The coupling of GPCRs with G-proteins leads to GDP release and Guanosine TriPhosphate (GTP) binding to the G_α subunit. Subsequently, the GTP binding induces conformational alterations on G_α subunit, promoting the release of G-proteins from GPCR and the dissociation of heterotrimeric G-proteins into G_α and $G_{\beta\gamma}$ subunits [25]. The G_α ($G_{\alpha s}$, $G_{\alpha i/o}$, $G_{\alpha q}$, $G_{\alpha 12/13}$) and $G_{\beta\gamma}$ subunits amplify and propagate their cell transduction signals through the modulation of various downstream effectors [26], including Adenylyl Cyclase (AC; EC 4.6.1.1) and PhosphoLipase C (PLC; EC 3.1.4.3), that, in turn, regulate the production of second messengers, such as Ca^{2+}, cyclic Adenosine MonoPhosphate (cAMP), cyclic Guanosine MonoPhosphate (cGMP), DiAcylGlycerol (DAG), and Inositol-1,4,5-triPhosphate (IP_3), the modulation of ion channels, and the activation of kinases cascades, triggering a wide array of cellular responses of physiological importance [27,28] (**Fig. 1**). Nevertheless, not all GPCR signaling events are dependent on the activation of G-proteins. In fact, upon prolonged or repeated stimulation of GPCRs by agonists, a process of receptor desensitization induces a progressive attenuation of receptor responsiveness. Second-messenger-dependent protein kinases, Protein Kinase A (PKA; EC 2.7.11.11) and Protein Kinase C (PKC; EC 2.7.11.13), and G-protein coupled Receptor Kinases (GRKs; EC 2.7.11.14, EC 2.7.11.15, and EC 2.7.11.16) are the two families of regulatory proteins that participate in the receptor signaling desensitization, a mechanism independent on the activation of G-proteins. While second-messenger-dependent protein kinases promotes phosphorylation of multiple GPCRs, suppressing agonist responsiveness to these receptors even in the absence of agonist occupation (heterologous desensitization), the recruitment of GRKs for

receptor phosphorylation preferentially requires an agonist-bound conformation of GPCRs (homologous desensitization), leading to an attenuation of receptor signaling [29,30]. GRK-dependent phosphorylation promotes GPCRs binding to a class of intracellular scaffolding proteins, *β*-arrestins, that sterically prevent further interactions between G-proteins and the activated receptors, causing desensitization [31] and ultimately internalization of GPCRs via clathrin-mediated endocytosis [32]. Additionally, *β*-arrestins are by themselves also able to stimulate different pathways, in particular ligand-bias signaling [33]. Receptor proteolysis mediated by lysosomes [34] and GTP hydrolysis by Regulators of G-protein Signaling (RGS) proteins [35,36] provide alternative mechanisms of GPCR downregulation. These regulatory mechanisms are critical not only for receptor desensitization but also for receptor resensitization for next round of GPCR activation and signaling [37].

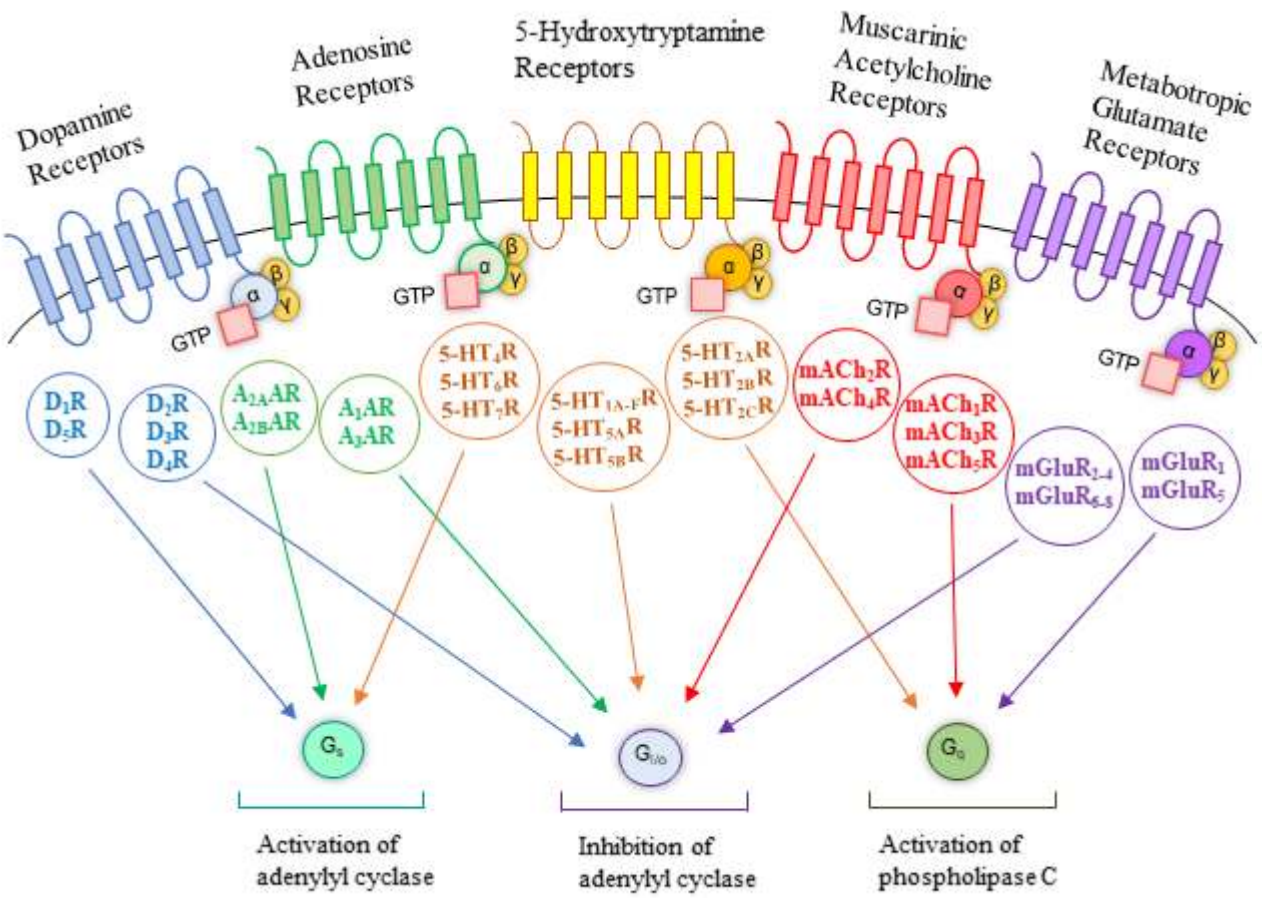

Fig. 1 – Signaling cascade of the distinct subtypes of GPCRs potentially involved in PD.

Drug discovery efforts targeting GPCRs have focused on the development of conventional agonists/antagonists that interact with the orthosteric binding site to modulate the activity of neurotransmitter receptors. However, the high conservation of orthosteric binding sites among subtypes of specific GPCR subfamilies has proven to

be challenging for design of therapeutic agents with high receptor subtype selectivity (reviewed in [38,39]). Additionally, the ligands that interact with orthosteric sites for some GPCRs, in particular peptide or protein receptors, possess physicochemical and pharmacokinetic properties that are unsuitable for drug discovery of small-molecule ligands (reviewed in [38,39]). Recently, the identification of novel therapeutic agents acting as allosteric modulators of GPCRs has provided an alternative approach for the development of subtype selective small molecules potentially useful for treatment of CNS disorders, such as PD. Allosteric modulators interact to topographically distinct binding sites (allosteric sites) from the orthosteric sites of the endogenous ligands, to either increase (positive allosteric modulators, PAMs) or reduce (negative allosteric modulators, NAMs) receptor responsiveness to ligands. The presence of less highly conserved regions often present in allosteric sites of GPCRs allows the molecular optimization of modulators in order to achieve higher subtype selectivity (reviewed in [38,39]). Overall, the exploration of allosteric sites of GPCRs for drug design is of utmost importance in medicinal chemistry, possessing several advantages including the possibility to target selective GPCR-signaling pathways without modulating others that may lead to adverse effects and to search for considerable diversity of chemical scaffolds to optimize the pharmacological profile of drug candidates (*e.g.* brain exposure) (reviewed in [38,39]).

Molecular Dynamics (MD) simulation studies have been widely employed as a useful complement to experimental methods in the determination of the atomic-level mechanisms for allostery, since these techniques can capture the motion of proteins in full atomic detail and predict the position of each atom in biomolecular systems as function of time using Newton's second law [40]. The identification of atomic-level mechanisms for allostery is relevant not only for understanding protein function but also for the application of structure-based drug design approaches [41]. MD simulations were employed already in order to understand how allostery is responsible for modulation of the behavior of different receptors. Experimental studies comparing the action of both agonists and antagonists have shed light on conformational changes on β_2AR upon binding to an irreversible agonist [42]. Another study used MD to compare the solved X-ray structure of an agonist-bound A_{2A}AR [43] with the previously determined X-ray structure of an antagonist-bound structure of the same receptor [44]. By doing so, the researchers were able to determine how the structure was affected by both classes of orthosteric ligands and concluded that TM3, TM5, TM6, and TM7 were the most affected domains. ECL2 and ECL3 also showed considerable displacement, explained by their proximity to the binding site. Interestingly, ICL3, critical for several GPCR functions such as activation and recycling [45-47], was also

shown to be considerably altered when comparing agonist- and antagonist-bound structures. This can highlight the ligand-bias mechanism and how it affects GPCR function. Only a few computational studies have addressed this problem. For example, a computational study by Dror *et al.* [48] using the M2 muscarinic receptor revealed that using cationic orthosteric ligands and cationic negative allosteric modulators hinders the binding of both, depending on total charge and charge location of both ligand and modulator. This was found to be due charge repulsion and, mostly, conformational rearrangements in orthosteric and allosteric binding sites upon allosteric modulator and orthosteric ligand binding, respectively. Additionally, the interaction between positive allosteric modulators and orthosteric ligands seem to increase binding affinity due to conformational changes as well, particularly binding site wider openings. Other computational studies addressed allostery only, such as the different conformational changes in 5-HT_{1A} upon agonist, partial agonist and antagonist [49] – which pointed towards TM5 and TM6 as the most altered domains when comparing agonist- and antagonist-bound structures – or how buspirone, a 5-HT_{1A} partial agonist, differently changes the 5-HT_{1A} and 5-HT_{2A} conformation upon binding [50]. To date, a substantial number of allosteric modulators of GPCRs have exhibited pharmacotherapeutic potential for the treatment of PD and other CNS diseases. Specifically, for PD, the development of allosteric modulators of muscarinic AcetylCholine Receptors (mAChRs) and metabotropic Glutamate Receptors (mGluRs) have demonstrated potential therapeutic applications in preclinical PD models.

2.1. Dopamine receptors

Dopamine is an endogenous chemical belonging to catecholamine and phenethylamine families that functions as a cathecolaminergic neurotransmitter and neurohormone, modulating various physiological actions on CNS such as voluntary movements, feeding, affect, reward, sleep, attention, working memory, and learning. In addition, hormonal regulation, cardiovascular functions, immune system, and renal functions are influenced by dopamine (reviewed in [51,52]). These physiological functions of dopamine are mainly mediated through activation of five subtypes of DRs, which are placed into two major classes, according to their ligand specificity, G-protein coupling, anatomical distribution, and physiological effects. The D_1-like receptors, including D_1R and D_5R, promotes the activation of AC with concomitante stimulation of cAMP production via $G_{s/olf}$ proteins, whereas the D_2-like receptors, including D_2R, D_3R, and D_4R, are preferentially coupled with $G_{i/o}$ proteins to inhibit AC activity and, consequently, the production of cAMP (reviewed in [51,52]).

The evidence of selective loss of dopaminergic neurons in SNc as the most relevant pathological hallmark of PD has suggested that the use of dopamine replacement therapies as therapeutic strategy to regulate dopamine levels in the brain may provide some symptomatic relief for PD patients. Despite the motor fluctuations and the occurrence of dyskinesias associated to a long-term administration of L-DOPA, alternative therapeutic opportunities have emerged as plausible approaches to counteract the prevalence of L-DOPA-induced motor complications. Apart from the combination of L-DOPA with AADC (EC 4.1.1.28), MAO-B (EC 1.4.3.4), and peripheral COMT (EC 2.1.1.6) inhibitors, the development of drug-delivery systems and the use of longer-acting drug candidates capable of stimulating presynaptic and postsynaptic DRs, such as the DR agonists may contribute to a more effective attenuation of motor fluctuations and reduction of the appearance dyskinesias. In MPTP-parkinsonian non-human primates, the administration of longer-acting selective D_2-like receptor agonists induced a significantly lower tendency to produce dyskinesia comparing to those treated with L-DOPA [53,54]. In addition, DR agonists act directly on their receptors without the necessity of metabolic conversion. DR agonists may also provide a wider therapeutic window with reduced risk of dyskinesias, presumably due to their longer plasma half-lives and better pharmacokinetic profiles than L-DOPA, thereby producing more prolonged receptor stimulation. Moreover, DR agonists possess the ability to target certain receptor subtypes, resulting in more specific therapeutic effects and avoiding the occurrence of side effects derived from non-specific activation of receptors induced by L-DOPA. Unlike L-DOPA, their metabolism does not produce hazardous reactive oxygen species (ROS) on dopaminergic neurons. Several studies have suggested that DR agonists might present neuroprotective properties via direct scavenging of free radicals or enhancing the activity of enzymes that scavenge these radicals, increasing neurotrophic activity. Therefore, the involvement of DRs in the modulation of PD has led medicinal chemists to invest on the research of DR agonists with higher subtype selectivity. Until recently, several classes of small molecules targeting D2R and D3R receptors have been discovered [55-67]. According to their chemical scaffolds, these DR agonists have been classified into two major classes (see **Fig. 2**): ergoline derivatives, including bromocriptine (**1**), cabergoline (**2**), lisuride (**3**), pergolide (**4**), and α-dihydroergocriptine (**5**), and nonergoline derivatives, including ropinirole (**6**), pramixepole (**7**), rotigotine (**8**), apomorphine (**9**), and piribedil (**10**). Both classes exhibit comparable antiparkinsonian efficacy. However, ergoline-derived DR agonists have been associated to the occurence of adverse effects such as cardiovascular, retroperitoneal, and pleuro-pulmonary fibrosis and, therefore, their use for clinical therapy

has been significantly diminished. Alternatively, the development of nonergoline derivatives may offer the same therapeutic benefits of ergoline derivatives without the mentioned side effects.

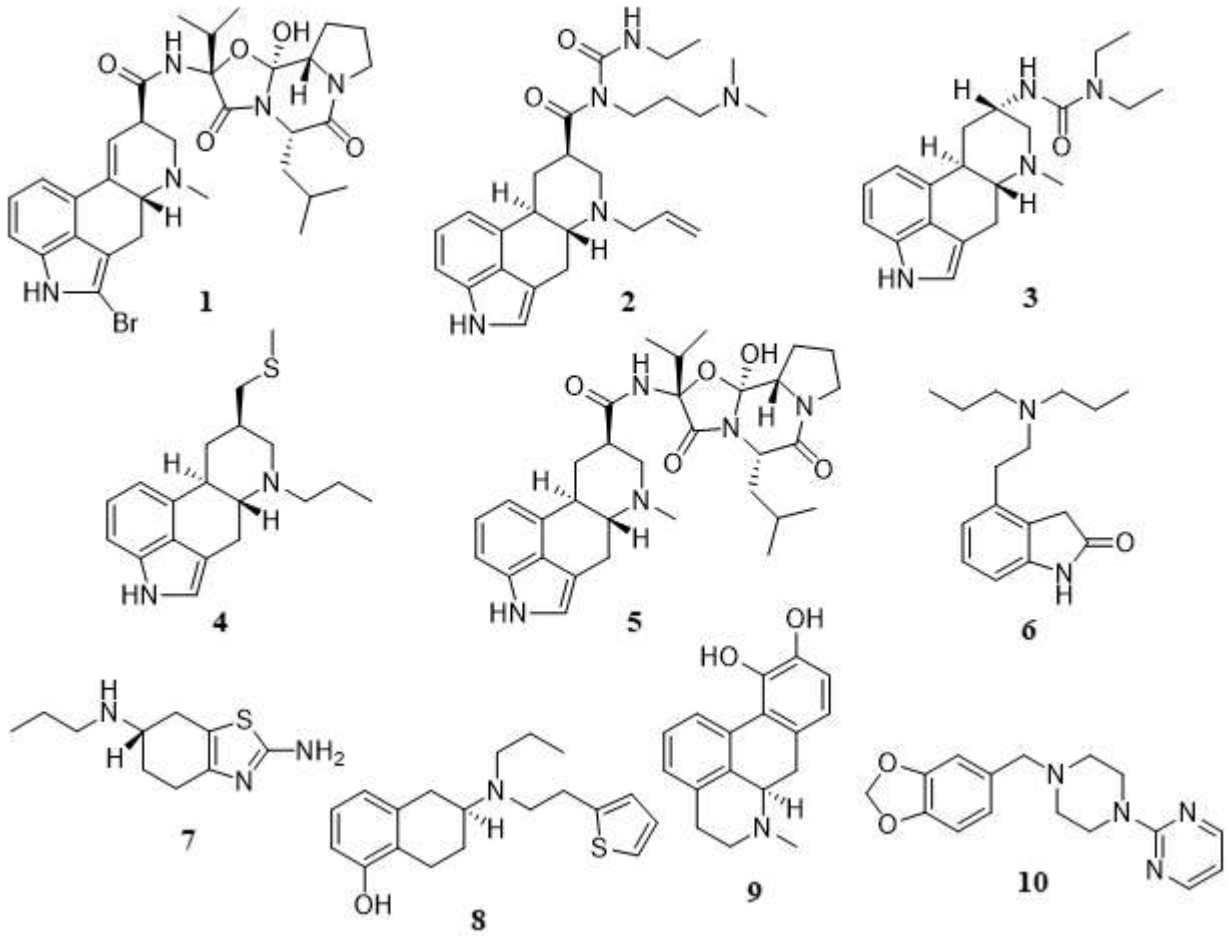

Fig. 2 – Chemical structures of ergoline (**1**-**5**) and non-ergolin derivatives (**6**-**10**): bromocriptine (**1**), cabergoline (**2**), lisuride (**3**), pergolide (**4**), α-dihydroergocriptine (**5**), ropinirole (**6**), pramixepole (**7**), rotigotine (**8**), apomorphine (**9**), and piribedil (**10**).

2.2. Adenosine receptors

Adenosine is an endogenous neuromodulator involved in various pathophysiological functions through interaction of four major subtypes of AR, A_1 (A_1AR), A_{2A} (A_{2A}AR), A_{2B} (A_{2B}AR), and A_3 (A_3AR) [68,69]. While A_1ARs and A_{3A}Rs are negatively coupled with AC via $G_{i/o}$ proteins, exerting an inhibitory effect on production of cAMP [69], the activation of A_{2A}ARs and A_{2B}ARs enhances AC activity via G_s proteins, causing an increase on cAMP levels [70]. In opposition to the ubiquitous distribution of A_1ARs and A_{2B}ARs in the brain, A_{2A}ARs are densely expressed in restricted regions within the CNS and exist primarily in stratium, nucleus accumbens, and olfactory tubercles [71,72], where they are coexpressed and physically interact with

dopamine D_2 receptors (D_2Rs) forming A_{2A}AR-D_2R heterodimers [73,74]. A_{2A}ARs and D_2Rs possess antagonistic effects on AC activity and experimental data have suggested the involvement of A_{2A}ARs-mediated adenosinergic neurotransmission on the negative regulation of D_2Rs-dependent dopaminergic signaling [75,76]. Preclinical studies have demonstrated that the pharmacological inhibition with selective A_{2A}AR antagonists induce significant beneficial effects in animal models of PD, reversing catalepsy induced by haloperidol (D_2R antagonist) in rodents [77] and cynomolgus monkeys [78], improving motor functions in 6-OHDA-lesioned rats [79], and attenuating PD-like lesions caused by administrarion of neurotoxin MPTP in mice [80] and cynomolgus monkeys [81]. Interestingly, coadministration of A_{2A}AR antagonists with L-DOPA not only enhance the therapeutic effects of L-DOPA on improvement of motor symptoms and on prevention of disease progression, but also can minimize the incidence of L-DOPA-induced wearing off and L-DOPA-related dyskinesias after long-term treatment [82]. Moreover, antiparkinsonian activity in preclinical animal models has been reported when A_{2A}AR antagonists are administered in combination with selective D_2R agonists. These evidences have led researchers to explore the inhibition of A_{2A}AR with selective antagonists as potential enhancers of dopaminergic neurotransmission for symptomatic treatment of PD. Also, the selective and restricted localization of A_{2A}AR in the basal ganglia provides a therapeutic opportunity for A_{2A}AR antagonists to regulate motor functions without inducing non-specific effects in other brain regions. Therefore, A_{2A}AR has been considered a promising therapeutic target for negative modulation by small-molecule drug candidates to be used either as monotherapy or in combination with dopaminergic drugs for PD therapeutics. A diverse plethora of chemical families of A_{2A}AR antagonists have been identified [83-99] and among these small-molecule drug candidates, eight A_{2A}AR antagonists have progressed to clinical studies (**Fig. 3**) to date by distinct pharmaceutical companies, including SYN-115 (**11**, Tozadenant) from Biotie Therapies and UCB Pharma S.A., KW-6002 (**12**, Istradefylline or NOURIAST®) from Kyowa Hakko Kirin Co. Ltd, ST1535 (**13**) and ST4206 (**14**) from Sigma-Tau, SCH-420814/MK-3814 (**15**, Preladenant) from Merck & Co. Inc., BIIB014/V2006 (**16**, Vipadenant) from Vernalis Plc-Biogen Idec Inc., V81444 (**17**) from Vernalis Plc and PBF-509 (chemical structure not disclosed) from PaloBiofarma S.L., and (reviewed in [100]). Apart from their encouraging pharmacokinetic properties, safety and tolerability profile, the reported clinical studies have demonstrated that A_{2A}AR antagonists significantly reduced L-DOPA-induced *wearing-off* effect, decreased the time spent by PD patients in a state of immobility (off-time) without impairing troublesome dyskinesia, and increased the time spent by PD patients in a state of mobility (on-time) with a moderate increase of non-troublesome dyskinesia, in

L-DOPA-administered patients at an advance stage of PD (reviewed in [100]). In 2013, KW6002 was approved for manufacturing and marketing in Japan as a novel therapeutic option for improvement of wearing-off effect in patients with PD when KW6002 is concomitantly administered with L-DOPA-containing products [101].

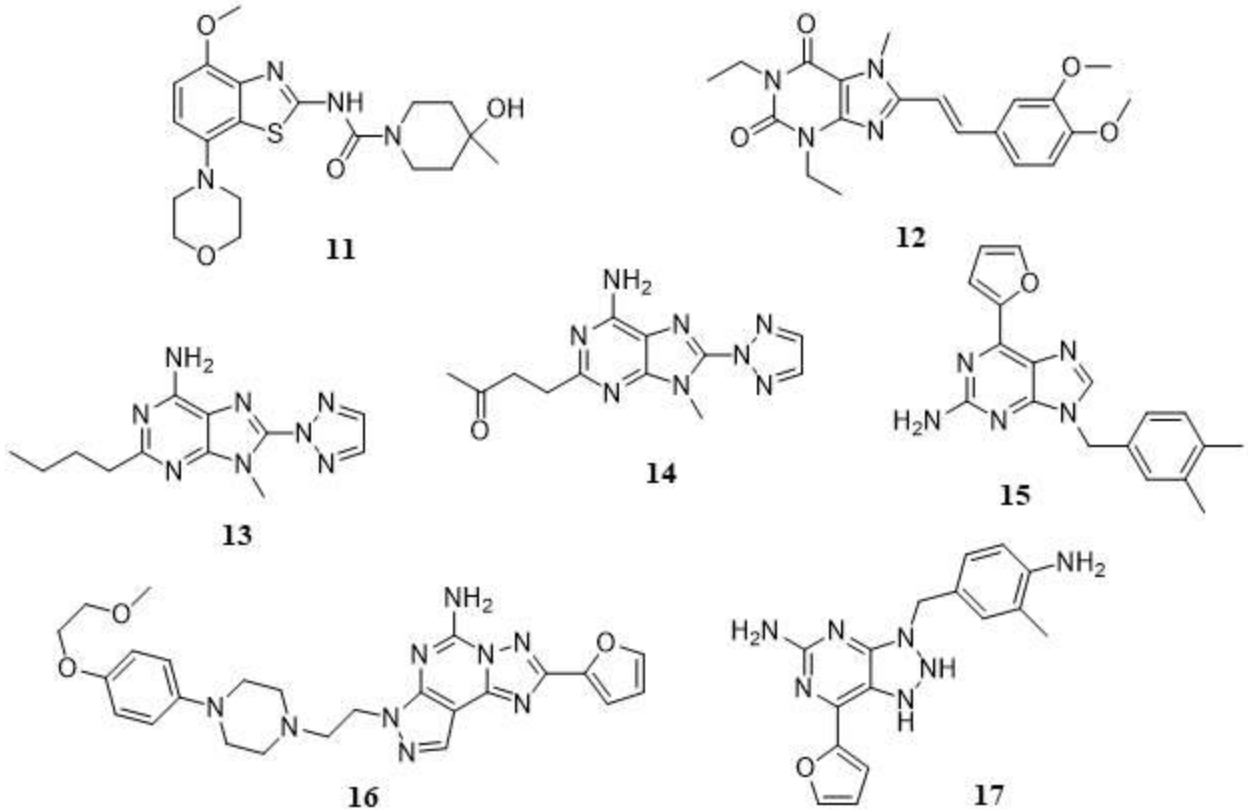

Fig. 3 – Chemical structures of $A_{2A}AR$ antagonists in clinical trails for PD treatment: SYN-115 or Tozadenant (**11**), KW-6002 or Istradefylline (**12**), ST1535 (**13**), ST4206 (**14**), BIIB014/V2006 (**15**), SCH-420814/MK-3814 or Preladenant (**16**), and V-81444 (**17**). The chemical structure of PBF-509 was not disclosed.

2.3. Muscarinic receptors

Five distinct subtypes of muscarinic AcetylCholine Receptors ($mAChR_1$-$mAChR_5$ or M_1-M_5) [102] mediate the metabotropic actions of acetylcholine through regulation of distinct signaling pathways: $mAChR_1$, $mAChR_3$, and $mAChR_5$ activate PLC via G_q proteins whereas $mAChR_2$ and $mAChR_3$ inhibit AC via $G_{i/o}$ proteins [103]. The modulation of cholinergic system dependent on mAChRs plays a critical role in a wide plethora of central nervous system (CNS) functions, including the modulation of neuronal excitability and synaptic plasticity, sensorimotor gating, locomotor activity, memory and learning mechanisms, among other functions [104,105]. Due to their role in a number of CNS processes, mAChRs have been recognized as an attractive therapeutic target for discovery of drug candidates targeting CNS pathologies, namely PD, AD, Attention Deficit

Hyperactivity Disorder (ADHD), and schizophrenia. Specifically, for PD, the characteristic dysfunction of dopaminergic neurotransmission in the stratium may contribute to a dysregulation of the dynamic equilibrum between cholinergic and dopaminergic systems. In fact, the loss of dopaminergic neurons triggers an excessive release of AcetylCholine (ACh) through activation of mACh autoreceptors and an overactivation of cholinergic system that results in the occurence of serious motor and cognitive disturbances associated to PD [106]. Therefore, inhibition of mAChRs has been suggested as a promising strategy to overcome the increased cholinergic activity and to reestablish the cholinergic/dopaminergic balance. Among the five subtypes of mAChRs, $mAChR_1$ and $mAChR_4$ subtypes have been suggested to participate in modulation of PD pathophysiology. Pharmacological blockade of $mAChR_1$ have shown therapeutic benefits in preclinical models of PD through blockade of carbachol-induced excitation of stratial medium spiny neurons, reversal of reserpine-induced akinesia and of haloperidol-induced catalepsy [107]. Additionally, selective $mAChR_1$ and $mAChR_4$ antagonists relieved unilateral 6-OHDA lesion-elicited motor deficits in mice [108] and $mAChR_4$ antagonism suppressed pilocarpine- and pimozide-induced tremulous jaw movements [109,110]. The $mAChR_4$ knockout enhanced dopaminergic neurotransmission [111], increased locomotor activity in D_1R agonist-treated mice [112], and attenuated haloperidol- and risperidone-induced catalepsy in scopolamine-treated mice [113]. These results have suggested the inactivation of $mAChR_1$ and $mAChR_4$ with small-molecule antagonists as an encouraging approach for PD therapeutics.

The high sequence conservation within the orthosteric binding site of the five mAChRs has demonstrated to be unfavorable for the discovery and development of antagonists which specifically target the blockade of one mAChR subtype. A highly subtype-selective mAChR antagonist provides a more direct pharmacological effect, contributing to the elimination of potential side effects. Also, a mAChR antagonist could be used as a pharmacological tool and aid in the development of selective mAChR antagonists, which in turn, may be useful for treatment of PD. Numerous small-molecule antagonists acting on $mAChR_1$ [114-126] and on $mAChR_4$ [127-133] have been identified.

2.4. Metabotropic glutamate receptors

The amino acid glutamate is considered the major excitatory neurotransmitter in the brain. Glutamate elicits and modulated synaptic responses in CNS by activating two classes of glutamate receptors: ionotropic (iGluRs) and metabotropic glutamate receptors (mGluRs). IGluRs constitute a class of ligand-based ion channels subdivided

into three families, including *N*-Methyl-D-Aspartate (NMDA), *α*-Amino-3-hydroxy-5-Methyl-4-isoxazole Propionic Acid (AMPA), and Kainate (KA) receptors. Belonging to *glutamate*-like or class C GPCRs, mGluRs are composed of eight subtypes which are classified into three groups according to the receptor structure, their pharmacological profile, and ligand binding specificity: Group I ($mGluR_1$ and $mGluR_5$), Group II ($mGluR_2$ and $mGluR_3$), and Group III ($mGluR_4$, $mGluR_6$, $mGluR_7$, and $mGluR_8$). The activation of group I mGluRs enhances the production of IP_3 and DAG through stimulation of PLC via G_q proteins, whereas group II and group III mGluRs inhibit AC activity-dependent on G_i/G_o proteins [134].

Several studies performed in preclinical animal PD models have suggested that the pharmacological blockade of group I mGluRs as well as the activation of group II and group III mGluRs may provide therapeutic strategies for treatment of PD. Regarding the group I mGluRs, the administration of $mGluR_5$ NAMs reversed parkinsonian symptoms, ranging from alleviation of akinesia in 6-OHDA-lesioned rats [135] to inhibition of muscle rigidity electromyographic activity, hypolocomotion, and catalepsy induced by haloperidol [136-138]. Interestingly, the coadministration of $mGluR_5$ antagonists with A_2AR antagonists produces a synergystic effect on stimulation of locomotor activity in both untreated and reserpine-treated mice [139] and promoted a complete recovery of akinesia in 6-OHDA-lesioned rats in reaction time tasks [140]. Similarly, the combination of $mGluR_5$ antagonists with NMDA receptor antagonists, at suboptimal doses, induced significant improvements on PD symptomatology, producing an anti-akinetic effect after 6-OHDA infusion in rats [141]. In rats with partial bilateral 6-hydroxydopamine lesions, the long-term administration of $mGluR_5$ antagonists significantly reversed the overactive glutamatergic neurotransmission of striatum and subthalamic nucleus (STN) and SNr, thereby resulting in the alleviation of motor symptoms [135,142,143]. In addition, acute and chronic administration of $mGluR_5$ NAMs significantly attenuate the development of L-DOPA induced dyskinesias in 6-OHDA-lesioned rats and in MPTP-treated monkeys chronically administered with L-DOPA [138,144,145]. In combination with L-DOPA, the $mGluR_5$ NAMs induced antidyskinetic effects and prolonged the motor stimulant effects of L-DOPA in both rat and monkey PD models [145]. These evidences suggest that $mGluR_5$ NAMs alone and/or coadministered with L-DOPA, A_2AR and NMDA receptor antagonists may provide a viable approach for symptomatic treatment of PD.

Interestingly, the mGluRs have shown to be implicated in processes of neurodegeneration/neuroprotection and to modulate excitatory synaptic neurotransmission, providing alternative therapeutic opportunities for neuroprotective drug candidates. More specifically, the $mGluR_5$ knock-out in mice protected against MPTP-

induced nigrostriatal damage, which suggested that blockade of $mGluR_5$ may confer neuroprotective effects in animal models [146]. Additionally, in rodents, the administration of $mGluR_5$ NAMs reduced the extent of nigrostriatal toxicity in rodents in response to MPTP [146,147], 6-OHDA [148,149], and methamphetamine [150], supporting the use of these drug candidates to exert neuroprotective activity and to slow the progression of neurodegeneration in PD. The relevance of pharmacological blockade of these receptors has inspired the researchers to discover antagonists and negative allosteric modulators [151-164] targeting $mGluR_5$.

The therapeutic benefits of activators of group II mGluRs have been demonstrated in several animal models. In fact, the intranigral or intracerebroventriular administration of $mGluR_2$/$mGluR_3$ agonists attenuated reserpine-induced akinesia and systemic administration of $mGluR_2$/$mGluR_3$ agonists impaired haloperidol-elicited catalepsy and muscle rigidity in rats [165,166]. Interestingly, the activation of group II mGluRs may exert neuroprotective effects in rat SNc neurons. Consistent with this hypothesis, administration of $mGluR_2$/$mGluR_3$ agonists decreased the extent of rat SNc neurodegeneration caused by 6-OHDA- [148] and MPTP-induced neurotoxicity [167, 168], underlying their role as disease-modifying agents in PD. Likewise, several evidences have suggested that the activation of group III mGluRs may alleviate PD symptoms by reducing glutamate and γ-aminobutyric acid (GABA) neurotransmission at both the stratiopallidal and STN-SNr synapses of the indirect pathway in the basal ganglia circuit [169-171]. Supporting this hypothesis, intracerebroventricular administration of group III mGluRs agonists has shown to reverse both acute (haloperidol-elicited catalepsy and reserpine-induced akinesia) and chronic (forelimb asymmetry caused by unilateral 6-OHDA-lesion) rat models of parkinsionism [170,172]. Intrapallidal administration of group III mGluRs agonists alleviate both cataleptic and akinetic effects in rodents [172,173], evidencing the importance of modulating synaptic neurotransmission as therapeutic strategy for symptomatic treatment of PD. In addition, the activation of group III mGluRs in the basal ganglia have displayed neuroprotective effects, reducing excitatory neurotransmission in the SNc by STN overactivity [174] and protecting against NMDA-elicited toxicity. The symptomatic and neuroprotective properties of group III mGluRs agonists are prevented in $mGluR_4$ knockout mice, which suggest that the modulation of $mGluR_4$ has the potential to exert antiparkinsonian activity in animal models. Overall, the pharmacological activation with $mGluR_2$/$mGluR_3$ [175-180] and $mGluR_4$ [181-186] with agonists and positive allosteric modulators may offer an alternative approach for PD therapeutics.

2.5. 5-Hydroxytryptamine receptors

Being one of the most commonly studied neurotransmitters, 5-HydroxyTryptamine (5-HT) or serotonin regulates a wide array of physiological functions in the brain, particularly in emotion, modulation of sleep-wake cycles, cognition, memory, and motor behaviour. These functions are mediated through the interaction with 5-HydroxyTryptamine (5-HTRs) or serotonin Receptors, which are subdivided into thirteen subclasses: (i) 5-HT_{1A}R, 5-HT_{1B}R, 5-HT_{1D}R, 5-HT_{1E}R, 5-HT_{1F}R, 5-HT_{5A}R, and 5-HT_{5B}R promote the downregulation of AC activity via G_i/G_o proteins; (ii) 5-HT_4R, 5-HT_6R, and 5-HT_7R stimulate the production of cAMP through activation of AC via G_s proteins; (iii) 5-HT_{2A}R, 5-HT_{2B}R, and 5-HT_{2C}R induce the activation of PLC [187]. Several studies have suggested that the serotonergic activity is markedly impaired in PD. In fact, in PD patients, serotonin has shown to be reduced in the cortex, caudate nucleus, and hippocampus [188], the raphe nucleus and in the substance P-containing preganglionic neurons in the dorsal motor vagal nucleus [189], while serotonin markers are decreased in the caudate nucleus and putamen [190]. Interestingly, the pharmacological activation/blockade of specific 5-HTR subtypes with small molecule drug candidates has displayed beneficial outcomes in preclinical PD models and clinical studies. Regarding the 5-HT_{1A}Rs, the administration of 5-HT_{1A}R agonists has shown to attenuate/reverse 6-OHDA- [191] and haloperidol-induced catalepsy [192,193], and to increase the motor activity in reserpine-administered rats [194]. In 6-OHDA-lesioned rats, 5-HT_{1A}R agonists improve the performance in the forepaw adjusting steps test, an indicator of antiparkinsonian activity [195]. Pharmacological modulation of 5-HT_{1A}R with agonists has shown to induce contraversive rotations in 6-OHDA-treated rats, to alleviate the parkinsonian symptoms in MPTP-lesioned common marmosets [196], and to attenuate L-DOPA induced motor complications [197-199]. Similarly to 5-HT_{1A}Rs, the activation of 5-HT_{1B}Rs mitigates the occurrence of dyskinesia and abnormal involuntary movements induced by L-DOPA [200-202]. Curiously, a synergystic effect on the decrease of abnormal involuntary movements was observed when 5-HT_{1B}R agonists were co-administered with 5-HT_{1A}R agonists [202]. Overall, targeting 5-HT_{1A}Rs [203-207] and 5-HT_{1B}Rs [208-211] with agonists may provide potential benefits on the reversal of PD symptoms.

On the other hand, the inactivation of 5-HT_{2A}R and 5-HT_{2C}R has demonstrated potential antiparkinsonian effects in human patients and animal models. In fact, trazodone, a dual 5-HT_{2A}R/5-HT_{2C}R antagonist, is effective on the treatment of PD-associated depression and on improvement of motor functions in human subjects [212]. Other dual 5-HT_{2A}R/5-HT_{2C}R antagonist, ritanserin, has shown to reduce bradykinesia and

ameliorate gait disorder in human patients [213]. In MPTP-treated mice, peripheral administration of 5-HT_{2A}R antagonists alone and in combination with dual 5-HT_{2A}R/5-HT_{2C}R antagonists enhanced motor performance on the beam walking apparatus [214,215]. Regarding the 5-HT_{2C}Rs, the intracerebral administration of 5-HT_{2C}R antagonists into the SNr elicited contraversive rotations to the injection side and enhanced antiparkinsonian action of D_1R and D_2R agonists in 6-OHDA-treated rats [216,217]. To date, diverse chemical families of antagonists of 5-HT_{2A}R [218-225] 5-HT_{2C}R [223-227] with potential effect on the reversal of PD have been reported.

2.6. GPCR-based drug discovery for PD: an overview of *in silico* methodologies

Over the last years, the development of Computer-Assisted Drug Design (CADD) methodologies has been of extreme relevance for the identification of GPCR modulators targeting PD, contributing to increase the cost-efficiency and to speed up the drug discovery process. *In silico* drug design of GPCR modulators can be achieved by applying structure-based and ligand-based drug design methodologies.

2.6.1. Application of structure-based design techniques for GPCR-based drug discovery

The field of structure-based drug design [228,229] has been a rapidly growing area in which many advances in the drug discovery process have occurred in recent years. The explosive development of the structural biology focused on determination of high resolution three-dimensional (3D) structures of GPCRs has furnished a myriad of therapeutic opportunities for drug design of GPCR modulators inspired by structure-based drug design methodologies such as molecular docking simulations, structure-based, and fragment-based virtual screening techniques. Since GPCRs are membrane-bound protein receptors, experimental elucidation of their 3D structure, by X-ray crystallography and Nuclear Magnetic Ressonance (NMR) studies, has been a tremendously challenging task comparing to globular proteins due to problems associated to receptor purification, receptor instability, among others (reviewed in [230]). Until the elucidation of the X-ray diffraction structure at 2.8 Å resolution of bovine rhodopsin in 2000 (PDBid 1F88) [231], no X-ray structures of any GPCR were available. The 3D structural determination of bovine rhodopsin allowed a deeper understanding of GPCR functioning at molecular level and, for many years, provided the only template for structure-based drug design approaches in homologus GPCRs for the study of drug-GPCR interactions. With the development of receptor crystallization strategies, a number of technical issues related to low expression of GPCRs and their structural instability have

been surmounted, thereby resulting in an accelerated increase of solved GPCR structures [230]. More than 200 3D structures of apo-GPCRs, protein-, natural ligand-, agonist-, and antagonist-bound GPCRs have been solved so far (Table 1), in which the *rhodopsin*-like GPCRs (or class A GPCRs) have been the most reported class [42-44, 231-346]. Additionally, the 3D structures of four subfamilies of *secretin*-like or class B GPCRs (Corticotropin-Releasing Factor Receptors, CRFRs; Calcitonin Receptor-Like Receptors, CRLRs; Glucagon-Like Peptide Receptors, GLPRs; ParaThyroid Hormone-related peptide Receptors, PTHRs) [347-359], two subfamilies of *glutamate*-like or class C GPCRs (metabotropic Glutamate Receptors, mGluRs; γ-AminoButyric Acid Receptors, GABARs) [360-366], one subfamily of *frizzled/taste2*-like or class F GPCR (Smoothened receptors, Smo) [367-372], and two subfamilies of *adhesion* GPCRs (Adhesion G-protein coupled Receptor G1, ADGRG1; Adhesion G-protein coupled Receptor L3, ADGRL3) [373-375] have been disclosed on PDB (reported until June 2017).

Table 1 – Three dimensional structures of GPCRs retrieved from the Research Collaboratory for Structural Bioinformatics Protein Data Bank (RCSB PDB) in June 2017.

***Rhodopsin*-like or class A GPCRs**					
PDBid	**GPCR**	**Main ligand(s) / binding partner(s)**	**Resolution / [Å]**	**Release date**	**Reference**
4IAQ	5-HT_{1B}R	Dihydroergotamine (agonist)	2.80	2013	[232]
4IAR	5-HT_{1B}R	Ergotamine (agonist)	2.70	2013	[232]
4IB4	5-HT_{2B}R	Ergotamine (agonist)	2.70	2013	[233]
4NC3	5-HT_{2B}R	Ergotamine (agonist)	2.80	2013	[234]
5TVN	5-HT_{2B}R	Lysergic acid diethylamide (agonist)	2.90	2017	[235]
5UEN	A_1R	DU172 (antagonist)	3.20	2017	[236]
2YDO	A_{2A}R	Adenosine (agonist)	3.00	2011	[237]
2YDV	A_{2A}R	5′-(*N*-Ethylcarboxamido)adenosine (agonist)	2.60	2011	[237]
3EML	A_{2A}R	ZM241385 (antagonist)	2.60	2008	[44]
3PWH	A_{2A}R	ZM241385 (antagonist)	3.30	2011	[238]
3QAK	A_{2A}R	UK-432097 (agonist)	2.71	2011	[43]
3REY	A_{2A}R	Xanthine amine congener (antagonist)	3.31	2011	[238]
3RFM	A_{2A}R	Caffeine (antagonist)	3.60	2011	[238]
3VG9	A_{2A}R	ZM241385 (antagonist) and Fab2838 (inverse agonist)	2.70	2012	[239]
3VGA	A_{2A}R	ZM241385 (antagonist) and Fab2838 (inverse agonist)	3.10	2012	[239]
3UZA	A_{2A}R	6-(2,6-Dimethylpyridin-4-yl)-5-phenyl-1,2,4-triazin-3-amine (antagonist)	3.27	2012	[240]
3UZC	A_{2A}R	4-(3-Amino-5-phenyl-1,2,4-triazin-6-yl)-2-chlorophenol (antagonist)	3.34	2012	[240]
4EIY	A_{2A}R	ZM241385 (antagonist)	1.80	2012	[241]
4UG2	A_{2A}R	CGS21680 (agonist)	2.60	2015	[242]
4UHR	A_{2A}R	CGS21680 (agonist)	2.60	2015	[242]
5JTB	A_{2A}R	ZM241385 (antagonist)	2.80	2017	[243]
5G53	A_{2A}R	5′-(*N*-Ethylcarboxamido)adenosine (agonist) and G_s proteins	3.40	2016	[244]
5IU4	A_{2A}R	ZM241385 (antagonist)	1.72	2016	[245]
5IU7	A_{2A}R	2-(Furan-2-yl)-N^5-(2-(4-phenylpiperidin-1-	1.90	2016	[245]

		yl)ethyl)-1,2-dihydro-[1,2,4]triazolo[1,5-*a*][1,3,5]triazine-5,7-diamine (antagonist)			
5IU8	$A_{2A}R$	2-(Furan-2-yl)-N^5-(2-(4-methylpiperazin-1-yl)ethyl)-1,2-dihydro-[1,2,4]triazolo[1,5-*a*][1,3,5]triazine-5,7-diamine (antagonist)	2.00	2016	[245]
5IUA	$A_{2A}R$	2-(Furan-2-yl)-N^5-(3-(4-phenylpiperazin-1-yl)propyl)-1,2-dihydro-[1,2,4]triazolo[1,5-*a*][1,3,5]triazine-5,7-diamine (antagonist)	2.20	2016	[245]
5IUB	$A_{2A}R$	N^5-(2-(4-(2,4-Difluorophenyl)piperazin-1-yl)ethyl)-2-(furan-2-yl)-1,2-dihydro-[1,2,4]triazolo[1,5-*a*][1,3,5]triazine-5,7-diamine (antagonist)	2.10	2016	[245]
5K2A	$A_{2A}R$	ZM241385 (antagonist)	2.50	2016	[246]
5K2B	$A_{2A}R$	ZM241385 (antagonist)	2.50	2016	[246]
5K2C	$A_{2A}R$	ZM241385 (antagonist)	1.90	2016	[246]
5K2D	$A_{2A}R$	ZM241385 (antagonist)	1.90	2016	[246]
5UIG	$A_{2A}R$	5-Amino-*N*-[(2-methoxyphenyl)methyl]-2-(3-methylphenyl)-2*H*-1,2,3-triazole-4-carboximidamide (antagonist)	3.50	2017	[247]
5UVI	$A_{2A}R$	ZM241385 (antagonist)	3.20	2017	[248]
5VBL	APJR	AMG3054 (agonist)	2.60	2017	[249]
4YAY	AT_1R	ZD7155 (antagonist)	2.90	2015	[250]
4ZUD	AT_2R	Olmesartan (inverse agonist)	2.80	2015	[251]
5UNF	AT_2R	L-161,638 (antagonist)	2.80	2017	[252]
5UNG	AT_2R	L-161,638 (antagonist)	2.80	2017	[252]
5UNH	AT_2R	(*N*-[(Furan-2-yl)methyl]-*N*-(4-oxo-2-propyl-3-{[2'-(2*H*-tetrazol-5-yl)[1,1'-biphenyl]-4-yl]methyl}-3,4-dihydroquinazolin-6-yl)benzamide) (antagonist)	2.90	2017	[252]
2VT4	β_1AR	Cyanopindolol (antagonist)	2.70	2008	[253]
2Y00	β_1AR	Dobutamine (partial agonist)	2.50	2011	[254]
2Y01	β_1AR	Dobutamine (partial agonist)	2.60	2011	[254]
2Y02	β_1AR	Carmoterol (agonist)	2.60	2011	[254]
2Y03	β_1AR	Isoprenaline (agonist)	2.85	2011	[254]
2Y04	β_1AR	Salbutamol (partial agonist)	3.05	2011	[254]
2YCY	β_1AR	Cyanopindolol (antagonist)	3.15	2011	[255]
2YCW	β_1AR	Carazolol (antagonist)	3.10	2011	[255]
2YCX	β_1AR	Cyanopindolol (antagonist)	3.25	2011	[255]
2YCZ	β_1AR	Iodocyanopindolol (antagonist)	3.65	2011	[255]
3ZPQ	β_1AR	4-(Piperazin-1-yl)-1*H*-indole (antagonist)	2.80	2013	[256]
3ZPR	β_1AR	4-Methyl-2-(piperazin-1-yl)quinoline (antagonist)	2.70	2013	[256]
4AMI	β_1AR	Bucindolol (agonist)	3.20	2012	[257]
4AMJ	β_1AR	Carvedilol (agonist)	2.30	2012	[257]
4BVN	β_1AR	Cyanopindolol (antagonist)	2.10	2014	[258]
4GPO	β_1AR	-	3.50	2013	[259]
5A8E	β_1AR	7-Methylcyanopindolol (inverse agonist)	2.40	2015	[260]
5F8U	β_1AR	Cyanopindolol (antagonist)	3.35	2015	[261]
2R4R	β_2AR	Fab5 (antibody) and carazolol (inverse agonist)	3.40	2007	[262]
2R4S	β_2AR	Fab5 (antibody) and carazolol (inverse agonist)	3.40	2007	[262]
2RH1	β_2AR	Carazolol (inverse agonist)	2.40	2007	[263]
3D4S	β_2AR	Timolol (partial inverse agonist)	2.80	2008	[264]
3KJ6	β_2AR	Fab5 (antibody)	3.40	2010	[265]
3NY8	β_2AR	ICI-118,551 (inverse agonist)	2.84	2010	[266]
3NY9	β_2AR	Ethyl 4-({(2*S*)-2-hydroxy-3-[(1-methylethyl)amino]propyl}oxy)-3-methyl-1-benzofuran-2-carboxylate (inverse agonist)	2.84	2010	[266]
3NYA	β_2AR	Alprenolol (antagonist)	3.16	2010	[266]
3P0G	β_2AR	Nb80 (nanobody) and BI-167107 (agonist)	3.50	2011	[267]

3PDS	β_2AR	FAUC50 (agonist)	3.50	2011	[42]
3SN6	β_2AR	Gs proteins	3.20	2011	[268]
4GBR	β_2AR	Carazolol (inverse agonist)	3.99	2012	[269]
5D5A	β_2AR	Carazolol (inverse agonist)	2.48	2016	[270]
5D5B	β_2AR	Carazolol (inverse agonist)	3.80	2016	[270]
5JQH	β_2AR	Nb60 (nanobody) and carazolol (inverse agonist)	3.20	2016	[271]
5U09	CB_1R	Taranabant (inverse agonist)	2.60	2016	[272]
5TGZ	CB_1R	AM6538 (antagonist)	2.80	2016	[273]
5T1A	CCR_2	BMS-681 (orthosteric antagonist) and CCR-RA-[*R*] (negative allosteric modulator)	2.81	2016	[274]
2RRS	CCR_5	-	NMR	2012	[275]
4MBS	CCR_5	Maraviroc (antagonist)	2.71	2013	[276]
5LWE	CCR_9	Vercirnon (negative allosteric modulator)	2.60	2016	[277]
2LNL	$CXCR_1$	-	NMR	2012	[278]
3ODU	$CXCR_4$	IT1t (antagonist)	2.50	2010	[279]
3OE0	$CXCR_4$	CVX15 (antagonist)	2.90	2010	[279]
3OE6	$CXCR_4$	IT1t (antagonist)	3.20	2010	[279]
3OE8	$CXCR_4$	IT1t (antagonist)	3.10	2010	[279]
3OE9	$CXCR_4$	IT1t (antagonist)	3.10	2010	[279]
4RWS	$CXCR_4$	vMIP-II complex (antagonist)	3.10	2015	[280]
2N55	$CXCR_5$	CXCL12 (agonist)	NMR	2016	[281]
3PBL	D_3R	Eticlopride (antagonist)	2.89	2010	[282]
4N6H	DOR	Naltrindole (antagonist)	1.80	2013	[283]
4RWA	DOR	DIPP-NH_2 (antagonist)	3.28	2015	[284]
4RWD	DOR	DIPP-NH_2 (antagonist)	2.70	2015	[284]
5GLH	ET_BR	Endothelin-1 (agonist)	2.80	2016	[285]
5GLI	ET_BR	-	2.50	2016	[285]
4PHU	$FFAR_1$	TAK-875 (positive allosteric modulator)	2.33	2014	[286]
5TZR	$FFAR_1$	MK-8666 (partial agonist)	2.20	2017	[287]
5TZY	$FFAR_1$	AP8 (ago-positive allosteric modulator) and MK-8666 (partial agonist)	3.22	2017	[287]
4AY9	FSHR	FSH (agonist)	2.50	2012	[288]
4MQW	FSHR	FSH (agonist)	2.90	2014	[289]
3RZE	H_1R	Doxepin (antagonist)	3.10	2011	[290]
4DJH	KOR	JDTic (antagonist)	2.90	2012	[291]
4Z34	$LPAR_1$	ONO9780307 (antagonist)	3.00	2015	[292]
4Z35	$LPAR_1$	ONO9910539 (antagonist)	2.90	2015	[292]
4Z36	$LPAR_1$	ONO3080573 (antagonist)	2.90	2015	[292]
5CXV	$mAChR_1$	Tiotropium (inverse agonist)	2.70	2016	[293]
3UON	$mAChR_2$	*R*-(-)-Quinuclidinyl benzilate (inverse agonist)	3.00	2012	[294]
4MQS	$mAChR_2$	Iperoxo (agonist)	3.50	2013	[295]
4MQT	$mAChR_2$	Iperoxo (agonist) and LY2119620 (positive allosteric modulator)	3.70	2013	[295]
4DAJ	$mAChR_3$	Tiotropium (inverse agonist)	3.40	2012	[296]
4U14	$mAChR_3$	Tiotropium (inverse agonist)	3.57	2014	[297]
4U15	$mAChR_3$	Tiotropium (inverse agonist)	2.80	2014	[297]
4U16	$mAChR_3$	*N*-Methylscopolamine (antagonist)	3.70	2014	[297]
5DSG	$mAChR_3$	Tiotropium (Inverse agonist)	2.60	2016	[293]
4DKL	MOR	*β*-Funaltrexamine (antagonist)	2.80	2012	[298]
5C1M	MOR	BU72 (agonist)	2.10	2015	[299]
4EJ4	N/OFQR	Naltrindole (antagonist)	3.40	2012	[300]
4GRV	N/OFQR	Neurotensin $_{8\text{-}13}$ (agonist)	2.80	2012	[301]
5DHG	N/OFQR	C35 (antagonist)	3.00	2015	[302]
5DHH	N/OFQR	SB612111 (antagonist)	3.00	2015	[302]
3ZEV	$NTSR_1$	TM86V-ΔIC3A	3.00	2014	[303]
4BUO	$NTSR_1$	TM86V-ΔIC3B	2.75	2014	[303]
4BV0	$NTSR_1$	OGG7V-ΔIC3A	3.10	2014	[303]
4BWB	$NTSR_1$	HTGH4-ΔIC3	3.57	2014	[303]

4XEE	$NTSR_1$	Neurotensin/Neuromedin N (agonist)	2.90	2015	[304]
4XES	$NTSR_1$	Neurotensin/Neuromedin N (agonist)	2.60	2015	[304]
5T04	$NTSR_1$	Neurotensin $_{8-13}$ (Arg-Arg-Pro-Tyr-Ile-Leu; agonist)	3.30	2016	[305]
4ZJ8	OX_1R	Suvorexant (antagonist)	2.75	2016	[306]
4ZJC	OX_1R	SB-674042 (antagonist)	2.83	2016	[306]
4S0V	OX_2R	Suvorexant (antagonist)	2.50	2015	[307]
4XNV	$P2Y_1R$	BPTU (antagonist)	2.20	2015	[308]
4XNW	$P2Y_1R$	MRS2500 (antagonist)	2.70	2015	[308]
4NTJ	$P2Y_{12}R$	AZD1283 (agonist)	2.62	2014	[309]
4PXZ	$P2Y_{12}R$	2MeSADP (agonist)	2.50	2014	[310]
4PY0	$P2Y_{12}R$	2MeSATP (partial agonist)	3.10	2014	[310]
3VW7	PAR_1	Vorapaxar (antagonist)	2.20	2012	[311]
5NDD	PAR_2	AZ8838 (antagonist)	2.80	2017	[312]
5NDZ	PAR_2	AZ3451 (antagonist)	3.60	2017	[312]
5NJ6	PAR_2	Fab3949 (antibody) and AZ7188 (antagonist)	4.00	2017	[312]
1F88	RHO	11-*cis*-Retinal (agonist)	2.80	2000	[231]
1GZM	RHO	11-*cis*-Retinal (agonist)	2.65	2003	[313]
1HZX	RHO	11-*cis*-Retinal (agonist)	2.80	2001	[314]
1JFP	RHO	11-*cis*-Retinal (agonist)	NMR	2001	[315]
1L9H	RHO	11-*cis*-Retinal (agonist)	2.60	2002	[316]
1LN6	RHO	11-*cis*-Retinal (agonist)	NMR	2002	[317]
1U19	RHO	11-*cis*-Retinal (agonist)	2.20	2014	[318]
2G87	RHO	11-*cis*-Retinal (agonist)	2.60	2006	[319]
2HPY	RHO	11-*cis*-Retinal (agonist)	2.80	2006	[320]
2I35	RHO	11-*cis*-Retinal (agonist)	3.80	2006	[321]
2I36	RHO	-	4.10	2006	[321]
2I37	RHO	-	4.15	2006	[321]
2J4Y	RHO	11-*cis*-Retinal (agonist)	3.40	2007	[322]
2PED	RHO	11-*cis*-Retinal (agonist)	2.95	2007	[323]
2X72	RHO	$G_{\alpha t1}$ and 11-*cis*-retinal (agonist)	3.00	2011	[324]
2Z73	RHO	11-*cis*-Retinal (agonist)	2.50	2008	[325]
2ZIY	RHO	11-*cis*-Retinal (agonist)	3.70	2008	[326]
3AYM	RHO	11-*cis*-Retinal (agonist)	2.80	2011	[327]
3AYN	RHO	11-*cis*-Retinal (agonist)	2.70	2011	[327]
3C9L	RHO	11-*cis*-Retinal (agonist)	2.65	2008	[328]
3C9M	RHO	11-*cis*-Retinal (agonist)	3.40	2008	[328]
3CAP	RHO	-	2.90	2008	[329]
3DQB	RHO	$G_{\alpha t1}$	3.20	2008	[330]
3PQR	RHO	$G_{\alpha t1}$ and 11-*cis*-retinal (agonist)	2.85	2011	[331]
3PXO	RHO	11-*cis*-Retinal (agonist)	3.00	2011	[331]
3OAX	RHO	*β*-Ionone and 11-*cis*-retinal (agonist)	2.60	2011	[332]
4A4M	RHO	$G_{\alpha t3}$ and 11-*cis*-retinal (agonist)	3.30	2012	[333]
4BEY	RHO	$G_{\alpha t2}$	2.90	2013	[334]
4BEZ	RHO	-	3.30	2013	[334]
4J4Q	RHO	$G_{\alpha t1}$	2.65	2013	[335]
4PXF	RHO	Arrestin-1	2.75	2014	[336]
4X1H	RHO	$G_{\alpha t1}$	2.29	2015	[337]
4ZWJ	RHO	-	3.30	2015	[338]
5DGY	RHO	Visual arrestin-1	7.70	2016	[339]
5DYS	RHO	11-*cis*-Retinal (agonist)	2.30	2016	[340]
5EN0	RHO	$G_{\alpha t3}$ and 11-*cis*-retinal (agonist)	2.81	2016	[340]
5TE3	RHO	-	2.70	2017	[341]
5TE5	RHO	(2*E*)-{(4*E*)-4-[(3*E*)-4-(2,6,6-Trimethylcyclohex-1-en-1-yl)but-3-en-2-ylidene]cyclohex-2-en-1-ylidene}acetaldehyde	4.01	2017	[341]
3V2W	$S1PR_1$	ML056 (antagonist)	3.35	2012	[342]
3V2Y	$S1PR_1$	CYM-5442 (agonist)	2.80	2012	[342]
2XWT	TSHR	K1-70 (antagonist)	1.90	2011	[343]
3G04	TSHR	Thyroid-stimulating human monoclonal	2.55	2009	[344]

		autoantibody (M22)			
4XT1	US28	CX3CL1 (agonist)	2.89	2015	[345]
4XT3	US28	CX3CL1 (agonist)	3.80	2015	[345]
4JQI	V_2R	Arrestin-2	2.60	2013	[346]
***Secretin*-like or class B GPCRs**					
PDBid	**GPCR**	**Ligand(s) / Binding Partner(s)**	**Resolution / [Å]**	**Release date**	**Reference**
3EHS	$CRFR_1$	-	2.76	2008	[347]
3EHT	$CRFR_1$	CRF (agonist)	3.4	2008	[347]
3EHU	$CRFR_1$	CRF (agonist)	1.96	2008	[347]
4K5Y	$CRFR_1$	CP-376395 (antagonist)	2.98	2013	[348]
4Z9G	$CRFR_1$	CP-376395 (antagonist)	3.18	2016	[349]
3AQF	CRLR	RAMP2	2.60	2011	[350]
3N7P	CRLR	RAMP1	2.80	2010	[351]
3N7R	CRLR	RAMP1 and telcagepant (antagonist)	2.90	2010	[351]
3N7S	CRLR	RAMP1 and olcegepant (antagonist)	2.10	2010	[351]
5UZ7	CRLR	G_s proteins	4.10	2017	[352]
4ERS	GLP_1R	mAb1 (antagonist)	2.64	2012	[353]
4L6R	GLP_1R	Glucagon (agonist)	3.30	2013	[354]
5EE7	GLP_1R	MK-0893 (antagonist)	2.50	2016	[355]
5NX2	GLP_1R	Peptide 5 (agonist)	3.70	2017	[356]
5VAI	GLP_1R	G_s proteins	4.10	2017	[357]
5VEW	GLP_1R	PF-06372222 (negative allosteric modulator)	2.70	2017	[358]
5VEX	GLP_1R	NNC0640 (negative allosteric modulator)	3.00	2017	[358]
3H3G	PTH_1R	xsdkd	1.94	2009	[359]
***Glutamate*-like or class C GPCRs**					
PDBid	**GPCR**	**Ligand(s) / Binding Partner(s)**	**Resolution / [Å]**	**Release date**	**Reference**
4MQE	GABABR	-	2.35	2013	[360]
4MQF	GABABR	2-Hydroxysaclofen (antagonist)	2.22	2013	[360]
4MR7	GABABR	CGP54626 (antagonist)	2.15	2013	[360]
4MR8	GABABR	CGP35348 (antagonist)	2.15	2013	[360]
4MR9	GABABR	SCH50911 (antagonist)	2.35	2013	[360]
4MRM	GABABR	Phaclofen (antagonist)	2.86	2013	[360]
4MS1	GABABR	CGP46381 (antagonist)	2.25	2013	[360]
4MS3	GABABR	γ-Aminobutyric acid (agonist)	2.50	2013	[360]
4MS4	GABABR	Baclofen (agonist)	1.90	2013	[360]
4OR2	$mGluR_1$	FITM (negative allosteric modulator)	2.80	2014	[361]
1EWK	$mGluR_1$	Glutamate (agonist)	2.20	2000	[362]
1EWT	$mGluR_1$	-	3.70	2000	[362]
1EWV	$mGluR_1$	-	4.00	2000	[362]
5CNI	$mGluR_2$	Glutamate (agonist)	2.69	2015	[363]
5CNJ	$mGluR_2$	LY2812223 (agonist)	2.65	2015	[363]
2E4U	$mGluR_3$	Glutamate (agonist)	2.35	2007	[364]
2E4V	$mGluR_3$	DCG-IV (agonist)	2.40	2007	[364]
2E4W	$mGluR_3$	1*S*,3*S*-ACPD (agonist)	2.40	2007	[364]
2E4X	$mGluR_3$	1*S*,3*R*-ACPD (agonist)	2.75	2007	[364]
2E4Y	$mGluR_3$	2*R*,4*R*-APDC (agonist)	3.40	2007	[364]
5CNK	$mGluR_3$	Glutamate (agonist)	3.15	2015	[363]
5CNM	$mGluR_3$	LY2812223 (agonist)	2.84	2015	[363]
4OO9	$mGluR_5$	Mavoglurant (negative allosteric modulator)	2.60	2014	[365]
5CGC	$mGluR_5$	3-Chloro-4-fluoro-5-[6-(1*H*-pyrazol-1-yl)pyrimidin-4-yl]benzonitrile (negative allosteric modulator)	3.10	2015	[366]
5CGD	$mGluR_5$	HTL14242 (negative allosteric modulator)	2.60	2015	[366]
2E4Z	$mGluR_7$	-	3.30	2007	[364]
***Frizzled/taste2*-like or class F GPCRs**					
PDBid	**GPCR**	**Ligand(s) / Binding Partner(s)**	**Resolution / [Å]**	**Release date**	**Reference**
4JKV	Smo	LY2940680 (antagonist)	2.45	2013	[367]
4N4W	Smo	SANT-1 (antagonist)	2.80	2014	[368]
4O9R	Smo	Cyclopamine (antagonist)	3.20	2014	[369]
4QIM	Smo	Anta XV (antagonist)	2.61	2014	[368]

4QIN	Smo	SAG1.5 (agonist)	2.60	2014	[368]
5KZV	Smo	20(*S*)-Hydroxycholesterol (agonist)	1.62	2016	[370]
5KZY	Smo	Cyclopamine (antagonist)	2.48	2016	[370]
5KZZ	Smo	-	1.33	2016	[370]
5L7D	Smo	Cholesterol (agonist)	3.20	2016	[371]
5L7I	Smo	Vismodegib (antagonist)	3.30	2016	[371]
5V56	Smo	TC114 (antagonist)	2.90	2017	[372]
5V57	Smo	TC114 (antagonist)	3.00	2017	[372]
***Adhesion* GPCRs**					
PDBid	**GPCR**	**Ligand(s) / Binding Partner(s)**	**Resolution / [Å]**	**Release date**	**Reference**
5KVM	$ADGRG_1$	FN3 monobody	2.45	2016	[373]
4RMK	$ADGRL_3$	-	1.61	2015	[374]
4RML	$ADGRL_3$	-	1.60	2015	[374]
5FTT	$ADGRL_3$	Unc5D and FLRT2	3.40	2016	[375]
5FTU	$ADGRL_3$	Unc5D and FLRT2	6.01	2016	[375]

(5-HTR - 5-HydroxyTryptamine receptor; ADGRG1 - Adhesion G-protein coupled Receptor G1; ADGRL3 - Adhesion G-protein coupled Receptor L3; AR - Adenosine Receptor; APJR - Apelin Receptor; ATR - Angiotensin II Receptor; βAR: - β-Adrenergic Receptor; CBR - Cannabinoid Receptor; CCR - CC Chemokine Receptor; CRF - Corticotropin Releasing Factor; CRFR - Corticotropin Releasing Factor Receptor; CRLR - Calcitonin Receptor-Like Receptor; CXCR - CXC Chemokine Receptor; DOR - δ-Opioid Receptor; DR - Dopamine Receptor; ETR - Endothelin Receptor; FFAR - Free Fatty Acid Receptor; FLRT2 - Fibronectin Leucin-Rich Transmembrane protein 2; FN3 - FibroNectin type III domain; FSH - Follicle-Stimulating Hormone; FSHR - Follicle-Stimulating Hormone Receptor; GABAR - γ-AminoButyric Acid Receptor; GLPR - Glucagon-Like Peptide Receptor; HR - Histamine Receptor; KOR - κ-Opioid Receptor; LPAR - LysoPhosphatidic Acid Receptor; mAChR - muscarinic AcetylCholine Receptor; mGluR - metabotropic Glutamate Receptor; MOR - μ-Opioid Receptor; N/OFQR - Nociceptin/Orphanin FQ Receptor; NTSR - Neurotensin Receptor; OXR - Orexin Receptor; P2YR - Purinergic P2Y Receptor; PAR - Protease-Activated Receptor; PTHR - ParaThyroid Hormone-related peptide Receptor; PTHrP - ParaThyroid Hormone-related Peptide; RAMP - Receptor-Activity Modifying Protein; RHO - Rhodopsin; S1PR - Sphingosine-1-Phosphate Receptor; Smo - Smoothened Receptor; TSHR - Thyroid-Stimulating Hormone Receptor; Unc5D - Unc5D guidance receptor; US28 - Cytomegalovirus-encoded chemokine Receptor; VIPR - Vasoactive Intestinal Peptide Receptor; VR - Vasopressin Receptor)

Molecular docking is one of the most frequently used methods in structure-based drug design due to its ability to predict the conformation of ligands within an appropriate binding site with a considerable degree of accuracy [376-380]. Each ligand is docked onto the X-ray or NMR structure of the target protein or, if the 3D structure is not available, onto a model of the target (retrived by homology modeling), applying molecular docking

algorithms that explore the different binding poses of the ligands inside the binding site of the target. The identification of the most likely binding conformations involves the exploration of a large conformational space representing the various potential binding poses of the ligands and the prediction of the interaction energy associated to each of the predicted binding poses. Regarding the conformational search step, the structural parameters of ligands (translational, torsional, and rotational degrees of freedom) are increasingly modified, and several conformational search algorithms execute this stage by employing stochastic and systematic search methods [376-380]. Independently of the specificities of each search method, any conformational search algorithm should explore a broader range of energy landscape within an affordable computational time. Subsequently, the strength of the binding affinity of the predicted ligand-protein complexes are estimated by the use of scoring functions, which are given in most cases by the Gibbs free energy (ΔG) and the dissociation constant (K_d). Scoring functions are estimated mathematical functions that evaluate the most relevant physicochemical parameters involved in ligand-protein interaction, in particular the intermolecular interactions, desolvation, and entropic effects. The use of a high number of physicochemical parameters seems to increase the accuracy of the scoring function [376-380]. The molecular docking programs are executed through a cyclic and iterative process, in which the different ligand binding conformations are evaluated by the scoring functions, until converging to a minimum energy conformation [376-380]. However, as the computational cost also increases proportionally with the number of included parameters, there should be a perfect combination between the accuracy and the speed of the calculation, which is crucial for databases containing a considerable number of chemical compounds. Nowadays, new scoring fucntions based on Machine-Learning (ML) algorithms are emerging [381,382].

The determination of the scoring functions can be extremely useful in drug discovery for the virtual screening of commercially available compounds and *in-house* ligands that have been already synthesized and tested *in vitro*, or even pre-assembled databases of virtual drug candidates in order to identify the ligand structures that are most likely to interact to a protein target of interest, according to their docking scores. Apart from their applicability to virtual screening, the scoring functions can also be employed for *de novo* drug design of novel chemical structures targeting a specific protein and for *hit-to-lead* optimization of pharmacodynamic parameters of drug candidates (reviewed in [376-380]). Table 2 describes the most relevant docking studies performed for distinct chemical classes of modulators of GPCRs potentially involved in PD, using X-ray structures of GPCRs available on PDB and receptor models constructed from GPCR templates.

Table 2. Structure-based drug design methodologies reported for ligands targeting GPCRs potentially involved in PD

Dopamine D_2 receptor (D_2R) agonists			
Entry	**Method(s)**	**Ligand(s)**	**Relevant ligand-receptor interactions**
1	Docking onto D_2R model using AutoDock 3.0.5 software package [383] (Template: X-ray structure of human β_2AR; PDBid 2RH1 [263])	Dopamine, 2-(aminomethyl)chromans	Dopamine: salt bridge interactions involving Asp114; hydrogen bond interactions with Ser193 and Ser197; π-π interactions involving Trp245, Phe248, and Phe249. 2-(Aminomethyl)chromans: salt bridge interactions involving Asp114; π-π interactions with Phe248; hydrogen bond interactions involving Ser193, Ser194, and/or Ser197 residues [384].
2	Docking onto D_2R model using MOE software package [385] (Template: X-ray structure of human β_2AR; PDBid 2RH1 [263])	(*R*)-(-)-2-OH-NPA	*R*-(-)-2-OH-NPA: salt bridge interactions involving Asp114; hydrogen bond interactions with Asn186, Ser193, and Ser393; hydrophobic interactions involving Thr412 and π-π interactions with Phe390 [386].
3	Docking onto D_2R model using GLIDE module from Schrödinger Suite [387-389] (Template: X-ray structure of D_3R; PDBid 3PBL [282])	Substituted piperidines, (2-methoxyphenyl) piperazines	Substituted piperidines: salt bridge interactions involving Asp114; π-π interactions with Phe393, His397, and the hydrophobic pocket composed by Phe386, Trp390, and Tyr420; hydrogen bond interactions with Ser193. (2-Methoxyphenyl) piperazines: salt bridge interactions involving Asp114; π-π interactions with Phe394 and the hydrophobic pocket composed by Phe386, Trp390, and Tyr420 [390].
4	Docking to D_2R model using GLIDE module of Schrödinger Suite [387-389] (Template: X-ray structure of D_3R; PDBid 3PBL [282])	1-(2-Methoxyphenyl)-4-(1-phenethylpiperidin-4-yl)piperazines, 1-(2-methoxyphenyl)-4-[(1-phenethylpiperidin-4-yl)methyl]-piperazines	1-(2-Methoxyphenyl)-4-(1-phenethylpiperidin-4-yl)piperazines: hydrophobic interactions with the hydrophobic pocket formed by Phe386, Trp390, and Tyr42 residues; salt bridge involving Asp114; hydrogen bond interactions involving Asp114, Ser194, and Ser197 residues. Two possible binding conformations for 1-(2-Methoxyphenyl)-4-[(1-phenethylpiperidin-4-yl)methyl]-piperazines: (i) arylpiperazine moiety interacts with hydrophobic pocket of orthosteric binding site and the head part makes hydrogen bond interactions with Ser194 and Ser197; (ii) the head part interacts with hydrophobic pocket and arylpiperazine group makes hydrogen bond interactions with Ser194 and Ser197 [391].
5	Docking onto $D_{2L}R$ model using AutoDock Vina [392] and AutoDock 4.2 [393] softwares (Template: X-ray structure of D_3R; PDBid 3PBL [282])	(*R*)-7-OH-DPAT, (*R*)-7-OH-PIPAT, pramipexole, ropinirole, rotigotine, quinpirole, dopamine, PD128907 and *cis*-8-OH-PBZI	Hydrogen bond interactions involving Asp114, Val190, Ser193, and Ser194 residues; hydrophobic interactions involving Phe110, Val111, Val115, Ile184, Trp386, Phe389, Phe390, His393, Gly415, and Tyr416 residues [394].
6	Docking onto D_2R model using AutoDock 3.0 software [383] (Template: X-ray structure of bovine RHO; PDBid 1F88 [231])	Raclopride, L-741,626	Raclopride: hydrogen bond interactions involving Asp114, Cys118, and Thr119; hydrophobic interactions with a hydrophobic region mainly composed by Tyr408 and Phe410 residues. L-741,626: Salt bridge interactions involving Asp114; hydrogen bond interactions with Ser221 and Thr412; π-π interactions involving Phe389 and Phe411 residues [395].
7	Docking onto D_2R model using Docking module of INSIGHT II software (Accelerys Inc., Cambridge, UK) [396] (Template: X-ray structure of bovine RHO; PDBid 1F88 [231])	5-{2-[4-(2-Methoxyphenyl)piperazin-1-yl]ethoxy)-1,3-dihydro-2*H*-benzimidazole-2-thione	5-{2-[4-(2-Methoxyphenyl)piperazin-1-yl]ethoxy)-1,3-dihydro-2*H*-benzimidazole-2-thione: salt bridge interactions involving Asp 86; hydrogen bond interactions with Trp115, Ser122, Ser141, Phe185, and His 189; π-π interactions involving Phe 178, Trp182, and Tyr216 residues [397].
8	Docking onto D_2R using LIBDOCK module from Discovery Studio software [398] (Template:	Arylpiperazines	Arylpiperazines: hydrophobic interactions involving Leu125, Leu126, Phe144, Val146, and Ile190 residues; hydrogen bond interactions involving Asn135 and Asn141; π-π interactions with Phe144 and His189 residues [399].

	X-ray structure of bovine RHO; PDBid 1F88 [231])		
Dopamine D_3 receptor (D_3R) agonists			
Entry	**Method(s)**	**Ligand(s)**	**Results/Conclusions**
9	Docking onto D_3R model performed by CERIUS^2 software (version 4.6) [400] (Template: X-ray structure of bovine RHO; PDBid 1F88 [231])	(*R*)-(+)-7-OH-DPAT	*R*-(+)-7-OH-DPAT: salt bridge interactions involving Asp110; hydrogen bond interactions with Ser192; hydrophobic interactions with Phe106, Val107, Val111, Cys114, Phe345, Phe346, and Tyr373 residues [401].
10	Docking onto X-ray structure of D_3R (PDBid 3PBL [282]) using AutoDock Vina [392] and AutoDock 4.0 softwares [402,403]	Glycyrrhetinic acid, E.resveratroloside, Curcumin, Hirsutanonol, Glabridin, Alloin, Diacerein, Bromocriptine, Apomorphine, Ropinirole	Hydrogen bond interactions with Asp110, Ser192, His349, Thr369, and Tyr373 residues; hydrophobic interactions involving the binding pocket Asp110, Ile183, Ser192, Phe346, His349, Thr369, and Tyr373 [404].
11	Docking onto X-ray structure of D_3R (PDB id 3PBL [282]) using SurFlex Dock software method of SYBYL-X 1.3 package [405]	(*E*)-*N*-((1*S*,4*r*)-4-(2-(((*S*)-2-amino-4,5,6,7-tetrahydro benzo[*d*]thiazol-6-yl)(propyl)amino)ethyl)cyclohexyl)-3-(4-chlorophenyl)acrylamide, *N*-((1*S*,4*r*)-4-(2-(((*S*)-2-amino-4,5,6,7-tetrahydrobenzo[*d*]thiazol-6-yl)(propyl) amino)ethyl)cyclohexyl)-3-(5-methyl-1,2,4-oxadiazol-3-yl)benzamide, *N*-((1*S*,4*r*)-4-(2-(((*S*)-2-amino-4,5,6,7-tetrahydrobenzo[*d*]thiazol-6-yl)(propyl)amino)ethyl) cyclohexyl)-2-chloropyridine-3-sulfonamide	(*E*)-*N*-((1*S*,4*r*)-4-(2-(((*S*)-2-amino-4,5,6,7-tetrahydrobenzo[*d*]thiazol-6-yl)(propyl)amino)ethyl) cyclohexyl)-3-(4-chlorophenyl)acrylamide: hydrogen bond interactions with Asp110 and Ile183; van der Waals interactions with Phe106, Phe345, Tyr365, and Tyr373 residues; hydrophobic interactions involving Ser182, Phe345, and Ser366 residues. *N*-((1*S*,4*r*)-4-(2-(((*S*)-2-amino-4,5,6,7-tetrahydrobenzo[*d*]thiazol-6-yl)(propyl)amino)ethyl) cyclohexyl)-3-(5-methyl-1,2,4-oxadiazol-3-yl)benzamide: hydrogen bond interactions with Asp110 and Ile183; hydrophobic interactions involving Val111, Ser182, Ile183, Val189, Ser192, Phe345, Phe346 residues. *N*-((1*S*,4*r*)-4-(2-(((*S*)-2-amino-4,5,6,7-tetrahydrobenzo[*d*]thiazol-6-yl)(propyl)amino)ethyl) cyclohexyl)-2-chloropyridine-3-sulfonamide: hydrogen bond interactions with Glu90 and Ser192; hydrophobic interactions with Asp110, Ser182, Ile 183, Phe345, Phe346, and Tyr373 residues [406].
12	Docking onto X-ray structure of D_3R (PDB id 3PBL [282]) using AutoDock Vina [392] and AutoDock 4.2 [393] softwares	*R*-7-OH-DPAT, *R*-7-OH-PIPAT, pramipexole, ropinirole, rotigotine, quinpirole, dopamine, PD128907 and *cis*-8-OH-PBZI	Hydrogen bond interactions involving Asp110, Val111, Thr115, Ser192, and Ser196 residues; hydrophobic interactions with Phe106, Val107, Val111, Ile183, Phe188, Trp342, Phe345, Phe346, His349, Thr369, and Tyr373 residues [394].
13	Docking onto X-ray structure of D_3R (PDB id 3PBL [282]) using InducedFit docking software [407-409]	[4-(4-Carboxamidobutyl)]-1-arylpiperazines	*N*-(4-(4-(2-(*tert*-Butyl)-6-(trifluoromethyl)pyrimidin-4-yl)-piperazin-1-yl)butyl)imidazo[1,2-*a*]pyridine-2-carboxamide: hydrogen bond interactions involving Thr115 and Ser196; hydrophobic interactions with Ile183, Val189, and Val350 residues. The arylamide moiety of this ligand and other analogues may adopt three different conformations: (i) the arylamide group is docked onto Glu90; (ii) the arylamide moiety is placed in proximity to Val180 and Ser182 residues; (iii) the arylamide moiety is involved in π-π interactions with Tyr365 and in hydrogen bond interactions with Thr369 [66].
Adenosine A_{2A} receptor ($A_{2A}AR$) antagonists			
Entry	**Method(s)**	**Ligand(s)**	**Results/Conclusions**
14	Docking onto $A_{2A}AR$ model using MOE software [410] (Template: X-ray structure of $A_{2A}AR$; PDBid 3EML [44])	8-Substituted 9-ethyladenine derivatives	Two different ligand binding orientations towards $A_{2A}AR$, interacting with key residues Phe163, Glu164, and Asn248 of $A_{2A}AR$ model (corresponding to Phe168, Glu169, and Asp253 of human $A_{2A}AR$). Ligand binding orientation 1: π-π interactions involving Phe163; hydrogen bond interactions with Glu164 and Asn248. Ligand binding orientation 2: π-π interactions involving Phe163; hydrogen bond interactions with Asn248 [96].
15	Docking onto X-ray structure of	3-[4-Amino-6-(2-	3-[4-Amino-6-(2-chlorobenzyl)thieno[2,3-*d*]pyrimidin-2-yl]benzonitrile: hydrophobic interactions

	A_{2A}AR (PDBid 4EIY [241]) using AutoDock 4.2 software [393]	chlorobenzyl)thieno[2,3-*d*] pyrimidin-2-yl]benzonitrile	involving Leu190, Leu194, Tyr197, Phe201, Ala236, Val239, and Ala243 residues [411].
16	Docking onto X-ray structure of A_{2A}AR (PDBid 3EML [44]) using GLIDE module from Schrödinger suite [387-389]	10 ligands with the best docking scores selected from a library of 46 A_{2A}AR antagonists	Hydrogen bond interactions involving Asn253 for all ligands and Ile180, Ala81, and Tyr271 residues for some ligands; π-π interactions with Phe168 [412].
17	Docking onto X-ray structure of A_{2A}AR (PDBid 3EML [44]) using DOCK 5.4 software [413]	7-Substituted 5-amino-2-(2-furyl)pyrazolo[4,3-*e*]-1,2,4-triazolo[1,5-*c*]pyrimidines, piperazine derivatives of triazolotriazine and triazolopyrimidines	7-Substituted 5-amino-2-(2-furyl)pyrazolo[4,3-*e*]-1,2,4-triazolo[1,5-*c*]pyrimidines: hydrogen bond interactions involving Thr88; π-π interactions involving Phe182 and Phe257 residues; hydrophobic interactions with Ile66, Ile92, Ile244, and Trp276 residues. Piperazine derivatives of triazolotriazine and triazolopyrimidines: hydrogen bond interactions involving Thr27; π-π stacking interactions with Phe182; hydrophobic interactions involving Ile92, Phe93, and Val186 residues [414].
18	Docking onto X-ray structure of A_{2A}AR (PDBid 4EIY [241]) using GLIDE module from Schrödinger suite [387-389]	5'-Substituted amiloride derivatives	5'-Substituted amiloride derivatives: hydrogen bond and salt bridge interactions with Asn52 and Thr88; π-π interactions with Trp246; hydrophobic interactions with Phe168, Met177, Leu249, and Ile274 residues [415].
19	Docking onto A_{2A}AR model using GLIDE module from Schrödinger suite [387-389] (Template: X-ray structure of β_1AR; PDBid 2VT4 [253])	4-(3-Aminoamino-5-phenyl-1,2,4-triazin-6-yl)-2-chlorophenol, 6-(2,6-dimethylpyridin-4-yl)-5-phenyl-1,2,4-triazin-3-amine	4-(3-Amino-5-phenyl-1,2,4-triazin-6-yl)-2-chlorophenol: hydrogen bond interactions involving Asn253 and His278; π-π interactions with Phe168, and hydrophobic interactions involving Met270. 6-(2,6-Dimethylpyridin-4-yl)-5-phenyl-1,2,4-triazin-3-amine: hydrogen bond interactions involving Asn253; π-π interactions with Phe168; and hydrophobic interactions with Met270, with a pocket comprised by Leu84, Leu85, Met177, Asn181, Trp246, Leu249, and His250 and a pocket formed by Ala63, Ile66, Ser277, and His278 residues [240].
20	Docking onto A_{2A}AR model using FlexiDock utility in the Biopolymer module of SYBYL 6.7.1 (Tripos, St Louis, MO) [416] (Template: structure of RHO; PDBid 1BRD [417])	CGS15943	CGS15943: hydrophobic interactions between quinazoline ring and Leu85, Ile135, Leu167, Phe168, Phe182, Val186, Trp246, and Leu249, and between furan ring and Ile80, Val84, and Ile274; hydrogen bond interactions involving Asn181 and Asn253 residues [418].
21	Docking onto X-ray structure of A_{2A}AR (PDBid 3EML [44]) using GLIDE module from Schrödinger suite software [387-389], InducedFit docking software [407-409], and ICM molecular modeling software (Molsoft, LLC) [419]	ZM241385	ZM241385: hydrogen bond interactions involving Glu169 and Asn253 residues; hydrophobic interactions with Phe168, His264, Ile267, Met270, and Ile274 residues [420-422].
22	Docking onto A_{2A}AR model using GLIDE module from Schrödinger suite software [387-389] and InducedFit docking software [407-409] (Template: X-ray structure of β_2AR; PDBid 2RH1 [263])	ZM241385	ZM241385: hydrogen bond interactions involving Asn253; hydrophobic interactions with Leu85, Thr88, Trp246, and Leu249 residues; π-π interactions with Phe168 [420].
23	Docking onto X-ray structure of A_{2A}AR (PDBid 3EML [44]) using	Caffeine	Five binding poses of caffeine to A_{2A}AR were analysed and the most relevant residues involved in caffeine-A_{2A}AR interaction are: Ala63, Val84, Leu85, Thr88, Phe168, Glu169, Met177, Trp246, Leu249,

	AutoDock Vina program [393].		His250, Asn253, Ile274, and His278 [423].
24	Docking onto A_{2A}AR model using CAChe 6.1 [424] and CAChe 7.5 softwares [424] (Template: X-ray structure of bovine RHO and β_2AR; PDBid 1U19 [318] and 2RH1 [263])	XAC, KW6002, ZM241385	In bovine rhodopsin, the purine ring of XAC and the phenyl rings of KW6002 and ZM241385 are accommodated in a pocket formed by Leu85, Thr88, Gln89, Ile135, Leu167, Phe168, Val178, Asn181, and Phe182. The purine ring of KW6002 and ZM241385 and the aminoethylphenoxyacetamid group of XAC occupies a pocket comprised by Glu13, Val55, Ile60, Ala63, Phe80, Ile274, Ile275, and His278. The furan moiety of ZM-241385 interacts with a lipophilic pocket formed by Phe62, Ile66, and Val164. In β_2AR, the purine ring of ligands is accommodated in a pocket formed by Leu48, Ala51, Asp52, Leu87, Thr88, Ser91, Leu95, Ile238, Phe242, Trp246, His250, Ser277, His278, Asn280, Ser281, and Asn285. The aromatic rings are placed in a pocket comprised by Val55, Ala59, Val60, Phe62, Ala63, Val84, Gln89, Glu169, Trp246, Ile274, and His278. XAC makes hydrogen bond interactions with Glu169, Ser277, His278, and Ser281 residues [425].
25	Docking onto a theoretical model of A_{2A}AR (PDBid 1MMH) using DOCK 5.4 software [413]	Xanthine derivatives (KW6002, KF17837, BS-DMPX) Non-xanthine derivatives (7-Substituted 5-amino-2-(2-furyl)pyrazolo[4,3-*e*]-1,2,4-triazolo[1,5-*c*]pyrimidines and piperazine derivatives of [1,2,4]triazolo[1,5-*a*]triazine)	Xanthine derivatives: hydrogen bond interactions involving Ser277; π-π interactions involving Tyr179, His250, and Phe257 residues; hydrophobic interactions with hydrophobic domains located at the entrance and at the bottom of binding pocket formed by Ser91, Ile92, Trp246, Leu249, Ala273, and His278 residues. Non-xanthine derivatives: hydrogen bond interactions involving Thr88 and Thr271 residues; π-π interactions involving Phe82 and Phe257 residues. The furan ring accomodates in a hydrophobic pocket comprised by Ile66, Ile92, Ile244, and Trp276 in 7-substituted 5-amino-2-(2-furyl)pyrazolo[4,3-*e*]-1,2,4-triazolo[1,5-*c*]pyrimidines and in a hydrophobic pocket comprised by Ile92, Phe93, and Val186 in piperazine derivatives of [1,2,4]triazolo[1,5-*a*]triazine) [426].
26	Docking onto TM2, TM3, TM5, TM6, and TM7 domains of A_{2A}AR (PDBid 3PWH [238]) performed by Autodock using Lamarckian Genetic Algorithm [383]	Pyrimidine and triazine derivatives, pyrazolo[3,4-*d*]pyrimidines, pyrrolo[2,3-*d*]pyrimidines, triazolo[4,5-*d*]pyrimidines, 6-arylpurines, thieno[3,2-*d*]pyrimidines	Hydrogen bond interactions involving Glu169 and Asn253 residues; hydrophobic interactions with Val84, Leu249, Met270 and Ile274; π-π interactions with Phe168 of A_{2A}AR [427].
27	Docking onto X-ray structure of A_{2A}AR (PDBid 3PWH [238]) using GLIDE module from Schrödinger suite [387-389]	2-(Furan-2-yl)-[1,2,4]triazolo[1,5-*f*]pyrimidin-5-amines, 2-(furan-2-yl)-[1,2,4]triazolo[1,5-*a*]pyrazin-8-amines, 2-(furan-2-yl)-[1,2,4]triazolo[1,5-*a*][1,3,5]triazin-7-amines	Hydrogen bond interactions involving Glu169 and Asn253 residues; π-π interactions with Phe168 and His250. Weak interactions with Ser67 (hydrogen bond interactions) and Tyr271 (π-π interactions) for some derivatives [428].
M_1 muscarinic acetylcholine receptor ($mAChR_1$) antagonists / negative allosteric modulators (NAMs)			
Entry	**Method(s)**	**Ligand(s)**	**Results/Conclusions**
28	Docking onto X-ray structure of $mAChR_1$ (PDBid 5CXV [293]) using GLIDE module from Schrödinger suite [387-389]	Tiotropium	Tiotropium: hydrogen bond interactions involving Asp residue [293].
29	Docking onto $mAChR_1$ model using DOCK 4.01 [429], FlexX 1.8 [430], and GOLD 1.1 softwares [431] (Template: X-ray structure of bovine RHO; PDBid 1F88 [231])	Pirenzepine	Pirenzepine: salt bridge interactions between the basic nitrogen atom and Asp residue at TM3, the lactam ring interacts with Asn residue at TM6 and its aromatic nitrogen atom with Thr residue at TM5 [432].
30	Docking onto $mAChR_1$ model using GOLD software [431]	*N*-Methyl-4-piperidyl benzylates	*N*-methyl-4-piperidyl benzylates: salt bridge interactions involving Asp105; hydrophobic interactions involving Tyr404; hydrogen bond interactions with Tyr179 [116].

	(Template: X-ray structure of bovine RHO; PDBid 1F88 [231])		
Metabotropic Glutamate Receptor 2 ($MGluR_2$) agonists / positive allosteric modulators (PAMs)			
Entry	**Method(s)**	**Ligand(s)**	**Results/Conclusions**
31	Docking onto $mGluR_2$ model using GLIDE module from Schrödinger suite [387-389] (Template: X-ray structures of $mGluR_1$, $mGluR_5$, and β_2-AR (PDBid 4OR2 [361], 4OO9 [365], and 3SN6 [268])	JNJ-42153605	JNJ-42153605: hydrophobic interactions involving Leu639, Phe643, Leu732, Trp773, and Phe776 residues; hydrogen bond interactions involving Ser731 and Asn735; π-π interactions with His723 [433].
32	Docking onto X-ray structure of $mGluR_2$ (PDBid 5CNJ [363]) using MOE v. 2013.08 [434]	LY2812223	LY2812223: salt bridge interactions involving Arg61, Asp295, and Lys377 residues; hydrogen bond interaction involving Ser165, Ala 166, Thr168, and Glu273 residues; water-mediated hydrogen bond interactions with Asp301; π-H interactions with the Ser272 [363].
Metabotropic Glutamate Receptor 3 ($MGluR_3$) agonists / positive allosteric modulators (PAMs)			
Entry	**Method(s)**	**Ligand(s)**	**Results/Conclusions**
32	Docking onto X-ray structure of $mGluR_3$ (PDBid 2E4U [364]) using Induced Fit algorithm [407-409]	Glutamate	Glutamate: hydrogen bond interactions with Ser151, Ala172, Ser173, and Thr174 residues; salt bridge interactions involving Arg64, Arg68, Asp301, and Lys389 residues [435].
33	Docking onto X-ray structures of $mGluR_3$ (PDBid 2E4V [364], 2E4W [364], 2E4X [364], and 2E4Y [364])	DCG-IV, *1S*,*3S*-ACPD, *1S*,*3R*-ACPD, *2R*,*4R*-APDC	DCG-IV: hydrogen bond interactions involving Arg68, Ser151, Ala172, Thr174, Tyr222, Ser278, Asp301, and Lys389; water-mediated hydrogen bond interactions with Arg64; van der Walls interactions involving Tyr150. *1S*,*3S*-ACPD: hydrogen bond interactions involving Arg68, Ser151, Ala172, Thr174, Asp301, and Lys389; water-mediated interactions with Arg64 and Ser278; van der Waals interactions involving Tyr222 and Gly302. *1S*,*3R*-ACPD: hydrogen bond interactions involving Arg68, Ser151, Ala172, Thr174, Asp301, and Lys389; van der Waals interactions with Tyr222 and Gly302. *2R*,*4R*-APDC: hydrogen bond interactions involving Arg68, Ser151, Ala172, Thr174, Asp301, and Lys389; van der Waals interactions with Tyr222 [364].
Metabotropic Glutamate Receptor 4 ($MGluR_4$) agonists / positive allosteric modulators (PAMs)			
Entry	**Method(s)**	**Ligand(s)**	**Results/Conclusions**
33	Docking onto $mGluR_4$ model using AutoDock 3.0 software [383] (Template: X-ray structure of $mGluR_1$; PDBid 1EWK [362])	L-Glutamate, L-AP4, *S*-PPG	L-Glutamate, L-AP4, and S-PPG interact with the agonist binding site of $mGluR_4$ composed by Arg78, Ser159, and Thr182 [436].
34	Docking onto VFT domain of $mGluR_4$ using Discovery Studio 2.5.5 software (Accelerys Inc., Cambridge, UK) [437]	LSP4-2022	The hydroxybenzilic moiety of LSP4-2022 interacts with Lys74 and Lys317 and the glutamate-like moiety interacts with Arg78, Ser159, Ala180, Thr182, Tyr230, Asp312, and Lys405. The phenoxyacetic acid group of LSP4-2022 is involved in hydrogen bond interactions with Thr108, Ser157, and Gly158 [438].
35	Docking onto $mGluR_4$ model using Discover 3.0 and WHATIF softwares [396] (Template: X-ray structures of LIVBP, LBP, and AmiC; PDBid 2LIV [439], 2LBP	ACTP-I	Docking to the open form of $mGluR_4$ model, built from LIVBP and LBP templates, has shown that ACTP-I interacts with Lys74, Arg78, Ser159, and Thr182. Docking to the closed form of $mGluR_4$ model, built from AmiC template, has shown that ACTP-1 interacts with Tyr230, Asp312, Ser313, and Lys317 [442].

	[440] and 1PEA [441])		
Metabotropic Glutamate Receptor 5 ($mGluR_5$) antagonists / negative allosteric modulators (NAMs)			
Entry	**Method(s)**	**Ligand(s)**	**Results/Conclusions**
36	Docking onto X-ray structure of $mGluR_5$ (PDBid 4OO9 [365]) using Maestro v.9.3 (Schrodinger) software [443]	Mavoglurant	Mavoglurant: hydrogen bond interactions involving Ser805, Ser809, and Asn747 residues; hydrophobic interactions involving two pockets (one hydrophobic pocket formed by Gly624, Ile625, Gly628, Ser654, Pro655, Ser658, Tyr659, Val806, Ser809, Ala810, and Ala813 residues, and other hydrophobic pocket consisted of Ile651, Val740, Pro743, and Leu744 residues) [365].
37	Docking onto X-ray structure of $mGluR_5$ (PDBid 5CGC [366], 5CGD [366]) using PyMOL (Schrodinger) [444]	3-Chloro-4-fluoro-5-[6-(1*H*-pyrazol-1-yl) pyrimidin-4-yl]benzonitrile, HTL14242	3-Chloro-4-fluoro-5-[6-(1*H*-pyrazol-1-yl) pyrimidin-4-yl]benzonitrile: hydrogen bond interactions involving Ser809; water-mediated hydrogen bond interaction with Val 740; π-π interactions with Trp785 and Phe788 residues. HTL14242: hydrogen bond interactions involving Ser809; water-mediated hydrogen bond interaction with Val 740; π-π interactions with Tyr659, Trp785, and Phe788 residues. The pyrazole and pyridyl rings of 3-Chloro-4-fluoro-5-[6-(1*H*-pyrazol-1-yl) pyrimidin-4-yl]benzonitrile and HTL14242, respectively, are docked onto a pocket defined by Ile625, Gly628, Ser654, Pro655, Ser658, Tyr659 and Ser809. The pyrimidine linker of both ligands is located in a pocket formed between Pro655, Tyr659, Val806, and Ser809 residues [366].
37	Docking onto X-ray structure of $mGluR_5$ (PDBid 4OO9 [365]) using CDocker [445] in Discovery Studio 3.1 (Accelrys Inc., Cambridge, UK)	4-Bromo-*N*-(3-bromophenyl)thiazole-2-carboxamide, 4-bromo-*N*-(6-methylpyridin-2-yl)thiazole-2-carboxamide	4-Bromo-*N*-(3-bromophenyl)thiazole-2-carboxamide: hydrogen bond interactions involving Tyr659; hydrophobic interactions involving two pockets (one hydrophobic pocket formed by Gly624, Ile625, Gly628, Ser654, Pro655, Ser658, Tyr659, Val806, Ser809, Ala810, and Ala813 residues, and other hydrophobic pocket defined by Pro655, Tyr659, Val806, and Ser809 residues. 4-Bromo-*N*-(6-methylpyridin-2-yl)thiazole-2-carboxamide: hydrogen bond interactions involving Tyr659; hydrophobic interactions with Ile625, Pro655, Ala810, and Ala813 residues [446].
38	Docking onto X-ray structure of $mGluR_5$ (PDBid 4OO9 [365]) using CDocker software [445]	Aglaiduline, 5-*O*-Ethyl-hirsutanonol, Yakuchinone A	Aglaiduline: hydrophobic interactions involving two pockets (one hydrophobic pocket formed by Arg648, Ile651, Val740, and Pro743 residues, and other hydrophobic pocket defined by Ser654, Pro655, and Ala810 residues; hydrogen bond interactions involving Asn747. Yakuchinone A: hydrophobic interactions involving two pockets (one hydrophobic pocket formed by Arg648, Ile651, Val740, and Pro743 residues, and other hydrophobic pocket defined by Ser654, Pro655, and Ala810; hydrogen bond interactions involving Ser805. 5-*O*-Ethyl-hirsutanonol: hydrogen bond interactions involving Ser805 and Ser809 [447].
39	Docking onto $mGluR_5$ model using AutoDock 3.0.5 software [383] (Template: X-ray structures of $mGluR_1$, PDBid 1EWK [362], 1EWV [362], 1EWT [362])	S4-CPG, MCPG	Hydrogen bond interactions involving Tyr43, Ser152, and Thr154 residues [448].
40	Docking onto $mGluR_5$ model using ROSETTA v3.4 software [449] (Template: X-ray structures of β_2AR, $S1PR_1$, and D_3R (PDBid 2RH1 [263], 3V2Y [342], and 3PBL [282])	CHPyEPC, 1,4-BisPEB, MPEP, 1,3-BisPEB	All NAM ligands make interactions with Leu630, Ile651, Gly652, Pro655, Trp785, Phe788, Tyr792, Val806, and Ser809 residues. CHPyEPC, 1,4-BisPEB, and 1,3-BisPEB interact with Val740, Pro743, Leu744, and Asn747 residues [450].
5-Hydroxytryptamine receptor 1A ($5\text{-}HT_{1A}R$) agonists			
Entry	**Method(s)**	**Ligand(s)**	**Results/Conclusions**
41	Docking onto $5\text{-}HT_{1A}R$ model	N^1-Substituted *N*-arylpiperazines	N^1-Substituted *N*-arylpiperazines: salt bridge interactions involving Asp116; π-π interactions involving

	using Affinity module from INSIGHT II software [396] (Template: X-ray structures of RHO; PDBid 1F88 [231], 1HZX [314], and 1L9H [316])		Phe361 and Tyr390 residues; hydrogen bond interactions with Thr188. Some ligands are involved in π-π interactions with hydrophobic pocket formed by Phe204, Leu 359, and Phe362 [451].
42	Docking onto 5-HT_{1A}R model using Affinity module from INSIGHT II software [396] (Template: X-ray structures of RHO; PDBid 1F88 [231], 1HZX [314], and 1L9H [316])	1-Cinnamyl-4-(2-methoxyphenyl) piperazines	1-Cinnamyl-4-(2-methoxyphenyl)piperazines: salt bridge interactions involving Asp116; π-π interactions involving Phe361 and Tyr390 residues; hydrogen bond interactions with Thr188 [452].
43	Docking onto 5-HT_{1A}R model using Affinity from INSIGHT II software [396] (Template: X-ray structures of RHO; PDBid 1F88 [231], 1HZX [314], and 1L9H [316])	4-Halo-6-[2-(4-arylpiperazin-1-yl)ethyl]-1*H*-benzimidazoles	4-Halo-6-[2-(4-arylpiperazin-1-yl)ethyl]-1*H*-benzimidazoles: salt bridge interactions involving Asp116; hydrogen bond interactions involving Ser199 and Trp358; π-π interactions involving Phe361 and Tyr390 residues [453].
44	Docking onto 5-HT_{1A}R model using FlexX-Pharm from SYBYL 7.0 software [454] (Template: X-ray structure of bovine RHO; PDBid 1F88 [231])	Arylpiperazines	Arylpiperazines: salt bridge interactions involving the Asp residue; π-π interactions with the Phe residue; hydrogen bond interactions with Asn, Cys, Ser, Thr, and Tyr residues [455].
45	Docking onto 5-HT_{1A}R model using AutoDock 3.0.5 software [383] (Template: X-ray structure of RHO; PDBid 2R4R [262])	Benzo[*b*]thiophen-2-yl-3-(4-arylpiperazin-1-yl)-propan-1-one derivatives	1-(Benzo[*b*]thiophen-2-yl)-3-(4-pyridin-2-yl)-piperazin-1-yl)-1-propanone: salt bridge and hydrogen bond interactions involving Asp116; ion-dipole interactions with Asn385; π-π interactions involving Phe361 [456].
46	Docking onto 5-HT_{1A}R model using GOLD 4.0 software [431] (Template: X-ray structure of β_1-AR; PDBid 2Y03 [254])	Carboxamide and sulphonamide alkyl piperazine analogues	Carboxamide and sulphonamide alkyl piperazine analogues: salt bridge interactions involving Asp116; hydrogen bond interactions with Ser199 and Thr200; π-π interactions involving Tyr96, Phe361, Phe362, Trp387, and Tyr390 residues [457].
47	Docking onto 5-HT_{1A}R model using AutoDock 4.0 software [393] (Template: X-ray structure of β_2-AR; PDBid 3P0G [267])	3-[3-(4-Aryl-1-piperazinyl)-propyl]-1*H*-indole derivatives	3-[3-(4-Aryl-1-piperazinyl)-propyl]-1*H*-indole derivatives: salt bridge interactions involving Asp116; π-π interactions with Phe and Tyr residues; hydrogen bond interactions with the Ser residue [458].
5-Hydroxytryptamine receptor 2A (5-HT_{2A}R) antagonists			
Entry	**Method(s)**	**Ligand(s)**	**Results/Conclusions**
48	Docking onto 5-HT_{2A}R model using QXP software [459] (Template: X-ray structure of bovine RHO; PDBid 1F88 [231])	(Aminoalkyl)benzo and heterocycloalkanones	(Aminoalkyl)benzo and heterocycloalkanones: hydrogen bond interactions involving Cys148, Asp155, and Ser159; hydrophobic interactions with residues located in TM2 and TM7 [460].
49	Docking onto X-ray structure of 5-HT_{2A}R (PDBid 2VT4 [253]) using GLIDE module from Schrödinger	4-Aryl-2,7,7-trimethyl-5-oxo-*N*-phenyl-1,4,5,6,7,8-hexahydroquinoline-3-carboxamides	4-Aryl-2,7,7-trimethyl-5-oxo-*N*-phenyl-1,4,5,6,7,8-hexahydroquinoline-3-carboxamides: interaction with Cys199, Asn310, and Asn329 residues [461].

	suite [387-389]		
50	Docking onto 5-HT_{2A}R model using GOLD 4.12 software [431] (Template: X-ray structure of β_2-AR; PDBid 2RH1 [263])	Ketanserin, 05245768	Ketanserin: salt bridge interactions involving the Asp residue; hydrogen bond interactions involving the Ser residue; hydrophobic interactions with Phe and Tyr residues. 05245768: salt bridge interactions involving the Asp residue; hydrogen bond interactions involving the Ser residue; hydrophobic interactions with Ile, Phe, and Tyr residues [462].
51	Docking onto 5-HT_{2A}R model using FlexiDock from SYBYL-X 1.2 software (Tripos, St Louis, MO) [416] (Template: X-ray structure of β_2-AR; PDBid 2RH1 [263])	(2*R*,4*S*)-PAT, (2*S*,4*R*)-PAT, (2*R*,4*S*)-4'-Cl-PAT, (2*S*,4*R*)-4'-Cl-PAT	(2*S*,4*R*)-PAT: salt bridge interactions involving the Asp residue; π-π interactions involving the Phe residue. (2*R*,4*S*)-PAT and (2*S*,4*R*)-4'-Cl-PAT: salt bridge interactions involving the Asp residue (2*R*,4*S*)-4'-Cl-PAT salt bridge interactions involving the Asp residue; hydrogen bond interactions with the Ser residue [463].
52	Docking onto 5-HT_{2A}R model using GLIDE module from Schrödinger suite [387-389] (Template: X-ray structure of β_2-AR; PDBid 2RH1 [263])	Nefazodone, Aripiprazole, Haloperidol, Cyproheptadine, Trazodone, Clozapine, Ketanserin, Spiperone, Risperidone	Interaction with a binding pocket comprised by Ile152, Asp155, Val156, Ser207, Met208, Pro211, Leu229, Asp231, Val235, Leu236, Ser239, Phe339, Asn343, and Asn363 residues [464].
53	Docking onto 5-HT_{2A}R model using AutoDock Vina 1.1.1 [392] (Template: X-ray structure of β_2-AR; PDBid 3D4S [264])	Arylpiperazines	Arylpiperazines: salt bridge interactions involving Asp155; hydrogen bond interactions with Asn343; hydrophobic interactions involving two hydrophobic pockets (one hydrophobic pocket comprised by Leu123, Ser159, Trp336, Phe339, Val366, and Tyr370 residues, and the other pocket formed by Trp151, Ile152, Leu229, Ala230, Phe234, and Val235 residues [465].
54	Docking onto 5-HT_{2A}R model using ICM Pro docking algorithm [419], GLIDE from Schrödinger suite [387-389], and GOLD programs [431] (Template: X-ray structures of bovine RHO and β_2-AR; PDBid 1U19 [318] and 2RH1 [263])	Nantenine analogues	Nantenine analogues: salt bridge interactions involving Asp155; hydrogen bond interactions involving Asn343. The majority of nantenin analogus interacts with Asp155, Val156, Ser159, Ile210, Leu228, Phe234, Gly238, Ser242, and Ile341 residues. Other ligands interact with Ile152, Thr160, Ile163, Ile206, Ser239, Phe243, Ser244, Pro338, Phe339, Phe340, Thr342, Asn343, Met345, Val366, and Gly369 residues [466].
55	Docking onto 5-HT_{2A}R model using GLIDE module from Schrödinger suite [387-389] (Template: X-ray structure of human A_{2A}R; PDBid 2YDV [237])	Ketanserin, Risperidone, Ziprasidone	Ketanserin: salt bridge and hydrogen bond interactions involving Asp155; hydrogen bond interactions with Trp151; hydrophobic interactions with Phe125 and Val130; van der Waals interactions involving Leu126, Pro129, Leu154, Phe158, Val204, and Met208 residues. Risperidone: salt bridge and hydrogen bond interactions involving Asp155; hydrogen bond interactions with Trp151; van der Waals interactions involving Leu126, Val130, Ile152, Leu154, Phe158, and Met208 residues. Ziprasidone: hydrogen bond interactions involving Trp151; π-π interactions involving Phe158; hydrophobic interactions involving Leu122, Leu126, and Phe158 residues; van der Waals interactions involving Ile118, Phe193, Ile196, Ile197, and Trp200 residues [467].
56	Docking onto 5-HT_{2A}R model using GLIDE module from Schrödinger suite [387-389] (Template: X-ray structure of human A_{2A}R; PDBid 2YDV [237])	*N*-[3-(4-(1*H*-indol-2-yl)phenoxy)propyl]-4-chlorophenylamine	*N*-[3-(4-(1*H*-indol-2-yl)phenoxy)propyl]-4-chlorophenylamine: hydrogen bond interactions involving Leu362 and Asn363 residues; π-π interactions involving Phe339; hydrophobic interactions with Thr342 and Asn343; van der Waals interactions with Leu136, Ala230, Phe339, Asn343, Ala346, Val347, Glu355 and Val366 residues [467].
57	Docking onto 5-HT_{2A}R model using AutoDock 4.2 software [393]	(*R*)-Roemerine	(*R*)-Roemerine: salt bridge and hydrogen bond interactions involving Asp155; dipole-dipole interactions involving Ser159 and Tyr370, van der Waals interactions involving Ser239, Ala242, Trp336, Phe339,

	(Template: X-ray structure of β_2AR; PDBid 2RH1 [263])		Phe340, Val366, and Tyr370 residues [468].
5-Hydroxytryptamine receptor 2C (5-HT_{2C}R) antagonists			
Entry	**Method(s)**	**Ligand(s)**	**Results/Conclusions**
58	Docking onto 5-HT_{2C}R model using QXP software [459] (Template: X-ray structure of bovine RHO; PDBid 1F88 [231])	(Aminoalkyl)benzo and heterocycloalkanones	(Aminoalkyl)benzo and heterocycloalkanones: hydrogen bond interactions involving Cys148, Asp155, and Ser159; hydrophobic interactions with residues located in TM2 and TM7 [460].
59	Docking onto 5-HT_{2C}R model using FlexX software [430] (Template: X-ray structure of β_2-AR; PDBid 2RH1 [263])	*N*-(3-(4-methylimidazolidin-1-yl)phenyl)-5,6-dihydrobenzo[*h*]quinazolin-4-amine, *N*-(4-methoxy-3-(4-methylpiperazin-1-yl)phenyl)-1,2-dihydro-3*H*-benzo[*e*] indole-3-carboxamide, 1-(3,5-difluoro phenyl)-3-(4-methoxy-3-(2-(piperidin-1-yl)ethoxy)phenyl) imidazolidin-2-one, *N*-(3-(2-((3-(piperazin-1-yl)pyrazin-2-yl) oxy)ethoxy) benzyl)propan-2-amine	Hydrophobic interactions involving Val106, Val135, Phe137, Phe214, Val215, Val221, Ala222, Phe223, Trp324, Phe327, Phe328, Leu350, and Leu354 residues. *N*-(3-(4-methylimidazolidin-1-yl)phenyl)-5,6-dihydrobenzo[*h*]quinazolin-4-amine: hydrogen bond interactions with Asp134 and Arg195 residues. *N*-(4-methoxy-3-(4-methylpiperazin-1-yl)phenyl)-1,2-dihydro-3*H*-benzo[*e*]indole-3-carboxamide: hydrogen bond interactions involving Asp134 and Tyr358 residues. 1-(3,5-difluorophenyl)-3-(4-methoxy-3-(2-(piperidin-1-yl)ethoxy)phenyl) imidazolidin-2-one: hydrogen bond interactions involving Arg195 and Tyr358 residues. *N*-(3-(2-((3-(piperazin-1-yl)pyrazin-2-yl)oxy)ethoxy)benzyl)propan-2-amine: hydrogen bond interactions involving Arg195, Val208, Asn351, and Tyr358 residues [469].
60	Docking onto 5-HT_{2C}R model using FlexiDock from SYBYL-X 1.2 software (Tripos, St Louis, MO) [416] (Template: X-ray structure of β_2-AR; PDBid 2RH1 [263])	(2*R*,4*S*)-PAT, (2*S*,4*R*)-PAT, (2*R*,4*S*)-4'-Cl-PAT, (2*S*,4*R*)-4'-Cl-PAT	(2*S*,4*R*)-PAT: salt bridge interactions involving the Asp residue; π-π interactions involving the Phe residue. (2*R*,4*S*)-PAT and (2*S*,4*R*)-4'-Cl-PAT: salt bridge interactions involving the Asp residue (2*R*,4*S*)-4'-Cl-PAT salt bridge interactions involving the Asp residue; hydrogen bond interactions with the Ser residue [463].
61	Docking onto 5-HT_{2C}R model using GLIDE module from Schrödinger suite [387-389] (Template: X-ray structure of β_2-AR; PDBid 2RH1 [263])	(*E*)-3-(2-chlorophenyl)-1-(5-methoxy-6-(2-(piperidin-1-yl)ethoxy)indolin-1-yl)prop-2-en-1-one	(*E*)-3-(2-chlorophenyl)-1-(5-methoxy-6-(2-(piperidin-1-yl)ethoxy)indolin-1-yl)prop-2-en-1-one: salt bridge interactions involving Asn331, Ser334 and Val354 residues; hydrogen bond interactions involving Asn331; hydrophobic interactions involving Val135, Val208, Phe214, Ala222, Phe327, Phe328, and Val354 residues [470].

2.6.2. Application of ligand-based and pharmacophore-based design techniques for GPCR-based drug discovery

The availability of structural data information for multiple GPCRs still remains scarce and, for that reason, computational drug design strategies have relied on theoretical models, in which the 3D model of a receptor structure is constructed by applying homology modeling techniques [471], and on ligand-based approaches [472]. The identification of an increasing number of small-molecule modulators with diverse chemical scaffolds together with experimental biological/pharmacological data (e.g. binding affinity values) has helped to the increased development of ligand-based drug design approaches. Among these ligand-based approaches, numerous CADD methodologies can be employed to large databases of compounds with drug-like properties ranging from pharmacophore modeling to quantitative structure-activity relationships (QSAR) and 3D-QSAR techniques such as Comparative Molecular Field Analysis (CoMFA) and Comparative Molecular Similarity Index Analysis (CoMSIA) [472].

The generation of pharmacophore models involves the identification of steric and electronic determining features that assure an optimal interaction towards a particular therapeutic target, triggering its pharmacological activity (reviewed in [473]). Thus, pharmacophore modeling is a computational tool that searches for common pharmacophoric patterns or chemical features (hydrogen bond acceptors and donors, hydrophobic groups, aromatic rings, etc.) shared by a set of active ligands with similar pharmacological activity and which may interact to the same binding sites. A pharmacophore model can be generated either in the absence of structural data information (ligand-based pharmacophore modeling) or based on the 3D structure of a therapeutic target (structure-based pharmacophore modeling) (reviewed in [473]). The development of structure-based pharmacophore models involves the examination of the pharmacophoric patterns in the binding site of the target and their spatial relationships. On the other hand, the ligand-based pharmacophore modeling implies the generation of a conformational space for each ligand of the training set to represent their conformational flexibility. A myriad of software tools and algorithms used for construction of a conformational space possess the ability to determine the different conformational geometries of the bioactive conformation and other similar geometries. An appropriate computational software for conformational search needs to generate all conformational geometries that the ligands can adopt when they are interacting with the therapeutic target. Subsequently, the multiple ligands of the training set are superimposed and the common 3D structural features

crucial for biological/pharmacological activity are uncovered (reviewed in [473]). Once a pharmacophore model is constructed, it can be used for *in silico* screening of large databases of virtual and *in-house* drug candidates, in which a pharmacophore hypothesis is considered as a template for the discovery of hit ligands with similar pharmacophoric characteristics. In addition, the pharmacophore modeling can be applied to the generation of new chemical scaffolds and/or structures (*de novo* drug design), which includes the chemical features of a given pharmacophore hypothesis [474].

On the other hand, the investigation of QSAR has been a remarkably useful technique in early stages of the drug discovery process. The fundamental basis of this ligand-based methodology is that variations in the biological/pharmacological activity for congeneric and non-congeneric series of chemical compounds (training set) that target a common mechanism of action are correlated with variations in their physicochemical and structural properties [475-477]. Since these structural features of the chemical ligands can be efficiently uncovered by experimental or computational approaches, a statiscally validated QSAR model is able to predict the biological/pharmacological activity of new chemical ligands, avoiding the time- and money-consuming chemical synthesis and biological evaluation of potentially uninteresting ligands. The generation of a QSAR model involves the collection of a statistical population of ligands and the determination of descriptor variables that can suitably explain the correlation of structural properties of ligands and their biological activity data (e.g. topological descriptors, electronic descriptors, geometrical descriptors, constitutional descriptors, etc.). Subsequently, various statistical methods within supervised machine learning (ML) techniques, including Partial Least Square (PLS) [478], Multiple (or multivariate) Linear Regression (MLR) [479], and Linear Discriminant Analysis (LDA) [480], and non-linear modeling, including Artificial Neural Networks (ANN) [481] and Support Vector Machines (SVM) [482] are applied to derive a robust mathematical correlation that explains the dependence of particular descriptor variables (independent variables) to the biological/pharmacological activity of a set of ligands (dependent variables). The resulting QSAR model is subjected to several validation tests to corroborate the reliability of the correlation models, in particular to internal validation or cross-validation and to external validation. The internal validation or cross-validation consists in the elimination one (Leave-One-Out cross-validation, LOO) or more (Leave Some-Out cross-validation, LSO; Leave-Many-Out cross-validation, LMO) ligands of the training set. The reconstruction of QSAR models is based on the remaining ligands of the training set using the combination of descriptor variables previously selected, and the pharmacological activity of the eliminated ligand(s) is predicted from the rebuilt QSAR model. Afterwards, the same methodology is

repeated until all or a definite portion the ligands have been removed once. The external validation consists in the prediction of biological/pharmacological activity using a group of ligands that are not included in the training set (test set) and the same descriptor variables are employed in the generation of the QSAR model [483].

The 3D QSAR CoMFA and CoMSIA methodologies have emerged as fundamental tools for design and molecular optimization of drug candidates targeting GPCRs. The CoMFA methodology provides information of whether differences in steric (Lennard-Jones potential functions) and electrostatic components (Coulomb potential functions) for field calculation of a training set of molecules in a given alignment can be correlated with differences in biological/pharmacological activity [484-486]. A comparable 3D QSAR-based methodology, CoMSIA, was developed based on arbitrary descriptors named similarity indices. In opposition to CoMFA, CoMSIA applies a smoother potential based on Gaussian functions, allowing the calculation of various similarity indices, such as steric, electrostatic, hydrophobic, hydrogen bond acceptor, and hydrogen bond donor parameters, that covers more extensively than the steric and electrostatic fields calculated by CoMFA, the most significant contributing factors for the binding free energy of ligands towards a putative target [487]. In both methodologies, the 3D alignment of the chemical structures of ligands is required, and should reveal the maximum superimposition of steric, electrostatic, hydrophobic, hydrogen bond acceptor, and hydrogen bond donor parameters that a database of ligands adopt when interacting with a specific therapeutic target. Each ligand on the training set is aligned to a template which exhibits a common molecular substructure and the aligned ligands are placed inside virtual 3D grid boxes. Subsequently, the interaction energies are calculated between the ligands and molecular fragments (molecular probes) at each grid point. Applying an appropriate statistical method for regression analysis, usually by PLS, the 3D-QSAR model is constructed to describe the variation of biological/pharmacological activity with the variation of CoMFA/CoMSIA interaction fields and the predictive ability of 3D-QSAR model is corroborated by cross-validation and prediction of activity of test set. The generated CoMFA/CoMSIA is typically represented as color-coded contoured 3D maps, which displays specific volumes of space where the magnitudes of steric, electrostatic, hydrophobic, hydrogen bond acceptor, and hydrogen bond donor parameters are positively or negatively correlated with the pharmacological activity [484-487]. This type of graphical representation can be presumed as a model of the binding site in which a training set of ligands is supposed to interact. Table 3 emphasizes the distinct ligand- and pharmacophore-based design approaches applied for the aforementioned GPCR-derived therapeutic targets potentially involved in PD.

Table 3. Ligand- and pharmacophore-based drug design methodologies reported for ligands targeting GPCRs potentially involved in PD

Dopamine D_2 receptor (D_2R) agonists			
Entry	**Method(s)**	**Ligand(s)**	**Results/Conclusions**
1	CoMFA using SYBYL 6.8 QSAR module [416]	Aminoindans, aminotetralins, dopamine analogs, ergolines, apomorphines, phenylpiperidines, benzo[*f*]quinolines	CoMFA maps showed that bulky substituents with low electronegativity on the fused piperidine ring nitrogen and small substituents with low electronegativity on the aromatic ring are favorable features for agonist activity [488].
2	CoMFA and CoMSIA using SYBYL 8.0 [416] and MOE v. 2011.10 [489] programs	(*S*)-6-((2-(4-phenylpiperazin-1-yl)-ethyl)(propyl)amino)-5,6,7,8-tetrahydronaphthalen-1-ol analogs	The key features for ligand activity are divided into two groups: near the aminotetralin head group and at/near the phenyl ring bound to piperazine moiety. Near the aminotetralin head group, the presence of bulky groups on 5-methoxy group of aminotetralin moiety is beneficial for activity; the introduction of bulky groups near the *N*-propyl group of aminotetraline moiety is expected to decrease the activity; the presence of electronegative substituents at 7-position of aminotetralin group and hydrophilic groups near the *N*-propyl group is predicted to enhance activity; a beneficial effect for activity is also expected upon the introduction of hydrogen bond donor groups near the 5- and 7-positions and near the *N*-propyl group of aminotetralin moiety. The presence of bulky substituents at 6-, 7-, and 8-positions of quinoline ring, electropositive groups on 3-position, and hydrophilic substituents on quinoline ring is favorable for activity. The introduction of hydrophilic substituents around the piperazine ring and hydrogen bond donor groups on the nitrogen atom of piperazine ring enhances the binding affinity [490].
3	Pharmacophore modeling using Discovery Studio software [398]	Arylpiperazines	Pharmacophore model including key features for ligand activity: (i) salt bridge formation between the basic nitrogen atom of piperazine ring and the receptor; (ii) one or more aromatic interactions involving arylpiperazine substructure; (iii) hydrogen bond interaction between the oxygen atom of methoxy group and the receptor; (iv) possibility of hydrogen bond interaction involving the linker part [399].
4	Pharmacophore modeling using MOE v. 2005.06 [491]	Aminotetralins, apomorphins, quinolines	Pharmacophore model including key features for ligand activity: (i) one excluded volume covering the projected feature Asp; (ii) one positively charged nitrogen atom interacting with Ser; (iii) one hydrogen bond donor feature interacting with Asp; (iv) one aromatic ring feature [492].
Dopamine D_3 receptor (D_3R) agonists			
Entry	**Method(s)**	**Ligand(s)**	**Results/Conclusions**
5	HQSAR and CoMFA using SYBYL 6.6 program [416]	Piperazinylalkylisoxazole analogues	The best HQSAR model was constructed using Atom, Bond, Connectivity, Donor and Acceptor (A/B/C/DA) as fragment type, 257 as hologram length, and 4–7 as fragment size. CoMFA models showed that the electrostatic parameters are the most contributing factor for D_3R agonist affinity of these ligands [493].
6	CoMFA using SYBYL-X 1.3 program [416]	Library of 34 structurally diverse D_3R agonists	Two representative molecules were used to analyze the key features for D_3R binding affinity.

			N-((1*S*,4*r*)-4-(2-(((*S*)-2-amino-4,5,6,7-tetrahydrobenzo[*d*]thiazol-6-yl)(propyl) amino)ethyl)cyclohexyl)-3-(5-methyl-1,2,4-oxadiazol-3-yl)benzamide: (i) the presence of bulky groups near the 2- and 3-position in pyridine ring enhances the binding affinity and near the 4-position of pyridine ring is expected to reduce the activity; (ii) the presence of electropositive groups near the 2-position and electronegative groups near the 4- and 5-position in pyridine ring may enhance activity. *N*-((1*S*,4*r*)-4-(2-(((*S*)-2-amino-4,5,6,7-tetrahydrobenzo[*d*]thiazol-6-yl)(propyl) amino)ethyl)cyclohexyl)-2-chloropyridine-3-sulfonamide: (i) the introduction of bulky and electronegative substituents near the 5-position of the benzene ring is expected to increase agonist activity; (ii) the introduction of electropositive groups near methyl position of 1,2,4-oxadiazole ring is favorable for activity [406].
7	CoMFA and CoMSIA using SYBYL 7.2 program [416]	Library of 41 structurally diverse D_3R agonists	The hydrophobic interactions are the most important contributing factor for D_3R agonist activity. Hydrogen bonding also contributes largely to the binding affinity and may confer receptor subtype selectivity [494].
8	CoMFA and CoMSIA using SYBYL 8.0 [416] and MOE v. 2011.10 [489] programs	(*S*)-6-((2-(4-phenylpiperazin-1-yl)-ethyl)(propyl)amino)-5,6,7,8-tetrahydronaphthalen-1-ol analogs	The key features for ligand activity are divided into two groups: near the aminotetralin head group and at/near the phenyl ring bound to piperazine moiety. Regarding the aminotetralin head group, the introduction of bulky substituents around 7- and 8-positions, hydrophobic and hydrophilic substituents on phenyl and cyclohexyl rings of aminoteralin moiety, respectively, is favorable for activity. The presence of bulky groups near the *N*-propyl group of aminotetraline moiety is expected to reduce the binding affinity to D_3R. The introduction of both hydrogen bond donor and acceptor substituents near piperazine ring is predicted to be favorable for agonist activity [490].
9	Pharmacophore modeling using Chem-X software	(*R*)-(+)-PD-128907, (*R*)-(+)-7-OH-DPAT, BP-897, (*S*)-(-)-3-PPP, Pramipexole, (+)-UH-232, (*S*)-(-)-DS-121, Quinelorane, (-)-Quinpirole, Ropinirole	Pharmacophore model including common key features for these ligands: (i) one aromatic ring and one sp^3 nitrogen bound to a propyl group and to two additional sp^3 carbons; (ii) the distance between the aromatic ring center and the basic sp^3 nitrogen within these compounds was found to be on approximately 5.16 ± 0.16 Å [401].
Adenosine A_{2A} receptor (A_{2A}AR) antagonists			
Entry	**Method(s)**	**Ligand(s)**	**Results/Conclusions**
10	HQSAR using SYBYL 7.2 program [416]	2-(Furan-2-yl)-[1,2,4]triazolo[1,5-*f*]pyrimidin-5-amines, 2-(furan-2-yl)-[1,2,4]triazolo[1,5-*a*]pyrazin-8-amines, 2-(furan-2-yl)-[1,2,4]triazolo[1,5-*a*][1,3,5]triazin-7-amines	The best HQSAR model includes the combination of fragment parameters A/B/C/DA, with a size fragment of 7-10 and a hologram length of 199. The structure features that contribute positively for the activity are: (i) for 2-(furan-2-yl)-[1,2,4]triazolo[1,5-*f*]pyrimidin-5-amines, the presence of a substituent at C3 of phenyl ring; (ii) for 2-(furan-2-yl)-[1,2,4]triazolo[1,5-*a*]pyrazin-8-amines, a short length of carbon chain between the piperazine moiety and the methylated nitrogen atom [428].
11	CoMFA using SYBYL 6.3 program [416]	Flavonoids	The key features for high affinity to A_{2A}AR are: (i) the presence of bulky substituents at C2, C7, and C8 of chromone ring; (ii) the absence of high electron density groups at *para* position of phenyl ring [495].
12	CoMFA using SYBYL-X 1.1.1	Substituted thieno[2,3-*d*]pyrimidines	The key features for A_{2A}AR antagonistic activity are: (i) the presence of bulky

	program [416]		substituents in the thiophen ring and small substituents in the pyrimidine ring; (ii) electropositive substituents between positions 1 and 2 and at position 4 of benzene ring located at pyrimidine ring; (iii) electronegative substituents at position 2 of the benzene ring located at the pyrimidine ring [411].
13	CoMFA and CoMSIA using DRAGON software [496]	Pyrimidine and triazine derivatives, pyrazolo[3,4-*d*]pyrimidines, pyrrolo[2,3-*d*]pyrimidines, triazolo[4,5-*d*]pyrimidines, 6-arylpurines, thieno[3,2-*d*]pyrimidines	For pyrimidine and triazine derivatives, the key features for A_{2A}AR antagonistic activity are: (i) the presence of a limitedly bulky, electronegative, and hydrophobic group at C6; (ii) the presence of a small, electronegative, and hydrophilic group at C2; (iii) a limitedly bulky, electronegative, and hydrophilic group (non hydrogen bond donor group) at C4. For pyrazolo[3,4-*d*]pyrimidines, pyrrolo[2,3-*d*]pyrimidines, triazolo[4,5-*d*]pyrimidines, and 6-arylpurines, the key features for A_{2A}AR antagonistic activity are: (i) the presence of a small, and electronegative group (hydrogen bond acceptor group) at C6; (ii) a hydrogen bond donor group at C2; (iii) a hydrogem bond acceptor group at N3. For thieno[3,2-*d*]pyrimidines, the key features for A_{2A}AR antagonistic activity are: (i) the presence of a limitedly bulky, electronegative, and hydrophilic group (hydrogen bond donor group) at C6, a small and electronegative group (hydrogen bond donor group) [427].
14	Pharmacophore modeling and GFA-based QSAR using Cerius^2 [400] and LigandScout programs [497]	4-Arylthieno[3,2-*d*]-pyrimidines	Molecular connectivity índex (SC-2), molecular surface area (AREA), graph-theoretical (WIENER), and molecular flexibility (PHI-MAG) descriptors influenced the activity of ligands against A_{2A}AR. Pharmacophore model including key features for ligand activity: (i) the presence of one hydrogen bond donor feature (amino group interacts with Asn253), two hydrophobic features (one group interacts with Leu85, Phe168, Met177, Trp246, and Leu249 residues; other group interacts wiith Leu269 and Met270 residues) [98].
15	Pharmacophore modeling and QSAR using PHASE 3.2 module of Schrodinger suite [498]	Library of 46 A_{2A}AR antagonists	Pharmacophore model including key features for ligand activity: (i) one hydrogen bond acceptor feature; (ii) one hydrogen bond donor feature; (iii) one hydrophobic feature; (iv) two aromatic ring features [412].
16	Pharmacophore modeling using CATALYST 4.11 software package [499]	Xanthine derivatives (KW6002, KF17837, BS-DMPX) Non-xanthine derivatives (7-Substituted 5-amino-2-(2-furyl)pyrazolo[4,3-*e*]-1,2,4-triazolo[1,5-*c*]pyrimidines and piperazine derivatives of [1,2,4]triazolo[1,5-*a*]triazine)	Pharmacophore models for xanthine and non-xanthine derivatives including key features for ligand activity: (i) two hydrophobic features; (ii) one hydrogen bond acceptor feature; (iii) one aromatic ring feature [427].
17	Pharmacophore modeling using PHASE 2.0 module of Schrodinger suite [498]	Library of 68 A_{2A}AR antagonists	Pharmacophore model 1 including key features for ligand activity: (i) two hydrogen bond acceptor features; (ii) two aromatic ring features; (iii) one hydrogen bond donor feature. Pharmacophore model 2 including key features for ligand activity: (i) two hydrogen bond acceptor features; (ii) one hydrogen bond donor feature; (iii) one aromatic ring; (iv) one hydrophobic feature [500].
18	Pharmacophore modeling using CATALYST 4.10 software package [499]	7-Substituted 5-amino-2-(2-furyl)pyrazolo[4,3-*e*]-1,2,4-triazolo[1,5-*c*]pyrimidines	Pharmacophore model including key features for ligand activity: (i) one ring aromatic feature; (ii) one positively ionizable feature; (iii) one hydrogen bond acceptor lipid feature, and one hydrophobic feature [501].
19	Pharmacophore modeling using CATALYST 4.11 program [499]	1,2,4-Triazole derivatives, pyrazolotriazolopyrimidines, trifluoropyrimidines, 9-ethyladenine derivatives,	Pharmacophore model including key features for ligand activity: (i) one hydrogen bond donor feature; (ii) three hydrophobic features; (iii) one aromatic ring feature

		thioacyhydrazones	[502].
20	Pharmacophore modeling using PHASE module of Schrodinger suite [498]	Library of 751 $A_{2A}AR$ antagonists	Pharmacophore model including key features for ligand activity: (i) one hydrogen bond acceptor feature; (ii) one hydrogen bond donor feature, and two aromatic ring features [503].
21	Pharmacophore modeling using FLAPPharm program [504]	Istradefyline, MSX-2, SYN-115, BIIB014, SCH-442416, ZM-241385, ST-1535, Preladenant	Pharmacophore model including key features for ligand activity: (i) three hydrogen bond acceptor features; (ii) one hydrogen bond donor feature; (iii) hydrophobic features. The proposed pharmacophore is predicted to interact Glu169 and Asn253 [505].
22	Pharmacophore modeling using CATALYST 4.11 program [499]	7-Substituted 5-amino-2-(2-furyl)pyrazolo[4,3-*e*]-1,2,4-triazolo[1,5-*c*]pyrimidines, piperazine derivatives of triazolotriazine and triazolopyrimidines	Pharmacophore model including key features for ligand activity: (i) two hydrophobic features, and one aromatic ring hydrophobic feature for 7-substituted 5-amino-2-(2-furyl)pyrazolo[4,3-*e*]-1,2,4-triazolo[1,5-*c*]pyrimidines; (ii) one hydrogen bond acceptor feature, two hydrophobic features, and one aromatic ring hydrophobic feature for piperazine derivatives of triazolotriazine and triazolopyrimidines [414].
M_1 muscarinic acetylcholine receptor ($mAChR_1$) antagonists / negative allosteric modulators (NAMs)			
Entry	**Method(s)**	**Ligand(s)**	**Results/Conclusions**
23	Pharmacophore modeling and 3D-QSAR using CATALYST 4.10 program [499]	α-Substituted 2,2-diphenylpropionates	The stereoelectronic properties including total energies, bond distances, valence angles, torsion angles, HOMO–LUMO energies, reactivity indices, vibrational frequencies of ether and carbonyl moieties, and nitrogen atom proton influnces the binding affinity of these ligands. Pharmacophore model including key features for ligand activity: (i) one aromatic ring feature; (ii) one hydrogen bond donor; (iii) basic nitrogen species at a distance of ~4Å from the hydrogen bond acceptor [506].
24	Pharmacophore modeling using PHASE module of Schrodinger suite [498]	Trihexylphenidyl, atropine, darifenacin, 4-DAMP, propantheline, pirenzepine	Pharmacophore model including the common molecular features: (i) molecular weight: 289.37–426.55; (ii) polar surface area: 23.47–68.78 $Å^2$; (iii) hydrogen bond acceptors: 1–3; (iv) hydrogen bond donors: 0–1; (v) rotatable bonds: 2–7; (vi) AlogP: 1.68–4.53 [507].
25	Pharmacophore modeling using CATALYST 4.10 program [499]	Caramiphen, indocaramiphen, nitrocaramiphen, atropine, dicyclomine, methoctramine, oxubutynin	Pharmacophore model including key features for ligand activity: (i) two hydrogen bond acceptor features; (ii) one aliphatic hydrophobic feature; (iii) one aromatic ring feature [508].
Metabotropic Glutamate Receptor 4 ($MGluR_4$) agonists / positive allosteric modulators (PAMs)			
Entry	**Method(s)**	**Ligand(s)**	**Results/Conclusions**
26	Pharmacophore modeling using APEX-3D software (MSI) [509]	(*S*)-Glu, (*S*)-Asp, (*S*)-AP4, (*S*)-SOP, (2*S*)-4CH_2Glu, (*S*)-Gla, (2*S*)-CCG-I, (2*SR*,3*RS*)-CPrAP4, (2*SR*,3*SR*)-CPrAP4, (1*S*,3*S*)-ACPD, (2*SR*,4*SR*)-CpeAP4, (2*SR*,4*RS*)-CpeAP4, ACPT-I, (+)-ACPT-III	Pharmacophore model including key features for ligand activity: (i) the presence of two hydrogen bond donor groups; (ii) the presence of three hydrogen bond acceptor groups. Additional regions are predicted to interact with $mGluR_4$, including the oxygen atom of phosphonic and phosphoric groups of (*S*)-Glu analogues, the carboxylic groups of (*S*)-Glu, ACPT-I, and (+)-ACPT-III, and the presence of cycloalkyl rings of CPrAP4, CpeAP4, ACPT-I, and (+)-ACPT-III [509].
Metabotropic Glutamate Receptor 5 ($MGluR_5$) antagonists / negative allosteric modulators (NAMs)			
Entry	**Method(s)**	**Ligand(s)**	**Results/Conclusions**
27	Pharmacophore modeling using Accelrys Discovery Studio 4.0	Pyridyl and phenyl substituted oxadiazoles, 5-aryl-3-acylpyridinyl-pyrazoles, 1-aryl-4-acylpyridinyl-	Pharmacophore model including common key features: (i) one hydrogen bond acceptor feature; (ii) one hydrophobic feature; (iii) two hydrophobic aromatic

	(DS) software [510]	imidazoles, aryl azetidinyl oxadiazoles, *N*-aryl pyrrolidinonyl oxadiazoles	features, (iv) two excluded volumes [447].
5-Hydroxytryptamine receptor 1A (5-HT_{1A}R) agonists			
Entry	**Method(s)**	**Ligand(s)**	**Results/Conclusions**
28	QSAR using 2D molecular descriptors by MOE v. 2004.0314 program [511]	2-[ω-(4-Arylpiperazin-1-yl)alkyl]perhydropyrrolo-[1,2-*c*]imidazoles, 2-[ω-(4-arylpiperazin-1-yl)alkyl]perhydroimidazo[1,5-*a*]pyridines	Steric parameters contribute most significantly for the 5-HT_{1A}R agonist activity. The number of rotatable bonds, partial charge descriptors, subdivided surface area descriptors, and an indicator variable for carbonyl oxygens also influence the 5-HT_{1A}R agonist activity of the ligands [512].
29	CoMFA using SYBYL 5.5 program [416]	Arylpiperazines, (aryloxy)propanolamines, tetrahydropyridylindoles	Arylpiperazines: the introduction of steric groups is favorable close to the aromatic ring and unfavorable near the basic nitrogen atom. The presence of electronegative substituents near the *ortho* position of the aromatic ring is beneficial for activity. (Aryloxy)propanolamines: the introduction of bulky and electronegative substituents close to the *ortho* and *meta* positions of the aromatic ring is beneficial for the activity. The presence of bulky and electropositive groups near the *para* position of the aromatic ring is favorable as well as the introduction of electropositive substituents near the basic nitrogen atom. Tetrahydropyridylindoles: the steric parameters contribute most significantly to the activity. The introduction of bulky and hydrogen bond donor groups at 5-position of índole ring is predicted to be beneficial for the activity [513].
30	CoMFA using SYBYL 5.5 program [416]	3-(1,2,5,6-Tetrahydropyridin-4-yl)índole derivatives	The steric parameters contribute most significantly to the 5-HT_{1A}R agonist activity. The presence of bulky substituents in the plane of índole 5-position is beneficial for 5-HT_{1A}R activity, whereas bulky substituents located out of plane is expected to decrease the activity. There is also a preference for coplanarity between indole and tetrahydropyridine rings. Using as reference a 5-$CONH_2$ analog, the presence of oxygen and hydrogen atoms of carboxamide moiety contributes positively for 5-HT_{1A}R activity [514].
31	CoMFA using SYBYL 6.0 program [416]	Bicyclohydantoin-phenylpiperazines	The electrostatic parameters contribute most significantly to the 5-HT_{1A}R agonist activity. The key features for agonist activity are: (i) the introduction of bulky substituents at *ortho* and *meta* positions of the phenyl ring; (ii) the introduction of electron-withdrawing substituents at *ortho* and *meta* positions of the phenyl ring. The presence of bulky and electron-withdrawing substituents is expected to have a negative effect on activity [515].
32	Pharmacophore modeling and CoMFA using DISCO [516] and SYBYL programs [416]	Pyridazinothiazepines, pyridazinooxazepines	Pharmacophore model including common key features for ligand activity: (i) two hydrophobic ring features (phenyl and 3(2*H*)-pyridazinone rings); (ii) four hydrogen bond donor features (*N* atom of protonated amine, N^1 atom and the two lone pairs of *O* atom of carbonyl group of 3(2*H*)-pyridazinone ring); (iii) two hydrogen bond acceptor features (*O* atom of carbonyl group and N^1 atom of 3(2*H*)-pyridazinone ring; (iv) *O* atom of carbonyl group interacting to the *N* atom of oxazepine or thiazepine rings), using as reference the ligand GYKI16527 [517].
33	Pharmacophore modeling and CoMFA using GALAHAD	Arylpiperazines	Pharmacophore model including common key features for ligand activity: (i) one hydrogen bond acceptor feature; (ii) one positively charged group; (iii) one aromatic

	program [518-520]		ring feature; (iv) one hydrophobic feature. The steric parameters contribute most significantly to the 5-HT_{1A}R agonist activity. The introduction of bulky substituents, as benzothiophene, and electropositive substituents attached to benzothiophene ring may enhance activity. Moreover, the presence of electronegative substituents surrounding the dihydrobenzodioxepin ring may have a positive effect on activity [521].
34	Pharmacophore modeling using CATALYST 4.6 program [499]	(2-Alkoxy)phenylpiperazine derivatives of 1-(2-hydroxy-3-(4-arylpiperazin-1-yl)propyl)-5,5-diphenylimidazolidine-2,4-dione with alkyl or ester substituents at N^3 of hydantoin ring	Pharmacophore model including common key features for ligand activity: (i) one hydrogen bond acceptor; (ii) one positively charged group; (iii) one aromatic ring feature; (iv) one hydrophobic feature. The interfeature distance ranges between hydrogen bond acceptor and hydrophobic features is [5.53-5.62 Å], between hydrogen bond acceptor and positively charged group is [5.13-6.00 Å], between hydrogen bond acceptor and aromatic ring is [10.08-11.68 Å], between hydrophobic feature and positively charged group is [7.60-8.08 Å], between hydrophobic and aromatic ring features is [12.24-13.91 Å], and between positively charged group and aromatic ring feature is [5.68-5.69 Å] [522,523].
35	Pharmacophore modeling using Accelrys Discovery Studio versions 3.5 (DS) software [524]	(*R*)-8-OH-DPAT, Quetiapine, Olanzepine, Ziprasidone, 5-Methyl Urapidil, BMY14802, JB788, S14671, F15599, F13714, 1,3-dioxolane derivatives, pyridyl-fused 3-amino chroman derivatives, 1-(*meta*-trifluoromethylphenyl) piperazines	Pharmacophore modeling including common key features for ligand activity: (i) one positively ionizable group; (ii) one hydrogen bond acceptor feature; (iii) three hydrophobic features; (iv) seven excluded volumes [525].
36	Pharmacophore modeling using GRID 22 program [526]	8-OH-DPAT, Buspirone, Vilazodone, Aripiprazole, F-13640	Pharmacophore modeling including common key features for ligand activity: two hydrophobic features surrounded by TM5/TM6 and by TM2/TM7/ECL2, one positive ionizable feature interacting with Asp, one hydrogen bond acceptor feature interacting with Tyr, and three excluded volumes [162].
5-Hydroxytryptamine receptor 2A (5-HT_{2A}R) antagonists			
Entry	**Method(s)**	**Ligand(s)**	**Results/Conclusions**
37	QSAR performed by GRID 22 [526] and GOLPE 4.6.0 programs [527] and using GRID/GOLPE descriptors	Butyrophenones	The interaction of hydrophobic groups in two areas, one at the bottom of the pocket near Leu163 and the other in the center near the side chains of Val and Phe residues, is expected to increase the binding affinity. The interaction of these ligands near of oxygen atom of Asp residue, indolic nitrogen of Trp residue, at the bottom near the Ser residue, to the side chain of Asn residue, and close to other Ser and Trp residues is favorable for antagonistic activity [528].
38	QSAR performed by MDL QSAR software package, version 2.2 (Symyx) using electronic and molecular parameters [529]	1-Benzhydryl-piperazines and 1-arylpiperazines with xanthine moiety at N^4	The binding affinity of these ligands to 5-HT_{2A}R correlates positively with the lipophilicity of ligands, the largest negative charge associated to O^6 atom of xanthine moiety, and with the partial atomic charge of N^4 atom of piperazine moiety [529].
39	QSAR by DRAGON software (version 1.11-2001) [496] and using DRAGON descriptors	2-Alkyl-4-aryl-pyrimidine fused heterocycles	A lower number of rotatable bonds, a more hydrophobic nature of the ligands, and lower polar surface area are expected to be favorable for binding affinity [530].
40	CoMFA using SYBYL 5.5 program [416]	3-(1,2,5,6-Tetrahydropyridin-4-yl)índole derivatives	The introduction of bulky substituents around the 5-position of indole ring is unfavorable for activity, whereas the presence of bulky groups at the N^1 position of

			pyridine ring and at the N^1 position of the indole ring is expected to be beneficial for activity. The introduction of electronegative substituents around the 5-position of the indole ring and of electropositive substituents above 5- and 6-carbons of the indole ring may increase the activity [514].
41	CoMFA using SYBYL 7.0 program [416]	Hexahydro- and octahydropyrido[1,2-*c*]pyrimidine derivatives	The introduction of bulky substituents in the proximity to *para* position in the benzene ring attached to the piperazine ring and the absence of substituents at *ortho* position may enhance activity. The presence of bulky groups placed in the proximity of piperazine ring and at C-4 position of the imide moiety is also beneficial for activity. The introduction of electronegative substituents in imide and piperazine moieties may increase the affinity [531].
42	CoMSIA using SYBYL 7.2 program [416]	Tetrahydrofuran derivatives, benzamides, 3-aminoethyl-1-tetralones, piperazines, benzothiazepines, pyrrolobenzazepines, clozapine, flupentixol, haloperidol, loxapine, mesoridazine, olanzapine, quetiapine, risperidone, sertindole, thiothixene, thioridazine, campazine, ziprazidone	The electrostatic, hydrophobic, and hydrogen bond donor parameters contribute most significantly to the binding affinity towards 5-HT_{2A}, comparing to steric and hydrogen bond acceptor parameters [532].
43	Pharmacophore modeling using MOE v. 2007.09 program [533]	Ketanserin, Risperidone, Ritanserin, Spiperone, Clozapine, Sertindole, Setoperone, Chlorpromazine, Cyproheptadine, Tefludazine, 5*H*-Thiazolo[3,2-*a*] pyrimidin-5-one derivatives	Pharmacophore model including common key features for 5-HT_{2A} antagonist activity: (i) two hydrogen bond acceptor features; (ii) one aromatic ring or hydrophobic feature with two parallel features for π orbital accommodation; (iii) one aromatic ring feature with one hydrogen bond donor group; (iv) one hydrophobic feature [534].
44	Pharmacophore modeling using MOE v. 2008.10 program [535]	Thiophene derivatives	Pharmacophore model including the common key features for ligand activity: (i) one aromatic ring feature; (ii) one positively ionizable group containing a nitrogen atom; (iii) one hydrogen bond acceptor feature; (iv) one hydrophobic or aromatic feature attached to the positively ionizable group. The interfeature distance ranges between the postively ionizable group and the hydrogen acceptor group is [6.6-10.3 Å], between aromatic ring feature and the hydrogen bond acceptor feature is [3.1-3.8 Å], between aromatic ring feature and the positively ionizable group is [7.4-8.8 Å], and the angle between the positively ionizable group and the plane of aromatic ring feature is [141.0-152.9 Å]^o [536].
45	Pharmacophore modeling using MOE v. 2008.10 program [535]	4-Nitroindole derivatives	Pharmacophore model including the common key features for ligand activity: (i) two aromatic ring features; (ii) one positively ionizable group; (iii) one hydrophobic feature [537].
46	Pharmacophore modeling using GRID 22 software [526]	Ketanserin	Pharmacophore model including the key features for ligand activity: (i) one positively ionizable amino group; (ii) two hydrophobic features; (iii) one hydrophobic feature [462].
5-Hydroxytryptamine receptor 2C (5-HT_{2C}R) antagonists			
Entry	**Method(s)**	**Ligand(s)**	**Results/Conclusions**
47	QSAR by DRAGON software (v.1.11-2001) [496] and using	Isoindolones	The binding affinity of these ligands are correlated to several atomic descriptors, in particular the eigenvalue n.2 and the eigenvalue n.5 of the Burden matrix, atomic

	Dragon descriptors		van der Waals volume to path length 2 and 8 of the Moran autocorrelations and path length 2 of Geary autocorrelation, polarizability to the highest eigenvalue n.1 and n.6 of the Burden matrix, and Sanderson electronegativity to path length 4 of Geary autocorrelation descriptors [538].
48	QSAR by D-CENT QSAR program [539,540] using quantum chemical parameters	*N*-Benzylphenethylamines	The binding affinity was correlated negatively with total atomic electrophilic superdelocalizability of atom 3 and atom 13, the orbital electrophilic superdelocalizability of the highest occupied molecular orbital localized on atom 20, and the local atomic electronic chemical potential of atom 22. On the other hand, the binding affinity was correlated positively with Fukui index of the second highest occupied molecular orbital localized on atom 15 and Fukui index of the lowest vacant molecular orbital localized on atom 17 [541].
49	CoMFA using SYBYL 7.0 program [416]	Library of 24 structurally diverse 5-HT_{2C}R antagonists	The introduction of bulky substituents in the regions where methyl and propyl groups are located may enhance activity, whereas the presence of bulky groups in the proximity of índole group is expected to decrease activity. The presence of electronegative substituents near the amide moiety and positively charged groups is favorable for antagonistic activity [470].
50	Pharmacophore modeling using Accelrys Discovery Studio version 2.1 (DS) software [542]	Library of 24 structurally diverse 5-HT_{2C}R antagonists	Pharmacophore model including the common key features for ligand activity: (i) three hydrophobic features; (ii) one positively ionizable group; (iii) one hydrogen acceptor feature [470].
51	Pharmacophore modeling using CATALYST 4.6 program [499]	Diaryl substituted pyrrolidinones and pyrrolones	Pharmacophore model including the common key features for ligand activity: (i) one positively ionizable group; (ii) one hydrogen bond acceptor feature; (iii) one aromatic ring feature; (iv) three hydrophobic features [543].

3. Relevant features in GPCR-ligand interactions

3.1. Impact of structural water molecules in GPCR-mediated interactions

Ubiquitous when considering biological interactions, water molecules display different and important roles in protein-protein in general and in GPCR associated interactions in particular. These molecules are not to be overlooked when considering drug design for either orthosteric or allosteric purposes. By forming a 'water pocket' network, they can play an important role on the transition between active and inactive states, by deforming TM7 and potentiating hydrogen bonds that stabilize the structure on the inactive state [22]. In the case of rhodopsin, water molecules tend to be clustered in the vicinity of the binding pockets, near highly conserved residues [316]. Furthermore, internal water networks connecting to the ligand binding site have found to be highly conserved, even for receptors from different subfamilies of GPCRs, in particular A_2AR and DOR, with associated recurring motifs [544]. The direct involvement of the structural water molecules in the interaction of ligands with GPCRs can be a major bottleneck for an efficient design of drug candidates without the proper structural data information, since the replacement of water molecules in the ligand binding site may induce a dramatic modification of Structure-Activity Relationships (SAR) [544]. Interestingly, the inclusion of structural water molecules in crystallographic structures without the knowledge of structural water positions can lead to an improvement of virtual screening enrichment of active drug candidates over decoys [545]. Apart from experimental approoaches, such as X-ray crystallography and NMR, MD simulations have been employed to predict the involvement of water molecules in GPCR-ligand interactions and to study the water networks within receptors in different activation states [546].

Homology modeling approaches, in particular, have found to significantly decrease in accuracy when the participation of structural water molecules is not considered. Hence, it is essential to always assess number and characteristics of the water-contacts of the GPCR in study [547]. In docking, the water molecules associated to the binding pockets can be determinant in the development of drugs, mediating interactions and, in some cases, establishing hydrogen bonds that bridge interactions between the ligand and the protein [44]. Several docking tools take into account the intervention of water molecules in protein–ligand interaction, such as Yet Another Docking Approach (YADA) [548], which considers the explicitly structural water molecules at the binding site and improves the prediction scores by up to 24%. Another docking software, Molegro Virtual Docker (MVD) [549], incorporates water molecules in protein-ligand complexes and considers that water molecules exhibit the same flexibility of the ligand. During the docking simulations, MVD solvates the ligands with the maximum

number of water molecules, and these are then retained or excluded depending on energy contributions. Each water molecule is a flexible on/off part of the ligand and is treated with the same flexibility as the ligand. To facilitate the removal of the water molecules, a constant (positive) entropy penalty value is introduced *per* included water molecule. This approach has found to be successful in docking simulations when the water molecules are included in ligands containing hydrogen bonding groups [549]. Also, a more recent approach incorporated Quantum Mechanics/Molecular Mechanics (QM/MM) calculations with implicit solvent for application to GPCR-targeted drug discovery, by considering the ligands and protein residues in the binding site as QM described regions [550].

In addition to the above-mentioned tools, alternative software packages are used to model water molecules, such as GRID [526], Hydrophobic INTeractions (HINT) [551], SuperStar [552], Just Add Water Molecules (JAWM) [553], WaterMap [554,555], water Potential of Mean Forces (wPMF) [556], Water Fingerprints for Ligand And Proteins (WaterFLAP) [504], among others. Overall, water molecules should be taken into consideration, since they may influence the ligand binding affinity, the binding free energy, and the protein mobility.

3.2. Analysis of the ligand-binding site of potential GPCR-derived therapeutic targets

Even though computational methods have proven to be effective to solve structural aspects of GPCR-ligand complexes, they rely on experimental work as both validation and as a starting point, such as homology modeling templates and actual structures from where to start a computational analysis. Recently, the determination of 3D structures of GPCR-ligand complexes had substantialy increased allowing shedding light on important patterns governing the interactions that lead to the formation and stabilization of these complexes. Among all the aforementioned GPCR-derived therapeutic targets of PD, the X-ray structure of five GPCRs (D_3R, $A_{2A}AR$, $mGluR_2$, $mGluR_3$, and $mGluR_5$) has been determined in complex with small-molecule modulators. Table 4 represents an overview of all known 3D structures of ligands in complex with GPCR-derived therapeutic targets of PD available on PDB and the important interacting residues involved in the GPCR-ligand interaction. Relevant interactions were retrieved from the G-Protein-Coupled Receptor database (GPCRdb) [557] for D_3R, $A_{2A}AR$ and $mGluR_5$, and from the PDBeMOTIF for $mGluR_2$ and $mGluR_3$.

From the analysis of the ligand-binding site of the distinct GPCR-derived therapeutic targets of PD, it is observed the presence of some residue patterns underlying the GPCR-ligand interaction.

The analysis of Table 4 shows that the majority of A_{2A}AR ligands makes hydrophobic interacions with Leu85 in TM3. Interestingly, the A_{2A}AR agonists and the A_{2A}AR antagonist 4-(3-Amino-5-phenyl-1,2,4-triazin-6-yl)-2-chlorophenol interact with Val83 in TM3. In ECL2, the A_{2A}AR modulators establish aromatic interactions with Phe168. More specifically, the A_{2A}AR agonists makes π-π interactions with the Phe168 and hydrogen bond interactions with Glu169. Considering the TM6 domain, the analysis of the Table 4 shows that the A2AAR ligands makes hydrophobic interactions with Trp248 and Leu249, π-π interactions with His250, and hydrogen bond interactions with Asn253. Some A_{2A}AR antagonists establishes hydrophobic interactions with Met177 in TM5 and π-π interactions with His264 located on ECL2. Similarly to TM6, a considerable number of residues located in TM7 domain are involved in A_{2A}AR-ligand interaction. Interesting, the A_{2A}AR agonists make hydrogen bond interactions with Ser277 and His278, while the A_{2A}AR antagonists makes hydrophobic interactions with Met270. In addition, some antagonists bind to Leu267, to Tyr271, and to Ile274. The structural details of agonists CGS21680 and 5′-(*N*-ethylcarboxamido)adenosine, and the antagonists ZM241385 and 4-(3-amino-5-phenyl-1,2,4-triazin-6-yl)-2-chlorophenol in complex with A_{2A}AR are represented in Fig. 4A, Fig. 4B, Fig. 5A, and Fig. 5B, respectively. Only one 3D structure of D_3R in complex with eticlopride is available on PDB, which does not permit us to shed light on important patterns underlying this interaction.

The mGluR2 orthosteric agonists mentioned on Table 4 make hydrogen bond interactions with Arg61, Ser145, Ala166, Tyr168, and Asp295 residues and van der Waals interactions with Arg57, Ser167, Tyr216, and Lys377 residues mainly located on the extracellular Amino-Terminal Domain (ATD). The structural details of the binding modes of mGluR2 orthosteric agonists are represented in Fig. 6A and 6B. Similarly, the mGluR3 orthosteric agonists interact with residues located on the extracellular ATD. The mGluR3 agonists make hydrogen bond and van der Waals interactions with Arg64, Arg68, Tyr150, Ser151, Ala172, Ser173, Thr174, and Lys389 residues. The structural details of the binding pose of glutamate (Fig. 7A) and DCG-IV (Fig. 7B) in complex with mGluR3 are represented. While mGluR2 and mGluR3 orthosteric agonists interacts with their receptors on extracellular Amino-Terminal Domain (ATD), the mGluR5 NAM binds exclusively to the TM domains (TM2, TM3, TM4, and TM7 domains for mavoglurant; TM3, TM5, TM6, and TM7 domains for HTL14242 and 3-chloro-4-fluoro-5-[6-(1*H*-pyrazol-1-yl)pyrimidin-4-yl]benzonitrile). In TM3, the mGluR5 NAM makes hydrophobic interactions with Ile651 and Pro655. Additionally, in TM7 domains, the mGluR5 NAM makes hydrophobic interactions with Val806 and hydrogen-bond interactions with Ser809. A

representation of the binding conformation of HTL14242 and 3-chloro-4-fluoro-5-[6-(1*H*-pyrazol-1-yl)pyrimidin-4-yl]benzonitrile is shown on Fig. 8A and 8B, respectively.

Across all GPCRs, some regions can also be pointed out, namely TM3, TM6 and TM7. However, contrary to the residue conservation observed in receptors belonging to the same subfamily, the residues are distinct, with some interactions being maintained – TM3 holds an apparent important hydrophobic interaction, while TM6 contributes mostly with hydrophobic interactions. These sorts of interactions, while revealing some light into coupling patterns, should not be regarded as the key drivers of GPCR-ligand interaction. Truly, the residues common across most GPCR-ligand structures when considering GPCRs individually are the most likely to be what defines these interactions. Some interesting studies that analyse the physicochemical aspects – interacting surface, hydrophobicity, among other features – should be carried out in order to elucidate important structural patterns that go beyond sequence.

Table 4. Residues involved in the interaction of ligands with potential GPCR-derived therapeutic targets of PD for which structural data information is available on PDB. Among all the aforementioned GPCR-derived therapeutic targets of PD, the X-ray structure of five GPCRs (D_3R, $A_{2A}AR$, $mGluR_2$, $mGluR_3$, and $mGluR_5$) has been determined in complex with small-molecule modulators. Relevant interactions were retrieved from the GPCRdb [557] and are divided into Hydrogen Bonds (HB), Salt Bridges (SB), HydroPhobic (HP), and ARomatic interactions (AR). For $mGluR_2$ and $mGluR_3$, the information related to ligand interaction was gathered using PDBeMOTIF [558], an online tool designed to analyse protein-ligand interaction by detecting Hydrogen Bonds (HB) and Van der Waals (VdW) interactions.

Receptor	**Main ligand(s)/binding partners**	**Localization of the interacting residues on GPCR structure**									
Dopamine D_3 receptor (D_3R)											
3PBL [282]	Eticlopride (antagonist)	**Extracellular ATD**: -									
		TM1: -	**TM2:** -	**ECL1:** -	**TM3:** Asp110 (HB and SB); Val111 (HP)	**TM4:** -	**ECL2:** Ile183 (HP)	**TM5:** -	**TM6:** Phe345 (AR); Phe346 (HP); His349 (HB)	**ECL3**: -	**TM7:** -
Adenosine A_{2A} receptor ($A_{2A}AR$)											
2YDO [237]	Adeonosine (agonist)	**Extracellular ATD**: -									
		TM1: -	**TM2:** -	**ECL1:** -	**TM3:** -	**TM4:** -	**ECL2:** Phe168 (AR); Glu169 (HB)	**TM5:** -	**TM6:** Trp246 (HP); Leu249 (HP); Asn253 (HB)	**ECL3**: -	**TM7:** Ser277 (HB); H278 (2HB)
2YDV [237]	5′-(*N*-Ethylcarboxamido)adenosine (agonist)	**Extracellular ATD**: -									
		TM1: -	**TM2:** -	**ECL1:** -	**TM3:** Val84 (HP); Val85 (HP); Thr88 (HB);	**TM4:** -	**ECL2:** Phe168 (AR); Glu169 (HB)	**TM5:** -	**TM6:** Trp246 (HP); Leu249 (HP); His250	**ECL3**: -	**TM7:** Ser277 (HB); His278 (HB)

									(HB); Asn253 (2HB)		
3EML [44]	ZM241385 (antagonist)	**Extracellular ATD**: -									
		TM1: -	**TM2: -**	**ECL1: -**	**TM3:** Leu85 (AR)	**TM4: -**	**ECL2: -**	**TM5:** Met177 (HP)	**TM6:** Trp246 (HP); Leu249 (HP); His250 (AR); Asn253 (HB)	**ECL3**: His264 (AR)	**TM7:** Lys267 (HP); Met270 (HP)
3PWH [238]	ZM 241385 (antagonist)	**Extracellular ATD**: -									
		TM1: -	**TM2: -**	**ECL1: -**	**TM3: -**	**TM4: -**	**ECL2:** Phe168 (AR)	**TM5:** Met177 (HP)	**TM6:** Leu249 (HP); His250 (AR); Asn253 (HB)	**ECL3**: -	**TM7:** Tyr271 (HP); Ile274 (HP)
3QAK [43]	UK-432097 (agonist)	**Extracellular ATD**: -									
		TM1: -	**TM2: -**	**ECL1: -**	**TM3:** Val84 (HP); Leu85 (HP)	**TM4:** -	**ECL2:** Phe168 (AR); Glu169 (2HB)	**TM5:** -	**TM6:** Trp246 (HP); Leu249 (HP); His250 (HB); Asn253 (HB)	**ECL3**: -	**TM7:** Met270 (HP); Tyr271 (HB and AR); Ile274 (HP); Ser277 (HB); His278 (2HB)
3REY [238]	Xanthine amine congener (antagonist)	**Extracellular ATD: -**									

		TM1: -	**TM2: -**	**ECL1: -**	**TM3: -**	**TM4:** -	**ECL2:** Phe168 (HP)	**TM5:** Met177 (HP)	**TM6:** Asn253 (HB)	**ECL3**: -	**TM7:** Met270 (HP); Ile274 (HP)
3RFM [238]	Caffeine (antagonist)	**Extracellular ATD: -**									
		TM1: -	**TM2: -**	**ECL1: -**	**TM3: -**	**TM4:** -	**ECL2:** Phe168 (HP)	**TM5: -**	**TM6: -**	**ECL3**: -	**TM7:** Ile274 (HP)
3UZA [240]	6-(2,6-Dimethylpyridin-4-yl)-5-phenyl-1,2,4-triazin-3-amine (antagonist)	**Extracellular ATD: -**									
		TM1: -	**TM2: -**	**ECL1: -**	**TM3: -**	**TM4: -**	**ECL2:** Phe168 (HP)	**TM5:** Met177 (HP)	**TM6:** Leu249 (HP); His250 (AR); Asn253 (2HB)	**ECL3**: -	**TM7:** Ile274 (HP)
3UZC [240]	4-(3-Amino-5-phenyl-1,2,4-triazin-6-yl)-2-chlorophenol (antagonist)	**Extracellular ATD: -**									
		TM1: -	**TM2: -**	**ECL1: -**	**TM3:** Val84 (HP); Leu85 (HP)	**TM4:** -	**ECL2:** Phe168 (AR)	**TM5:** Met177 (HP)	**TM6:** Trp246 (HP); Leu249 (HP); His250 (AR); Asn253 (2HB)	**ECL3**: -	**TM7:** Ile274 (HP); His278 (HB)
3VG9 [229]	ZM241385 (antagonist)	**Extracellular ATD: -**									
		TM1: -	**TM2: -**	**ECL1: -**	**TM3:** Leu85 (HP)	**TM4:** -	**ECL2:** Phe168 (HP)	**TM5:** -	**TM6:** Trp246 (HP); Leu249 (HP); His250 (AR); Asn253 (HB)	**ECL3**: -	**TM7:** Met270 (HP); Tyr271 (HP)
3VGA	ZM241385	**Extracellular ATD: -**									

[239]	(antagonist)	**TM1: -**	**TM2: -**	**ECL1: -**	**TM3:** Leu85 (HP)	**TM4:** -	**ECL2:** Phe168 (AR)	**TM5:** Met177 (HP)	**TM6:** Leu249 (HP); His250 (AR)	**ECL3**: -	**TM7:** Met270 (HP)
4EIY [241]	ZM241385 (antagonist)	**Extracellular ATD: -**									
		TM1: -	**TM2: -**	**ECL1:-**	**TM3: -**	**TM4: -**	**ECL2:** Phe168 (AR); Glu169 (HB)	**TM5:** Met177 (HP)	**TM6:** Trp246 (HP); Leu249 (HP); His250 (AR); Asn253 (3HB)	**ECL3**: His264 (AR)	**TM7:** Leu267 (HP); Met270 (HP)
4UG2 [242]	CGS21680 (agonist)	**Extracellular ATD: -**									
		TM1: -	**TM2:** Ser67 (HB)	**ECL1:** -	**TM3:** Val84 (HP); Leu85 (HP); Thr88 (HB)	**TM4:** -	**ECL2:** Phe168 (AR); Glu169 (HB)	**TM5:** -	**TM6:** Trp246 (HP); Leu249 (HP); His250 (HB); Asn253 (2HB)	**ECL3**: -	**TM7:** Met270 (HP); Ile274 (HP); Ser277 (HB); His278 (2HB)
4UHR [242]	CGS21680 (agonist)	**Extracellular ATD: -**									
		TM1: -	**TM2: -**	**ECL1: -**	**TM3:** Val84 (HP); Leu85 (HP); Thr88 (HB)	**TM4:** -	**ECL2:** Phe168 (AR)	**TM5:** -	**TM6:** Trp246 (HP); Leu249 (HP); His250 (HB); Asn253 (HB)	**ECL3**: -	**TM7:** Ile274 (HP); Ser277 (HB); His278 (2HB)
5G53 [244]	5′-(*N*-Ethylcarboxamido)adenosine (agonist)	**Extracellular ATD: -**									

		TM1: -	**TM2: -**	**ECL1: -**	**TM3:** Val84 (HP); Leu85 (HP); Thr88 (HB)	**TM4:** -	**ECL2:** Phe168 (AR); Glu169 (HB)	**TM5:** -	**TM6:** Trp246 (HP); Leu249 (HP); His250 (HB); Asn253 (2HB)	**ECL3**: -	**TM7:** Ser277 (HB); His278 (2HB)
5IU4 [245]	ZM241385 (antagonist)	**Extracellular ATD: -**									
		TM1: -	**TM2: -**	**ECL1: -**	**TM3:** Leu85 (HP)	**TM4:** -	**ECL2:** Phe168 (AR); Glu169 (HB)	**TM5:** Met177 (HP)	**TM6:** Trp246 (HP); Leu249 (HP); His250 (AR); Asn253 (3HB)	**ECL3**: His264 (AR)	**TM7:** Met270 (HP)
5IU7 [245]	2-(Furan-2-yl)-N^5-(2-(4-phenylpiperidin-1-yl)ethyl)-1,2-dihydro-[1,2,4]triazolo[1,5-*a*][1,3,5]triazine-5,7-diamine (antagonist)	**Extracellular ATD: -**									
		TM1: -	**TM2: -**	**ECL1: -**	**TM3:** Leu85 (HP)	**TM4:** -	**ECL2:** Phe168 (AR); Glu169 (HB)	**TM5:** Met177 (HP)	**TM6:** Trp246 (HP); Leu249 (HP); His250 (AR); Asn253 (3HB)	**ECL3**: His264 (AR)	**TM7:** Met270 (HP)
5IU8 [245]	2-(Furan-2-yl)-N^5-(2-(4-phenylpiperidin-1-yl)ethyl)-1,2-dihydro-[1,2,4]triazolo[1,5-*a*][1,3,5]triazine-5,7-diamine (antagonist)	**Extracellular ATD: -**									
		TM1: -	**TM2: -**	**ECL1: -**	**TM3:** Leu85 (HP)	**TM4:** -	**ECL2:** Phe168 (AR); Glu169 (HB)	**TM5:** Met177 (HP)	**TM6:** Trp246 (HP); Leu249 (HP); His250 (AR); Asn253 (2HB)	**ECL3**: -	**TM7:** Met270 (HP)
5IUA	2-(Furan-2-yl)-N^5-	**Extracellular ATD: -**									

[245]	(3-(4-phenylpiperazin-1-yl)propyl)-1,2-dihydro-[1,2,4]triazolo[1,5-*a*][1,3,5]triazine-5,7-diamine (antagonist)	**TM1: -**	**TM2: -**	**ECL1: -**	**TM3:** Leu85 (HP)	**TM4: -**	**ECL2:** Phe168 (AR); Glu169 (HB)	**TM5:** Met177 (HP)	**TM6:** Trp246 (HP); Leu249 (HP); His250 (AR); Asn253 (HB)	**ECL3**: -	**TM7:** Leu267 (HP); Met270 (HP)
5IUB [245]	N^5-(2-(4-(2,4-Difluorophenyl)piperazin-1-yl)ethyl)-2-(furan-2-yl)-1,2-dihydro-[1,2,4]triazolo[1,5-*a*][1,3,5]triazine-5,7-diamine (antagonist)	**Extracellular ATD: -**									
		TM1: -	**TM2: -**	**ECL1: -**	**TM3:** Leu85 (HP)	**TM4: -**	**ECL2:** Phe168 (AR); Glu169 (HB)	**TM5:** Met177 (HP)	**TM6:** Trp246 (HP); Leu249 (HP); His250 (AR); Asn253 (3HB)	**ECL3**: His264 (AR); Ala265	**TM7:** Leu267 (HB); Met270 (HP); Ile274 (HP)
5K2A [246]	ZM241385 (antagonist)	**Extracellular ATD: -**									
		TM1: -	**TM2: -**	**ECL1: -**	**TM3: -**	**TM4: -**	**ECL2:** Phe168 (AR); Glu169 (HB)	**TM5:** Met177 (HP)	**TM6:** Trp246 (HP); Leu249 (HP); His250 (AR); Asn253 (3HB)	**ECL3**: His264 (AR); Ala265	**TM7:** Leu267 (HP); Met270 (HP)
5K2B [246]	ZM241385 (antagonist)	**Extracellular ATD: -**									
		TM1: -	**TM2: -**	**ECL1: -**	**TM3: -**	**TM4: -**	**ECL2:** Phe168 (AR); Glu169 (HB)	**TM5: -**	**TM6:** Trp246 (HP); Leu249 (HP); His250 (AR); Asn253 (3HB)	**ECL3**: -	**TM7:** Leu267 (HP); Met270 (HP)
	ZM241385	**Extracellular ATD: -**									

5K2C [246]	(antagonist)	**TM1: -**	**TM2: -**	**ECL1: -**	**TM3: -**	**TM4: -**	**ECL2:** Phe168 (AR); Glu169 (HB)	**TM5:** Met177 (HP)	**TM6:** Leu249 (HP); His250 (AR); Asn253 (3HB)	**ECL3**: His264 (AR)	**TM7:** Met270 (HP)
5K2D [246]	ZM241385 (antagonist)	**Extracellular ATD: -**									
		TM1: -	**TM2: -**	**ECL1: -**	**TM3: -**	**TM4: -**	**ECL2:** Phe168 (AR); Glu169 (HB)	**TM5:** Met177 (HP)	**TM6:** Leu249 (HP); His250 (AR); Asn253 (3HB)	**ECL3**: His264 (AR)	**TM7:** Met270 (HP)
5UIG [247]	5-Amino-*N*-[(2-methoxyphenyl)methyl]-2-(3-methylphenyl)-2*H*-1,2,3-triazole-4-carboximidamide (antagonist)	**Extracellular ATD: -**									
		TM1: -	**TM2: -**	**ECL1: -**	**TM3:** Leu85 (HP)	**TM4: -**	**ECL2:** Phe168 (AR)	**TM5:** Met177 (HP)	**TM6:** Trp246 (HP); Leu249 (HP); His250 (AR)	**ECL3**: -	**TM7:** Tyr271 (HP); Ile274 (HP)
Metabotropic Glutamate Receptor 2 ($MGluR_2$)											
5CNI [363]	Glutamate (agonist)	**Extracellular ATD:** Arg57 (VdW); Arg61 (HB); Tyr144 (VdW); Ser145 (HB); Ala166 (HB); Ser167 (VdW); Thr168 (HB); Tyr216 (VdW); Asp295 (HB); Lys377 (VdW)									
		TM1: -	**TM2: -**	**ECL1: -**	**TM3: -**	**TM4: -**	**ECL2: -**	**TM5: -**	**TM6: -**	**ECL3**: -	**TM7: -**
5CNJ [363]	LY2812223 (agonist)	**Extracellular ATD:** Arg57 (VdW); Arg61 (HB); Ser143 (VdW); Tyr144 (SB); Ser145 (HB); Ala166 (HB); Ser167 (VdW); Thr168 (HB); Tyr216 (VdW); Arg271 (VdW); Ser272 (VdW); Glu273 (VdW); Asp295 (HB); Gly296 (VdW); Lys377 (VdW) – chain A Arg57 (VdW); Arg61 (HB); Ser143 (VdW); Tyr144 (VdW); Ser145 (HB); Ala166 (VdW); Ser167 (VdW); Thr168 (HB); Tyr216 (VdW); Arg271 (VdW); Ser272 (VdW); Glu273 (VdW); Asp295 (HB); Gly296 (VdW); Lys377 (VdW) – chain B									
		TM1: -	**TM2: -**	**ECL1: -**	**TM3: -**	**TM4: -**	**ECL2: -**	**TM5: -**	**TM6: -**	**ECL3**: -	**TM7: -**
Metabotropic Glutamate Receptor 3 ($MGluR_3$)											
2E4U [364]	Glutamate (agonist)	**Extracellular ATD:** Arg64 (VdW); Arg68 (HB); Ser149 (VdW); Tyr150 (VdW); Ser151 (HB); Ala172 (VdW); Ser173 (VdW); Thr174 (HB); Tyr222 (VdW); Asp301 (HB); Lys389 (VdW)									
		TM1: -	**TM2: -**	**ECL1: -**	**TM3: -**	**TM4: -**	**ECL2: -**	**TM5: -**	**TM6: -**	**ECL3**: -	**TM7: -**
2E4V [364]	DCG-IV (agonist)	**Extracellular ATD:** Arg64 (VdW); Arg68 (HB); Ser149 (VdW); Tyr150 (VdW); Ser151 (HB); Ala172 (VdW); Ser173 (VdW); Thr174 (HB); Tyr222 (VdW); Arg277 (VdW); Ser278 (HB); Asp301 (HB); Gly302 (VdW); Lys389 (VdW)									
		TM1: -	**TM2: -**	**ECL1: -**	**TM3: -**	**TM4: -**	**ECL2: -**	**TM5: -**	**TM6: -**	**ECL3**: -	**TM7: -**
2E4W	1*S*,3*S*-ACPD	**Extracellular ATD:** Arg64 (VdW); Arg68 (HB); Ser149 (VdW); Tyr150 (VdW); Ser151 (HB); Ala172 (HB); Ser173 (VdW); Thr174 (HB);									

[364]	(agonist)	Tyr222 (VdW); Asp301 (HB); Gly302 (VdW); Lys389 (VdW)								
		TM1: -	**TM2: -**	**ECL1: -**	**TM3: -**	**TM4: -**	**ECL2: -**	**TM5: -**	**TM6: -**	**ECL3**: **-**	**TM7: -**
2E4X [364]	1*S*,3*R*-ACPD (agonist)	**Extracellular ATD:** Arg64 (VdW); Arg68 (HB); Ser149 (VdW); Tyr150 (VdW); Ser151 (HB); Ala172 (HB); Ser173 (VdW); Thr174 (HB); Tyr222 (VdW); Asp301 (HB); Gly302 (VdW); Lys389 (VdW)								
		TM1: -	**TM2: -**	**ECL1: -**	**TM3: -**	**TM4: -**	**ECL2: -**	**TM5: -**	**TM6: -**	**ECL3**: **-**	**TM7: -**
2E4Y [364]	2*R*,4*R*-APDC (agonist)	**Extracellular ATD:** Arg64 (SB); Arg68 (HB); Ser149 (HB); Tyr150 (VdW); Ser151 (HB); Ala172 (HB); Ser173 (VdW); Thr174 (VdW); Tyr222 (VdW); Asp301 (HB) – chain A Arg64 (HB); Arg68 (HB); Tyr150 (VdW); Ser151 (HB); Ala172 (VdW); Ser173 (VdW); Thr174 (HB); Tyr222 (SB); Asp301 (HB); Gly302 (VdW); Lys389 (VdW) – chain B								
		TM1: -	**TM2: -**	**ECL1: -**	**TM3: -**	**TM4: -**	**ECL2: -**	**TM5: -**	**TM6: -**	**ECL3**: **-**	**TM7: -**
5CNK [363]	Glutamate (agonist)	**Extracellular ATD:** Arg64 (VdW); Arg68 (HB); Ser149 (VdW); Tyr150 (VdW); Ser151 (HB); Ala172 (HB); Thr174 (VdW); Tyr222 (VdW); Asp301 (HB); Lys389 (HB) – chain A Arg64 (VdW); Arg68 (HB); Ser149 (VdW); Tyr150 (VdW); Ser151 (HB); Ala172 (HB); Thr174 (VdW); Tyr222 (VdW); Asp301 (HB); Lys389 (HB) – chain B								
		TM1: -	**TM2: -**	**ECL1: -**	**TM3: -**	**TM4: -**	**ECL2: -**	**TM5: -**	**TM6: -**	**ECL3**: **-**	**TM7: -**
5CNM [363]	LY2812223 (agonist)	**Extracellular ATD:** Arg64 (VdW); Arg68 (HB); Tyr150 (VdW); Ser151 (HB); Ala172 (HB); Ser173 (VdW); Thr174 (VdW); Lys389 (HB)								
		TM1: -	**TM2: -**	**ECL1: -**	**TM3: -**	**TM4: -**	**ECL2: -**	**TM5: -**	**TM6: -**	**ECL3**: **-**	**TM7: -**
Metabotropic Glutamate Receptor 5 ($MGluR_5$)											
4OO9 [365]	Mavoglurant (negative allosteric modulator)	**Extracellular ATD: -**								
		TM1: -	**TM2:** Ile625 (HP)	**ECL1: -**	**TM3:** Ile651 (HP); Pro655 (HP); Tyr659 (HP)	**TM4:** Leu744 (HP); Asn747 (HB)	**ECL2: -**	**TM5: -**	**TM6: -**	**ECL3**: **-**	**TM7:** Ser805 (2HB); Val806 (HP); Ser809 (HB); Ala810 (HP)
5CGC [366]	3-Chloro-4-fluoro-5-[6-(1*H*-pyrazol-1-yl)pyrimidin-4-yl]benzonitrile (negative allosteric modulator)	**Extracellular ATD: -**								
		TM1: -	**TM2: -**	**ECL1: -**	**TM3:** Ile651 (HP); Pro655 (HP)	**TM4: -**	**ECL2: -**	**TM5:** Leu744 (HP)	**TM6:** Trp785 (AR); Phe788 (HP)	**ECL3**: **-**	**TM7:** Val806 (HP); Ser809 (HB); Ala810 (HP)
5CGD [366]	HTL14242 (negative allosteric modulator)	**Extracellular ATD: -**								
		TM1: -	**TM2:** Ile625 (HP)	**ECL1: -**	**TM3:** Ile651 (HP); Pro655 (HP)	**TM4: -**	**ECL2: -**	**TM5:** Leu744 (HP)	**TM6:** Trp785 (HP); Phe788	**ECL3**: **-**	**TM7:** Val806 (HP); Ser809 (HB)

									(AR)		

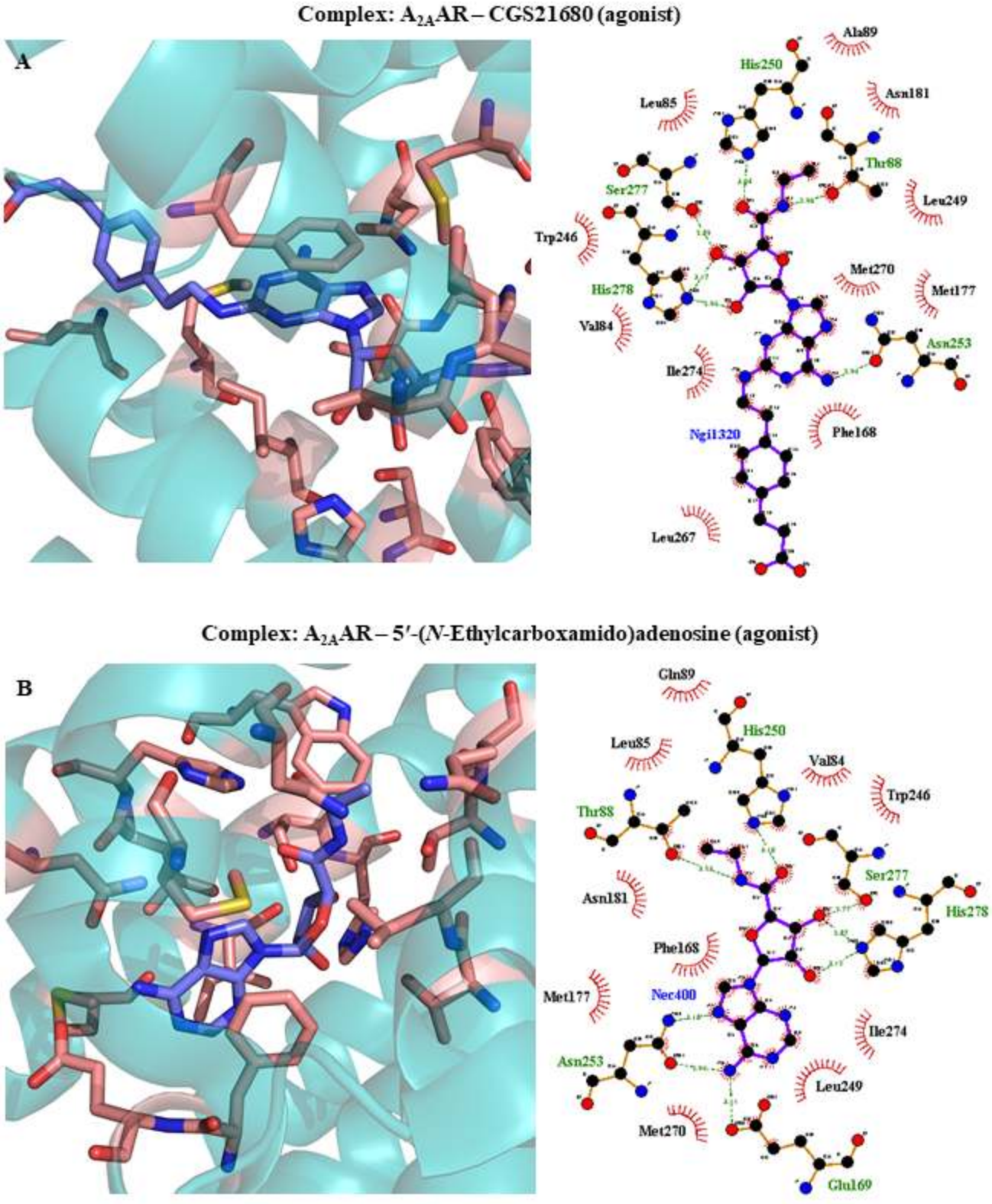

Fig. 4 - Structural detail of the interaction between $A_{2A}AR$ and agonists. A) Complex between $A_{2A}AR$ and CGS21680 (PDBid 4UHR [242]); B) Complex between $A_{2A}AR$ and 5′-(*N*-Ethylcarboxamido)adenosine (PDBid 5G53 [244]).

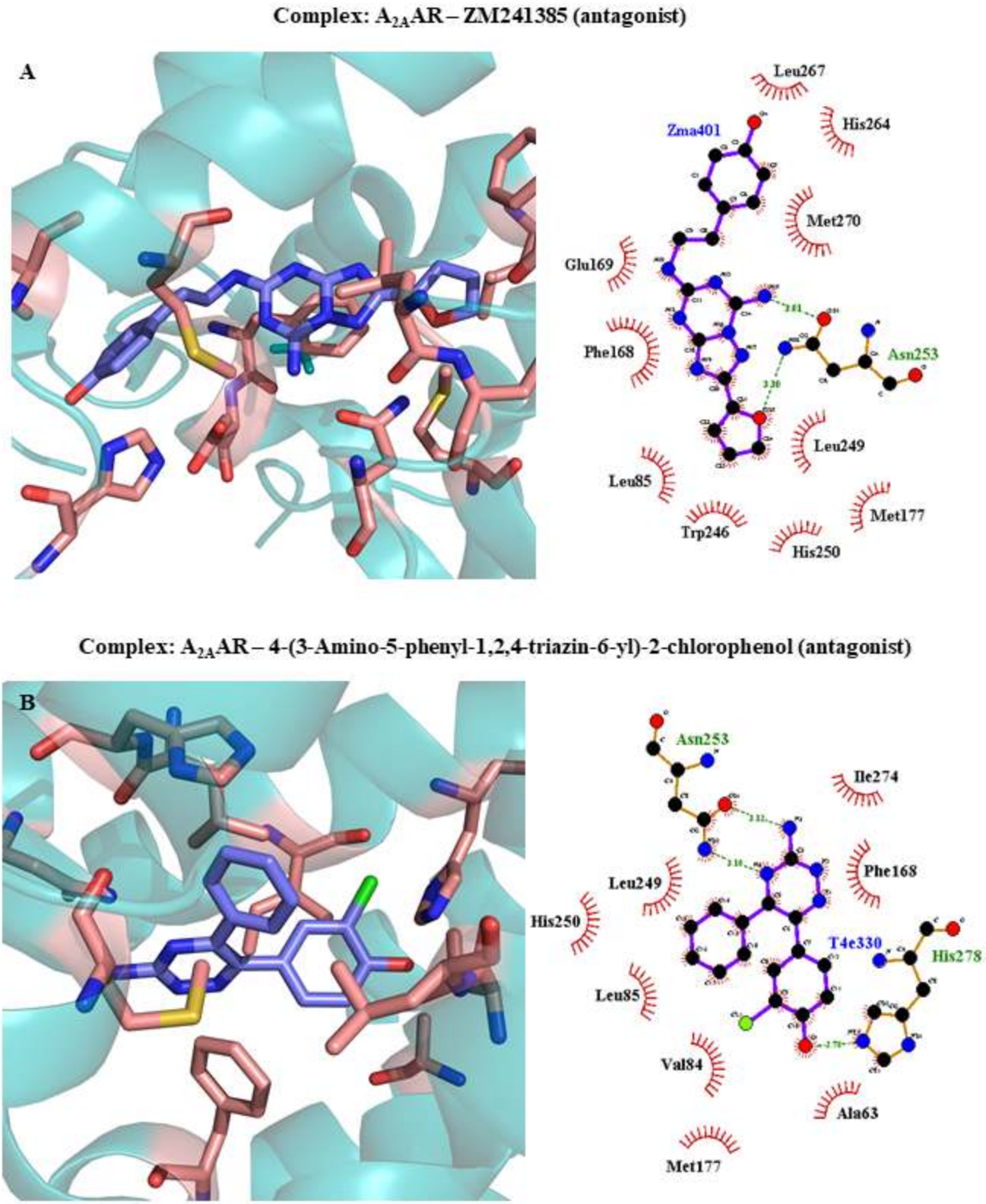

Fig. 5 - Structural detail of the interaction between $A_{2A}AR$ and antagonists. A) Complex between $A_{2A}AR$ and ZM241385 (PDBid 3EML [44]); B) Complex between $A_{2A}AR$ and 4-(3-amino-5-phenyl-1,2,4-triazin-6-yl)-2-chlorophenol (PDBid 3UZC [240]).

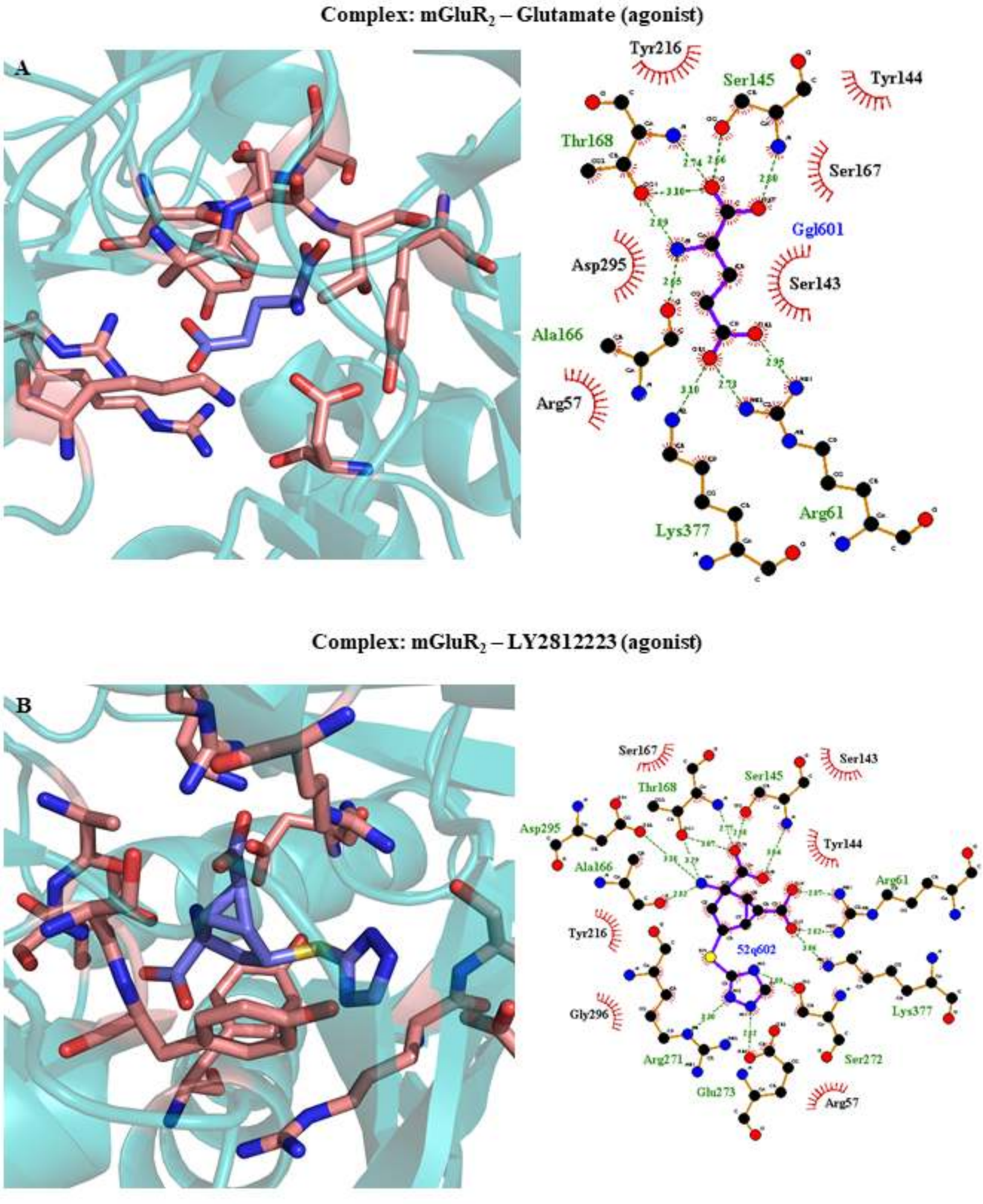

Fig. 6 - Structural detail of the interaction between $mGluR_2$ and orthosteric agonists. A) Complex between $mGluR_2$ and glutamate (PDBid 5CNI [363]); B) Complex between $mGluR_2$ and LY2812223 (PDBid 5UNJ [363]).

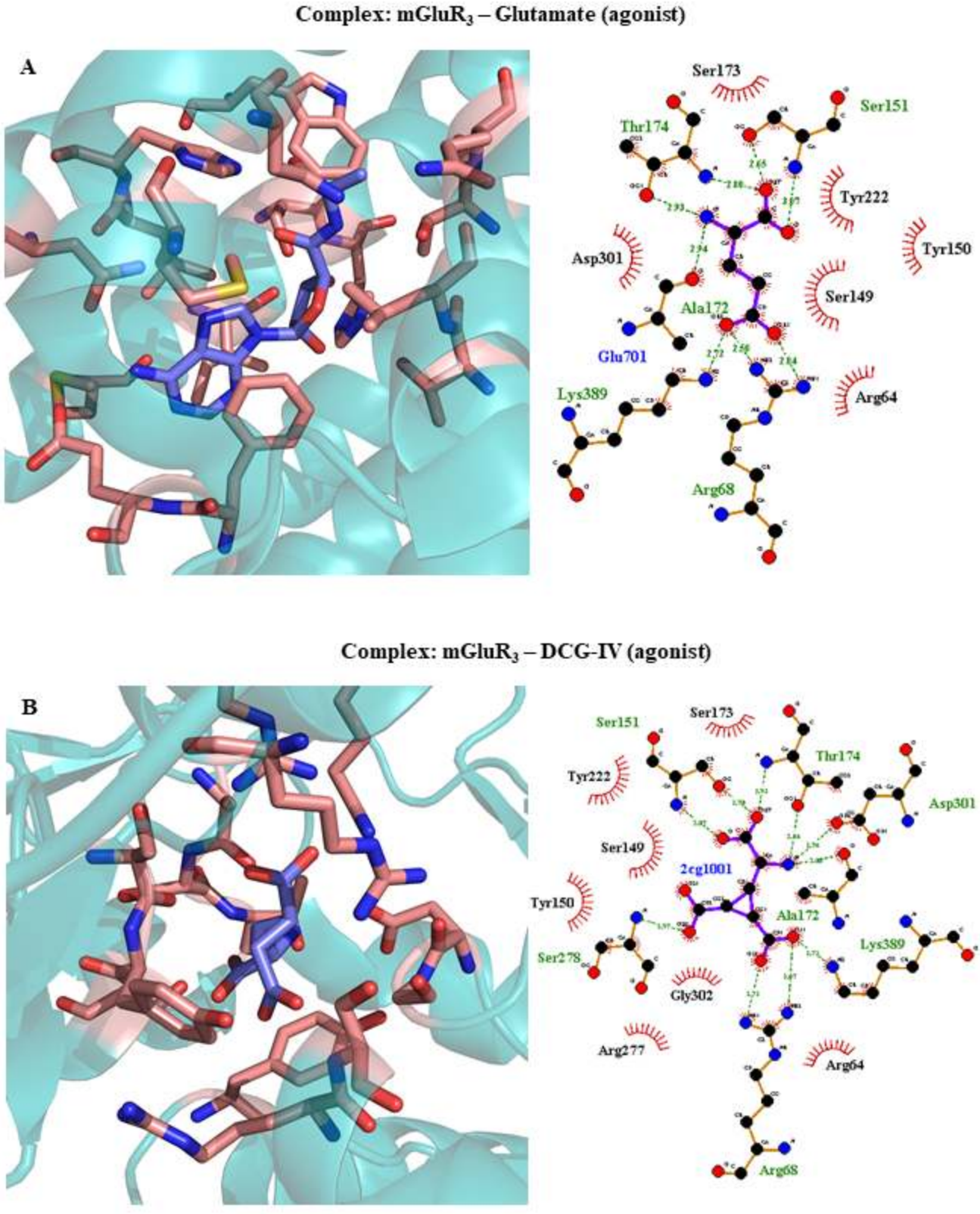

Fig. 7 - Structural detail of the interaction between $mGluR_3$ and orthosteric agonists. A) Complex between $mGluR_3$ and glutamate (PDBid 2E4U [364]); B) Complex between $mGluR_3$ and DCG-IV (PDBid 2E4V [364]).

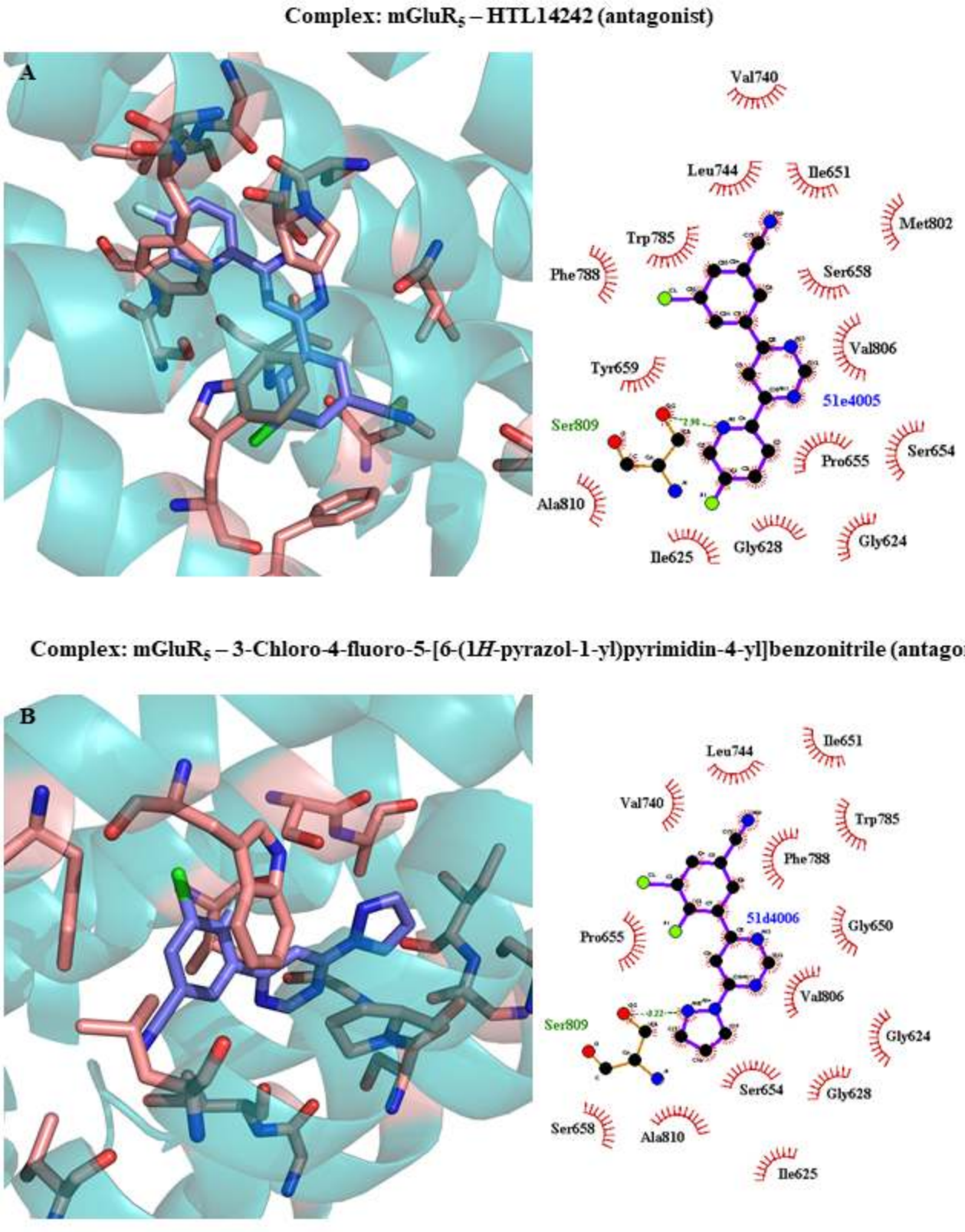

Fig. 8 - Structural detail of the interaction between $mGluR_5$ and antagonists/NAM. A) Complex between $mGluR_5$ and HTL14242 (PDBid 5CGD [366]); B) Complex between $mGluR_2$ and 3-chloro-4-fluoro-5-[6-(1*H*-pyrazol-1-yl)pyrimidin-4-yl]benzonitrile (PDBid 5CGC [366]).

CONCLUSION

GPCRs are practically ubiquitous proteins and drug targets, making them of high interest when dealing with a wide range of emerging diseases as PD. Drug discovery efforts targeting alternative therapeutic targets have been made to reduce the occurence of these side effects. In fact, the pharmacological activation/inhibition of all the aforementioned GPCR subtypes with small-molecule drug candidates may reduce L-DOPA induced dyskinesias. This raises the need for novel and subtype selective drug candidates useful for PD therapy.

The design of receptor subtype ligands that interact with the orthosteric binding site of GPCRs has proven to be ineffective, specifically for muscarinic acetylcholine receptors and metabotropic glutamate receptors, because of the high homology across binding sites of different GPCR subtypes, leading to a decreased subtype selectivity and specificity and unfavorable side effect profiles. Taking this into account, allosteric modulators are preferrable to target subtype specific GPCRs by interacting with a protein region that is both larger and more diverse. Experimentally, these structure-based drug design methologies have the advantage of understanding drug-GPCR interactions at a molecular level, which is vital for the development of new and reliable pharmacophore models. Nevertheless, the drug design of GPCR modulators based on orthosteric or allosteric binding site requires prior structural data information, which is scarce for the majority of GPCRs. In fact, future drugs acting on GPCRs are likely to rely on ligand-based computational methodologies to tackle missing structural data information. Overall, these *in silico* approaches have been extremely relevant in early stages of drug discovery, particularly in lead optimization of drug candidates, in order to determine the most favorable molecular modifications for the identification of more potent and subtype selective GPCR modulators targeting PD. Another aspect of extremely importance in drug discovery process of GPCR modulators resides in their pharmacokinetic and toxicological profile since usually drug candidates with a favorable pharmacodynamic profile fail to advance at late stages of drug discovery process due to their unfavorable pharmacokinetic properties and toxicity. A drug design strategy that perfectly combines favorable pharmacodynamic properties of small molecule GPCR modulators with encouraging pharmacokinetic properties (e.g. blood-brain barrier permeability, brain exposure, *etc*) is crucial for the development of promising anti-parkinsonian agents with potential clinical efficacy.

LIST OF ABBREVIATIONS

5-HTR – 5-HydroxyTryptamine Receptor

6-OHDA - 6-HydroxyDopamine

AADC - Aromatic L-Amino acid DeCarboxylase

AC – Adenylyl Cyclase

AD – Alzheimer's Disease

ADGRG1 - ADhesion G-protein coupled Receptor G1

ADGRL3 - ADhesion G-protein coupled Receptor L3

ADHD - Attention Deficit Hyperactivity Disorder

AMPA - *α*-Amino-3-hydroxy-5-Methyl-4-isoxazolePropionic Acid

ANN – Artificial Neural Networks

APEX-3D - Activity Prediction EXpert system-3D

APJR - Apelin Receptor

AR – Adenosine Receptor

ATD – Amino-Terminal Domain

ATR - AngioTensin II Receptor

AutoDock – Automated Docking

***β*AR** - *β*-Adrenergic Receptor

BBB – Blood-Brain Barrier

CAChe – Computer-Aided Chemistry consulting

cAMP - cyclic Adenosine MonoPhosphate

CADD - Computer-Assisted Drug Design

CBR - Cannabinoid Receptor

CCR - CC Chemokine Receptor

CDocker – CHARMm-based Docker

cGMP - cyclic Guanosine MonoPhosphate

CNS – Central Nervous System

CoMFA - Comparative Molecular Field Analysis

CoMSIA - Comparative Molecular Similarity Index Analysis

COMT - Catechol-*O*-MethylTransferase

CRF - Corticotropin Releasing Factor

CRFR - Corticotropin Releasing Factor Receptor

CRLR - Calcitonin Receptor-Like Receptor

CXCR - CXC Chemokine Receptor

CV – Cross-Validation

DAG – DiAcylGlycerol

DISCO - DIscrete Surface Charge Optimization

DOR - δ-Opioid Receptor

DR – Dopamine Receptor

ECL – ExtraCellular Loop

ETR - EndoThelin Receptor

FFAR - Free Fatty Acid Receptor

FLAP – Fingerprints for Ligands And Proteins

FlexiDock – Flexible Docking

FLRT2 - Fibronectin Leucin-Rich Transmembrane protein 2

FN3 - FibroNectin type III domain

FSH - Follicle-Stimulating Hormone

FSHR - Follicle-Stimulating Hormone Receptor

GABA – γ-AminoButyric Acid

GABAR - γ-AminoButyric Acid Receptor

GALAHAD - Genetic Algorithm with Linear Assignment of Hypermolecular Alignment of Database

GDP - Guanosine DiPhoshate

GFA – Genetic Function Approximation

GLIDE – Grid-based LIgand-Docking with Energetics

GLPR - Glucagon-Like Peptide Receptor

GOLD - Genetic Optimization for Ligand Docking

GOLPE - General Optimal Linear PLS Estimation

GPCR – G-Protein Coupled Receptors

GPCRdb - G-Protein Coupled Receptors database

GRK - G-protein coupled Receptor Kinase

GTP - Guanosine TriPhoshate

HINT – Hydrophobic INTeractions

HQSAR – Hologram Quantitative Structure-Activity Relationship

HR – Histamine Receptor

ICL – IntraCellular Loop

ICM – Internal Coordinate Mechanics

iGluR – Ionotropic Glutamate Receptor

IP_3 - Inositol-1,4,5-triPhosphate

JAWM – Just Add Water Molecules

KA – Kainic Acid

KOR - κ-Opioid Receptor

LDA – Linear Discriminant Analysis

LibDock – Library Docking

LPAR - LysoPhosphatidic Acid Receptor

L-DOPA - L-3,4-Dihydroxyphenylalanine or LevoDOPA

mAChR - Muscarinic AcetylCholine Receptor

MAO-B – MonoAmino Oxidase-B

MD – Molecular Dynamics

mGluR – Metabotropic Glutamate Receptor

ML – Machine Learning

MLR - Multiple Linear Regression

MOE – Molecular Operating Environment

MOR - μ-Opioid Receptor

MPTP - 1-Methyl-4-Phenyl-1,2,3,6-TetrahydroPyridine

MVD – Molegro Virtual Docker

N/OFQR - Nociceptin/Orphanin FQ Receptor

NAM – Negative Allosteric Modulator

NMDA - *N*-Methyl-D-Aspartate

NMR – Nuclear Magnetic Resonance

NTSR - Neurotensin Receptor

OXR – OreXin Receptor

P2YR - Purinergic P2Y Receptor

PAM – Positive Allosteric Modulator

PAR - Protease-Activated Receptor

PD – Parkinson's Disease

PHASE - PHarmacophore Alignment and Scoring Engine

PKA – Protein Kinase A

PKC – Protein Kinase C

PLC – PhosphoLipase C

PLS – Partial Least Square

PNS – Peripheral Nervous System

PTHR - ParaThyroid Hormone-related peptide Receptor

PTHrP - ParaThyroid Hormone-related Peptide

QM/MM – Quantum Mechanics/Molecular Mechanics

QSAR - Quantitative Structure-Activity Relationship

RAMP - Receptor-Activity Modifying Protein

REM – Rapid Eye Movement

RGS - Regulators of G-protein Signaling

RHO – Rhodopsin

S1PR - Sphingosine-1-Phosphate Receptor

SAR – Structure-Activity Relationships

Smo - Smoothened Receptor

SNc - Substantia Nigra pars compacta

SNr – Substantia Nigra pars reticulata

STN – SubThalamic Nucleus

SVM - Support Vector Machines

TM – TransMembrane

TSHR -Thyroid-Stimulating Hormone Receptor

Unc5D - Unc5D guidance receptor

US28 - Cytomegalovirus-encoded chemokine Receptor

VFT – Venus FlyTrap

VIPR - Vasoactive Intestinal Peptide Receptor

VR - Vasopressin Receptor

wPMF – water Potential of Mean Forces

YADA – Yet Another Docking Approach

CONFLICT OF INTEREST

The authors declare no conflict of interests.

ACKNOWLEDGEMENTS

This work had the financial support of Fundação para a Ciência e a Tecnologia (FCT/MEC) through national funds and co-financed by FEDER, under the Partnership Agreement PT2020 (projects UID/QUI/50006/2013 and POCI/01/0145/FEDER/007265). Irina S. Moreira acknowledges support by the FCT - Investigator programme - IF/00578/2014 (co-financed by European Social Fund and Programa Operacional Potencial Humano), a Marie Skłodowska-Curie Individual Fellowship MSCA-IF-2015 [MEMBRANEPROT 659826], the FEDER (Programa Operacional Factores de Competitividade - COMPETE 2020) and FCT–project: UID/NEU/04539/2013. Rita Melo acknowledges support from the FCT (SFRH/BPD/97650/2013 and UID/Multi/04349/2013 project). MNDSC further acknowledges FCT for the sabbatical grant SFRH/BSAB/127789/2016.

REFERENCES

1. Parkinson, J. An Essay On The Shaking Palsy. Whittingham and Rowland: London, UK, **1817**.

2. Dauer, W.; Przedborski, S. Parkinson's disease: mechanisms and models. *Neuron*, **2003**, *39*(6), 889-909.

3. Lew, M. Overview of Parkinson's Disease. *Pharmacother.*, **2007**, *27*(12P2), 155S-160S.

4. Schapira, A.H. Neurobiology and treatment of Parkinson's disease. *Trends Pharmacol. Sci.*, **2009**, *30*(1), 41-47.

5. Chaudhuri, K.R.; Healy, D.G.; Schapira, A.H. Non-motor symptoms of Parkinson's disease: diagnosis and management. *Lancet Neurol.*, **2006**, *5*(3), 235-245.

6. Poewe, W. Non-motor symptoms in Parkinson's disease. *Eur. J. Neurol.*, **2008**, *15*(S1), 14-20.

7. Warner, T.T.; Schapira, A.H.V. Genetic and environmental factors in the cause of Parkinson's disease. *Ann. Neurol.*, **2003**, *53*(S3), S16-S25.

8. Smith, Y.; Wichmann, T.; Factor, S.A.; DeLong, M.R. Parkinson's disease therapeutics: new developments and challenges since the introduction of levodopa. *Neuropsychopharmacology*, **2012**, *37*(1), 213-246.

9. Carlsson, A.; Lindqvist, M.; Magnusson, T.O.R. 3,4-Dihydroxyphenylalanine and 5-hydroxytryptophan as reserpine antagonists. *Nature*, **1957**, *180*(4596), 1200-1200.

10. Birkmayer, W.; Hornykiewicz, O. The L-3,4-dihydroxyphenylalanine (DOPA)-effect in Parkinson-akinesia. *Wien Klin Wochenschr*, **1961**, *73*, 787-788.

11. Barbeau, A.; Sourkes, T.L.; Murphy, C.F. Les catecholamines de la maladie de parkinsons. In: Monoamines et Systeme Nervoux Central; de Ajuriaguerra, J., Ed.; Goerg & Cie SA: Geneve, **1962**; pp. 247-262.

12. Baas, H.; Beiske, A.G.; Ghika, J.; Jackson, M.; Oertel, W.H.; Poewe, W.; Ransmayr, G. Catechol-O-methyltransferase inhibition with tolcapone reduces the "wearing off" phenomenon and levodopa requirements in fluctuating parkinsonian patients. *Neurology*, **1998**, *50*(5 S5), S46-S53.

13. Youdim, M.B.; Edmondson, D.; Tipton, K.F. The therapeutic potential of monoamine oxidase inhibitors. *Nat. Rev. Neurosci.*, **2006**, *7*(4), 295-309.

14. Porras, G.; Deurwaerdere, P.D.; Li, Q; Marti, M.; Morgenstern, R.; Sohr, R.; Bezard, E.; Morari, M.; Meissner, W.G. L-DOPA-induced dyskinesia: beyond an excessive dopamine tone in the stratium. *Sci. Rep.*, **2014**, *4*, 3730.

15. Pahwa, R.; Lyons, K.E. Levodopa-related wearing-off in Parkinson's disease: identification and management. *Curr. Med. Res. Opin.*, **2009**, *25*(4), 841-849.

16. Jenner, P. Wearing Off, Dyskinesia, and the Use of Continuous Drug Delivery in Parkinson's Disease. *Neurol. Clin.*, **2013**, *31*(3, Supplement), S17-S35.

17. Eriksson, T.; Magnusson, T.; Carlsson, A.; Linde, A.; Granérus, A.K. "On-off" phenomenon in Parkinson's disease: correlation to the concentration of DOPA in plasma. *J. Neural Transm.*, **1984**, *59*(3), 229-240.

18. Schrag, A.; Quinn, N. Dyskinesias and motor fluctuations in Parkinson's disease: A community-based study. *Brain*, **2000**, *123*(11), 2297-2305.

19. Thanvi, B.; Lo, N.; Robinson, T. Levodopa- induced dyskinesia in Parkinson's disease: clinical features, pathogenesis, prevention and treatment. *Postgrad. Med. J.*, **2007**, *83*(980), 384-388.

20. Pangalos, M.N.; Schechter, L.E.; Hurko, O. Drug development for CNS disorders: strategies for balancing risk and reducing attrition. *Nat. Rev. Drug Discov.*, **2007**, *6*(7), 521-532.

21. Moreira, I.S. Structural features of the G-protein/GPCR interactions. *BBA-General Subjects*, **2014**, *1840*(1), 16-33.

22. Rosenbaum, D.M.; Rasmussen, S.G.; Kobilka, B.K. The structure and function of G-protein-coupled receptors. *Nature*, **2009**, *459*(7245), 356-363.

23. Schioth, H.B.; Fredriksson, R. The GRAFS classification system of G-protein coupled receptors in comparative perspective. *Gen. Comp. Endocrinol.*, **2005**, *142*(1-2), 94-101.

24. Marinissen, M.J.; Gutkind, J.S. G-protein-coupled receptors and signaling networks: emerging paradigms. *Trends Pharmacol. Sci.*, **2001**, *22*(7), 368-376.

25. Lang, M.; Beck-Sickinger, A.G. Structure-activity relationship studies: methods and ligand design for G-protein coupled peptide receptors. *Curr. Protein Pept. Sci.*, **2006**, *7*(4), 335-353.

26. Gilman, A.G. G proteins: transducers of receptor-generated signals. *Annu. Rev. Biochem.*, **1987**, *56*, 615-649.

27. Birnbaumer, L. The discovery of signal transduction by G proteins: a personal account and an overview of the initial findings and contributions that led to our present understanding. *Biochim. Biophys. Acta*, **2007**, *1768*(4), 756-771.

28. Kontoyianni, M.; Liu, Z. Structure-based design in the GPCR target space. *Curr. Med. Chem.*, **2012**, *19*(4), 544-556.

29. Ghadessy, R.S.; Kelly, E. Second messenger-dependent protein kinases and protein synthesis regulate endogenous secretin receptor responsiveness. *Br. J. Clin. Pharmacol.*, **2002**, *135*(8), 2020-2028.

30. Shukla, A.K.; Xiao, K.; Lefkowitz, R.J. Emerging paradigms of *β*-arrestin-dependent seven transmembrane receptor signaling. *Trends Biochem. Sci.*, **2011**, *36*(9), 457-469.

31. Lefkowitz, R.J. G protein-coupled receptors. III. New roles for receptor kinases and *β*-arrestins in receptor signaling and desensitization. *J. Biol. Chem.*, **1998**, *273*(30), 18677-18680.

32. Wolfe, B.L.; Trejo, J. Clathrin-dependent mechanisms of G protein-coupled receptor endocytosis. *Traffic*, **2007**, *8*(5), 462-470.

33. Reiter, E.; Ahn, S.; Shukla, A.K.; Leftkowitz, R.J. Molecular Mechanism of *β*-Arrestin-Biased Agonism at Seven-Transmembrane Receptors. *Annu. Rev. Pharmacol. Toxicol.*, **2012**, *52*, 179-197.

34. Tsao, P.; von Zastrow, M. Downregulation of G protein-coupled receptors. *Curr. Opin. Neurobiol.*, **2000**, *10*(3), 365-369.

35. De Vries, L.; Zheng, B.; Fischer, T.; Elenko, E.; Farquhar, M.G. The regulator of G protein signaling family. *Annu. Rev. Pharmacol. Toxicol.*, **2000**, *40*, 235-271.

36. Ross, E.M.; Wilkie, T.M. GTPase-activating proteins for heterotrimeric G proteins: regulators of G protein signaling (RGS) and RGS-like proteins. *Annu. Rev. Biochem.*, **2000**, *69*, 795-827.

37. Mohan, M.L.; Vasudevan, N.T.; Gupta, M.K.; Martelli, E.E.; Naga Prasad, S.V. G-protein coupled receptor resensitization-appreciating the balancing act of receptor function. *Curr. Mol. Pharmacol.*, **2012**: Available from: https://www.ncbi.nlm.nih.gov/pmc/articles/PMC4607669/.

38. Christopoulos, A. Allosteric binding sites on cell-surface receptors: novel targets for drug discovery. *Nat. Rev. Drug Discov.*, **2002**, *1*(3), 198-210.

39. Conn, P.J.; Christopoulos, A; Lindsley, C.W. Allosteric modulators of GPCRs: a novel approach for the treatment of CNS disorders. *Nat. Rev. Drug Discov.*, **2009**, *8*(1), 41-54.

40. Karplus, M.; Kuriyan, J. Molecular dynamics and protein function. *Proc Natl. Acad. Sci*., **2005**, *102*(19), 6679–6685.

41. Nussinov, R.; Tsai, C-J. Allostery in disease and in drug discovery. *Cell*, **2013**, *153*(2), 293–305.

42. Rosenbaum, D.M.; Zhang, C.; Lyons, J.A.; Holl, R.; Aragao, D.; Arlow, D.H.; Rasmussen, S.G.F.; Choi, H.J.; Devree, B.T.; Sunahara, R.K.; Chae, P.S.; Gellman, S.H.; Dror, R.O.; Shaw, D.E.; Weis,

W.I.; Caffrey, M.; Gmeiner, P.; Kobilka, B.K. Structure and function of an irreversible agonist-β_2 adrenoceptor complex. *Nature*, **2011**, *469*(7329), 236-240.

43. Xu, F.; Wu, H.; Katritch, V.; Han, G.W.; Jacobson, K.A.; Gao, Z.G.; Cherezov, V.; Stevens, R.C. Structure of an agonist-bound human A_{2A} adenosine receptor. *Science*, **2011**, *332*(6027), 322-327.

44. Jaakola, V.P.; Griffith, M.T.; Hanson, M.A.; Cherezov, V.; Chien, E.Y.; Lane, J.R.; Ijzerman, A.P.; Stevens, R.C. The 2.6 Å crystal structure of a human A_{2A} adenosine receptor bound to an antagonist. *Science*, **2008**, *322*(5905), 1211-1217.

45. Ozcan, O.; Uyar, A.; Doruker, P.; Akten, E.D. Effect of intracellular loop 3 on intrinsic dynamics of human β_2-adrenergic receptor. *BMC Struct. Biol.*, **2013**, *13*, 29. Available from: https://bmcstructbiol.biomedcentral.com/articles/10.1186/1472-6807-13-29.

46. Pydi, S.P.; Singh, N.; Upadhyaya, J.; Bhullar, R.P.; Chelikani, P. The third intracellular loop plays a critical role in bitter taste receptor activation. *Biochim. Biophys. Acta,* **2014**, *1838*(1 Pt B), 231-236.

47. Gómez-Moutón, C.; Fischer, T.; Peregil, R.M.; Jiménez-Baranda, S.; Stossel, T.P.; Nakamura, F.; Mañes, S. Filamin A interaction with the $CXCR_4$ third intracellular loop regulates endocytosis and signaling of WT and WHIM-like receptors. *Blood,* **2015**, *125*(7), 1116-1125.

48. Dror, R.O.; Green, H.F.; Valant, C.; Borhani, D.W.; Valcourt, J.R.; Pan, A.C.; Arlow, D.H.; Canals, M.; Lane, J.R.; Rahmani, R.; Baell, J.B.; Sexton, P.M.; Christopoulos, A.; Shaw, D.E. Structural basis for modulation of a G-protein-coupled receptor by allosteric drugs. *Nature*, **2013**, *503*(7475), 295-299.

49. Sylte, I.; Bronowska, A.; Dahl, S.G. Ligand induced conformational states of the 5-HT_{1A} receptor. *Eur. J. Pharmacol.*, **2001**, *416*(1-2), 33-41.

50. Bronowska, A.; Leś, A.; Chilmonczyk, Z.; Filipek, S.; Edvardsen, O.; Ostensen, R.; Sylte, I. Molecular dynamics of buspirone analogues interacting with the 5-HT_{1A} and 5-HT_{2A} serotonin receptors. *Bioorg. Med. Chem.*, **2001**, *9*(4), 881-895.

51. Beaulieu, J.-M.; Gainetdinov, R.R. The Physiology, Signaling, and Pharmacology of Dopamine Receptors. *Pharmacol. Rev*., **2011**, *63*(1), 182-217.

52. Beaulieu, J.M.; Espinoza, S.; Gainetdinov, R.R. Dopamine receptors - IUPHAR Review 13. *Br. J. Pharmacol.*, **2015**, *172*(1), 1-23.

53. Bedard, P.J.; Di Paolo, T.; Falardeau, P.; Boucher, R. Chronic treatment with L-DOPA, but not bromocriptine induces dyskinesia in MPTP-parkinsonian monkeys. Correlation with [^{3}H]-spiperone binding. *Brain Res*., **1986**, *379*(2), 294-299.

54. Pearce, R.K.B.; Banerji, T.; Jenner, P.; Marsden, C.D. *De novo* administration of ropinirole and bromocriptine induces less dyskinesia than L-DOPA in the MPTP-treated marmoset. *Mov. Disord.*, **1998**, *13*(2), 234-241.

55. Chen, X.; McCorvy, J.D.; Fischer, M.G.; Butler, K.V.; Shen, Y.; Roth, B.L.; Jin, J. Discovery of G Protein-Biased D_2 Dopamine Receptor Partial Agonists. *J. Med. Chem.*, **2016**, *59*(23), 10601-10618.

56. Hiller, C.; Kling, R.C.; Heinemann, F.W.; Meyer, K.; Hübner, H.; Gmeiner, P. Functionally selective dopamine D_2/D_3 receptor agonists comprising an enyne moiety. *J. Med. Chem.*, **2013**, *56*(12), 5130-5141.

57. Kühhorn, J.; Hübner, H.; Gmeiner, P. Bivalent Dopamine D_2 Receptor Ligands: Synthesis and Binding Properties. *J. Med. Chem.*, **2011**, *54*(13), 4896-4903.

58. Weichert, D.; Banerjee, A.; Hiller, C.; Kling, R.C.; Hübner, H.; Gmeiner, P. Molecular Determinants of Biased Agonism at the Dopamine D_2 Receptor. *J. Med. Chem.*, **2015**, *58*(6), 2703-2717.

59. Mewshaw, R.E.; Kavanagh, J.; Stack, G.; Marquis, K.L.; Shi, X.; Kagan, M.Z.; Webb, M.B.; Katz, A.H.; Park, A.; Kang, Y.H.; Abou-Gharbia, M.; Scerni, R.; Wasik, T.; Cortes-Burgos, L.; Spangler, T.; Brennan, J.A.; Piesla, M.; Mazandarani, H.; Cockett, M.I.; Ochalski, R.; Coupet, J.; Andree, T.H. New Generation Dopaminergic Agents. 1. Discovery of a Novel Scaffold Which Embraces the D_2 Agonist Pharmacophore. Structure−Activity Relationships of a Series of 2-(Aminomethyl)chromans. *J. Med. Chem.*, **1997**, *40*(26), 4235-4256.

60. Boeckler, F.; Ohnmacht, U.; Lehmann, T.; Utz, W.; Hübner, H.; Gmeiner, P. CoMFA and CoMSIA investigations revealing novel insights into the binding modes of dopamine D_3 receptor agonists. *J. Med. Chem.*, **2005**, *48*(7), 2493-2508.

61. Hübner, H.; Haubmann, C.; Utz, W.; Gmeiner, P. Conjugated Enynes as Nonaromatic Catechol Bioisosteres: Synthesis, Binding Experiments, and Computational Studies of Novel Dopamine Receptor Agonists Recognizing Preferentially the D_3 Subtype. *J. Med. Chem.*, **2000**, *43*(4), 756-762.

62. Garcia-Ladona, F.J.; Cox, B.F. BP 897, a selective dopamine D_3 receptor ligand with therapeutic potential for the treatment of cocaine-addiction. *CNS Drug Rev*., **2003**, *9*(2), 141-158.

63. Tschammer, N.; Elsner, J.; Goetz, A.; Ehrlich, K.; Schuster, S.; Ruberg, M.; Kühhorn, J.; Thompson, D.; Whistler, J.; Hübner, H.; Gmeiner, P. Highly Potent 5-Aminotetrahydropyrazolopyridines: Enantioselective Dopamine D_3 Receptor Binding, Functional Selectivity, and Analysis of Receptor−Ligand Interactions. *J. Med. Chem.*, **2011**, *54*(7), 2477-2491.

64. Hackling, A.; Ghosh, R.; Perachon, S.; Mann, A.; Holtje, H.D.; Wermuth, C.G.; Schwartz, J.C.; Sippl, W.; Sokoloff, P.; Stark, H. *N*-(*ω*-(4-(2-Methoxyphenyl)piperazin-1-yl)alkyl)carboxamides as Dopamine D_2 and D_3 Receptor Ligands. *J. Med. Chem.*, **2003**, *46*(18), 3883-3899.

65. Chen, J.; Collins, G.T.; Zhang, J.; Yang, C.Y.; Levant, B.; Woods, J.; Wang, S. Design, Synthesis, and Evaluation of Potent and Selective Ligands for the Dopamine 3 (D_3) Receptor with a Novel *in Vivo* Behavioral Profile. *J. Med. Chem.*, **2008**, *51*(19), 5905-5908.

66. Ananthan, S.; Saini, S.K.; Zhou, G.; Hobrath, J.V.; Padmalayam, I.; Zhai, L.; Bostwick, J.R.; Antonio, T.; Reith, M.E.; McDowell, S.; Cho, E.; McAleer, L.; Taylor, M.; Luedtke, R.R. Design, Synthesis, and Structure−Activity Relationship Studies of a Series of [4-(4-Carboxamidobutyl)]-1-arylpiperazines: Insights into Structural Features Contributing to Dopamine D_3 versus D_2 Receptor Subtype Selectivity. *J. Med. Chem.*, **2014**, *57*(16), 7042-7060.

67. Leopoldo, M.; Berardi, F.; Colabufo, N.A.; De Giorgio, P.; Lacivita, E., Perrone, R.; Tortorella, V. Structure−Affinity Relationship Study on *N*-[4-(4-Arylpiperazin-1-yl)butyl]arylcarboxamides as Potent and Selective Dopamine D_3 Receptor Ligands. *J. Med. Chem.*, **2002**, *45*(26), 5727-5735.

68. Fredholm, B.B. Adenosine receptors as drug targets. *Exp. Cell Res*., **2010**, *316*(8), 1284-1288.

69. Fredholm, B.B.; Ijzerman, A.P.; Jacobson, K.A.; Linden, J.; Muller, C.E. International Union of Basic and Clinical Pharmacology. LXXXI. Nomenclature and classification of adenosine receptors-an update. *Pharmacol. Rev.*, **2011**, *63*(1), 1-34.

70 Chen, J.F.; Eltzschig, H.K.; Fredholm, B.B. Adenosine receptors as drug targets-what are the challenges? *Nat. Rev. Drug Discov.*, **2013**, *12*(4), 265-286.

71. Moreau, J.-L.; Huber, G. Central adenosine A_{2A} receptors: an overview. *Brain Res Rev*, **1999**, *31*(1), 65-82.

72. Svenningsson, P.; Le Moine, C.; Fisone, G.; Fredholm, B.B. Distribution, biochemistry and function of striatal adenosine A_{2A} receptors. *Prog. Neurobiol.*, **1999**, *59*(4), 355-396.

73. Torvinen, M.; Kozell, L.B.; Neve, K.A.; Agnati, L.F.; Fuxe, K. Biochemical identification of the dopamine D_2 receptor domains interacting with the adenosine A_{2A} receptor. *J. Mol. Neurosci.*, **2004**, *24*(2), 173-180.

74. Canals, M.; Marcellino, D.; Fanelli, F.; Ciruela, F.; de Benedetti, P.; Goldberg, S.R.; Neve, K.; Fuxe, K.; Agnati, L.F.; Woods, A.S.; Ferré, S.; Lluis, C.; Bouvier, M.; Franco, R. Adenosine A_{2A}-dopamine D_2 receptor-receptor heteromerization: qualitative and quantitative assessment by fluorescence and bioluminescence energy transfer. *J. Biol. Chem.*, **2003**, *278*(47), 46741-46749.

75. Ferre, S.; Fuxe, K.; von Euler, G.; Johansson, B.; Fredholm, B.B. Adenosine-dopamine interactions in the brain. *Neuroscience*, **1992**, *51*(3), 501-512.

76. Ferre, S.; Fredholm, B.B.; Morelli, M.; Popoli, P.; Fuxe, K. Adenosine-dopamine receptor-receptor interactions as an integrative mechanism in the basal ganglia. *Trends Neurosci*., **1997**, *20*(10), 482-487.

77. Trevitt, J.; Vallance, C.; Harris, A.; Goode, T. Adenosine antagonists reverse the cataleptic effects of haloperidol: implications for the treatment of Parkinson's disease. *Pharmacol. Biochem. Behav.*, **2009**, *92*(3), 521-527.

78. Varty, G.B.; Hodgson, R.A.; Pond, A.J.; Grzelak, M.E.; Parker, E.M.; Hunter, J.C. The effects of adenosine A_{2A} receptor antagonists on haloperidol-induced movement disorders in primates. *Psychopharmacology (Berl)*, **2008**, *200*(3), 393-401.

79. Lundblad, M.; Vaudano, E.; Cenci, M.A. Cellular and behavioural effects of the adenosine A_{2A} receptor antagonist KW-6002 in a rat model of L-DOPA-induced dyskinesia. *J. Neurochem.*, **2003**, *84*(6), 1398-1410.

80. Chen, J.F.; Xu, K.; Petzer, J.P.; Staal, R.; Xu, Y.H.; Beilstein, M.; Sonsalia, P.K.; Castagnoli, K.; Castagnoli, N. Jr.; Schwarzschild MA. Neuroprotection by caffeine and A_{2A} adenosine receptor inactivation in a model of Parkinson's disease. *J. Neurosci.*, **2001**, *21*(10), Rc143.

81. Grondin, R.; Bédard, P.J.; Hadj Tahar, A.; Grégoire, L.; Mori, A.; Kase, H. Antiparkinsonian effect of a new selective adenosine A_{2A} receptor antagonist in MPTP-treated monkeys. *Neurology*, **1999**, *52*(8), 1673-1677.

82. Kanda, T.; Jackson, M.J.; Smith, L.A.; Pearce, R.K.; Nakamura, J.; Kase, H.; Kuwana, Y.; Jenner, P. Combined use of the adenosine A_{2A} antagonist KW-6002 with L-DOPA or with selective D_1 or D_2

dopamine agonists increases antiparkinsonian activity but not dyskinesia in MPTP-treated monkeys. *Exp. Neurol.*, **2000**, *162*(2), 321-327.

83. Baraldi, P.G.; Cacciari, B.; Spalluto, G.; Pineda de las Infantas y Villatoro, M.J.; Zocchi, C.; Dionisotti, S.; Ongini, E. Pyrazolo[4,3-*e*]-1,2,4-triazolo[1,5-*c*]pyrimidine Derivatives: Potent and Selective A_{2A} Adenosine Antagonists. *J. Med. Chem*., **1996**, *39*(5), 1164-1171.

84. Baraldi, P.G.; Cacciari, B.; Spalluto, G.; Bergonzoni, M.; Dionisotti, S.; Ongini, E.; Varani, K.; Borea, P.A. Design, Synthesis, and Biological Evaluation of a Second Generation of Pyrazolo[4,3-*e*]-1,2,4-triazolo[1,5-*c*]pyrimidines as Potent and Selective A_{2A} Adenosine Receptor Antagonists. *J. Med. Chem.*, **1998**, *41*(12), 2126-2133.

85. Neustadt, B.R.; Hao, J.; Lindo, N.; Greenlee, W.J.; Stamford, A.W.; Tulshian, D.; Ongini, E.; Hunter, J.; Monopoli, A; Bertorelli, R.; Foster, C.; Arik, L.; Lachowicz, J.; Ng, K.; Feng, K.I. Potent, selective, and orally active adenosine A_{2A} receptor antagonists: arylpiperazine derivatives of pyrazolo[4,3-*e*]-1,2,4-triazolo[1,5-*c*]pyrimidines. *Bioorg. Med. Chem. Lett.*, **2007**, *17*(5), 1376-1380.

86. Vu, C.B.; Peng, B.; Kumaravel, G.; Smits, G.; Jin, X.; Phadke, D.; Engber, T.; Huang, C.; Reilly, J.; Tam, S.; Grant, D.; Hetu, G.; Chen, L.; Zhang, J,; Petter, R.C. Piperazine derivatives of [1,2,4]triazolo[1,5-*a*][1,3,5]triazine as potent and selective adenosine A_{2A} receptor antagonists. *J. Med. Chem.*, **2004**, *47*(17), 4291-4299.

87. Vu, C.B.; Pan, D.; Peng, B.; Kumaravel, G.; Smits, G.; Jin, X.; Phadke, D.; Engber, T.; Huang, C.; Reilly, J.; Tam, S.; Grant, D.; Hetu, G.; Petter, R.C. Novel diamino derivatives of [1,2,4]triazolo[1,5-*a*][1,3,5]triazine as potent and selective adenosine A_{2A} receptor antagonists. *J. Med. Chem.*, **2005**, *48*(6), 2009-2018.

88. Gillespie, R.J.; Bamford, S.J.; Botting, R.; Comer, M.; Denny, S.; Gaur, S.; Griffin, M.; Jordan, A.M.; Knight, A.R.; Lerpiniere, J.; Leonardi, S.; Lightowler, S.; McAteer, S.; Merrett, A.; Misra, A.; Padfield, A.; Reece, M.; Saadi, M.; Selwood, D.L.; Stratton, G.C.; Surry, D.; Todd, R.; Tong, X.; Ruston, V.; Upton, R.; Weiss, S.M. Antagonists of the human A_{2A} adenosine receptor. 4. Design, synthesis, and preclinical evaluation of 7-aryltriazolo[4,5-*d*]pyrimidines. *J. Med. Chem*., **2009**, *52*(1), 33-47.

89. Jacobson, K.A.; Gallo-Rodriguez, C.; Melman, N.; Fischer, B.; Maillard, M.; van Bergen, A.; van Galen, P.J.; Karton, Y. Structure-activity relationships of 8-styrylxanthines as A_2-selective adenosine antagonists. *J. Med. Chem.*, **1993**, *36*(10), 1333-1342.

90. Mantri, M.; de Graaf, O.; van Veldhoven, J.; Goblyos, A.; von Frijtag Drabbe Kunzel, J.K.; Mulder-Krieger, T.; Link, R.; de Vries, H.; Beukers, M.W.; Brussee, J.; Ijzerman, A.P. 2-Amino-6-furan-2-yl-4-substituted nicotinonitriles as A_{2A} adenosine receptor antagonists. *J. Med. Chem.*, **2008**, *51*(15), 4449-4455.

91. Muller, C.E.; Geis, U.; Hipp, J.; Schobert, U.; Frobenius, W.; Pawlowski, M.; Suzuki, F.; Sandoval-Ramirez, J. Synthesis and structure-activity relationships of 3,7-dimethyl-1-propargylxanthine derivatives, A_{2A}-selective adenosine receptor antagonists. *J. Med. Chem.*, **1997**, *40*(26), 4396-4405.

92. Shook, B.C.; Rassnick, S.; Osborne, M.C.; Davis, S.; Westover, L.; Boulet, J.; Hall, D.; Rupert, K.C.; Heintzelman, G.R.; Hansen, K.; Chakravarty, D.; Bullington, J.L.; Russell, R.; Branum, S.; Wells, K.M.; Damon, S.; Youells, S.; Li, X.; Beauchamp, D.A.; Palmer, D.; Reyes, M.; Demarest, K.; Tang, Y.; Rhodes, K.; Jackson, P.F. *In vivo* characterization of a dual adenosine A_{2A}/A_1 receptor antagonist in animal models of Parkinson's disease. *J. Med. Chem.*, **2010**, *53*(22), 8104-8115.

93. Shook, B.C.; Rassnick, S.; Wallace, N.; Crooke, J.; Ault, M.; Chakravarty, D.; Barbay, J.K.; Wang, A.; Powell, M.T.; Leonard, K.; Alford, V.; Scannevin, R.H.; Carroll, K.; Lampron, L.; Westover, L.; Lim, H.K.; Russell, R.; Branum, S.; Wells, K.M.; Damon, S.; Youells, S.; Li, X.; Beauchamp, D.A.; Rhodes, K.; Jackson, P.F. Design and characterization of optimized adenosine A_{2A}/A_1 receptor antagonists for the treatment of Parkinson's disease. *J. Med. Chem.*, **2012**, *55*(3), 1402-1417.

94. Slee, D.H.; Zhang, X.; Moorjani, M,; Lin, E.; Lanier, M.C.; Chen, Y.; Rueter, J.K.; Lechner, S.M.; Markison, S.; Malany, S.; Joswig, T.; Santos, M.; Gross, R.S.; Williams, J.P.; Castro-Palomino, J.C.; Crespo, M.I.; Prat, M.; Gual, S.; Diaz, J.L.; Wen, J.; O'Brien, Z.; Saunders, J. Identification of novel, water-soluble, 2-amino-*N*-pyrimidin-4-yl acetamides as A_{2A} receptor antagonists with *in vivo* efficacy. *J. Med. Chem.*, **2008**, *51*(3), 400-406.

95. Zhang, X.; Tellew, J.E.; Luo, Z.; Moorjani, M.; Lin, E.; Lanier, M.C.; Chen, Y,; Williams, J.P.; Saunders, J.; Lechner, S.M.; Markison, S.; Joswig, T.; Petroski, R.; Piercey, J.; Kargo, W.; Malany, S.; Santos, M.; Gross, R.S.; Wen, J.; Jalali, K.; O'Brien, Z.; Stotz, C.E.; Crespo, M.I.; Diaz, J.L.; Slee, D.H. Lead optimization of 4-acetylamino-2-(3,5-dimethylpyrazol-1-yl)-6-pyridylpyrimidines as A_{2A} adenosine receptor antagonists for the treatment of Parkinson's disease. *J. Med. Chem.*, **2008**, *51*(22), 7099-7110.

96. Volpini, R.; Dal Ben, D.; Lambertucci, C.; Marucci, G.; Mishra, R.C.; Ramadori, A.T.; Klotz, K.N.; Trincavelli, M.L.; Martini, C.; Cristalli, G. Adenosine A_{2A} receptor antagonists: new 8-substituted 9-ethyladenines as tools for *in vivo* rat models of Parkinson's disease. *ChemMedChem*, **2009**, *4*(6), 1010-1019.

97. Zhou, G.; Aslanian, R.; Gallo, G.; Khan, T.; Kuang, R.; Purakkattle, B.; De Ruiz, M.; Stamford, A.; Ting, P.; Wu, H.; Wang, H.; Xiao, D.; Yu, T.; Zhang, Y.; Mullins, D.; Hodgson, R. Discovery of aminoquinazoline derivatives as human A_{2A} adenosine receptor antagonists. *Bioorg. Med. Chem. Lett.*, **2016**, *26*(4), 1348-1354.

98. Ahmed, S.S.S.J.; Ahameethunisa, A.; Santos, W. QSAR and pharmacophore modeling of 4-arylthieno [3, 2-*d*] pyrimidine derivatives against adenosine receptor of Parkinson's Disease. *J. Theor. Comput. Chem.*, ***2010***, *9*(6), 975-991.

99. Ghatol, S.P.; Verma, S.; Agarwal, K.; Sharon, A. Pharmacophore Distance Mapping and Docking Study of Some Benzimidazole Analogs as A_{2A} Receptor Antagonists. *Receptor*, **2010**, *16*(C2), 2.413.

100. Preti, D.; Baraldi, P.G.; Moorman, A.R.; Borea, P.A.; Varani, K. History and perspectives of A_{2A} adenosine receptor antagonists as potential therapeutic agents. *Med. Res. Rev.*, **2015**, *35*(4), 790-848.

101. Dungo, R.; Deeks, E.D. Istradefylline: first global approval. *Drugs*, **2013**, *73*(8), 875-882.

102. Caulfield, M.P.; Birdsall, N.J. International Union of Pharmacology. XVII. Classification of muscarinic acetylcholine receptors. *Pharmacol. Rev.*, **1998**, *50*(2), 279-290.

103. Langmead, C.J.; Watson, J.; Reavill, C. Muscarinic acetylcholine receptors as CNS drug targets. *Pharmacol. Ther.*, **2008**, *117*(2), 232-243.

104. Hasselmo, M.E. The Role of Acetylcholine in Learning and Memory. *Curr. Opin. Neurobiol.*, **2006**, *16*(6), 710-715.

105. Maehara, S.; Hikichi, H.; Ohta, H. Behavioral effects of *N*-desmethylclozapine on locomotor activity and sensorimotor gating function in mice - possible involvement of muscarinic receptors. *Brain Res.*, **2011**, *1418*, 111-119.

106. Lehmann, J.; Langer, S.Z. The striatal cholinergic interneuron: Synaptic target of dopaminergic terminals? *Neuroscience*, **1983**, *10*(4), 1105-1120.

107. Xiang, Z.; Thompson, A.D.; Jones, C.K.; Lindsley, C.W.; Conn, P.J. Roles of the M_1 Muscarinic Acetylcholine Receptor Subtype in the Regulation of Basal Ganglia Function and Implications for the Treatment of Parkinson's Disease. *J. Pharmacol. Exp. Ther.*, **2012**, *340*(3), 595-603.

108. Ztaou, S.; Maurice, N.; Camon, J. Guiraudie-Capraz, G.; Kerkerian-Le Goff, L.; Beurrier, C.; Liberge, M.; Amalric, M. Involvement of Striatal Cholinergic Interneurons and M_1 and M_4 Muscarinic Receptors in Motor Symptoms of Parkinson's Disease. *J. Neurosci.*, **2016**, *36*(35), 9161-9172.

109. Mayorga, A.J.; Cousins, M.S.; Trevitt, J.T.; Conlan, A.; Gianutsos, G.; Salamone, J.D. Characterization of the muscarinic receptor subtype mediating pilocarpine-induced tremulous jaw movements in rats. *Eur. J. Pharmacol.*, **1999**, *364*(1), 7-11.

110. Betz, A.J.; McLaughlin, P.J.; Burgos, M.; Weber, S.M.; Salamone, J.D. The muscarinic receptor antagonist tropicamide suppresses tremulous jaw movements in a rodent model of parkinsonian tremor: possible role of M_4 receptors. *Psychopharmacology (Berl)*, **2007**, *194*(3), 347-359.

111. Tzavara, E.T.; Bymaster, F.P.; David, R.J.; Wade, M.R.; Perry, K.W.; Wess, J.; McKinzie, D.L.; Felder, C.; Nomikos, G.G. M_4 muscarinic receptors regulate the dynamics of cholinergic and dopaminergic neurotransmission: relevance to the pathophysiology and treatment of related CNS pathologies. *FASEB J.*, **2004**, *18*(12), 1410-1412.

112. Gomeza, J.; Zhang, L.; Kostenis, E.; Felder, C.C.; Bymaster, F.P.; Brodkin, J.; Shannon, H.; Xia, B.; Duttaroy, A.; Deng, C.-x. Generation and pharmacological analysis of M_2 and M_4 muscarinic receptor knockout mice. *Life Sci.*, **2001**, *68*(22), 2457-2466.

113. Fink-Jensen, A.; Schmidt, L.S.; Dencker, D.; Schulein, C.; Wess, J.; Wortwein, G.; Woldbye, D.P.D. Antipsychotic-induced catalepsy is attenuated in mice lacking the M_4 muscarinic acetylcholine receptor. *Eur. J. Pharmacol.*, **2011**, *656*(0), 39-44.

114. Augelli-Szafran, C.E.; Blankley, C.J.; Jaen, J.C.; Moreland, D.W.; Nelson, C.B.; Penvose-Yi, J.R.; Schwarz, R.D.; Thomas, A.J. Identification and characterization of M_1 selective muscarinic receptor antagonists. *J. Med. Chem.*, **1999**, *42*(3), 356-363.

115. Eberlein, W.G.; Engel, W.W.; Trummlitz, G.; Schmidt, G.; Hammer, R. Tricyclic compounds as selective antimuscarinics. 2. Structure-activity relationships of M_1-selective antimuscarinics related to pirenzepine. *J. Med. Chem.*, **1988**, *31*(6), 1169-1174.

116. Selent, J.; Brandt, W.; Pamperin, D.; Gober, B. Enantiomeric *N*-methyl-4-piperidyl benzilates as muscarinic receptor ligands: Radioligand binding studies and docking studies to models of the three muscarinic receptors M_1, M_2 and M_3. *Bioorg. Med. Chem.*, **2006**, *14*(6), 1729-1736.

117. Miller, N.R.; Daniels, R.N.; Lee, D.; Conn, P.J.; Lindsley, C.W. Synthesis and SAR of *N*-(4-(4-alklylpiperazin-1-yl)phenyl)benzamides as muscarinic acetylcholine receptor subtype 1 (M_1) antagonists. *Bioorg. Med. Chem. Lett.*, **2010**, *20*(7), 2174-2177.

118. Weaver, C.D.; Sheffler, D.J.; Lewis, L.M.; Bridges, T.M.; Williams, R.; Nalywajko, N.T.; Kennedy, J.P.; Mulder, M.M.; Jadhav, S.; Aldrich, L.A.; Jones, C.K.; Mario, J.E.; Niswender, C.M.; Mock, M.M.; Zheng, F.; Conn, P.J.; Lindsley, C.W. Discovery and development of a potent and highly selective small molecule muscarinic acetylcholine receptor subtype I ($mAChR_1$ or M_1) antagonist *in vitro* and *in vivo* probe. *Curr. Top. Med. Chem.*, **2009**, *9*(13), 1217-1226.

119. Melancon, B.J.; Lamers, A.P.; Bridges, T.M.; Sulikowski, G.A.; Utley, T.J.; Sheffler, D.J.; Noetzel, M.J.; Morrison, R.D.; Scott Daniels, J.; Niswender, C.M.; Jones, C.K.; Jeffrey Conn, P.; Lindsley, C.W.; Wood, M.R. Development of a more highly selective M_1 antagonist from the continued optimization of the MLPCN Probe ML012. *Bioorg. Med. Chem. Lett.*, **2012**, *22*(2), 1044-1048.

120. Melancon, B.J.; Utley, T.J.; Sevel, C.; Mattmann, M.E.; Cheung, Y.-Y.; Bridges, T.M.; Morrison, R.D.; Sheffler, D.J.; Niswender, C.M.; Scott Daniels, J.; Jeffrey Conn, P.; Lindsley, C.W.; Wood, M.R. Development of novel M1 antagonist scaffolds through the continued optimization of the MLPCN probe ML012. *Bioorg. Med. Chem. Lett.*, **2012**, *22*(15), 5035-5040.

121. Poslusney, M.S.; Sevel, C.; Utley, T.J.; Bridges, T.M.; Morrison, R.D.; Kett, N.R.; Sheffler, D.J.; Niswender, C.M.; Daniels, J.S.; Conn, P.J.; Lindsley, C.W.; Wood, M.R. Synthesis and biological characterization of a series of novel diaryl amide M_1 antagonists. *Bioorg. Med. Chem. Lett.*, **2012**, *22*(22), 6923-6928.

122. Ramos, A.C.; Andersen, M.L.; Oliveira, M.G.; Soeiro, A.C.; Galduroz, J.C. Biperiden (M_1 antagonist) impairs the expression of cocaine conditioned place preference but potentiates the expression of cocaine-induced behavioral sensitization. *Behav. Brain Res.*, **2012**, *231*(1), 213-216.

123. Giachetti, A.; Giraldo, E.; Ladinsky, H.; Montagna, E. Binding and functional profiles of the selective M1 muscarinic receptor antagonists trihexyphenidyl and dicyclomine. *Br. J. Pharmacol.*, **1986**, *89*(1), 83-90.

124. Thomas, D.R.; Dada, A.; Jones, G.A.; Deisz, R.A.; Gigout, S.; Langmead, C.J.; Werry, T.D.; Hendry, N.; Hagan, J.J.; Davies, C.H.; Watson, J.M. *N*-desmethylclozapine (NDMC) is an antagonist at the human native muscarinic M_1 receptor. Neuropharmacology, **2010**, *58*(8), 1206-1214.

125. Cazzola, M.; Matera, M.G.; Liccardi, G.; Sacerdoti, G.; D'Amato, G.; Rossi, F. Effect of telenzepine, an M_1-selective muscarinic receptor antagonist, in patients with nocturnal asthma. *Pulm. Pharmacol.*, **1994**, *7*(2), 91-97.

126. Hammer, R.; Berrie, C.P.; Birdsall, N.J.M.; Burgen, A.S.V., Hulme, E.C. Pirenzepine distinguishes between different subclasses of muscarinic receptors. *Nature*, **1980**, *283*(5742), 90-92.

127. Augelli-Szafran, C.E.; Jaen, J.C.; Moreland, D.W.; Nelson, C.B.; Penvose-Yi, J.R.; Schwarz, R.D. Identification and characterization of M_4 selective muscarinic antagonists. *Bioorg. Med. Chem. Lett.*, **1998**, *8*(15), 1991-1996.

128. Varoli, L.; Andreani, A.; Burnelli, S.; Granaiola, M.; Leoni, A.; Locatelli, A.; Morigi, R.; Rambaldi, M.; Bedini, A.; Fazio, N.; Spampinato, S. Diphenol-related diamines as novel muscarinic M_4 receptor antagonists. *Bioorg. Med. Chem. Lett.*, **2008**, *18*(9), 2972-2976.

129. Varoli, L., Angeli, P. Buccioni, M.; Burnelli, S.; Fazio, N; Marucci, G.; Recanatini, M.; Spampinato, S. Synthesis and pharmacological profile of a series of 1-substituted-2-carbonyl derivatives of Diphenidol: novel M_4 muscarinic receptor antagonists. *Med. Chem.*, **2008**, *4*(2), 121-128.

130. Michelle Lewis, L.; Sheffler, D.; Williams, R.; Bridges, T.M.; Kennedy, J.P.; Brogan, J.T.; Mulder, M.J.; Williams, L.; Nalywajko, N.T.; Niswender, C.M.; Weaver, C.D.; Conn, P.J.; Lindsley, C.W. Synthesis and SAR of selective muscarinic acetylcholine receptor subtype 1 (M_1 mAChR) antagonists. *Bioorg. Med. Chem. Lett.*, **2008**, *18*(3), 885-890.

131. Böhme, T.M.; Augelli-Szafran, C.E.; Hallak, H.; Pugsley, T.; Serpa, K.; Schwarz, R.D. Synthesis and Pharmacology of Benzoxazines as Highly Selective Antagonists at M_4 Muscarinic Receptors. *J. Med. Chem.*, **2002**, *45*(14), 3094-3102.

132. Croy, C.H.; Chan, W.Y.; Castetter, A.M.; Watt, M.L.; Quets, A.T.; Felder, C.C. Characterization of PCS1055, a novel muscarinic M_4 receptor antagonist. *Eur. J. Pharmacol.*, **2016**, *782*, 70-76.

133. Veeraragavan, S.; Bui, N.; Perkins, J.R.; Yuva-Paylor, L.A.; Paylor, R. The modulation of fragile X behaviors by the muscarinic M_4 antagonist, tropicamide. *Behav. Neurosci.*, **2011**, *125*(5), 783-790.

134. Hovelsø, N.; Sotty, F.; Montezinho, L.P.; Pinheiro, P.S.; Herrik, K.F.; Mørk, A. Therapeutic Potential of Metabotropic Glutamate Receptor Modulators. *Curr. Neuropharmacol.*, **2012**, *10*(1), 12-48.

135. Breysse, N.; Amalric, M.; Salin, P. Metabotropic glutamate 5 receptor blockade alleviates akinesia by normalizing activity of selective basal-ganglia structures in parkinsonian rats. *J. Neurosci.,* **2003**. *23*(23), 8302-8309.

136. Ossowska, K.; Konieczny, J.; Wolfarth, S.; Pilc, A. MTEP, a new selective antagonist of the metabotropic glutamate receptor subtype 5 ($mGluR_5$), produces antiparkinsonian-like effects in rats. *Neuropharmacology*, **2005**, *49*(4), 447-455.

137. Ossowska, K.; Konieczny, J.; Wolfarth, S.; Wieronska, J.; Pilc, A. Blockade of the metabotropic glutamate receptor subtype 5 ($mGluR_5$) produces antiparkinsonian-like effects in rats. *Neuropharmacology*, **2001**, *41*(4), 413-420.

138. Dekundy, A.; Pietraszek, M.; Schaefer, D.; Cenci, M.A.; Danysz, W. Effects of group I metabotropic glutamate receptors blockade in experimental models of Parkinson's disease. *Brain Res. Bull.*, **2006**, *69*(3), 318-326.

139. Kachroo, A.; Orlando, L.R.; Grandy, D.K.; Chen, J.F.; Young, A.B.; Schwarschild, M.A. Interactions between metabotropic glutamate 5 and adenosine A_{2A} receptors in normal and parkinsonian mice. *J. Neurosci.*, **2005**, *25*(45), 10414-10419.

140. Coccurello, R.; Breysse, N.; Amalric, M. Simultaneous blockade of adenosine A_{2A} and metabotropic glutamate $mGlu_5$ receptors increase their efficacy in reversing Parkinsonian deficits in rats. *Neuropsychopharmacology*, **2004**, *29*(8), 1451-1461.

141. Turle-Lorenzo, N.; Breysse, N.; Baunez, C.; Amalric, M. Functional interaction between $mGlu_5$ and NMDA receptors in a rat model of Parkinson's disease. *Psychopharmacology (Berl)*, **2005**, *179*(1), 117-127.

142. Armentero, M.T., Fancellu, R.; Nappi, G.; Bramanti, P.; Blandini, F. Prolonged blockade of NMDA or mGluR5 glutamate receptors reduces nigrostriatal degeneration while inducing selective metabolic changes in the basal ganglia circuitry in a rodent model of Parkinson's disease. *Neurobiol. Dis.*, **2006**, *22*(1), 1-9.

143. Oueslati, A.; Breysse, N.; Amalric, M.; Kerkerian-Le Goff, L.; Salin, P. Dysfunction of the cortico-basal ganglia-cortical loop in a rat model of early parkinsonism is reversed by metabotropic glutamate receptor 5 antagonism. *Eur. J. Neurosci.,* **2005**, *22*(11), 2765-2774.

144. Levandis, G.; Bazzini, E.; Armentero, M.T.; Nappi, G.; Blandini, F. Systemic administration of an $mGluR_5$ antagonist, but not unilateral subthalamic lesion, counteracts L-DOPA-induced dyskinesias in a rodent model of Parkinson's disease. *Neurobiol. Dis.*, **2008**, *29*(1), 161-168.

145. Rylander, D.; Iderberg, H.; Li, Q.; Dekundy, A.; Zhang, J.; Li, H.; Baishen, R.; Danysz, W.; Bezard, E.; Cenci, M.A. A $mGluR_5$ antagonist under clinical development improves L-DOPA-induced dyskinesia in parkinsonian rats and monkeys. *Neurobiol. Dis.*, **2010**, *39*(3), 352-361.

146. Battaglia, G.; Busceti, C.L.; Molinaro, G.; Biagioni, F.; Storto, M.; Fornai, F.; Nicoletti, F.; Bruno, V. Endogenous activation of $mGlu_5$ metabotropic glutamate receptors contributes to the development of nigro-striatal damage induced by 1-methyl-4-phenyl-1,2,3,6-tetrahydropyridine in mice. *J. Neurosci.*, **2004**, *24*(4), 828-835.

147. Aguirre, J.A.; Kehr, J. Yoshitake, T.; Liu, F.L.; Rivera, A.; Fernandez-Espinola, S.; Andbjer, B.; Leo, G.; Medhurst, A.D.; Agnati, L.F.; Fuxe, K. Protection but maintained dysfunction of nigral dopaminergic nerve cell bodies and striatal dopaminergic terminals in MPTP-lesioned mice after acute treatment with the $mGluR_5$ antagonist MPEP. *Brain Res*., **2005**, *1033*(2), 216-220.

148. Vernon, A.C.; Palmer, S.; Datla, K.P.; Zbarsky, V.; Croucher, M.J.; Dexter, D.T. Neuroprotective effects of metabotropic glutamate receptor ligands in a 6-hydroxydopamine rodent model of Parkinson's disease. *Eur. J. Neurosci.*, **2005**, *22*(7), 1799-1806.

149. Vernon, A.C.; Zbarsky, V.; Datla, K.P.; Croucher, M.J.; Dexter, D.T. Subtype selective antagonism of substantia nigra pars compacta Group I metabotropic glutamate receptors protects the nigrostriatal system against 6-hydroxydopamine toxicity *in vivo*. *J. Neurochem.*, **2007**, *103*(3), 1075-1091.

150. Battaglia, G.; Fornal, F.; Busceti, C.L.; Aloisi, G.; Cerrito, F.; De Blasi, A.; Melchiorri, D.; Nicoletti, F. Selective blockade of $mGlu_5$ metabotropic glutamate receptors is protective against methamphetamine neurotoxicity. *J. Neurosci.*, **2002**, *22*(6), 2135-2141.

151. Zhang, L.; Balan, G.; Barreiro, G.; Boscoe, B.P.; Chenard, L.K.; Cianfrogna, J.; Claffey, M.M.; Chen, L.; Coffman, K.J.; Drozda, S.E.; Dunetz, J.R.; Fonseca, K.R.; Galatsis, P.; Grimwood, S.; Lazzaro, J.T.; Mancuso, J.Y.; Miller, E.L.; Reese M.R.; Rogers, B.N.; Sakurada, I.; Skaddan, M.; Smith, D.L.; Stepan,

A.F.; Trapa, P.; Tuttle, J.B.; Verhoest, P.R.; Walker, D.P.; Wright, A.S.; Zaleska, M.M.; Zasadny, K.; Shaffer, C.L. Discovery and Preclinical Characterization of 1-Methyl-3-(4-methylpyridin-3-yl)-6-(pyridin-2-ylmethoxy)-1*H*-pyrazolo-[3,4-*b*]pyrazine (PF470): A Highly Potent, Selective, and Efficacious Metabotropic Glutamate Receptor 5 ($mGluR_5$) Negative Allosteric Modulator. *J. Med. Chem.*, **2014**, *57*(3), 861-877.

152. Burdi, D.F.; Hunt, R.; Fan, L.; Hu, T.; Wang, J.; Guo, Z.; Huang, Z.; Wu, C.; Hardy, L.; Detheux, M.; Orsini, M.A.; Quinton, M.S.; Lew, R.; Spear, K. Design, Synthesis, and Structure−Activity Relationships of Novel Bicyclic Azole-amines as Negative Allosteric Modulators of Metabotropic Glutamate Receptor 5. *J. Med. Chem.*, **2010**, *53*(19), 7107-7118.

153. Keck, T.M.; Zou, M.-F.; Zhang, P.; Rutledge, R.P.; Newman, A.H. Metabotropic Glutamate Receptor 5 Negative Allosteric Modulators as Novel Tools for *in Vivo* Investigation. *ACS Med. Chem. Lett.*, **2012**, *3*(7), 544-549.

154. Cosford, N.D.; Tehrani, L.; Roppe, J.; Schweiger, E.; Smith, N.D.; Anderson, J.; Bristow, L.; Brodkin, J.; Jiang, X.; McDonald, I.; Rao, S.; Washburn, M.; Varney, M.A. 3-[(2-Methyl-1,3-thiazol-4-yl)ethynyl]-pyridine: a potent and highly selective metabotropic glutamate subtype 5 receptor antagonist with anxiolytic activity. *J. Med. Chem.*, **2003**, *46*(2), 204-206.

155. Sharma, S.; Kedrowski, J.; Rook, J.M.; Smith, R.L.; Jones, C.K.; Rodriguez, A.L.; Conn, P.J.; Lindsley, C.W. Discovery of Molecular Switches That Modulate Modes of Metabotropic Glutamate Receptor Subtype 5 ($mGlu_5$) Pharmacology *in Vitro* and *in Vivo* within a Series of Functionalized, Regioisomeric 2- and 5-(Phenylethynyl)pyrimidines. *J. Med. Chem.*, **2009**, *52*(14), 4103-4106.

156. Hirose, W.; Kato, Y.; Yamamoto, T.; Kassai, M.; Takata, M.; Hayashi, S.; Arai, Y.; Imai, S.; Yoshida, K. Synthesis, structure–activity relationships and biological evaluation of 4,5,6,7-tetrahydropyrazolopyrazines as metabotropic glutamate receptor 5 negative allosteric modulators. *Bioorg. Med. Chem. Lett.*, **2016**, *26*(16), 3866-3869.

157. Yoshikawa, K.; Ohyama, T.; Takahashi, E.; Numajiri, Y.; Konno, M.; Moriyama, M.; Takemi, N.; Kunita, K.; Nishimura, K.; Hayashi, R. Identification of α-substituted acylamines as novel, potent, and orally active $mGluR_5$ negative allosteric modulators. *Bioorg. Med. Chem. Lett.*, **2015**, *25*(16), 3135-3141.

158. Nógrádi, K.; Wágner, G.; Domány, G.; Bobok. A.; Magdó, I.; Kiss, B.; Kolok, S.; Fónagy, K.; Gyertyán, I.; Háda, V.; Kóti, J.; Gál, K.; Farkas, S.; Keseru, G.M.; Greiner, I.; Szombathelyi, Z. Thieno[2,3-*b*]pyridines as negative allosteric modulators of metabotropic $GluR_5$ receptors: Hit-to-lead optimization. *Bioorg. Med. Chem. Lett.*, **2014**, *24*(16), 3845-3849.

159. Kubas, H.; Meyer, U.; Hechenberger, M.; Klein, K.U.; Plitt, P.; Zemribo, R.; Spexgoor, H.W.; Van Assema, S.G.A.; Abel, U. Scaffold hopping approach towards various AFQ-056 analogs as potent metabotropic glutamate receptor 5 negative allosteric modulators. *Bioorg. Med. Chem. Lett.*, **2013**, *23*(23), 6370-6376.

160. Kubas, H.; Meyer, U.; Krueger, B.; Hechenberger, M.; Vanejevs, M.; Zemribo, R.; Kauss, V.; Ambartsumova, R.; Pyatkin, I.; Polosukhin, A.I.; Abel, U. Discovery, synthesis, and structure-activity relationships of 2-aminoquinazoline derivatives as a novel class of metabotropic glutamate receptor 5 negative allosteric modulators. *Bioorg. Med. Chem. Lett.*, **2013**, *23*(16), 4493-4500.

161. Chae, E.; Shin, Y.J.; Ryu, E.J.; Ji, M.K.; Ryune Cho, N.; Lee, K.H.; Jeong, H.J.; Kim, S.J.; Choi, Y.; Seok Oh, K.; Park, C.E.; Soo Yoon, Y. Discovery of biological evaluation of pyrazole/imidazole amides as $mGlu_5$ receptor negative allosteric modulators. *Bioorg. Med. Chem. Lett.*, **2013**, *23*(7), 2134-2139.

162. Xu, L.; Zhou, S.; Yu, K.; Gao, B.; Jiang, H.; Zhen, X.; Fu, W. Molecular Modeling of the 3D Structure of 5-HT_{1A}R: Discovery of Novel 5-HT_{1A}R Agonists via Dynamic Pharmacophore-Based Virtual Screening. *J Chem Inf Model*, **2013**, ***53***(12), 3202-3211.

163. Koller, M.; Carcache, D.A.; Orain, D.; Ertl, P.; Behnke, D.; Desrayaud, S.; Laue, G.; Vranesic, I. Discovery of 1*H*-pyrrolo[2,3-*c*]pyridine-7-carboxamides as novel, allosteric $mGluR_5$ antagonists. *Bioorg. Med. Chem. Lett*, **2012**, *22*(20), 6454-6459.

164. Packiarajan, M.; Ferreira, C.G.M.; Hong, S.P.; White, A.D.; Chandrasena, G.; Pu, X.; Brodbeck, R.M.; Robichaud, A.J. Azetidinyl oxadiazoles as potent mGluR5 positive allosteric modulators. *Bioorg. Med. Chem. Lett.*, **2012**, *22*(20), 6469-6474.

165. Konieczny, J.; Ossowska, K.; Wolfwarth, S.; Pilc, A. LY354740, a group II metabotropic glutamate receptor agonist with potential antiparkinsonian properties in rats. *Naunyn Schmiedeberg's Arch. Pharmacol.*, **1998**, *358*(4), 500-502.

166. Bradley, S.R.; Marino, M.J.; Wittmann, M.; Rouse, S.T.; Awad, H.; Levey, A.I.; Conn, P.J. Activation of group II metabotropic glutamate receptors inhibits synaptic excitation of the substantia Nigra *pars reticulata*. *J. Neurosci.*, **2000**, *20*(9), 3085-3094.

167. Matarredona, E.R.; Santiago, M.; Venero, J.L.; Cano, J.; Machado, A. Group II metabotropic glutamate receptor activation protects striatal dopaminergic nerve terminals against MPP^+-induced neurotoxicity along with brain-derived neurotrophic factor induction. *J. Neurochem.*, **2001**, *76*(2), 351-360.

168. Battaglia, G.; Busceti, C.L.; Pontarelli, F.; Biagioni, F.; Fornai, F.; Paparelli, A.; Bruno, V.; Ruggieri, S.; Nicoletti, F. Protective role of group-II metabotropic glutamate receptors against nigro-striatal degeneration induced by 1-methyl-4-phenyl-1,2,3,6-tetrahydropyridine in mice. *Neuropharmacology*, **2003**, *45*(2), 155-166.

169. Matsui, T.; Kita, H. Activation of group III metabotropic glutamate receptors presynaptically reduces both GABAergic and glutamatergic transmission in the rat globus pallidus. *Neuroscience*, **2003**, *122*(3), 727-737.

170. Valenti, O.; Marino, M.J.; Wittmann, M.; Lis, E.; DiLella, A.G.; Kinney, G.G.; Conn, P.J. Group III metabotropic glutamate receptor-mediated modulation of the striatopallidal synapse. *J. Neurosci.*, **2003**. *23*(18), 7218-7226.

171. Wittmann, M., Marino, M.J.; Bradley, S.R.; Conn, P.J. Activation of group III mGluRs inhibits GABAergic and glutamatergic transmission in the substantia nigra pars reticulata. *J. Neurophysiol.*, **2001**, *85*(5), 1960-1968.

172. MacInnes, N.; Messenger, M.J.; Duty, S. Activation of group III metabotropic glutamate receptors in selected regions of the basal ganglia alleviates akinesia in the reserpine-treated rat. *Br. J. Pharmacol.*, **2004**, *141*(1), 15-22.

173. Lopez, S.; Turle-Lorenzo, N.; Acher, F.; De Leonibus, E.; Mele, A.; Amalric, M. Targeting group III metabotropic glutamate receptors produces complex behavioral effects in rodent models of Parkinson's disease. *J. Neurosci.*, **2007**, *27*(25), 6701-6711.

174. Valenti, O.; Mannaloni, G.; Seabrook, G.R.; Conn, P.J.; Marino, M.J. Group III metabotropic glutamate-receptor-mediated modulation of excitatory transmission in rodent substantia nigra *pars compacta* dopamine neurons. *J. Pharmacol. Exp. Ther.*, **2005**, *313*(3), 1296-1304.

175. Zhang, L.; Brodney, M.A.; Candler, J.; Doran, A.C.; Duplantier, A.J.; Efremov, I.V.; Evrard, E.; Kraus, K.; Ganong, A.H.; Haas, J.A.; Hanks, A.N.; Jenza, K.; Lazzaro, J.T.; Maklad, N.; McCarthy, S.A.; Qian, W.; Rogers, B.N.; Rottas, M.D.; Schmidt, C.J.; Sluciak, J.A.; Tingley, F.D.; Zhang, A.Q. 1-[(1-Methyl-1*H*-imidazol-2-yl)methyl]-4-phenylpiperidines as $mGluR_2$ Positive Allosteric Modulators for the Treatment of Psychosis. *J. Med. Chem.*, **2011**, *54*(6), 1724-1739.

176. Andrés, J.I.,; Alcázar, J.; Cid, J.M.; De Angelis, M.; Iturrino, L.; Langlois, X.; Lavreysen, H.; Trabanco, A.A.; Celen, S.; Bormans, G. Synthesis, evaluation, and radiolabeling of new potent positive allosteric modulators of the metabotropic glutamate receptor 2 as potential tracers for positron emission tomography imaging. *J. Med. Chem.*, **2012**, *55*(20), 8685-8699.

177. Trabanco, A.A.; Duvey, G.; Cid, J.M.; MacDonald, G.J.; Cluzeau, P.; Nhem, V.; Furnari, R.; Behaj, N.; Poulain, G.; Finn, T.; Lavreysen, H.; Poli, S.; Raux, A.; Thollon, Y.; Poirier, N.; Daddona, D.; Andrés, J.I.; Lutjens, R.; Poul, E.L.; Imogai, H.; Rocher, J.P. New positive allosteric modulators of the metabotropic glutamate receptor 2 ($mGluR_2$): Identification and synthesis of *N*-propyl-8-chloro-6-substituted isoquinolones. *Bioorg. Med. Chem. Lett.*, **2011**, *21*(3), 971-976.

178. Cid, J.M.; Duvey, G.; Cluzeau, P.; Nhem, V.; MacAry, K.; Raux, A.; Poirier, N.; Muller, J.; Boléa, C.; Finn, T.; Poli, S.; Epping-Jordan, M.; Chamelot, E.; Derouet, F.; Girard, F.; MacDonald, G.J.; Vega, J.A.; De Lucas, A.I.; Matesanz, E.; Lavreysen, H.; Linares, M.L.; Oehlrich, D.; Oyarzábal, J.; Tresadern, G.; Trabanco, A.A.; Andrés, J.I.; Le Poul, E.; Imogai, H.; Lutjens, R.; Rocher, J.P. Discovery of 1,5-disubstituted pyridones: A new class of positive allosteric modulators of the metabotropic glutamate 2 receptor. *ACS Chem. Neurosci.*, **2010**, *1*(12), 788-795.

179. Garbaccio, R.M.; Brnardic, E.J.; Fraley, M.E.; Hartman, G.D.; Hutson. P.H.; O'Brien, J.A.; Magliaro, B.C.; Uslaner, J.M.; Huszar, S.L.; Fillgrove, K.L.; Small, J.H.; Tang, C.; Kuo, Y.; Jacobson, M.A. Discovery of oxazolobenzimidazoles as positive allosteric modulators for the $mGluR_2$ receptor. *ACS Med. Chem. Lett.*, **2010**, *1*(8), 406-410.

180. Brnardic, E.J.; Fraley, M.E.; Garbaccio, R.M.; Layton, M.E.; Sanders, J.M.; Culberson, C.; Jacobson, M.A.; Magliaro, B.C.; Hutson, P.H.; O'Brien, J.A.; Huszar, S.L.; Uslaner, J.M.; Fillgrove, K.L.; Tang, C.; Kuo, Y.; Sur, S.M.; Hartman, G.D. 3-Aryl-5-phenoxymethyl-1,3-oxazolidin-2-ones as positive allosteric modulators of $mGluR_2$ for the treatment of schizophrenia: Hit-to-lead efforts. *Bioorg. Med. Chem. Lett.*, **2010**, *20*(10), 3129-3133.

181. Tresadern, G.; Cid, J.M.; MacDonald, G.J.; Vega, J.A.; de Lucas, A.I.; García, A.; Matesanz, E.; Linares, M.L.; Oehlrich, D.; Lavreysen, H.; Biesmans, I.; Trabanco, A.A. Scaffold hopping from pyridones to imidazo[1,2-*a*]pyridines. New positive allosteric modulators of metabotropic glutamate 2 receptor. *Bioorg. Med. Chem. Lett.*, **2010**, *20*(1), 175-179.

182. Huynh, T.H.V.; Erichsen, M.N.; Tora, A.S.; Goudet, C.; Sagot, E.; Assaf, Z.; Thomsen, C.; Brodbeck, R.; Stensbøl, T.B.; Bjørn-Yoshimoto, W.E.; Nielsen, B.; Pin, J.P.; Gefflaut, T.; Bunch, L. New 4-Functionalized Glutamate Analogues Are Selective Agonists at Metabotropic Glutamate Receptor Subtype 2 or Selective Agonists at Metabotropic Glutamate Receptor Group III. *J. Med. Chem.*, **2016**, *59*(3), 914-924.

183. Engers, D.W.; Niswender, C.M.; Weaver, C.D.; Jadhav. S.; Menon, U.N.; Zamorano, R.; Conn, P.J.; Lindsley, C.W.; Hopkins, C.R. Synthesis and Evaluation of a Series of Heterobiarylamides That Are Centrally Penetrant Metabotropic Glutamate Receptor 4 ($mGluR_4$) Positive Allosteric Modulators (PAMs). *J. Med. Chem.*, **2009**, *52*(14), 4115-4118.

184. Jones, C.K.; Engers, D.W.; Thompson, A.D.; Field, J.R.; Blobaum, A.L.; Lindsley, S.R.; Zhou, Y.; Gogliotti, R.D.; Jadhav, S.; Zamorano, R.; Bogenpohl, J.; Smith, Y.; Morrison, R.; Daniels, J.S.; Weaver, C.D.; Conn, P.J.; Lindsley, C.W.; Niswender, C.M.; Hopkins, C.R. Discovery, Synthesis, and Structure–Activity Relationship Development of a Series of *N*-4-(2,5-Dioxopyrrolidin-1-yl)phenylpicolinamides (VU0400195, ML182): Characterization of a Novel Positive Allosteric Modulator of the Metabotropic Glutamate Receptor 4 ($mGlu_4$) with Oral Efficacy in an Antiparkinsonian Animal Model. *J. Med. Chem.*, **2011**, *54*(21), 7639-7647.

185. Niswender, C.M.; Johnson, K.A.; Weaver, C.D.; Jones, C.K.; Xiang, Z.; Luo, Q.; Rodriguez, A.L.; Mario, J.E.; de Paulis, T.; Thompson, A.D.; Days, E.L.; Nalywajko, T.; Austin, C.A.; Williams, M.B.; Ayala, J.E.; Williams, R.; Lindsley, C.W.; Conn, P.J. Discovery, characterization, and antiparkinsonian effect of novel positive allosteric modulators of metabotropic glutamate receptor 4. *Mol. Pharmacol.*, **2008**, *74*(5), 1345-1358.

186. Niswender, C.M.; Lebois, E.P.; Luo, Q.; Kim, K.; Muchalski, H.; Yin, H.; Conn, P.J.; Lindsley, C.W. Positive allosteric modulators of the metabotropic glutamate receptor subtype 4 ($mGluR_4$): Part I. Discovery of pyrazolo[3,4-*d*]pyrimidines as novel $mGluR_4$ positive allosteric modulators. *Bioorg. Med. Chem. Lett.*, **2008**, *18*(20), 5626-5630.

187. Pithadia, A.B.; Jain, S.M. 5-Hydroxytryptamine Receptor Subtypes and their Modulators with Therapeutic Potentials**.** *J. Clin. Med. Res.*, **2009**, *1*(2), 72-80.

188. Scatton, B.; Javoy-Agid, F.; Rouquier, L.; Dubois, B.; Agid, Y. Reduction of cortical dopamine, noradrenaline, serotonin and their metabolites in Parkinson's disease. *Brain Res.*, **1983**, *275*(2), 321-328.

189. Halliday, G.M.; Blumbergs, P.C.; Cotton, R.G.; Blessing, W.W.; Geffen, L.B. Loss of brainstem serotonin- and substance P-containing neurons in Parkinson's disease. *Brain Res.*, **1990**, *510*(1), 104-107.

190. Kish, S.J.; Tong, J.; Hornykiewicz, O.; Rajput, A.; Chang, L.J.; Guttman, M.; Furukawa, Y. Preferential loss of serotonin markers in caudate versus putamen in Parkinson's disease. *Brain*, **2008**, *131*(Pt 1), 120-131.

191. Nayebi, A.M.; Rad, S.R.; Saberian, M.; Azimzadeh, S.; Samini, M. Buspirone improves 6-hydroxydopamine-induced catalepsy through stimulation of nigral 5-HT_{1A} receptors in rats. *Pharmacol. Rep.*, **2010**, *62*(2), 258-264.

192. Kleven, M.S.; Barret-Grévoz, C.; Slot, L.B.; Newman-Tancredi, A. Novel antipsychotic agents with 5-HT_{1A} agonist properties: Role of 5-HT_{1A} receptor activation in attenuation of catalepsy induction in rats. *Neuropharmacology*, **2005**, *49*(2), 135-143.

193. Ohno, Y.; Shimizu, S.; Imaki, J. Effects of tandospirone, a 5-HT_{1A} agonistic anxiolytic agent, on haloperidol-induced catalepsy and forebrain Fos expression in mice. *J. Pharmacol. Sci.*, **2009**, *109*(4), 593-599.

194. Mignon, L.; Wolf, W.A. Postsynaptic 5-HT_{1A} receptors mediate an increase in locomotor activity in the monoamine-depleted rat. *Psychopharmacology (Berl)*, **2002**, *163*(1), 85-94.

195. Dupre, K.B.; Eskow, K.L.; Barnum, C.J.; Bishop, C. Striatal 5-HT_{1A} receptor stimulation reduces D1 receptor-induced dyskinesia and improves movement in the hemiparkinsonian rat. *Neuropharmacology*, **2008**, *55*(8), 1321-1328.

196. Jones, C.A.; Johnston, L.C.; Jackson, M.J.; Smith, L.A.; van Scharrenburg, G.; Rose, S.; Jenner, P.G.; McCreary, A.C. An *in vivo* pharmacological evaluation of pardoprunox (SLV308)--a novel combined dopamine D_2/D_3 receptor partial agonist and 5-HT_{1A} receptor agonist with efficacy in experimental models of Parkinson's disease. *Eur. Neuropsychopharmacol.*, **2010**, *20*(8), 582-593.

197. Carta, M.; Carlsson, T.; Kirik, D.; Bjorklund, A. Dopamine released from 5-HT terminals is the cause of L-DOPA-induced dyskinesia in parkinsonian rats. *Brain*, **2007**, *130*(Pt 7), 1819-1833.

198. Lindgren, H.S.; Andersson, D.R.; Lagerkvist, S.; Nissbrandt, H.; Cenci, M.A. L-DOPA-induced dopamine efflux in the striatum and the substantia nigra in a rat model of Parkinson's disease: temporal and quantitative relationship to the expression of dyskinesia. *J. Neurochem.*, **2010**, *112*(6), 1465-1476.

199. Tayarani-Binazir, K.; Jackson, M.J.; Rose, S.; McCreary, A.C.; Jenner, P. The partial dopamine agonist pardoprunox (SLV308) administered in combination with L-DOPA improves efficacy and decreases dyskinesia in MPTP treated common marmosets. *Exp. Neurol.*, **2010**, *226*(2), 320-327.

200. Zhang, X.; Andren, P.E.; Greengard, P.; Svenningsson, P. Evidence for a role of the 5-HT_{1B} and its adaptor protein, p11, in L-DOPA treatment of an animal model of Parkinsonism. *Proc. Natl. Acad. Sci. U.S.A.*, **2008**, *105*(6), 2163-2168.

201. Jackson, M.J.; Al-Barghouthy, G.; Pearce, R.K.; Smith, L.; Hagan, J.J.; Jenner, P. Effect of 5-$HT_{1B/D}$ receptor agonist and antagonist administration on motor function in haloperidol and MPTP-treated common marmosets. *Pharmacol. Biochem. Behav.*, **2004**, *79*(3), 391-400.

202. Muñoz, A.; Carlsson, T.; Tronci, E.; Kirik, D.; Bjorklund, A.; Carta, M. Serotonin neuron-dependent and -independent reduction of dyskinesia by 5-HT_{1A} and 5-HT_{1B} receptor agonists in the rat Parkinson model. *Exp. Neurol.*, **2009**, *219*(1), 298-307.

203. Dhanawat, M.; Das, N.; Shrivastava, S.K. Design, synthesis, anticonvulsant screening and $5HT_{1A/2A}$ receptor affinity of N^3-substituted 2,4-imidazolidinediones and oxazolidinediones. *Drug Discov. Ther.*, **2016**, *5*(5), 227-237.

204. Pytka, K.; Walczak, M.; Kij. A.; Rapacz, A.; Siwek, A.; Kasek, G.; Olczyk, A.; Galuszka, A.; Waszkielewicz, A.; Marona, H.; Sapa, J.; Filipek, B. The antidepressant-like activity of 6-methoxy-2-[4-(2-methoxyphenyl)piperazin-1-yl]-9*H*-xanthen-9-one involves serotonergic 5-HT_{1A} and 5-$HT_{2A/C}$ receptors activation. *Eur. J. Pharmacol.*, **2015**, *764*, 537-546.

205. Partyka, A.; Chlon-Rzepa, G.; Wasik, A.; Jastrzebska-Wiesek, M.; Bucki, A.; Kolaczkowski, M.; Satala, G.; Bojarski, A.J.; Wesolowska, A. Antidepressant- and anxiolytic-like activity of 7-phenylpiperazinylalkyl-1,3-dimethyl-purine-2,6-dione derivatives with diversified 5-HT_{1A} receptor functional profile. *Bioorg. Med. Chem.*, **2015**, *23*(1), 212-221.

206. Bollinger, S.; Hubner, H.; Heinemann, F.W.; Meyer, K.; Gmeiner, P. Novel pyridylmethylamines as highly selective 5-HT_{1A} superagonists. *J. Med. Chem.*, **2010**, *53*(19), 7167-7179.

207. Franchini, S.; Prandi, A.; Baraldi, A.; Sorbi, C.; Tait, A.; Buccioni, M.; Marucci, G.; Cilia, A.; Pirona, L.; Fossa, P.; Cichero, E.; Brasili, L. 1,3-Dioxolane-based ligands incorporating a lactam or imide moiety: Structure-affinity/activity relationship at α_1-adrenoceptor subtypes and at 5-HT_{1A} receptors. *Eur. J. Med. Chem.*, **2010**, *45*(9), 3740-3751.

208. Carr, M.A.; Creviston, P.E.; Hutchison, D.R.; Kennedy, J.H.; Khau, V.V.; Kress, T.J.; Leanna, M.R.; Marshall, J.D.; Martinelli, M.J.; Peterson, B.C.; Varie, D.L.; Wepsiec, J.P. Synthetic Studies toward the Partial Ergot Alkaloid LY228729, a Potent $5HT_{1A}$ Receptor Agonist. *J. Org. Chem.*, **1997**, *62*(25), 8640-8653.

209. Neale, R.F.; Faillon, S.L.; Boyar, W.C.; Wasley, J.W.F.; Martin, L.L; Stone, G.A.; Glaeser, B.S.; Sinton, C.M.; Williams, M. Biochemical and pharmacological characterization of CGS 12066B, a selective serotonin-1B agonist. *Eur. J. Pharmacol.*, **1987**, *136*(1), 1-9.

210. Edmeads, J.G.; Millson D.S. Tolerability profile of zolmitriptan (Zomig™ 311C90), a novel dual central and peripherally acting $5HT_{1B/1D}$ agonist. *Cephalalgia*, **1997**, *17*(18_suppl), 41-52.

211. Jandu, K.S.; Barrett, V.; Brockwell, M.; Cambridge, D.; Farrant, D.R.; Foster, C.; Giles, H.; Glen, R.C.; Hill, A.P.; Hobbs, H.; Honey, A.; Martin, G.R.; Salmon, J.; Smith, D.; Woollard, P.; Selwood, D.L. Discovery of 4-[3-(trans-3-Dimethylaminocyclobutyl)-1*H*-indol-5-ylmethyl](4*S*)-oxazolidin-2-one (4991W93), a $5HT_{1B/1D}$ receptor partial agonist and a potent inhibitor of electrically induced plasma extravasation. *J. Med. Chem*., **2001**, *44*(5), 681-693.

212. Werneck, A.L.; Rosso, A.L.; Vincent, M.B. The use of an antagonist 5-$HT_{2A/C}$ for depression and motor function in Parkinson' disease. *Arq. Neuropsiquiatr.*, **2009**, *67*, 407-412.

213. Henderson, J.; Yiannikas, C.; Graham, J.S. Effect of ritanserin, a highly selective 5-HT_2 receptor antagonist, on Parkinson's disease. *Clin. Exp. Neurol.*, **1992**, *29*, 277-282.

214. Ferguson, M.C.; Nayyar, T.; Deutch, A.Y.; Ansah, T.A. 5-HT_{2A} receptor antagonists improve motor impairments in the MPTP mouse model of Parkinson's disease. *Neuropharmacology*, **2010**, *59*(1-2), 31-36.

215. Ansah, T.; Ferguson, M.; Nayyar, T. The 5-HT_{2A} Receptor Antagonist M100907 Produces Antiparkinsonian Effects and Decreases Striatal Glutamate. *Front. Syst. Neurosci.*, **2011**, *5*(48). Available from: https://www.ncbi.nlm.nih.gov/pmc/articles/PMC3117200/

216. Fox, S.H.; Moser, B.; Brotchie, J.M. Behavioral Effects of 5-HT_{2C} Receptor Antagonism in the Substantia Nigra Zona Reticulata of the 6-Hydroxydopamine-Lesioned Rat Model of Parkinson's Disease. *Exp. Neurol.*, **1998**, *151*(1), 35-49.

217. Fox, S.H.; Brotchie, J.M. 5-HT_{2C} receptor antagonists enhance the behavioural response to dopamine D_1 receptor agonists in the 6-hydroxydopamine-lesioned rat. *Eur. J. Pharmacol.*, **2000**, *398*(1), 59-64.

218. Watt, A.P.; Hitzel, L.; Mortishire-Smith, R.J. Enantiomeric separation of substituted 2-arylindoles on derivatised polysaccharide chiral stationary phases. *J. Biochem. Biophys. Methods*, **2002**, *54*(1-3), 275-286.

219. Campiani, G.; Butini, S.; Fattorusso, C.; Catalanotti, B.; Gemma, S.; Nacci, V.; Morelli, E.; Cagnotto, A.; Mereghetti, I.; Mennini, T.; Carli, M.; Minetti, P.; Di Cesare, M.A.; Mastroianni, D.; Scafetta, N.; Galletti, B.; Stasi, M.A.; Castorina, M.; Pacifici, L.; Vertechy, M.; Di Serio, S.; Ghirardi, O.; Tinti, O.; Carminati, P. Pyrrolo[1,3]benzothiazepine-Based Seroonin and Dopamine Receptor Antagonists. Molecular Modeling, Further Structure-Activity Relationship Studies, and Identification of Novel Atypical Antipsychotic Agents. *J. Med. Chem.*, **2004**, *47*(1), 143-157.

220. Johnsen, M.; Rehse, K.; Pertz, H.; Stasch, J.P.; Bischoff, E. New antithrombotic 1-Phthalazinamines with Serotonin Antagonistic Properties. *Arch. Pharm. (Weinheim)*, **2003**, *336*(12), 591-597.

221. González-Gómez, J.C.; Santana, L.; Uriarte, E.; Brea, J.; Villazón, M.; Loza, M.I.; De Luca, M.; Rivas, M.E.; Montenegro, G.Y.; Fontenla, J.A. New arylpiperazine derivatives with high affinity for α_{1A}, D_2 and 5-HT_{2A} receptors. *Bioorg. Med. Chem. Lett.*, **2003**, *13*(2), 175-178.

222. Swain, C.J.; Teran, A.; Maroto, M.; Cabello, A. Identification and optimisation of 5-amino-7-aryldihydro-1,4-diazepines as 5-HT_{2A} ligands. *Bioorg. Med. Chem. Lett.*, **2006**, *16*(23), 6058-6062.

223. Awouters, F.; Niemegeers, C.J.E.; Megens, A.A.H.P.; Meert, T.F.; Janssen, P.A.J. Pharmacological profile of ritanserin: A very specific central serotonin S_2-antagonist. *Drug Dev. Res.*, **1988**, *15*(1), 61-73.

224. Akhondzadeh, S.; Malek-Hosseini, M.; Ghoreishi, A.; Raznahan, M.; Rezazadeh, S.A. Effect of ritanserin, a $5HT_{2A/2C}$ antagonist, on negative symptoms of schizophrenia: A double-blind randomized placebo-controlled study. *Prog. Neuropsychopharmacol. Biol. Psychiatry*, **2008**, *32*(8), 1879-1883.

225. Carro, L.; Torrado, M.; Raviña, E.; Masaguer, C.F.; Lage, S.; Brea, J.; Loza, M.I. Synthesis and biological evaluation of a series of aminoalkyl-tetralones and tetralols as dual dopamine/serotonin ligands. *Eur. J. Med. Chem.*, **2014**, *71*, 237-249.

226. Tosh D.K.; Ciancetta, A.; Warnick, E.; Crane, S.; Gao, Z.G.; Jacobson, K.A.; Structure-based scaffold repurposing for G protein coupled receptors: Transformation of adenosine derivatives into $5HT_{2B}/5HT_{2C}$ serotonin receptor antagonists. *J. Med. Chem.*, **2016**, *59*(24), 11006-11026.

227. Di Matteo, V.; Di Giovanni, G.; Esposito, E.; SB 242084: A selective 5-HT_{2C} receptor antagonist. *CNS Drug Rev.*, **2000**, *6*(3), 195-205

228. De Azevedo Jr, W.F.; Canduri, F., Basso, L.A.; Palma, M.S.; Santos, D.S. Determining the structural basis for specificity of ligands using crystallographic screening, *Cell. Biochem. Biophys.*, **2006**, *44*(3), 405-411.

229. Levin, N.M.B.; Pintro, V.O.; De Avila, M.B.; De Mattos, B.B.; De Azevedo Jr, W.F. Understanding the Structural Basis for Inhibition of Cyclin-Dependent Kinases. New pieces in the Molecular Puzzle. *Curr. Drug Targets*. **2017**, *18*(9), 1104-1111.

230. Ghosh, E.; Kumari, P.; Jaiman, D.; Shukla, A.K. Methodological advances: the unsung heroes of the GPCR structural revolution. *Nat. Rev. Mol. Cell. Biol.*, **2015**, *16*(2), 69-81.

231. Palczewski, K.; Kumasaka, T.; Hori, T.; Behnke, C.A.; Motoshima, H.; Fox, B.A.; Le Trong, I.; Teller, D.C.; Okada, T.; Stenkamp, R.E.; Yamamoto, M.; Miyano, M. Crystal structure of rhodopsin: A G protein-coupled receptor. *Science*, **2000**, *289*(5480), 739-745.

232. Wang, C.; Jiang, Y.; Ma, J.; Wu, H.; Wacker, D.; Katritch, V.; Han, G.W.; Liu, W.; Huang, X.P.; Vardy, E.; McCorvy, J.D.; Gao, X.; Zhou, X.E.; Melcher, K.; Zhang, C.; Bai, F.; Yang, H.; Yang, L.; Jiang, H.; Roth, B.L.; Cherezov, V.; Stevens, R.C.; Xu, H.E. Structural basis for molecular recognition at serotonin receptors. *Science*, **2013**, *340*(6132), 610-614.

233. Wacker, D.; Wang, C.; Katritch, V.; Han, G.W.; Huang, X.P.; Vardy, E.; McCorvy, J.D.; Jiang, Y.; Chu, M.; Siu, F.Y.; Liu, W.; Xu, H.E.; Cherezov, V.; Roth, B.L.; Stevens, R.C. Structural features for functional selectivity at serotonin receptors. *Science*, **2013**, *340*(6132), 615-619.

234. Liu, W.; Wacker, D.; Gati, C.; Han, G.W.; James, D.; Wang, D.; Nelson, G.; Weierstall, U.; Katritch, V.; Barty, A.; Zatsepin, N.A.; Li, D.; Messerschmidt, M.; Boutet, S.; Williams, G.J.; Koglin, J.E.; Seibert, M.M.; Wang, C.; Shah, S.T.; Basu, S.; Fromme, R.; Kupitz, C.; Rendek, K.N.; Grotjohann, I.; Fromme, P.; Kirian, R.A.; Beyerlein, K.R.; White, T.A.; Chapman, H.N.; Caffrey, M.; Spence, J.C.; Stevens, R.C.; Cherezov, V. Serial femtosecond crystallography of G protein-coupled receptors. *Science*, **2013**, *342*(6165), 1521-1524.

235. Wacker, D.; Wang, S.; McCorvy, J.D.; Betz, R.M.; Venkatakrishnan, A.J.; Levit, A.; Lansu, K.; Schools, Z.L.; Che, T.; Nichols, D.E.; Shoichet, B.K.; Dror, R.O.; Roth, B.L. Crystal Structure of an LSD-Bound Human Serotonin Receptor, *Cell*, **2017**, *168*(3), 377-389.

236. Glukhova, A.; Thal, D.M.; Nguyen, A.T.; Vecchio, E.A.; Jorg, M.; Scammells, P.J.; May, L.T.; Sexton, P.M.; Christopoulos, A. Structure of the Adenosine A_1 Receptor Reveals the Basis for Subtype Selectivity. *Cell*, **2017**, *168*(5), 867-877.

237. Lebon, G.; Warne, T.; Edwards, P.C.; Bennett, K.; Langmead, C.J.; Leslie, A.G.W.; Tate, C.G. Agonist-Bound Adenosine A_{2A} Receptor Structures Reveal Common Features of GPCR Activation. *Nature*, **2011**, *474*, 521-525.

238. Dore, A.S.; Robertson, N.; Errey, J.C.; Ng, I.; Hollenstein, K.; Tehan, B.; Hurrell, E.; Bennett, K.; Congreve, M.; Magnani, F.; Tate, C.G.; Weir, M.; Marshall, F.H. Structure of the adenosine A_{2A} receptor in complex with ZM241385 and the xanthines XAC and cafeine. *Structure*, **2011**, *19*(9), 1283-1293.

239. Hino, T.; Arakawa, T.; Iwanari, H.; Yurugi-Kobayashi, T.; Ikeda-Suno, C.; Nakada-Nakura, Y.; Kusano-Arai, O.; Weyand, S.; Shimamura, T.; Nomura, N.; Cameron, A.D.; Kobayashi, T.; Hamakubo, T.; Iwata, S.; Murata, T. G-protein-coupled receptor inactivation by an allosteric inverse-agonist antibody. *Nature*, **2012**, *482*(7384), 237-240.

240. Congreve, M.; Andrews, S.P.; Dore, A.S.; Hollenstein, K.; Hurrell, E.; Langmead, C.J.; Mason, J.S.; Ng, I.W.; Tehan, B.; Zhukov, A.; Weir, M.; Marshall, F.H. Discovery of 1,2,4-Triazine Derivatives as Adenosine A_{2A} Antagonists using Structure Based Drug Design. *J. Med. Chem.*, **2012**, *55*(5), 1898-1903.

241. Liu, W.; Chun, E.; Thompson, A.A.; Chubukov, P.; Xu, F.; Katritch, V.; Han, G.W.; Roth, C.B.; Heitman, L.H.; IJzerman, A.P.; Cherezov, V.; Stevens, R.C. Structural basis for allosteric regulation of GPCRs by sodium ions. *Science*, **2012**, *337*(6091), 232-236.

242. Lebon, G.; Edwards, P.C.; Leslie, A.G.W.; Tate, C.G. Molecular Determinants of CGS21680 Binding to the Human Adenosine A_{2A} Receptor. *Mol. Pharmacol.*, **2015**, *87*(6), 907-915.

243. Melnikov, I.; Polovinkin, V.; Kovalev, K.; Gushchin, I.; Shevtsov, M.; Shevchenko, V.; Mishin, A.; Alekseev, A.; Rodriguez-Valera, F.; Borshchevskiy, V.; Cherezov, V.; Leonard, G.A.; Gordeliy, V.; Popov, A. Fast iodide-SAD phasing for high-throughput membrane protein structure determination. *Sci. Adv.*, **2017**, *3*, e1602952. Available from: https://www.ncbi.nlm.nih.gov/pmc/articles/PMC5429034/.

244. Carpenter, B.; Nehme, R.; Warne, T.; Leslie, A.G.W.; Tate, C.G. Structure of the Adenosine A_{2A} Receptor Bound to an Engineered G Protein. *Nature*, **2016**, *536*(7614), 104-107.

245. Segala, E.; Guo, D.; Cheng, R.K.; Bortolato, A.; Deflorian, F.; Dore, A.S.; Errey, J.C.; Heitman, L.H.; IJzerman, A.P.; Marshall, F.H.; Cooke, R.M. Controlling the Dissociation of Ligands from the Adenosine A_{2A} Receptor through Modulation of Salt Bridge Strength. *J. Med. Chem.*, **2016**, *59*(13), 6470-6479.

246. Batyuk, A.; Galli, L.; Ishchenko, A.; Han, G.W.; Gati, C.; Popov, P.A.; Lee, M.Y.; Stauch, B.; White, T.A.; Barty, A.; Aquila, A.; Hunter, M.S.; Liang, M.; Boutet, S.; Pu, M.; Liu, Z.J.; Nelson, G.; James, D.; Li, C.; Zhao, Y.; Spence, J.C.; Liu, W.; Fromme, P.; Katritch, V.; Weierstall, U.; Stevens, R.C.; Cherezov, V. Native phasing of X-ray free-electron laser data for a G protein–coupled receptor. *Sci. Adv.*, **2016**, *2*, e1600292.

247. Sun, B.; Bachhawat, P.; Chu, M.L.; Wood, M.; Ceska, T.; Sands, Z.A.; Mercier, J.; Lebon, F.; Kobilka, T.S.; Kobilka, B.K. Crystal structure of the adenosine A_{2A} receptor bound to an antagonist reveals a potential allosteric pocket. *Proc. Natl. Acad. Sci. U.S.A.*, **2017**, *114*(8), 2066-2071.

248. Martin-Garcia, J.M.; Conrad, C.E.; Nelson, G.; Stander, N.; Zatsepin, N.A.; Zook, J.; Zhu, L.; Geiger, J.; Chun, E.; Kissick, D.; Hilgart, M.C.; Ogata, C.; Ishchenko, A.; Nagaratnam, N.; Roy-Chowdhury, S.; Coe, J.; Subramanian, G.; Schaffer, A.; James, D.; Ketawala, G.; Venugopalan, N.; Xu, S.; Corcoran, S.; Ferguson, D.; Weierstall, U.; Spence, J.C.H.; Cherezov, V.; Fromme, P.; Fischetti, R.F.; Liu, W. Serial Millisecond Crystallography of Membrane and Soluble Protein Micro-crystals using Synchrotron Radiation. *IUCrJ*, **2017**, *4*. Available from: https://doi.org/10.1107/S205225251700570X.

249. Ma, Y.; Yue, Y.; Ma, Y.; Zhang, Q.; Zhou, Q.; Song, Y.; Shen, Y.; Li, X.; Ma, X.; Li, C.; Hanson, M.A.; Han, G.W.; Sickmier, E.A.; Swaminath, G.; Zhao, S.; Stevems, R.C.; Hu, L.A.; Zhong, W.; Zhang, M.; Xu, F. Structural Basis for Apelin Control of the Human Apelin Receptor. *Structure*, **2017**, *25*(6), 858-866.

250. Zhang, H.; Unal, H.; Gati, C.; Han, G.W.; Liu, W.; Zatsepin, N.A.; James, D.; Wang, D.; Nelson, G.; Weierstall, U.; Sawaya, M.R.; Xu, Q.; Messerschmidt, M.; Williams, G.J.; Boutet, S.; Yefanov, O.M.; White, T.A.; Wang, C.; Ishchenko, A.; Tirupula, K.C.; Desnoyer, R.; Coe, J.; Conrad, C.E.; Fromme, P.; Stevens, R.C.; Katritch, V.; Karnik, S.S.; Cherezov, V. Structure of the Angiotensin receptor revealed by serial femtosecond crystallography. *Cell*, **2015**, *161*(4), 833-844.

251. Zhang, H.; Unal, H.; Desnoyer, R.; Han, G.W.; Patel, N.; Katritch, V.; Karnik, S.S.; Cherezov, V.; Stevens, R.C. Structural Basis for Ligand Recognition and Functional Selectivity at Angiotensin Receptor. *J. Biol. Chem.*, **2015**, *290*(49), 29127-29139.

252. Zhang, H.; Han, G.W.; Batyuk, A.; Ishchenko, A.; White, K.L.; Patel, N.; Sadybekov, A.; Zamlynny, B.; Rudd, M.T.; Hollenstein, K.; Tolstikova, A.; White, T.A.; Hunter, M.S.; Weierstall, U.; Liu, W.; Babaoglu, K.; Moore, E.L.; Katz, R.D.; Shipman, J.M.; Garcia-Calvo, M.; Sharma, S.; Sheth, P.; Soisson, S.M.; Stevens, R.C.; Katritch, V.; Cherezov, V. Structural basis for selectivity and diversity in angiotensin II receptors. *Nature*, **2017**, *544*(7650), 327-332.

253. Warne, T.; Serrano-Vega, M.J.; Baker, J.G.; Moukhametzianov, R.; Edwards, P.C.; Henderson, R.; Leslie, A.G.; Tate, C.G.; Schertler, G.F. Structure of a β_1-adrenergic G-protein-coupled receptor. *Nature*, **2008**, *454*(7203), 486-491.

254. Warne, A.; Moukhametzianov, R.; Baker, J.G.; Nehme, R.; Edwards, P.C.; Leslie, A.G.W.; Schertler, G.F.X.; Tate, C.G. The Structural Basis for Agonist and Partial Agonist Action on a β_1-Adrenergic Receptor. *Nature*, **2011**, *469*(7329), 241-244.

255. Moukhametzianov, R.; Warne, T.; Edwards, P.C.; Serrano-Vega, M.J.; Leslie, A.G.W.; Tate, C.G.; Schertler, G.F.X. Two Distinct Conformations of Helix 6 Observed in Antagonist-Bound Structures of a β_1-Adrenergic Receptor. *Proc. Natl. Acad. Sci. U.S.A.*, **2011**, *108*(20), 8228-8232.

256. Christopher, J.; Brown, J.; Dore, A.; Errey, J.; Koglin, M.; Marshall, F.H.; Myszka, D.; Rich, R.L.; Tate, C.G.; Tehan, B.; Warne, T.; Congreve, M. Biophysical Fragment Screening of the β_1-Adrenergic

Receptor: Identification of High Affinity Aryl Piperazine Leads Using Structure-Based Drug Design. *J. Med. Chem.*, **2013**, *56*(9), 3446-3455.

257. Warne, T.; Edwards, P.C.; Leslie, A.G.; Tate, C.G. Crystal Structures of a Stabilized β_1-Adrenoceptor Bound to the Biased Agonists Bucindolol and Carvedilol. *Structure*, **2012**, *20*(5), 841-849.

258. Miller-Gallacher, J.L.; Nehme, R.; Warne, T.; Edwards, P.C.; Schertler, G.F.X.; Leslie, A.G.W.; Tate, C.G. The 2.1 Å Resolution Structure of Cyanopindolol-Bound β_1-Adrenoceptor Identifies an Intramembrane Na^+ Ion that Stabilises the Ligand-Free Receptor. *PLoS One*, **2014**, *9*(3), 92727.

259. Huang, J.; Chen, S.; Zhang, J.J.; Huang, X.Y. Crystal structure of oligomeric β_1-adrenergic G protein-coupled receptors in ligand-free basal state. *Nat. Struc. Mol. Biol.*, **2013**, *20*, 419-425.

260. Sato, T.; Baker, J.; Warne, T.; Brown, G.; Leslie, A.; Congreve, M.; Tate, C. Pharmacological Analysis and Structure Determination of 7-Methylcyanopindolol-Bound β_1-Adrenergic Receptor. *Mol. Pharmacol*., **2015**, *88*(6), 1024-1034.

261. Leslie, A.G.W.; Warne, T.; Tate, C.G. Ligand occupancy in crystal structure of β_1 adrenergic G protein coupled receptor. *Nat. Struct. Mol. Biol*., **2015**, *22*(12), 941-942.

262. Cherezov, V.; Rosenbaum, D.M.; Hanson, M.A.; Rasmussen, S.G.; Thian, F.S.; Kobilka, T.S.; Choi, H.J.; Kuhn, P.; Weis, W.I.; Kobilka, B.K.; Stevens, R.C. High-resolution crystal structure of an engineered human β_2-adrenergic G protein-coupled receptor. *Science*, **2007**, *318*(5854), 1258-1265.

263. Hanson, M.A.; Cherezov, V.; Griffith, M.T.; Roth, C.B.; Jaakola, V.P.; Chien, E.Y.; Velasquez, J.; Kuhn, P.; Stevens, R.C. A specific cholesterol binding site is established by the 2.8 Å structure of the human β_2-adrenergic receptor. *Structure*, **2008**, *16*(6), 897-905.

264. Bokoch, M.P.; Zou, Y.; Rasmussen, S.G.; Liu, C.W.; Nygaard, R.; Rosenbaum, D.M.; Fung, J.J.; Choi, H.J.; Thian, F.S.; Kobilka, T.S.; Puglisi, J.D.; Weis, W.I.; Pardo, L.; Prosser, R.S.; Mueller, L.; Kobilka, B.K. Ligand-specific regulation of the extracellular surface of a G-protein-coupled receptor. *Nature*, **2010**, *463*(7277), 108-112.

265. Wacker, D.; Fenalti, G.; Brown, M.A.; Katritch, V.; Abagyan, R.; Cherezov, V.; Stevens, R.C. Conserved Binding Mode of Human β_2 Adrenergic Receptor Inverse Agonists and Antagonist Revealed by X-ray Crystallography. *J. Am. Chem. Soc.*, **2010**, *132*(33), 11443-11445.

266. Rasmussen, S.G.; Choi, H.J.; Fung, J.J.; Pardon, E.; Casarosa, P.; Chae, P.S.; Devree, B.T.; Rosenbaum, D.M.; Thian, F.S.; Kobilka, T.S.; Schnapp, A.; Konetzki, I.; Sunahara, R.K.; Gellman, S.H.; Pautsch,

A.; Steyaert, J.; Weis, W.I.; Kobilka, B.K. Structure of a nanobody-stabilized active state of the β_2 adrenoceptor. *Nature*, **2011**, *469*(7329), 175-180.

267. Rasmussen, S.G.; DeVree, B.T.; Zou, Y.; Kruse, A.C.; Chung, K.Y.; Kobilka, T.S.; Thian, F.S.; Chae, P.S.; Pardon, E.; Calinski, D.; Mathiesen, J.M.; Shah, S.T.; Lyons, J.A.; Caffrey, M.; Gellman, S.H.; Steyaert, J.; Skiniotis, G.; Weis, W.I.; Sunahara, R.K.; Kobilka, B.K. Crystal structure of the β_2 adrenergic receptor-G_s protein complex. *Nature*, **2011**, *477*(7366), 549-555.

268. Zou, Y.; Weis, W.I.; Kobilka, B.K. N-terminal T4 lysozyme fusion facilitates crystallization of a G protein coupled receptor. *PLoS One*, **2012**, *7*(10), e46039. Available from: https://doi.org/10.1371/journal.pone.0046039.

269. Huang, C.Y.; Olieric, V.; Ma, P.; Howe, N.; Vogeley, L.; Liu, X.; Warshamanage, R.; Weinert, T.; Panepucci, E.; Kobilka, B.; Diederichs, K.; Wang, M.; Caffrey, M. In meso in situ serial X-ray crystallography of soluble and membrane proteins at cryogenic temperatures. *Acta Crystallogr. D Struct. Biol.*, **2016**, *72*(Pt 1), 93-112.

270. Staus, D.P.; Strachan, R.T.; Manglik, A.; Pani, B.; Kahsai, A.W.; Kim, T.H.; Wingler, L.M.; Ahn, S.; Chatterjee, A.; Masoudi, A.; Kruse, A.C.; Pardon, E.; Steyaert, J.; Weis, W.I.; Prosser, R.S.; Kobilka, B.K.; Costa, T.; Lefkowitz, R.J. Allosteric nanobodies reveal the dynamic range and diverse mechanisms of G-protein-coupled receptor activation. *Nature*, **2016**, *535*(7612), 448-452.

271. Shao, Z.; Yin, J.; Chapman, K.; Grzemska, M.; Clark, L.; Wang, J.; Rosenbaum, D.M. High-resolution crystal structure of the human CB_1 cannabinoid receptor. *Nature*, **2017**, *540*(7634), 602-606.

272. Hua, T.; Vemuri, K.; Pu, M.; Qu, L.; Han, G.W.; Wu, Y.; Zhao, S.; Shui, W.; Li, S.; Korde, A.; Laprairie, R.B.; Stahl, E.L.; Ho, J.H.; Zvonok, N.; Zhou, H.; Kufareva, I.; Wu, B.; Zhao, Q.; Hanson, M.A.; Bohn, L.M.; Makriyannis, A.; Stevens, R.C.; Liu, Z.J. Crystal Structure of the Human Cannabinoid Receptor CB_1. *Cell*, **2016**, *167*(3), 750-762.e14.

273. Zheng, Y.; Qin, L.; Zacarias, N.V.; de Vries, H.; Han, G.W.; Gustavsson, M.; Dabros, M.; Zhao, C.; Cherney, R.J.; Carter, P.; Stamos, D.; Abagyan, R.; Cherezov, V.; Stevens, R.C.; IJzerman, A.P.; Heitman, L.H.; Tebben, A.; Kufareva, I.; Handel, T.M. Structure of CC Chemokine Receptor 2 with Orthosteric and Allosteric Antagonists. *Nature*, **2016**, *540*(7633), 458-461.

274. Miyamoto, K.; Togiya, K. Solution Structure of LC4 Transmembrane Segment of CCR_5. *PLoS One,* **2011**, *6*, e20452. Available from: https://doi.org/10.1371/journal.pone.0020452.

275. Tan, Q.; Zhu, Y.; Li, J.; Chen, Z.; Han, G.W.; Kufareva, I.; Li, T.; Ma, L.; Fenalti, G.; Li, J.; Zhang, W.; Xie, X.; Yang, H.; Jiang, H.; Cherezov, V.; Liu, H.; Stevens, R.C.; Zhao, Q.; Wu, B. Structure of the CCR_5 chemokine receptor-HIV entry inhibitor maraviroc complex. *Science*, **2013**, *341*(6152), 1387-1390.

276. Oswald, C.; Rappas, M.; Kean, J.; Dore, A.S.; Errey, J.C.; Bennett, K.; Deflorian, F.; Christopher, J.A.; Jazayeri, A.; Mason, J.S.; Congreve, M.; Cooke, R.M.; Marshall, F.H. Intracellular allosteric antagonism of the CCR_9 receptor. *Nature*, **2016**, *540*(7633), 462-465.

277. Park, S.H.; Das, B.B.; Casagrande, F.; Tian, Y.; Nothnagel, H.J.; Chu, M.; Kiefer, H.; Maier, K.; De Angelis, A.A.; Marassi, F.M.; Opella, S.J. Structure of the chemokine receptor $CXCR_1$ in phospholipid bilayers. *Nature*, **2012**, *491*(7426), 779-793.

278. Wu, B.; Chien, E.Y.; Mol, C.D.; Fenalti, G.; Liu, W.; Katritch, V.; Abagyan, R.; Brooun, A.; Wells, P.; Bi, F.C.; Hamel, D.J.; Kuhn, P.; Handel, T.M.; Cherezov, V.; Stevens, R.C. Structures of the $CXCR_4$ chemokine GPCR with small-molecule and cyclic peptide antagonists. *Science*, **2010**, *330*(6007), 1066-1071.

279. Qin, L.; Kufareva, I.; Holden, L.G.; Wang, C.; Zheng, Y.; Zhao, C.; Fenalti, G.; Wu, H.; Han, G.W.; Cherezov, V.; Abagyan, R.; Stevens, R.C.; Handel, T.M. Crystal structure of the chemokine receptor $CXCR_4$ in complex with a viral chemokine. *Science*, **2015**, *347*(6226), 1117-1122.

280. Ziarek, J.J.; Kleist, A.B.; London, N.; Raveh, B.; Montpas, N.; Bonneterre, J.; St-Onge, G.; DiCosmo-Ponticello, C.J.; Koplinski, C.A.; Roy, I.; Stephens, B.; Thelen, S.; Veldkamp, C.T.; Coffman, F.D.; Cohen, M.C.; Dwinell, M.B.; Thelen, M.; Peterson, F.C.; Heveker, N.; Volkman, B.F. Structural basis for chemokine recognition by a G protein-coupled receptor and implications for receptor activation. *Sci. Signal.*, **2017**, *10*(471), eaah5756. Available from: http://stke.sciencemag.org/content/10/471/eaah5756.long

281. Chien, E.Y., Liu, W., Zhao, Q., Katritch, V., Han, G.W., Hanson, M.A., Shi, L., Newman, A.H., Javitch, J.A., Cherezov, V., Stevens, R.C. Structure of the human dopamine D_3 receptor in complex with a D_2/D_3 selective antagonist. *Science*, **2010**, *330*(6007), 1091-1095.

282. Fenalti, G.; Giguere, P.M.; Katritch, V.; Huang, X.P.; Thompson, A.A.; Cherezov, V.; Roth, B.L.; Stevens, R.C. Molecular control of δ-opioid receptor signaling. *Nature*, **2014**, *506*(7487), 191-196.

283. Fenalti, G.; Zatsepin, N.A.; Betti, C.; Giguere, P.; Han, G.W.; Ishchenko, A.; Liu, W.; Guillemyn, K.; Zhang, H.; James, D.; Wang, D.; Weierstall, U.; Spence, J.C.; Boutet, S.; Messerschmidt, M.; Williams, G.J.; Gati, C.; Yefanov, O.M.; White, T.A.; Oberthuer, D.; Metz, M.; Yoon, C.H.; Barty, A.; Chapman, H.N.; Basu, S.; Coe, J.; Conrad, C.E.; Fromme, R.; Fromme, P.; Tourwe, D.; Schiller, P.W.; Roth, B.L.; Ballet, S.; Katritch, V.; Stevens, R.C.; Cherezov, V. Structural basis for bifunctional peptide recognition at human *δ*-opioid receptor. *Nat. Struct. Mol. Biol.*, **2015**, *22*(3), 265-268.

284. Shihoya, W.; Nishizawa, T.; Okuta, A.; Tani, K.; Dohmae, N.; Fujiyoshi, Y.; Nureki, O.; Doi, T. Activation mechanism of endothelin ETB receptor by endothelin-1. *Nature*, **2016**, *537*(7620), 363-368.

285. Srivastava, A.; Yano, J.; Hirozane, Y.; Kefala, G.; Gruswitz, F.; Snell, G.; Lane, W.; Ivetac, A.; Aertgeerts, K.; Nguyen, J.; Jennings, A.; Okada, K. High-resolution structure of the human GPR40 receptor bound to allosteric agonist TAK-875. *Nature*, **2014**, *513*(7516), 124-127.

286. Lu, J.; Byrne, N.; Wang, J.; Bricogne, G.; Brown, F.K.; Chobanian, H.R.; Colletti, S.L.; Di Salvo, J.; Thomas-Fowlkes, B.; Guo, Y.; Hall, D.L.; Hadix, J.; Hastings, N.B.; Hermes, J.D.; Ho, T.; Howard, A.D.; Josien, H.; Kornienko, M.; Lumb, K.J.; Miller, M.W.; Patel, S.B.; Pio, B.; Plummer, C.W.; Sherborne, B.S.; Sheth, P.; Souza, S.; Tummala, S.; Vonrhein, C.; Webb, M.; Allen, S.J.; Johnston, J.M.; Weinglass, A.B.; Sharma, S.; Soisson, S.M. Structural basis for the cooperative allosteric activation of the free fatty acid receptor GPR40. *Nat. Struc. Mol. Biol.*, **2017**.

287. Jiang, X.; Liu, H.; Chen, X.; Chen, P.; Fischer, D.; Sriraman, V.; Yu, H.N.; Arkinstall, S.; He, X. Structure of Follicle-Stimulating Hormone in Complex with the Entire Ectodomain of its Receptor. *Proc. Natl. Acad. Sci. U.S.A.*, **2012**, *109*(31), 12491-12496.

288. Jiang, X.; Fischer, D.; Chen, X.; McKenna, S.D.; Liu, H.; Sriraman, V.; Yu, H.N.; Goutopoulos, A.; Arkinstall, S.; He, X. Evidence for Follicle-stimulating Hormone Receptor as a Functional Trimer. *J. Biol. Chem.*, **2014**, *289*, 14273-14282.

289. Shimamura, T.; Shiroishi, M.; Weyand, S.; Tsujimoto, H.; Winter, G.; Katritch, V.; Abagyan, R.; Cherezov, V.; Liu, W.; Han, G.W.; Kobayashi, T.; Stevens, R.C.; Iwata, S. Structure of the human histamine H_1 receptor complex with doxepin. *Nature*, **2011**, *475*(7354), 65-70.

290. Wu, H.; Wacker, D.; Mileni, M.; Katritch, V.; Han, G.W.; Vardy, E.; Liu, W.; Thompson, A.A.; Huang, X.P.; Carroll, F.I.; Mascarella, S.W.; Westkaemper, R.B.; Mosier, P.D.; Roth, B.L.; Cherezov, V.;

Stevens, R.C. Structure of the human κ-opioid receptor in complex with JDTic. *Nature*, **2012**, *485*(7398), 327-332.

291. Chrencik, J.E.; Roth, C.B.; Terakado, M.; Kurata, H.; Omi, R.; Kihara, Y.; Warshaviak, D.; Nakade, S.; Asmar-Rovira, G.; Mileni, M.; Mizuno, H.; Griffith, M.T.; Rodgers, C.; Han, G.W.; Velasquez, J.; Chun, J.; Stevens, R.C.; Hanson, M.A. Crystal Structure of Antagonist Bound Human Lysophosphatidic Acid Receptor 1. *Cell*, **2015**, *161*(7), 1633-1643.

292. Cherezov, V.; Rosenbaum, D.M.; Hanson, M.A.; Rasmussen, S.G.; Thian, F.S.; Kobilka, T.S.; Choi, H.J.; Kuhn, P.; Weis, W.I.; Kobilka, B.K.; Stevens, R.C. High-resolution crystal structure of an engineered human β_2-adrenergic G protein-coupled receptor. *Science*, **2007**, *318*(5854), 1258-1265.

293. Thal, D.M.; Sun, B.; Feng, D.; Nawaratne, V.; Leach, K.; Felder, C.C.; Bures, M.G.; Evans, D.A.; Weis, W.I.; Bachhawat, P.; Kobilka, T.S.; Sexton, P.M.; Kobilka, B.K.; Christopoulos, A. Crystal structures of the M_1 and M_4 muscarinic acetylcholine receptors. *Nature*, **2016**, *531*(7594), 335-340.

294. Haga, K.; Kruse, A.C.; Asada, H.; Yurugi-Kobayashi, T.; Shiroishi, M.; Zhang, C.; Weis, W.I.; Okada, T.; Kobilka, B.K.; Haga, T.; Kobayashi, T. Structure of the human M_2 muscarinic acetylcholine receptor bound to an antagonist. *Nature*, **2012**, *482*(7386), 547-551.

295. Kruse, A.C.; Ring, A.M.; Manglik, A.; Hu, J.; Hu, K.; Eitel, K.; Hubner, H.; Pardon, E.; Valant, C.; Sexton, P.M.; Christopoulos, A.; Felder, C.C.; Gmeiner, P.; Steyaert, J.; Weis, W.I.; Garcia, K.C.; Wess, J.; Kobilka, B.K. Activation and allosteric modulation of a muscarinic acetylcholine receptor. *Nature*, **2013**, *504*(7478), 101-106.

296. Kruse, A.C.; Hu, J.; Pan, A.C.; Arlow, D.H.; Rosenbaum, D.M.; Rosemond, E.; Green, H.F.; Liu, T.; Chae, P.S.; Dror, R.O.; Shaw, D.E.; Weis, W.I.; Wess, J.; Kobilka, B.K. Structure and dynamics of the M_3 muscarinic acetylcholine receptor. *Nature*, **2012**, *482*(7386), 552-556.

297. Thorsen, T.S.; Matt, R.; Weis, W.I.; Kobilka, B.K. Modified T4 Lysozyme Fusion Proteins Facilitate G Protein-Coupled Receptor Crystallogenesis. *Structure*, **2014**, *22*(11), 1657-1664.

298. Manglik, A.; Kruse, A.C.; Kobilka, T.S.; Thian, F.S.; Mathiesen, J.M.; Sunahara, R.K.; Pardo, L.; Weis, W.I.; Kobilka, B.K.; Granier, S. Crystal structure of the μ-opioid receptor bound to a morphinan antagonist. *Nature*, **2012**, *485*(7398), 321-326.

299. Huang, W.; Manglik, A.; Venkatakrishnan, A.J.; Laeremans, T.; Feinberg, E.N.; Sanborn, A.L.; Kato, H.E.; Livingston, K.E.; Thorsen, T.S.; Kling, R.C.; Granier, S.; Gmeiner, P.; Husbands, S.M.; Traynor,

J.R.; Weis, W.I.; Steyaert, J.; Dror, R.O.; Kobilka, B.K. Crystal structure of the μ-opioid receptor bound to a morphinan antagonist. *Nature*, **2015**, *524*(7565), 315-321.

300. Granier, S.; Manglik, A.; Kruse, A.C.; Kobilka, T.S.; Thian, F.S.; Weis, W.I.; Kobilka, B.K. Structure of the μ-opioid receptor bound to naltrindole. *Nature*, **2012**, *485*(7398), 400-404.

301. White, J.F.; Noinaj, N.; Shibata, Y.; Love, J.; Kloss, B.; Xu, F.; Gvozdenovic-Jeremic, J.; Shah, P.; Shiloach, J.; Tate, C.G.; Grisshammer, R. Structure of the agonist-bound neurotensin receptor. *Nature*, **2012**, *490*(7421), 508-513.

302. Miller, R.L.; Thompson, A.A.; Trapella, C.; Guerrini, R.; Malfacini, D.; Patel, N.; Han, G.W.; Cherezov, V.; Calo, G.; Katritch, V.; Stevens, R.C. The Importance of Ligand-Receptor Conformational Pairs in Stabilization: Spotlight on the N/OFQ G Protein-Coupled Receptor. *Structure*, **2015**, *23*(12), 2291-2299.

303. Egloff, P.; Hillenbrand, M.; Klenk, C.; Batyuk, A.; Heine, P.; Balada, S.; Schlinkmann, K.M.; Scott, D.J.; Schuetz, M.; Plueckthun, A. Structure of Signaling-Competent Neurotensin Receptor 1 Obtained by Directed Evolution in *Escherichia Coli*. *Proc. Natl. Acad. Sci. U.S.A.*, **2014**, *111*(6), e655-e662.

304. Krumm, B.E.; White, J.F.; Shah, P.; Grisshammer, R. Structural prerequisites for G-protein activation by the neurotensin receptor. *Nat. Commun.*, **2015**, *6*, 7895-7895.

305. Krumm, B.E.; Lee, S.; Bhattacharya, S.; Botos, I.; White, C.F.; Du, H.; Vaidehi, N.; Grisshammer, R. Structure and dynamics of a constitutively active neurotensin receptor. *Sci. Rep.*, **2016**, *6*, 38564-38564.

306. Yin, J.; Babaoglu, K.; Brautigam, C.A.; Clark, L.; Shao, Z.; Scheuermann, T.H.; Harrell, C.M.; Gotter, A.L.; Roecker, A.J.; Winrow, C.J.; Renger, J.J.; Coleman, P.J.; Rosenbaum, D.M. Structure and ligand-binding mechanism of the human OX_1 and OX_2 orexin receptors. *Nat. Struc. Mol. Biol.*, **2016**, *23*(4), 293-299.

307. Yin, J.; Mobarec, J.C.; Kolb, P.; Rosenbaum, D.M. Crystal structure of the human OX_2 orexin receptor bound to the insomnia drug suvorexant. *Nature*, **2015**, *519*(7542), 247-250.

308. Zhang, D.; Gao, Z.G.; Zhang, K.; Kiselev, E.; Crane, S.; Wang, J.; Paoletta, S.; Yi, C.; Ma, L.; Zhang, W.; Han, G.W.; Liu, H.; Cherezov, V.; Katritch, V.; Jiang, H.; Stevens, R.C.; Jacobson, K.A.; Zhao, Q.; Wu, B. Two disparate ligand-binding sites in the human $P2Y_1$ receptor. *Nature*, **2015**, *520*(7547), 317-321.

309. Zhang, K.; Zhang, J.; Gao, Z.-G.; Zhang, D.; Zhu, L.; Han, G.W.; Moss, S.M.; Paoletta, S.; Kiselev, E.; Lu, W.; Fenalti, G.; Zhang, W.; Muller, C.E.; Yang, H.; Jiang, H.; Cherezov, V.; Katritch, V.; Jacobson, K.A.; Stevens, R.C.; Wu, B.; Zhao, Q. Structure of the human $P2Y_{12}$ receptor in complex with an antithrombotic drug. *Nature*, **2014**, *509*(7498), 115-118.

310. Zhang, J.; Zhang, K.; Gao, Z.G.; Paoletta, S.; Zhang, D.; Han, G.W.; Li, T.; Ma, L.; Zhang, W.; Muller, C.E.; Yang, H.; Jiang, H.; Cherezov, V.; Katritch, V.; Jacobson, K.A.; Stevens, R.C.; Wu, B.; Zhao, Q. Agonist-bound structure of the human $P2Y_{12}$ receptor. *Nature*, **2014**, *509*(7498), 119-122.

311. Zhang, C.; Srinivasan, Y.; Arlow, D.H.; Fung, J.J.; Palmer, D.; Zheng, Y.; Green, H.F.; Pandey, A.; Dror, R.O.; Shaw, D.E.; Weis, W.I.; Coughlin, S.R.; Kobilka, B.K. High-resolution crystal structure of human protease-activated receptor 1. *Nature*, **2012**, *492*(7429), 387-392.

312. Cheng, R.K.Y.; Fiez-Vandal, C.; Schlenker, O.; Edman, K.; Aggeler, B.; Brown, D.G.; Brown, G.A.; Cooke, R.M.; Dumelin, C.E.; Dore, A.S.; Geschwindner, S.; Grebner, C.; Hermansson, N.O.; Jazayeri, A.; Johansson, P.; Leong, L.; Prihandoko, R.; Rappas, M.; Soutter, H.; Snijder, A.; Sundstrom, L.; Tehan, B.; Thornton, P.; Troast, D.; Wiggin, G.; Zhukov, A.; Marshall, F.H.; Dekker, N. Structural insight into allosteric modulation of protease-activated receptor 2. *Nature*, **2017**, *545*(7652), 112-115.

313. Li, J.; Edwards, P.; Burghammer, M.; Villa, C.; Schertler, G.F.X. Structure of Bovine Rhodopsin in a Trigonal Crystal Form. *J. Mol. Biol.*, **2004**, *343*(5), 1409-1438.

314. Teller, D.C.; Okada, T.; Behnke, C.A.; Palczewski, K.; Stenkamp, R.E. Advances in determination of a high-resolution three-dimensional structure of rhodopsin, a model of G-protein-coupled receptors (GPCRs). *Biochemistry*, **2001**, *40*(26), 7761-7772.

315. Yeagle, P.L.; Choi, G.; Albert, A.D. Studies on the structure of the G-protein-coupled receptor rhodopsin including the putative G-protein binding site in unactivated and activated forms. *Biochemistry*, **2001**, *40*(39), 11932-11937.

316. Okada, T.; Fujiyoshi, Y.; Silow, M.; Navarro, J.; Landau, E.M.; Shichida, Y. Functional role of internal water molecules in rhodopsin revealed by X-ray crystallography. *Proc. Natl. Acad. Sci. U.S.A.*, **2002**, *99*(9), 5982-5987.

317. Choi, G.; Landin, J.; Galan, J.F.; Birge, R.R.; Albert, A.D.; Yeagle, P.L. Structural studies of metarhodopsin II, the activated form of the G-protein coupled receptor, rhodopsin. *Biochemistry*, **2002**, *41*(23), 7318-7324.

318. Okada, T.; Sugihara, M.; Bondar, A.N.; Elstner, M.; Entel, P.; Buss, V. The retinal conformation and its environment in rhodopsin in light of a new 2.2 Å crystal structure. *J. Mol. Biol.*, **2004**, *342*(2), 571-583.

319. Nakamichi, H.; Okada, T. Crystallographic analysis of primary visual photochemistry. *Angew. Chem. Int. Ed. Engl.*, **2006**, *45*(26), 4270-4273.

320. Nakamichi, H., Okada, T. Local peptide movement in the photoreaction intermediate of rhodopsin. *Proc. Natl. Acad. Sci. U.S.A.*, **2006**, *103*(34), 12729-12734.

321. Salom, D.; Lodowski, D.T.; Stenkamp, R.E.; Trong, I.L.; Golczak, M.; Jastrzebska, B.; Harris, T.; Ballesteros, J.A.; Palczewski, K. Crystal structure of a photoactivated deprotonated intermediate of rhodopsin. *Proc. Natl. Acad. Sci. U.S.A.*, **2006**, *103*(44), 16123-16128.

322. Standfuss, J.; Xie, G.; Edwards, P.C.; Burghammer, M.; Oprian, D.D.; Schertler, G.F.X. Crystal Structure of a Thermally Stable Rhodopsin Mutant. *J. Mol. Biol.*, **2007**, *372*(5), 1179-1188.

323. Nakamichi, H.; Buss, V.; Okada, T. Photoisomerization mechanism of rhodopsin and 9-*cis*-rhodopsin revealed by X-ray crystallography. *Biophys. J.*, **2007**, *92*(12), L106-L108.

324. Standfuss, J.; Edwards, P.C.; Dantona, A.; Fransen, M.; Xie, G.; Oprian, D.D.; Schertler, G.F.X. The Structural Basis of Agonist Induced Activation in Constitutively Active Rhodopsin. *Nature*, **2011**, *471*(7340), 656-660.

325. Murakami, M.; Kouyama, T. Crystal structure of squid rhodopsin, *Nature,* **2008**, *453*(7193), 363-367.

326. Shimamura, T.; Hiraki, K.; Takahashi, N.; Hori, T.; Ago, H.; Masuda, K.; Takio, K.; Ishiguro, M.; Miyano, M. Crystal structure of squid rhodopsin with intracellularly extended cytoplasmic region. *J. Biol. Chem.*, **2008**, *283*(26), 17753-17756.

327. Murakami, M.; Kouyama, T. Crystallographic Analysis of the Primary Photochemical Reaction of Squid Rhodopsin. *J. Mol. Biol.*, **2011**, *413*(3), 615-627.

328. Stenkamp, R.E. Alternative models for two crystal structures of bovine rhodopsin. *Acta Crystallogr. Sect. D*, **2008**, *64*(Pt 8), 902-904.

329. Park, J.H.; Scheerer, P.; Hofmann, K.P.; Choe, H.-W.; Ernst, O.P. Crystal structure of the ligand-free G-protein-coupled receptor opsin. *Nature*, **2008**, *454*(7201), 183-187.

330. Scheerer, P.; Park, J.H.; Hildebrand, P.W.; Kim, Y.J.; Krauss, N.; Choe, H.-W.; Hofmann, K.P.; Ernst, O.P. Crystal structure of opsin in its G-protein-interacting conformation. *Nature*, **2008**, *455*(7212), 497-502.

331. Choe, H.W.; Kim, Y.J.; Park, J.H.; Morizumi, T.; Pai, E.F.; Krauss, N.; Hofmann, K.P.; Scheerer, P.; Ernst, O.P. Crystal structure of metarhodopsin II. *Nature*, **2011**, *471*(7340), 651-655.

332. Makino, C.L.; Riley, C.K.; Looney, J.; Crouch, R.K.; Okada, T. Binding of more than one retinoid to visual opsins. *Biophys. J.*, **2010**, *99*(7), 2366-2373.

333. Deupi, X.; Edwards, P.; Singhal, A.; Nickle, B.; Oprian, D.; Schertler, G.; Standfuss, J. Stabilized G Protein Binding Site in the Structure of Constitutively Active Metarhodopsin-II. *Proc. Natl. Acad. Sci. U.S.A.*, **2012**, *109*(1), 119-124.

334. Singhal, A.; Ostermaier, M.K.; Vishnivetskiy, S.A.; Panneels, V.; Homan, K.T.; Tesmer, J.J.; Veprintsev, D.; Deupi, X.; Gurevich, V.V.; Schertler, G.F.; Standfuss, J. Insights Into Congenital Stationary Night Blindness Based on the Structure of G90D Rhodopsin. *EMBO Rep.*, **2013**, *14*(6), 520-526.

335. Park, J.H.; Morizumi, T.; Li, Y.; Hong, J.E.; Pai, E.F.; Hofmann, K.P.; Choe, H.W.; Ernst, O.P. Opsin, a structural model for olfactory receptors? *Angew. Chem. Int. Ed. Engl.*, **2013**, *52*(42), 11021-11024.

336. Szczepek, M.; Beyriere, F.; Hofmann, K.P.; Elgeti, M.; Kazmin, R.; Rose, A.; Bartl, F.J.; von Stetten, D.; Heck, M.; Sommer, M.E.; Hildebrand, P.W.; Scheerer, P. Crystal structure of a common GPCR-binding interface for G protein and arrestin. *Nat. Commun.*, **2014**, *5*, 4801-4801.

337. Blankenship, E.; Vahedi-Faridi, A.; Lodowski, D.T. The High-Resolution Structure of Activated Opsin Reveals a Conserved Solvent Network in the Transmembrane Region Essential for Activation. *Structure*, **2015**, *23*(12), 2358-2364.

338. Kang, Y.; Zhou, X.E.; Gao, X.; He, Y.; Liu, W.; Ishchenko, A.; Barty, A.; White, T.A.; Yefanov, O.; Han, G.W.; Xu, Q.; de Waal, P.W.; Ke, J.; Tan, M.H.; Zhang, C.; Moeller, A.; West, G.M.; Pascal, B.D.; Van Eps, N.; Caro, L.N.; Vishnivetskiy, S.A.; Lee, R.J.; Suino-Powell, K.M.; Gu, X.; Pal, K.; Ma, J.; Zhi, X.; Boutet, S.; Williams, G.J.; Messerschmidt, M.; Gati, C.; Zatsepin, N.A.; Wang, D.; James, D.; Basu, S.; Roy-Chowdhury, S.; Conrad, C.E.; Coe, J.; Liu, H.; Lisova, S.; Kupitz, C.; Grotjohann, I.; Fromme, R.; Jiang, Y.; Tan, M.; Yang, H.; Li, J.; Wang, M.; Zheng, Z.; Li, D.; Howe, N.; Zhao, Y.; Standfuss, J.; Diederichs, K.; Dong, Y.; Potter, C.S.; Carragher, B.; Caffrey, M.; Jiang, H.; Chapman, H.N.; Spence, J.C.; Fromme, P.; Weierstall, U.; Ernst, O.P.; Katritch, V.; Gurevich, V.V.; Griffin, P.R.; Hubbell, W.L.; Stevens, R.C.; Cherezov, V.; Melcher, K.; Xu, H.E. Crystal structure of rhodopsin bound to arrestin by femtosecond X-ray laser. *Nature*, **2015**, *523*(7562), 561-567.

339. Zhou, X.E.; Gao, X.; Barty, A.; Kang, Y.; He, Y.; Liu, W.; Ishchenko, A.; White, T.A.; Yefanov, O.; Han, G.W.; Xu, Q.; de Waal, P.W.; Suino-Powell, K.M.; Boutet, S.; Williams, G.J.; Wang, M.; Li, D.; Caffrey, M.; Chapman, H.N.; Spence, J.C.; Fromme, P.; Weierstall, U.; Stevens, R.C.; Cherezov, V.; Melcher, K.; Xu, H.E. X-ray laser diffraction for structure determination of the rhodopsin-arrestin complex. *Sci. Data*, **2016**, *3*, 160021-160021.

340. Singhal, A.; Guo, Y.; Matkovic, M.; Schertler, G.; Deupi, X.; Yan, E.C.; Standfuss, J. Structural role of the T94I rhodopsin mutation in congenital stationary night blindness. *EMBO Rep.*, **2016**, *17*(10), 1431-1440.

341. Gulati, S.; Jastrzebska, B.; Banerjee, S.; Placeres, A.L.; Miszta, P.; Gao, S.; Gunderson, K.; Tochtrop, G.P.; Filipek, S.; Katayama, K.; Kiser, P.D.; Mogi, M.; Stewart, P.L.; Palczewski, K. Photocyclic behavior of rhodopsin induced by an atypical isomerization mechanism. *Proc. Natl. Acad. Sci. U.S.A.*, **2017**, *114*(13), e2608-e2615.

342. Hanson, M.A.; Roth, C.B.; Jo, E.; Griffith, M.T.; Scott, F.L.; Reinhart, G.; Desale, H.; Clemons, B.; Cahalan, S.M.; Schuerer, S.C.; Sanna, M.G.; Han, G.W.; Kuhn, P.; Rosen, H.; Stevens, R.C. Crystal structure of a lipid G protein-coupled receptor. *Science*, **2012**, *335*(6070), 851-855.

343. Sanders, P.; Young, S.; Sanders, J.; Kabelis, K.; Baker, S.; Sullivan, A.; Evans, M.; Clark, J.; Wilmot, J.; Hu, X.; Roberts, E.; Powell, M.; Nunez Miguel, R.; Furmaniak, J.; Rees Smith, B. Crystal Structure of the TSH Receptor (TSHR) Bound to a Blocking-Type TSHR Autoantibody. *J. Mol. Endocrinol.*, **2011**, *46*(2), 81-99.

344. Sanders, J.; Chirgadze, D.Y.; Sanders, P.; Baker, S.; Sullivan, A.; Bhardwaja, A.; Bolton, J.; Reeve, M.; Nakatake, N.; Evans, M.; Richards, T.; Powell, M.; Miguel, R.N.; Blundell, T.L.; Furmaniak, J.; Smith, B.R. Crystal structure of the TSH receptor in complex with a thyroid-stimulating autoantibody. *Thyroid*, **2007**, *17*(5), 395-410.

345. Burg, J.S.; Ingram, J.R.; Venkatakrishnan, A.J.; Jude, K.M.; Dukkipati, A.; Feinberg, E.N.; Angelini, A.; Waghray, D.; Dror, R.O.; Ploegh, H.L.; Garcia, K.C. Structural basis for chemokine recognition and activation of a viral G protein-coupled receptor. *Science*, **2015**, *347*(6226), 1113-1117.

346. Shukla, A.K.; Manglik, A.; Kruse, A.C.; Xiao, K.; Reis, R.I.; Tseng, W.C.; Staus, D.P.; Hilger, D.; Uysal, S.; Huang, L.Y.; Paduch, M.; Tripathi-Shukla, P.; Koide, A.; Koide, S.; Weis, W.I.; Kossiakoff,

A.A.; Kobilka, B.K.; Lefkowitz, R.J. Structure of active *β*-arrestin-1 bound to a G-protein-coupled receptor phosphopeptide. *Nature*, **2013**, *497*(7447), 137-141.

347. Pioszak, A.A.; Parker, N.R.; Suino-Powell, K.; Xu, H.E. Molecular Recognition of Corticotropin-releasing Factor by Its G-protein-coupled Receptor $CRFR_1$. *J. Biol. Chem.*, **2008**, *283*(47), 32900-32912.

348. Hollenstein, K.; Kean, J.; Bortolato, A.; Cheng, R.K.; Dore, A.S.; Jazayeri, A.; Cooke, R.M.; Weir, M.; Marshall, F.H. Structure of class B GPCR corticotropin-releasing factor receptor 1. *Nature*, **2013**, *499*(7459), 438-443.

349. Dore, A.S.; Bortolato, A.; Hollenstein, K.; Cheng, R.K.Y.; Read, R.J.; Marshall, F.H. Decoding Corticotropin-Releasing Factor Receptor Type 1 Crystal Structures. *Curr. Mol. Pharmacol.*, **2017**.

350. Kusano, S., Kukimoto-Niino, M., Hino, N., Ohsawa, N., Okuda, K., Sakamoto, K., Shirouzu, M., Shindo, T., Yokoyama, S. Structural basis for extracellular interactions between calcitonin receptor-like receptor and receptor activity-modifying protein 2 for adrenomedullin-specific binding. *Protein Sci*., **2012**, *21*(2), 199-210.

351. Ter Haar, E.; Koth, C.M.; Abdul-Manan, N.; Swenson, L.; Coll, J.T.; Lippke, J.A.; Lepre, C.A.; Garcia-Guzman, M.; Moore, J.M. Crystal Structure of the Ectodomain Complex of the CGRP Receptor, a Class-B GPCR, Reveals the Site of Drug Antagonism. *Structure*, **2010**, *18*(9), 1083-1093.

352. Liang, Y.L.; Khoshouei, M.; Radjainia, M.; Zhang, Y.; Glukhova, A.; Tarrasch, J.; Thal, D.M.; Furness, S.G.B.; Christopoulos, G.; Coudrat, T.; Danev, R.; Baumeister, W.; Miller, L.J.; Christopoulos, A.; Kobilka, B.K.; Wootten, D.; Skiniotis, G.; Sexton, P.M. Phase-plate cryo-EM structure of a class B GPCR-G-protein complex. *Nature*, **2017**, *546*(7656), 118-123.

353. Koth, C.M.; Murray, J.M.; Mukund, S.; Madjidi, A.; Minn, A.; Clarke, H.J.; Wong, T.; Chiang, V.; Luis, E.; Estevez, A.; Rondon, J.; Zhang, Y.; Hotzel, I.; Allan, B.B. Molecular basis for negative regulation of the glucagon receptor. *Proc. Natl. Acad. Sci. U.S.A.*, **2012**, *109*(36), 14393-14398.

354. Siu, F.Y.; He, M.; de Graaf, C.; Han, G.W.; Yang, D.; Zhang, Z.; Zhou, C.; Xu, Q.; Wacker, D.; Joseph, J.S.; Liu, W.; Lau, J.; Cherezov, V.; Katritch, V.; Wang, M.W.; Stevens, R.C. Structure of the human glucagon class B G-protein-coupled receptor. *Nature*, **2013**, *499*(7459), 444-449.

355. Jazayeri, A.; Dore, A.S.; Lamb, D.; Krishnamurthy, H.; Southall, S.M.; Baig, A.H.; Bortolato, A.; Koglin, M.; Robertson, N.J.; Errey, J.C.; Andrews, S.P.; Teobald, I.; Brown, A.J.; Cooke, R.M.; Weir,

M.; Marshall, F.H. Extra-helical binding site of a glucagon receptor antagonist. *Nature*, **2016**, *533*(7602), 274-277.

356. Jazayeri, A.; Rappas, M.; Brown, A.J.H., Kean, J., Errey, J.C., Robertson, N.J., Fiez-Vandal, C., Andrews, S.P., Congreve, M.; Bortolato, A.; Mason, J.S.; Baig, A.H.; Teobald, I.; Dore, A.S.; Weir, M.; Cooke, R.M.; Marshall, F.H. Crystal structure of the GLP-1 receptor bound to a peptide agonist. *Nature*, **2017**, *546*(7657), 254-258.

357. Zhang, Y.; Sun, B.; Feng, D.; Hu, H.; Chu, M.; Qu, Q.; Tarrasch, J.T.; Li, S.; Sun Kobilka, T.; Kobilka, B.K.; Skiniotis, G. Cryo-EM structure of the activated GLP-1 receptor in complex with a G protein. *Nature*, **2017**, *546*(7657), 248-253.

358. Song, G.; Yang, D.; Wang, Y.; de Graaf, C.; Zhou, Q.; Jiang, S.; Liu, K.; Cai, X.; Dai, A.; Lin, G.; Liu, D.; Wu, F.; Wu, Y.; Zhao, S.; Ye, L.; Han, G.W.; Lau, J.; Wu, B.; Hanson, M.A.; Liu, Z.J.; Wang, M.W.; Stevens, R.C. Human GLP-1 receptor transmembrane domain structure in complex with allosteric modulators. *Nature*, **2017**, *546*(7657), 312-315.

359. Pioszak, A.A.; Parker, N.R.; Gardella, T.J.; Xu, H.E. Structural basis for parathyroid hormone-related protein binding to the parathyroid hormone receptor and design of conformation-selective peptides. *J. Biol. Chem.*, **2009**, *284*(41), 28382-28391.

360. Geng, Y.; Bush, M.; Mosyak, L.; Wang, F.; Fan, Q.R. Structural mechanism of ligand activation in human GABA(B) receptor. *Nature*, **2013**, *504*(7479), 254-259.

361. Wu, H.; Wang, C.; Gregory, K.J.; Han, G.W.; Cho, H.P.; Xia, Y.; Niswender, C.M.; Katritch, V.; Meiler, J.; Cherezov, V.; Conn, P.J.; Stevens, R.C. Structure of a class C GPCR metabotropic glutamate receptor 1 bound to an allosteric modulator. *Science*, **2014**, *344*(6179), 58-64.

362. Kunishima, N., Shimada, Y., Tsuji, Y., Sato, T., Yamamoto, M., Kumasaka, T., Nakanishi, S., Jingami, H., Morikawa, K. Structural basis of glutamate recognition by a dimeric metabotropic glutamate receptor. *Nature*, **2000**, *407*(6807), 971-977.

363. Monn, J.A.; Prieto, L.; Taboada, L.; Hao, J.; Reinhard, M.R.; Henry, S.S.; Beadle, C.D.; Walton, L.; Man, T.; Rudyk, H.; Clark, B.; Tupper, D.; Baker, S.R.; Lamas, C.; Montero, C.; Marcos, A.; Blanco, J.; Bures, M.; Clawson, D.K.; Atwell, S.; Lu, F.; Wang, J.; Russell, M.; Heinz, B.A.; Wang, X.; Carter, J.H.; Getman, B.G.; Catlow, J.T.; Swanson, S.; Johnson, B.G.; Shaw, D.B.; McKinzie, D.L. Synthesis and Pharmacological Characterization of C4-(Thiotriazolyl)-substituted-2-

aminobicyclo[3.1.0]hexane-2,6-dicarboxylates. Identification of (1*R*,2*S*,4*R*,5*R*,6*R*)-2-Amino-4-(1*H*-1,2,4-triazol-3-ylsulfanyl)bicyclo[3.1.0]hexane-2,6-dicarboxylic Acid (LY2812223), a Highly Potent, Functionally Selective mGlu2 Receptor Agonist. *J. Med. Chem.*, **2015**, *58*(18), 7526-7548.

364. Muto, T.; Tsuchiya, D.; Morikawa, K.; Jingami, H. Structures of the extracellular regions of the group II/III metabotropic glutamate receptors. *Proc. Natl. Acad. Sci. U.S.A.*, **200**7, 104(10), 3759-3764.

365. Dore, A.S.; Okrasa, K.; Patel, J.C.; Serrano-Vega, M.; Bennett, K.; Cooke, R.M.; Errey, J.C.; Jazayeri, A.; Khan, S.; Tehan, B.; Weir, M.; Wiggin, G.R.; Marshall, F.H. Structure of class C GPCR metabotropic glutamate receptor 5 transmembrane domain. *Nature*, **2014**, *511*(7511), 557-562.

366. Christopher, J.A.; Aves, S.J.; Bennett, K.A.; Dore, A.S.; Errey, J.C.; Jazayeri, A.; Marshall, F.H.; Okrasa, K.; Serrano-Vega, M.J.; Tehan, B.G.; Wiggin, G.R.; Congreve, M. Fragment and Structure-Based Drug Discovery for a Class C GPCR: Discovery of the mGlu5 Negative Allosteric Modulator HTL14242 (3-Chloro-5-[6-(5-fluoropyridin-2-yl)pyrimidin-4-yl]benzonitrile). *J. Med. Chem.*, **2015**, *58*(16), 6653-6664.

367. Wang, C.; Wu, H.; Katritch, V.; Han, G.W.; Huang, X.P.; Liu, W.; Siu, F.Y.; Roth, B.L.; Cherezov, V.; Stevens, R.C. Structure of the human smoothened receptor bound to an antitumour agent. *Nature*, **2013**, *497*(7449), 338-343.

368. Wang, C.; Wu, H.; Evron, T.; Vardy, E.; Han, G.W.; Huang, X.P.; Hufeisen, S.J.; Mangano, T.J.; Urban, D.J.; Katritch, V.; Cherezov, V.; Caron, M.G.; Roth, B.L.; Stevens, R.C. Structural basis for Smoothened receptor modulation and chemoresistance to anticancer drugs. *Nat. Commun.*, **2014**, *5*, 4355-4355.

369. Weierstall, U.; James, D.; Wang, C.; White, T.A.; Wang, D.; Liu, W.; Spence, J.C.; Bruce Doak, R.; Nelson, G.; Fromme, P.; Fromme, R.; Grotjohann, I.; Kupitz, C.; Zatsepin, N.A.; Liu, H.; Basu, S.; Wacker, D.; Han, G.W.; Katritch, V.; Boutet, S.; Messerschmidt, M.; Williams, G.J.; Koglin, J.E.; Marvin Seibert, M.; Klinker, M.; Gati, C.; Shoeman, R.L.; Barty, A.; Chapman, H.N.; Kirian, R.A.; Beyerlein, K.R.; Stevens, R.C.; Li, D.; Shah, S.T.; Howe, N.; Caffrey, M.; Cherezov, V. Lipidic cubic phase injector facilitates membrane protein serial femtosecond crystallography. *Nat. Commun.,* **2014**, *5*, 3309-3309.

370. Huang, P.; Nedelcu, D.; Watanabe, M.; Jao, C.; Kim, Y.; Liu, J.; Salic, A. Cellular Cholesterol Directly Activates Smoothened in Hedgehog Signaling. *Cell*, **2016**, *166*(5), 1176-1187.e14

371. Byrne, E.F.; Sircar, R.; Miller, P.S.; Hedger, G.; Luchetti, G.; Nachtergaele, S.; Tully, M.D.; Mydock-McGrane, L.; Covey, D.F.; Rambo, R.P.; Sansom, M.S.; Newstead, S.; Rohatgi, R.; Siebold, C. Structural basis of Smoothened regulation by its extracellular domains. *Nature*, **2016**, *535*(7613), 517-522.

372. Zhang, X.; Zhao, F.; Wu, Y.; Yang, J.; Han, G.W.; Zhao, S.; Ishchenko, A.; Ye, L.; Lin, X.; Ding, K.; Dharmarajan, V.; Griffin, P.R.; Gati, C.; Nelson, G.; Hunter, M.S.; Hanson, M.A.; Cherezov, V.; Stevens, R.C.; Tan, W.; Tao, H.; Xu, F. Crystal structure of a multi-domain human smoothened receptor in complex with a super stabilizing ligand. *Nat. Commun*. **2017**, *8*, 15383-15383.

373. Salzman, G.S.; Ackerman, S.D.; Ding, C.; Koide, A.; Leon, K.; Luo, R.; Stoveken, H.M.; Fernandez, C.F.; Tall, G.G.; Piao, X.; Monk, K.R.; Koide, S.; Arac, D. Structural basis for regulation of GPR56/ADGRG1 by its alternatively spliced extracellular domains. *Neuron*, **2016**, *91*(6), 1292-1304.

374. Ranaivoson, F.M.; Liu, Q.; Martini, F.; Bergami, F.; von Daake, S.; Li, S.; Lee, D.; Demeler, B.; Hendrickson, W.A.; Comoletti, D. Structural and Mechanistic Insights into the Latrophilin3-FLRT3 Complex that Mediates Glutamatergic Synapse Development. *Structure*, **2015**, *23*(9), 1665-1677.

375. Lima, C.D.; Klein, M.G.; Hendrickson, W.A. Super-Complexes of Adhesion GPCRs and Neural Guidance Receptors. *Nat. Commun.*, **2016**, *7*, 11184. Available from: https://www.nature.com/articles/ncomms11184.

376. Kitchen, D.B.; Decornez, H.; Furr, J.R.; Bajorath, J. Docking and scoring in virtual screening for drug discovery: methods and applications. *Nat. Rev. Drug Discov.*, **2004**, *3*(11), 935-949.

377. Lemos, A.; Leão, M.; Soares, J- Palmeira, A.; Pinto, M.; Saraiva, L.; Sousa, M.E. Medicinal Chemistry Strategies to Disrupt the p53-MDM2/MDMX Interaction. *Med. Res. Rev.*, **2016**, *36*(5), 789-844.

378. Azevedo, L.S.; Moraes, F.P.; Xavier, M.M.; Pantoja, E.O.; Villavicencio, B.; Finck, J.A.; Proença, A.M.; Rocha, K.B.; De Azevedo Jr, W.F. Recent Progress of Molecular Docking Simulations Applied to Development of Drugs, *Curr. Bioinform*., **2012**, *7*(4), 352-365.

379. Xavier, M.M.; Heck, G.S.; Avila, M.B.; Levin, N.M.B.; Pintro, V.O.; Carvalho, N.L.; De Azevedo Jr, W.F. SAnDReS a Computational Tool for Statistical Analysis of Docking Results and Development of Scoring Functions, Comb. *Chem. High Throughout Screen*., **2016**, *19*(10), 801-812.

380. Ferreira, L.G.; Dos Santos, R.N.; Oliva, G.; Andricopulo, A.D. Molecular docking and structure-based drug design strategies. *Molecules,* **2015**, *20*(7), 13384-13421.

381. Ericksen, S.S.; Wu, H.; Zhang, H.; Michael, L.A.; Newton, M.A.; Hoffmann, F.M.; Wildman, S.A. Machine Learning Consensus Scoring Improves Performance Across Targets in Structure-Based Virtual Screening. *J. Chem. Inf. Model.*, **2017**. Available from: http://pubs.acs.org/doi/abs/10.1021/acs.jcim.7b00153.

382. Wójcikowski, M.; Ballester, P.J.; Siedlecki, P. Performance of machine-learning scoring functions in structure-based virtual screening. *Sci. Rep.*, **2017**, *7*, 46710. Available from: https://www.nature.com/articles/srep46710.

383. Morris, G.M.; Goodsell, D.S.; Halliday, R.S.; Huey, R.; Hart, W.E.; Belew, R.K.; Olson, A.J. Automated docking using a Lamarckian genetic algorithm and an empirical binding free energy function. *J. Comput. Chem.*, **1998**, *19*(14), 1639-1662.

384. Ostopovici-Halip, L.; Rad-Curpan, R. Modeling of ligand binding to dopamine D_2 receptor. *J. Serb. Chem. Soc.*, **2014**, *79*(2), 175-183.

385. *Molecular Operating Environment (MOE)*, 2009.10; Chemical Computing Group Inc., 1010 Sherbooke St. West, Suite #910, Montreal, QC, Canada, H3A 2R7, **2009**.

386. Malo, M.; Brive, L.; Luthman, K.; Svensson, P. Investigation of D_2 Receptor–Agonist Interactions Using a Combination of Pharmacophore and Receptor Homology Modeling. *ChemMedChem*, **2012**, *7*(3), 471-482.

387. Friesner, R.A.; Banks, J.L.; Murphy, R.B.; Halgren, T.A.; Klicic, J.J.; Mainz, D.T.; Repasky, M.P.; Knoll, E.H.; Shelley, M.; Perry, J.K.; Shaw, D.E.; Francis, P.; Shenkin, P.S. Glide: A New Approach for Rapid, Accurate Docking and Scoring. 1. Method and Assessment of Docking Accuracy. *J. Med. Chem.*, **2004**, *47*(7), 1739-1749.

388. Friesner, R.A.; Murphy, R.B.; Repasky, M.P.; Frye, L.L.; Greenwood, J.R.; Halgren, T.A.; Sanschagrin, P.C.; Mainz, D.T. Extra Precision Glide: Docking and Scoring Incorporating a Model of Hydrophobic Enclosure for Protein−Ligand Complexes. *J. Med. Chem.*, **2006**, *49*(21), 6177-6196.

389. Halgren, T.A.; Murphy, R.B.; Friesner, R.A.; Beard, H.S.; Frye, L.L.; Pollard, W.T.; Banks, J.L. GLIDE: A New Approach for Rapid, Accurate Docking and Scoring. 2. Enrichment Factors in Database Screening. *J. Med. Chem.*, **2004**, *47*(7), 1750-1759.

390. Penjisevic, J.Z.; Sukalovic, V.V.; Andric, D.B.; Roglic, G.M.; Novakovic, I.; Soskic, V.; Kostic-Rajacic, S.V. Synthesis, biological evaluation and docking analysis of substituted piperidines and (2-methoxyphenyl) piperazines. *J. Serb. Chem. Soc.*, **2016**, *81*(4), 347-356.

391. Penjišević, J.Z.; Sukalovic, V.V.; Andric, D.B.; Roglic, G.M.; Soskic, V.; Kostic-Rajacic, S.V. Synthesis, Biological, and Computational Evaluation of Substituted 1-(2-Methoxyphenyl)-4-(1-phenethylpiperidin-4-yl)piperazines and 1-(2-Methoxyphenyl)-4-[(1-phenethylpiperidin-4-yl)methyl]piperazines as Dopaminergic Ligands. *Arch. Pharm. (Weinheim)*, **2016**, *349*(8), 614-626.

392. Trott, O.; Olson, A.J. AutoDock Vina: Improving the speed and accuracy of docking with a new scoring function, efficient optimization, and multithreading. *J. Comput. Chem.*, **2010**, *31*(2), 455-461.

393. Morris, G.M.; Huey, R.; Lindstrom, W.; Sanner, M.F.; Belew, R.K.; Goodsell, D.S.; Olson, A.J. AutoDock4 and AutoDockTools4: Automated Docking with Selective Receptor Flexibility. *J. Comput. Chem.*, **2009**, *30*(16), 2785-2791.

394. Platania, C.B.M.; Salomone, S.; Leggio, G.M.; Drago, F.; Bucolo, C. Homology Modeling of Dopamine D_2 and D_3 Receptors: Molecular Dynamics Refinement and Docking Evaluation. *PLoS One*, **2012**, *7*(9), e44316. Available from: https://doi.org/10.1371/journal.pone.0044316.

395. Ortore, G.; Tuccinardi, T.; Bertini, S.; Martinelli, A. A Theoretical Study To Investigate D_2DAR/D_4DAR Selectivity: Receptor Modeling and Molecular Docking of Dopaminergic Ligands. *J. Med. Chem.*, **2006**, *49*(4), 1397-1407.

396. Cerius^2 Modeling Environment, March 2000. San Diego: Molecular Simulations Inc., **2000**.

397. Sukalovic, V.; Andric, D.; Roglic, G.; Kostic-Rajacic, S.; Schrattenholz, A.; Soskic, V. Synthesis, dopamine D_2 receptor binding studies and docking analysis of 5-[3-(4-arylpiperazin-1-yl)propyl]-1*H*-benzimidazole, 5-[2-(4-arylpiperazin-1-yl)ethoxy]-1*H*-benzimidazole and their analogs. *Eur. J. Med. Chem.*, **2005**, *40*(5), 481-493.

398. Accelrys Software Inc., *Discovery Studio Modeling Environment*, *Release* 2.5, San Diego, CA, **2009**.

399. Sukalovic, V.; Soskic, V.; Andric, D.; Roglic, G.; Kostic-Rajacic, S. Modeling key interactions between dopamine D_2 receptor second extracellular loop and arylpiperazine ligands. *J. Serb. Chem. Soc.*, **2012**, *77*(3), 259-277.

400. Cerius^2 User Guide; Accelrys, Inc., Cerius^2 Modeling Environment, Release 4.8, San Diego: Accelrys Software Inc., **2005**.

401. Varady, J.; Wu, X.; Fang, X.; Min, J.; Hu, Z.; Levant, B.; Wang, S. Molecular modeling of the three-dimensional structure of dopamine 3 (D_3) subtype receptor: discovery of novel and potent D_3 ligands through a hybrid pharmacophore- and structure-based database searching approach. *J. Med. Chem.*, ***2003***, *46*(21), 4377-4392.

402. Huey, R.; Goodsell, D.S.; Morris, G.M.; Olson, A.J. Grid-Based Hydrogen Bond Potentials with Improved Directionality. *Lett. Drug Des. Discov.*, **2004**, *1*(2), 178-183.

403. Huey, R.; Morris, G.M.; Olson, A.J.; Goodsell, D.S. A semiempirical free energy force field with charge-based desolvation. *J. Comput. Chem.*, **2007**, *28*(6), 1145-1152.

404. Mirza, M.U.; Mirza, A.H.; Ghori, N.-U.-H.; Ferdous, S. Glycyrrhetinic acid and E.resveratroloside act as potential plant derived compounds against dopamine receptor D_3 for Parkinson's disease: a pharmacoinformatics study. *Drug Des. Dev. Ther.*, **2015**, *9*, 187-198.

405. Jain A. Surflex-Dock 2.1: robust performance from ligand energetic modeling, ring flexibility, and knowledge-based search. *J. Comput. Aided Mol. Des.*, **2007**. *21*(5), 281-306.

406. Duan, X.; Zhang, X.; Xu, B.; Wang, F.; Lei, M. Computational Study and Modified Design of Selective Dopamine D_3 Receptor Agonists. *Chem. Biol. Drug Des.*, **2016**, *88*(1), 142-154.

407. Farid, R.; Day, T.; Friesner, R.A.; Pearlstein, R.A. New insights about HERG blockade obtained from protein modeling, potential energy mapping, and docking studies. *Bioorg. Med. Chem.*, **2006**, *14*(9), 3160-3173.

408. Sherman, W.; Beard, H.S.; Farid, R. Use of an Induced Fit Receptor Structure in Virtual Screening. *Chem. Biol. Drug Des.*, **2006**, *67*(1), 83-84.

409. Sherman, W.; Day, T.; Jacobson, M.P.; Friesner, R.A.; Farid, R. Novel Procedure for Modeling Ligand/Receptor Induced Fit Effects. *J. Med. Chem.*, **2006**, *49*(2), 534-553.

410. *Molecular Operating Environment (MOE)*, Chemical Computing Group Inc., 1255 University St., Suite #1600, Montreal, QC, Canada, H3B 3X3, **2005**.

411. Pourbasheer, E.; Shokouhi Tabar, S.; Masand, V.; Aalizadeh, R.; Ganjali, M. 3D-QSAR and docking studies on adenosine A_{2A} receptor antagonists by the CoMFA method. *SAR QSAR Environ. Res.*, **2015**, *26*(6), 461-477.

412. Mustyala, K.K.; Chitturi, A.R.; Naikal James, P.S.; Vuruputuri, U. Pharmacophore mapping and *in silico* screening to identify new potent leads for A_{2A} adenosine receptor as antagonists. *J. Recept. Sig. Transd.*, **2012**, *32*(2), 102-113.

413. Moustakas, D.T.; Lang, P.T.; Pegg, S.; Pettersen, E.; Kuntz, I.D.; Brooijmans, N.; Rizzo, R.C. Development and validation of a modular, extensible docking program: DOCK 5. *J. Comput. Aided Mol. Des.*, **2006**, *20*(10), 601-619.

414. Wei, J.; Qu, W.; Ye, Y.; Gao, Q. 3D pharmacophore based virtual screening of A_{2A} adenosine receptor antagonists. *Protein Pept. Lett.*, **2010**, *17*(3), 332-339.

415. Massink, A.; Louvel, J.; Adiere, I.; van Veen, C.; Huisman, B.J.H.; Dijksteel, G.S.; Guo, D.; Lenselink, E.B.; Buckley, B.J.; Matthews, H.; Ranson, M.; Kelso, M.; Ijzerman, A. 5′-Substituted Amiloride Derivatives as Allosteric Modulators Binding in the Sodium Ion Pocket of the Adenosine A_{2A} Receptor. *J. Med. Chem.*, **2016**, *59*(10), 4769-4777.

416. Vanopdenbosch, N.; Cramer, R.; Giarrusso, F.F. SYBYL, the integrated molecular modeling system. *J. Mol. Graphic*., **1985**, *3*, 110–111.

417. Henderson, R.; Baldwin, J.M.; Ceska, T.A.; Zemlin, F.; Beckmann, E.; Downing, K.H. Model for the structure of bacteriorhodopsin based on high-resolution electron cryo-microscopy. *J. Mol. Biol.*, **1990**, *213*(4), 899-929.

418. Kim, S.-K.; Gao, Z.-G.; Van Rompaey, P.; Gross, A.S.; Chen, A.; Van Calenbergh, S.; Jacobson, K.A. Modeling the Adenosine Receptors: Comparison of the Binding Domains of A_{2A} Agonists and Antagonists. *J. Med. Chem.*, **2003**, *46*(23), 4847-4859.

419. Abagyan, R. A.; Orry, A.; Raush, E.; Budagyan, L.; Totrov, M. ICM Manual, 3.0; MolSoft LLC: La Jolla, CA, **2009**.

420. Ivanov, A.A.; Barak, D.; Jacobson, K.A. Evaluation of Homology Modeling of G-Protein-Coupled Receptors in Light of the A_{2A} Adenosine Receptor Crystallographic Structure. *J. Med. Chem.*, **2009**, *52*(10), 3284-3292.

421. Katritch, V.; Jaakola, V.-P.; Lane, J.R.; Lin, J.; Ijzerman, A.P.; Yeager, M.; Kufareva, I.; Stevens, R.C.; Abagyan, R. Structure-Based Discovery of Novel Chemotypes for Adenosine A_{2A} Receptor Antagonists. *J. Med. Chem*., **2010**, *53*(4), 1799-1809.

422. Jaakola, V.-P.; Ijzerman, A.P. The crystallographic structure of the human adenosine A_{2A} receptor in a high-affinity antagonist-bound state: implications for GPCR drug screening and design. *Curr. Opin. Struct. Biol.*, **2010**, *20*(4), 401-414.

423. Liu, Y.; Burger, S.K.; Ayers, P.W.; Vohringer-Martinez, E. Computational Study of the Binding Modes of Caffeine to the Adenosine A_{2A} Receptor. *J. Phys. Chem. B*, **2011**, *115*(47), 13880-13890.

424. Crouch, R.D.; Holden, M.S.; Samet, C. CAChe Molecular Modeling: A Visualization Tool Early in the Undergraduate Chemistry Curriculum. *J. Chem. Educ.*, **1996**, *73*(10), 916.

425. Yuzlenko, O.; Kieć- Kononowicz, K. Molecular modeling of A_1 and A_{2A} adenosine receptors: Comparison of rhodopsin- and β_2- adrenergic- based homology models through the docking studies. *J. Comput. Chem.*, **2009**, *30*(1), 14-32.

426. Ye, Y.; Wei, J.; Dai, X.; Gao, Q. Computational studies of the binding modes of A_{2A} adenosine receptor antagonists. *Amino Acids*, **2008**, *35*(2), 389-396.

427. Zhang, L.; Liu, T.; Wang, X.; Wang, J.; Li, G.; Li, Y.; Yang, L.; Wang, Y. Insight into the binding mode and the structural features of the pyrimidine derivatives as human A_{2A} adenosine receptor antagonists. *Biosystems*, **2014**, *115*, 13-22.

428. Muñoz-Gutiérrez, C.; Caballero, J.; Morales-Bayuelo, A. HQSAR and molecular docking studies of furanyl derivatives as adenosine A_{2A} receptor antagonists. *Med. Chem. Res.*, **2016**, *25*(7), 1316-1328.

429. Ewing, T.J.A.; Kuntz, I.D. Critical evaluation of search algorithms for automated molecular docking and database screening. *J. Comput. Chem.*, **1997**, *18*(9), 1175-1189.

430. Rarey, M.; Kramer, B.; Lengauer, T.; Klebe, G. A Fast Flexible Docking Method using an Incremental Construction Algorithm. *J. Mol. Biol.*, **1996**, *261*(3), 470-489

431. Jones, G.; Willett, P.; Glen, R.C.; Leach, A.R.; Taylor, R. Development and validation of a genetic algorithm for flexible docking. *J. Mol. Biol.*, **1997**, *267*(3), 727-748.

432. Bissantz, C.; Bernard, P.; Hibert, M. Rognan, D. Protein-based virtual screening of chemical databases. II. Are homology models of G-Protein Coupled Receptors suitable targets? *Proteins*, **2003**, *50*(1), 5-25.

433. Ahnaou, A.; Lavreysen, H.; Tresadern, G.; Cid, J.M.; Drinkenburg, W.H. mGlu2 Receptor Agonism, but Not Positive Allosteric Modulation, Elicits Rapid Tolerance towards Their Primary Efficacy on Sleep Measures in Rats. *PLoS One*, **2015**, *10*(12), e0144017. Available from: https://doi.org/10.1371/journal.pone.0144017.

434. *Molecular Operating Environment (MOE)*, 2013.08; Chemical Computing Group, Inc; 1010 Sherbrooke St. West, Suite #910, Montreal, QC, Canada, H3A 2R7, **2013.**

435. Huynh, T.H.; Erichsen, M.N.; Tora, A.S.; Goudet, C.; Sagot, E.; Assaf, Z.; Thomsen, C.; Brodbeck, R.; Stensbol, T.B.; Bjorn-Yoshimoto, W.E.; Nielsen, B.; Pin, J.P.; Gefflaut, T.; Bunch, L. New 4-Functionalized Glutamate Analogues Are Selective Agonists at Metabotropic Glutamate Receptor Subtype 2 or Selective Agonists at Metabotropic Glutamate Receptor Group III. *J. Med. Chem.*, **2016**, *59*(3), 914-924.

436. Macchiarulo, A.; Costantino, G.; Sbaglia, R.; Aiello, S.; Meniconi, M.; Pellicciari, R. The role of electrostatic interaction in the molecular recognition of selective agonists to metabotropic glutamate receptors. *Proteins*, **2003**, *50*(4), 609-619.

437. Accelrys Software Inc., *Discovery Studio Modeling Environment*, *Release* 2.5.5, San Diego, CA, **2010**.

438. Goudet, C.; Vilar, B.; Courtiol, T.; Deltheil, T.; Bessiron, T.; Brabet, I.; Oueslati, N.; Rigault, D.; Bertrand, H.O.; McLean, H.; Daniel, H.; Amalric, M.; Acher, F.; Pin, J.P. A novel selective metabotropic glutamate receptor 4 agonist reveals new possibilities for developing subtype selective ligands with therapeutic potential. *FASEB J.*, **2012**, *26*(4), 1682-1693.

439. Sack, J.S.; Saper, M.A.; Quiocho, F.A. Periplasmic binding protein structure and function. Refined X-ray structures of the leucine/isoleucine/valine-binding protein and its complex with leucine. *J. Mol. Biol.*, **1989**, *206*(1), 171-191.

440. Sack, J.S.; Trakhanov, S.D.; Tsigannik, I.H.; Quiocho, F.A. Structure of the L-leucine-binding protein refined at 2.4 Å resolution and comparison with the Leu/Ile/Val-binding protein structure. *J. Mol. Biol.*, **1989**, *206*(1), 193-207.

441. Pearl, L.; O'Hara, B.; Drew, R.; Wilson, S. Crystal structure of AmiC: the controller of transcription antitermination in the amidase operon of Pseudomonas aeruginosa. *The EMBO journal*, **1994**, *13*(24), 5810-5817.

442. Bessis, A.S.; Bertrand, H.O.; Galvez, T.; De Colle, C.; Pin, J.P.; Acher, F. Three-dimensional model of the extracellular domain of the type 4a metabotropic glutamate receptor: new insights into the activation process. *Protein Sci.*, **2000**, *9*(11), 2200-2209.

443. Schrodinger Release 2013-2: Maestro, Schrödinger, LLC, New York, NY, **2013**.

444. The PyMOL Molecular Graphics System, version 1.7.4; Schrodinger, LLC.

445. Wu, G.; Robertson, D.H.; Brooks, C.L.; Vieth, M. Detailed analysis of grid-based molecular docking: A case study of CDOCKER-A CHARMm-based MD docking algorithm. *J. Comput. Chem.*, **2003**, *24*(13), 1549-1562.

446. Vu, H.N.; Kim, J.Y.; Hassan, A.H.E.; Choi, K.; Park, J.-H.; Park, K.D.; Lee, J.K.; Pae, A.N.; Choo, H.; Min, S.-J.; Cho, Y.S. Synthesis and biological evaluation of picolinamides and thiazole-2-carboxamides as $mGluR_5$ (metabotropic glutamate receptor 5) antagonists. *Bioorg. Med. Chem. Lett.*, **2016**, *26*(1), 140-144.

447. Jiang, L.; Li, Y.; Qiao, L.; Chen, X.; He, Y.; Zhang, Y.; Li, G. Discovery of potential negative allosteric modulators of $mGluR_5$ from natural products using pharmacophore modeling, molecular docking, and molecular dynamics simulation studies. *Can. J. Chem.*, **2015**, *93*(11), 1199-1206.

448. Casoni, A.; Clerici, F.; Contini, A. Molecular dynamic simulation of $mGluR_5$ amino terminal domain: essential dynamics analysis captures the agonist or antagonist behaviour of ligands. *J. Mol. Graph. Model.*, **2013**, *41*, 72-78.

449. Misura, K.M.; Chivian, D.; Rohl, C.A.; Kim, D.E.; Baker, D. Physically realistic homology models built with ROSETTA can be more accurate than their templates. *Proc. Natl. Acad. Sci. U.S.A.*, **2006**, *103*(14), 5361−5366.

450. Dalton, J.A.; Gomez-Santacana, X.; Llebaria, A.; Giraldo, J. Computational analysis of negative and positive allosteric modulator binding and function in metabotropic glutamate receptor 5 (in)activation. *J. Chem. Inf. Model.*, **2014**, *54*(5), 1476-1487.

451. Zlatovic, M.V.; Sukalovic, V.; Kostic-Rajacic, S.V.; Andric, D.B.; Roglic, G.M. Influence of N-1 substituent properties on binding affinities of arylpiperazines to the binding site of 5-HT_{1A} receptor. *J. Serb. Chem. Soc*., **2006**, *71*(11), 1125-1135.

452. Penjisevic, J.; Sukalovic, V.; Andric, D.; Kostic-Rajacic, S.; Soskic, V.; Roglic, G. 1- Cinnamyl- 4- (2- methoxyphenyl) piperazines: Synthesis, Binding Properties, and Docking to Dopamine (D_2) and Serotonin (5- HT_{1A}) Receptors. *Arch. Pharm. (Weinheim)*, **2007**, *340*(9), 456-465.

453. Andrić, D.; Roglic, G.; Sukalovic, V.; Soskic, V.; Kostic-Rajacic, S. Synthesis, binding properties and receptor docking of 4-halo-6-[2-(4-arylpiperazin-1-yl) ethyl]-1*H*-benzimidazoles, mixed ligands of D_2 and 5-HT_{1A} receptors. *Eur. J. Med. Chem.*, **2008**, *43*(8), 1696-1705.

454. Hindle, S.A.; Rarey, M.; Buning, C.; Lengauer, T. Flexible docking under pharmacophore type constraints. *J. Comput. Aided Mol. Des.*, **2002**, *16*(2), 129-149.

455. Nowak, M.; Kolaczkowski, M.; Pawlowski, M.; Bojarski, A.J. Homology modeling of the serotonin 5-HT_{1A} receptor using automated docking of bioactive compounds with defined geometry. *J. Med. Chem.*, **2006**, *49*(1), 205-214.

456. Pessoa-Mahana, H; Recabarren-Gajardo, G.; Temer, J.F.; Zapata-Torres, G.; Pessoa-Mahana, C.D.; Barria, C.S.; Araya-Maturana, R. Synthesis, Docking Studies and Biological Evaluation of Benzo-[*b*]-thiophen-2-yl-3-(4-arylpiperazin-1-yl)-propan-1-one derivatives on 5-HT_{1A} Serotonin Receptors. *Molecules*, **2012**, *17*(2), 1388-1407.

457. Dilly, S.; Scuvée-Moreau, J.; Wouters, J.; Liégeois, J.-F. The 5-HT_{1A} Agonism Potential of Substituted Piperazine-Ethyl-Amide Derivatives Is Conserved in the Hexyl Homologues: Molecular Modeling and Pharmacological Evaluation. *J. Chem. Inf. Model.*, **2011**, *51*(11), 2961-2966.

458. Pessoa-Mahana, H.; Nunez, C.U.; Araya-Maturana, R.; Barria, C.S.; Zapata-Torres, G.; Pessoa-Mahana, C.D.; Iturriaga-Vasquez, P.; Mella-Raipan, J.; Reyes-Parada, M.; Celis-Barros, C. Synthesis, 5-hydroxytryptamine 1A receptor affinity and docking studies of 3-[3-(4-aryl-1-piperazinyl)-propyl]-1_H-indole derivatives. *Chem. Pharm. Bull.*, **2012**, *60*(5), 632-638.

459. McMartin, C.; Bohacek, R.S. QXP: Powerful Rapid Computer Algorithms for Structure-Based Drug Design. *J. Comput.-Aided Mol. Des.* **1997**, *11*(4), 333-344.

460. Brea, J.; Rodrigo, J.; Carrieri, A.; Sanz, F.; Cadavid, M.I.; Enguix, M.J.; Villazón, M.; Mengod, G.; Caro, Y.; Masaguer, C.F. New serotonin 5-HT_{2A}, 5-HT_{2B}, and 5-HT_{2C} receptor antagonists: synthesis, pharmacology, 3D-QSAR, and molecular modeling of (aminoalkyl) benzo and heterocycloalkanones. *J. Med. Chem.*, **2002**, *45*(1), 54-71.

461. Ahmed, K.; Dubey, B.; Shrivastava, B.; Sharma, P.; Nadeem, S. Anxiolytic effects of newly synthesized derivatives in mice and molecular docking studies as serotonin $5HT_{2A}$ receptor inhibitor. *Pharm. Lett.*, **2015**, *7*(6), 93-101.

462. Xiong, Z.-J.: Du, P.; Li, B.; Zhen, X.-C.; Fu, U. Discovery of a Novel 5-HT_{2A} Inhibitor by Pharmacophore-based Virtual Screening. *Chem. Res. Chin. Univ.*, **2011**, *27*, 655-660.

463. Córdova-Sintjago, T.; Sakhuja, R.; Kondabolu, K.; Canal, C.E.; Booth, R.G. Molecular determinants for ligand binding at serotonin 5-HT_{2A} and 5-HT_{2C} GPCRs: Experimental affinity results analyzed by molecular modeling and ligand docking studies. *Int. J. Quant. Chem.*, **2012**, *112*(24), 3807-3814.

464. Gandhimathi, A.; Sowdhamini, R. Molecular modelling of human 5-hydroxytryptamine receptor (5-HT_{2A}) and virtual screening studies towards the identification of agonist and antagonist molecules. *J. Biomol. Struct. Dyn.*, **2016**, *34*(5), 952-970.

465. Sencanski, M.; Sukalovic, V.; Shakib, K.; Soskic, V.; Dosen-Micovic, L.; Kostic-Rajacic, S. Molecular modeling of $5HT_{2A}$ receptor - arylpiperazine ligands interactions. *Chem. Biol. Drug Des.*, **2014**, *83*(4), 462-471.

466. Pecic, S.; Makkar, P.; Chaudhary, S.; Reddy, B.V.; Navarro, H.A.; Harding, W.W. Affinity of aporphines for the human 5-HT_{2A} receptor: insights from homology modeling and molecular docking studies. *Bioorg. Med. Chem.*, **2010**, *18*(15), 5562-5575.

467. Bali, A., Sen, U.; Peshin, T. Synthesis, docking and pharmacological evaluation of novel indole based potential atypical antipsychotics. *Eur. J. Med. Chem.*, **2014**, *74*, 477-490.

468. Munusamy, V.; Yap, B.K.; Buckle, M.J.; Doughty, S.W.; Chung, L.Y. Structure-based identification of aporphines with selective 5-HT_{2A} receptor-binding activity. *Chem. Biol. Drug Des.*, **2013**, *81*(2), 250-256.

469. Ahmad, A.; Nagarajan, S.; Doddareddy, M.R.; Cho, Y.-S.; Pae, A.-N. Binding mode prediction of 5-hydroxytryptamine 2C receptor ligands by homology modeling and molecular docking analysis. *Bull. Korean Chem. Soc.*, **2011**, *32*(6), 2008-2014

470. Lu, C.; Jin, F.; Li, C.; Li, W.; Liu, G.; Tang, Y. Insights into binding modes of 5-HT_{2C} receptor antagonists with ligand-based and receptor-based methods. *J. Mol. Model.*, **2011**, *17*(10), 2513-2523.

471. Cavasotto, C.N.; Phatak, S.S. Homology modeling in drug discovery: current trends and applications. *Drug Discov. Today*, **2009**, *14*(13-14), 676-683.

472. Bacilieri, M.; Moro, S. Ligand-based drug design methodologies in drug discovery process: an overview. *Curr. Drug Discov. Technol.*, **2006**, *3*(3), 155-165.

473. Yang, S.Y. Pharmacophore modeling and applications in drug discovery: challenges and recent advances. *Drug Discov. Today*, **2010**, *15*(11-12), 444-450.

474. Dror, O.; Shulman-Peleg, A.; Nussinov, R.; Wolfson, H.J. Predicting molecular interactions *in silico*: I. A guide to pharmacophore identification and its applications to drug design. *Curr. Med. Chem.*, **2004**, *11*(1), 71-90.

475. Winkler, D.A. The role of quantitative structure--activity relationships (QSAR) in biomolecular discovery. *Brief Bioinform*., **2002**, *3*(1), 73-86.

476. Perkins, R.; Fang, H.; Tong, W.; Welsh, W.J. Quantitative structure-activity relationship methods: perspectives on drug discovery and toxicology. *Environ. Toxicol. Chem.*, **2003**, *22*(8), 1666-1679.

477. Dudek, A.Z.; Arodz, T.; Galvez, J. Computational methods in developing quantitative structure-activity relationships (QSAR): a review. *Comb. Chem. High Throughput Screen.*, **2006**, *9*(3), 213-228.

478. Boulesteix, A.L.; Strimmer, K. Partial least squares: a versatile tool for the analysis of high-dimensional genomic data. *Brief Bioinform*., **2007**, *8*(1), 32-44.

479. Alexopoulos, E.C. Introduction to Multivariate Regression Analysis. *Hippokratia*, **2010**, *14*(Suppl 1), 23-28.

480. Speck-Planche, A., Kleandrova, V.V.; Luan, F.; Cordeiro, M.N.D.S. Multi-target inhibitors for proteins associated with Alzheimer: *in silico* discovery using fragment-based descriptors. *Curr. Alzheimer Res.*, **2013**, *10*(2), 117-124.

481. Speck-Planche, A.; Kleandrova, V.V. QSAR and molecular docking techniques for the discovery of potent monoamine oxidase B inhibitors: computer-aided generation of new rasagiline bioisosteres. *Curr. Top. Med. Chem.*, **2012**, *12*(16), 1734-1747.

482. Chapelle, O.; Vapnik, V.; Bousquet, O.; Mukherjee, S. Choosing Multiple Parameters for Support Vector Machines. *Mach. Learn.*, **2002**, *46*(1), 131-159.

483. Roy, K., Kar, S.; Das, R.N. Statistical Methods in QSAR/QSPR. In *A Primer on QSAR/QSPR Modeling: Fundamental Concepts*. Springer International Publishing: Cham, **2015**; pp. 37-59.

484. Cramer, R.D.; Patterson, D.E.; Bunce, J.D. Comparative molecular field analysis (CoMFA). 1. Effect of shape on binding of steroids to carrier proteins. *J. Am. Chem. Soc*., **1988**, *110*(18), 5959-5967.

485. Kubinyi, H. *Comparative molecular field analysis (CoMFA). Handbook of Chemoinformatics: From Data to Knowledge in 4 Volumes*, **2008**, 1555-1574.

486. Ghemtio, L.; Zhang, Y.; Xhaard, H. CoMFA/CoMSIA and pharmacophore modelling as a powerful tools for efficient virtual screening: Application to anti-leishmanial betulin derivatives. *Virtual Screen.*, **2012**, 55-82.

487. Klebe, G.; Abraham, U.; Mietzner, T. Molecular Similarity Indices in a Comparative Analysis (CoMSIA) of Drug Molecules to Correlate and Predict Their Biological Activity. *J. Med. Chem.*, **1994**, *37*(24), 4130-4146.

488. Zhu, N.; Liang, L.; Stevens, C.L.K. A CoMFA Study of Dopamine D_2 Receptor Agonists and X-Ray Crystal Structure of Quinelorane Dihydrochloride Dihydrate, R(−)-Apomorphine Hydrochloride and *R*(−)-*N*-n-Propylnorapomorphine Hydrochloride. *Struct. Chem*., **2004**, *15*(6), 553-565.

489. *Molecular Operating Environment (MOE)*, 2011.10; Chemical Computing Group, Inc; 1010 Sherbrooke St. West, Suite #910, Montreal, QC, Canada, H3A 2R7, **2011**.

490. Modi, G.; Sharma, H.; Kharkar, P.S.; Dutta, A.K. Understanding the Structural Requirements of Hybrid (*S*)-6-((2-(4-Phenylpiperazin-1-yl)ethyl)(propyl)amino)-5,6,7,8-tetrahydronaphthalen-1-ol and its Analogs as D_2/D_3 Receptor Ligands: A Three-Dimensional Quantitative Structure-Activity Relationship (3D QSAR) Investigation. *MedChemComm*, **2014**, *5*(9), 1384-1399.

491. *Molecular Operating Environment (MOE)*, 2005.06; Chemical Computing Group Inc., 1010 Sherbrooke St. West, Suite #910, Montreal, QC, Canada, **2005**.

492. Malo, M.; Brive, L.; Luthman, K.; Svensson, P. Selective pharmacophore models of dopamine D_1 and D_2 full agonists based on extended pharmacophore features. *ChemMedChem*, **2010**, *5*(2), 232-246.

493. Cha, M.Y.; Lee, I.Y.; Cha, J.H.; Choi, K.I.; Cho, Y.S.; Koh, H.Y.; Pae, A.N. QSAR studies on piperazinylalkylisoxazole analogues selectively acting on dopamine D_3 receptor by HQSAR and CoMFA. *Bioorg. Med. Chem.*, **2003**, *11*(7), 1293-1298.

494. Wang, Q.; Mach, R.H.; Luedtke, R.R.; Reichert, D.E. Subtype Selectivity of Dopamine Receptor Ligands: Insights from Structure and Ligand-Based Methods. *J. Chem. Inf. Model.*, **2010**, *50*(11), 1970-1985.

495. Moro, S.; van Rhee, A.M.; Sanders, L.H.; Jacobson, K.A. Flavonoid Derivatives as Adenosine Receptor Antagonists: A Comparison of the Hypothetical Receptor Binding Site Based on a Comparative Molecular Field Analysis Model. *J. Med. Chem.*, **1998**, *41*(1), 46-52.

496. Mauri, A.; Consonni, V.; Pavan, M.; Todeschini, R. DRAGON software: An easy approach to molecular descriptor calculations. *MATCH Commun. Math. Comput. Chem.*, **2006**, *56*, 237-248.

497. Wolber, G.; Langer, T. LigandScout: 3-D pharmacophores derived from protein-bound ligands and their use as virtual screening filters. *J. Chem. Inf. Model.*, **2005**, *45*(1), 160-169.

498. Dixon S.L.; Smondyrev A.M.; Rao S.N. PHASE: a novel approach to pharmacophore modeling and 3D database searching. *Chem. Biol. Drug Des.*, **2006**, *67*(5), 370–372.

499. Sprague, P.W.; Hoffmann, R. In: *Computer-Assisted Lead Finding and Optimization: Current Tools for Medicinal Chemistry*; Han van de Waterbeemd, Bernard Testa, and Gerd Folkers Eds.; Verlag Helvetica Chimica Acta, Zürich, **1997**; doi: 10.1002/9783906390406.ch14.

500. Parenti, M.D.; Fioravanzo, E.; Mabilia, M.; Gallo, G.; Ciacci, A. Induced fit and pharmacophore generation approach applied to A_{2A} adenosine receptor antagonists. *Arkivoc*, **2006**, *8*, 74-82.

501. Wei, J.; Wang, S.; Gao, S.; Dai, X.; Gao, Q. 3D-Pharmacophore Models for Selective A_{2A} and A_{2B} Adenosine Receptor Antagonists. *J. Chem. Inf. Model.*, **2007**, *47*(2), 613-625.

502. Xu, Z.; Cheng, F.; Da, C.; Liu, G.; Tang, Y. Pharmacophore modeling of human adenosine receptor A_{2A} antagonists. *J. Mol. Model.*, **2010**, *16*(12), 1867-1876.

503. Bacilieri, M.; Ciancetta, A.; Paoletta, S.; Federico, S.; Cosconati, S.; Cacciari, B.; Taliani, S.; Da Settimo, F.; Novellino, E.; Klotz, K.N.; Spalluto, G.; Moro, S. Revisiting a Receptor-Based Pharmacophore Hypothesis for Human A_{2A} Adenosine Receptor Antagonists. *J. Chem. Inf. Model*., **2013**, *53*(7), 1620-1637.

504. Baroni, M.; Cruciani, G.; Sciabola, S.; Perruccio, F.; Mason, J.S. A common reference framework for analyzing/comparing proteins and ligands. Fingerprints for Ligands and Proteins (FLAP): theory and application. *J. Chem. Inf. Model*., **2007**, *47*(2), 279-294.

505. Sirci, F.; Goracci, L.; Rodriguez, D.; van Muijlwijk-Koezen, J.; Gutiérrez-de-Terán, H.; Mannhold, R. Ligand-, structure- and pharmacophore-based molecular fingerprints: a case study on adenosine A_1, A_{2A}, A_{2B}, and A_3 receptor antagonists. *J. Comput. Aided Mol. Des*., **2012**, *26*(11), 1247-1266.

506. Bhattacharjee, A.K.; Gordon, J.A.; Marek, E.; Campbell, A.; Gordon, R.K. 3D-QSAR studies of 2,2-diphenylpropionates to aid discovery of novel potent muscarinic antagonists. *Bioorg. Med. Chem.*, **2009**, *17*(11), 3999-4012.

507. Bhandare, R.R.; Gao, R.; Canney, D.J.; Kharkar, P.S. Novel γ-Butyrolactone Derivatives as Muscarinic Receptor Antagonists: Pharmacophore Elucidation and Docking Analyses. In *Crystallizing Ideas – The Role of Chemistry*, Ramasami, P.; Gupta Bhowon, M.; Jhaumeer Laulloo, S.; Li Kam Wah, H., Eds; Springer International Publishing: Cham. **2016**; pp. 155-179.

508. Bhattacharjee, A.K.; Pomponio, J.W.; Evans, S.A.; Pervitsky, D.; Gordon, R.K. Discovery of subtype selective muscarinic receptor antagonists as alternatives to atropine using in silico pharmacophore modeling and virtual screening methods. *Bioorg. Med. Chem.*, **2013**, *21*(9), 2651-2662.

509. Bessis, A.S.; Jullian, N.; Coudert, E.; Pin, J.P.; Acher, F. Extended glutamate activates metabotropic receptor types 1, 2 and 4: selective features at $mGluR_4$ binding site. *Neuropharmacology*, **1999**, *38*(10), 1543-1551.

510. Accelrys Software Inc., *Discovery Studio Modeling Environment*, *Release* 4.0, San Diego, CA, **2013**.

511. *Molecular Operating Environment (MOE)*, 2004.03; Chemical Computing Group Inc., 1010 Sherbrooke St. West, Suite #910, Montreal, QC, Canada, H3A 2R7, **2004**.

512. Joshi, U.J.; Tikhele, S.H.; Shah, F. 2D QSAR of arylpiperazines as 5-HT_{1A} receptor agonists. *Indian J. Pharm. Sci.*, **2007**, *69*(6); 800-804.

513. Gaillard, P.; Carrupt, P.-A.; Testa, B.; Schambel, P. Binding of Arylpiperazines, (Aryloxy)propanolamines, and Tetrahydropyridylindoles to the 5-HT_{1A} Receptor: Contribution of the Molecular Lipophilicity Potential to Three-Dimensional Quantitative Structure−Affinity Relationship Models. *J. Med. Chem.*, **1996**, *39*(1), 126-134.

514. Agarwal, A.; Pearson, P.P.; Taylor, E.W.; Li, H.B.; Dahlgren, T.; Herslof, M.; Yang, Y.; Lambert, G.; Nelson, D.L.; Regan, J.W. Three-dimensional quantitative structure-activity relationships of 5-HT receptor binding data for tetrahydropyridinylindole derivatives: a comparison of the Hansch and CoMFA methods. *J. Med. Chem.*, **1993**, *36*(25), 4006-4014.

515. López-Rodríguez, M.L.; Rosado, M.L.; Benhamú, B.; Morcillo, M.J.; Fernández, E.; Schaper, K.-J. Synthesis and Structure−Activity Relationships of a New Model of Arylpiperazines. 2. Three-Dimensional Quantitative Structure−Activity Relationships of Hydantoin−Phenylpiperazine Derivatives with Affinity for 5-HT_{1A} and α_1 Receptors. A Comparison of CoMFA Models. *J. Med. Chem.*, **1997**, *40*(11), 1648-1656.

516. Patel Y.; Gillet V.J.; Bravi G.; Leach A.R. A comparison of the pharmacophore identification programs: Catalyst, DISCO and GASP. *J. Comput. Aided Mol. Des.*, 2002**,** *16*(8-9), 653-681

517. Borosy, A.; Morvay, M.; Mátyus, P. 3D QSAR analysis of novel 5-HT_{1A} receptor ligands. *Chemometr. Intell. Lab. Syst.*, **1999**, *47*(2), 239-252.

518. Richmond, N.J.; Abrams, C.A.; Wolohan, P.R.; Abrahamian, E.; Willett, P.; Clark, R.D. GALAHAD: 1. Pharmacophore identification by hypermolecular alignment of ligands in 3D. *J. Comput. Aided Mol. Des*., **2006**, *20*(9), 567–587.

519. Shepphird, J.K.; Clark, R.D. A marriage made in torsional space: Using GALAHAD models to drive pharmacophore multiplet searches. *J. Comput. Aided Mol. Des*., **2006**, *20*(12), 763–771.

520. Andrade, C.H.; Salum, L.B.; Pasqualoto, K.F.M.; Ferreira, E.I.; Andricopulo, A.D. Three-dimensional quantitative structure-activity relationships for a large series of potent antitubercular agents. *Lett. Drug Des. Discov*., **2008**, *5*(6), 377–387.

521. Weber, K.C.; Salum, L.B.; Honorio, K.M.; Andricopulo, A.D.; da Silva, A.B. Pharmacophore-based 3D QSAR studies on a series of high affinity 5-HT_{1A} receptor ligands. *Eur. J. Med. Chem.*, **2010**, *45*(4), 1508-1514.

522. Lepailleur, A.; Bureau, R.; Paillet-Loilier, M.; Fabis, F.; Saettel, N.; Lemaitre, S.; Dauphin, F.; Lesnard, A.; Lancelot, J.-Ch.; Rault, S. Molecular modeling studies focused on 5-HT_7 versus 5-HT_{1A} selectivity. Discovery of novel phenylpyrrole derivatives with high affinity for 5-HT_7 receptors. *J. Med. Chem*., **2005**, *45*(4), 1075-1081.

523. Handzlik, J.; Szymanska, E.; Nedza, K.; Kubacka, M.; Siwek, A.; Mogilski, S.; Handzlik, J.; Filipek, B.; Kiec-Kononowicz, K. Pharmacophore models based studies on the affinity and selectivity toward 5-HT_{1A} with reference to alpha1-adrenergic receptors among arylpiperazine derivatives of phenytoin. *Bioorg. Med. Chem.*, **2011**, *19*(3), 1349-1360.

524. Accelrys Software Inc., *Discovery Studio Modeling Environment*, *Release* 3.5, San Diego, CA, **2013**.

525. Ngo, T.; Nicholas, T.J.; Chen, J.; Finch, A.M.; Griffith, R. 5-HT_{1A} receptor pharmacophores to screen for off-target activity of α_1-adrenoceptor antagonists. *J. Comput. Aided Mol. Des.*, **2013**, *27*(4), 305-319.

526. Goodford, P.J. A computational procedure for determining energetically favorable binding sites on biologically important macromolecules. *J. Med. Chem*. **1985**, *28*(7), 849−857.

527. GOLPE 4.6.0.; Multivariate Infometric Analysis: Srl. Perugia, Italy, **2003**.

528. Dezi, C.; Brea, J.; Alvarado, M.; Ravina, E.; Masaguer, C.F.; Loza, M.I.; Sanz, F.; Pastor, M. Multistructure 3D-QSAR studies on a series of conformationally constrained butyrophenones docked into a new homology model of the 5-HT_{2A} receptor. *J. Med. Chem.*, **2007**, *50*(14), 3242-3255.

529. Valkova, I.; Zlatkov, A.; Nedza, K.; Doytchinova, I. Synthesis, 5-HT_{1A} and 5-HT_{2A} receptor affinity and QSAR study of 1-benzhydryl-piperazine derivatives with xanthine moiety at N4. *Med. Chem. Res*., **2012**, *21*(4), 477-486.

530. Choudhary, M.; Pilania, P.; Sharma, B.K. QSAR rationales for the 5-HT_{2A} receptor antagonistic activity of 2-alkyl-4-aryl-pyrimidine fused heterocycles. *Res. J. Pharm. Biol. Chem. Sci.*, **2015**, *6*(2), 326-338.

531. Maciejewska, D.; Zolek, T.; Herold, F. CoMFA methodology in structure-activity analysis of hexahydro- and octahydropyrido[1,2-*c*]pyrimidine derivatives based on affinity towards 5-HT_{1A}, 5-HT_{2A} and α_1-adrenergic receptors. *J. Mol. Graph. Model.*, **2006**, *25*(3), 353-362.

532. Avram, S.; Duda-Seiman, D.; Borcan, F.; Wolschann, P. QSAR-CoMSIA applied to antipsychotic drugs with their dopamine D_2 and serotonine $5HT_{2A}$ membrane receptors. *J. Serb. Chem. Soc.*, **2011**, *76*(2), 263-281.

533, *Molecular Operating Environment (MOE)*, 2007.09; Chemical Computing Group Inc., 1010 Sherbrooke St. West, Suite #910, Montreal, QC, Canada, **2007**.

534. Awadallah, F.M. Synthesis, Pharmacophore modeling, and biological evaluation of novel 5*H*-thiazolo [3,2-*a*] pyrimidin-5-one derivatives as 5-HT_{2A} receptor antagonists. *Sci. Pharm.*, **2008**, *76*, 415-438.

535. *Molecular Operating Environment (MOE)*, 2008.10; Chemical Computing Group Inc., 1010 Sherbrooke St. West, Suite #910, Montreal, QC, Canada, **2008**.

536. El-Kerdawy, M.M.; El-Bendary, E.R.; Abdel-Aziz, A.A.; El-Wasseef, D.R.; El-Aziz, N.I. Synthesis and pharmacological evaluation of novel fused thiophene derivatives as 5-HT_{2A} receptor antagonists: molecular modeling study. *Eur. J. Med. Chem*., **2010**, *45*(5), 1805-1820.

537. Hayat, F.; Viswanath, A.N.; Pae, A.N.; Rhim, H.; Park, W.K.; Choo, H.Y. Synthesis and biological evaluation of 4-nitroindole derivatives as 5-HT_{2A} receptor antagonists. *Bioorg. Med. Chem.*, **2015**, *23*(6), 1313-1320.

538. Choudhary, M.; Sharma, B.K. QSAR rationales for the isoindolone derivatives as 5-HT_{2C} receptor antagonists. *Res. J. Pharm. Biol. Chem. Sci.*, **2015**, *6*(3), 1725-1736.

539. Gómez-Jeria, J.S. D-Cent-QSAR: A program to generate Local Atomic Reactivity Indices from Gaussian 03 log files. 1.0, Santiago, Chile, **2014**.

540. Gómez-Jeria, J.S., An empirical way to correct some drawbacks of mulliken population analysis. *J. Chil. Chem. Soc.*, **2009**, *54*, 482-485.

541. Gómez-Jeria, J.S.; Robles-Navarro, A. A quantum chemical study of the relationships between electronic structure and cloned rat 5-HT_{2C} receptor binding affinity in *N*-benzylphenethylamines. *Res. J. Pharm. Biol. Chem. Sci.*, **2015**, *6*(3), 1358-1373.

542. Accelrys Software Inc., *Discovery Studio Modeling Environment*, *Release* 2.1, San Diego, CA, **2004**.

543. Micheli, F.; Pasquarello, A.; Tedesco, G.; Hamprecht, D.; Bonanomi, G.; Checchia, A.; Jaxa-Chamiec, A.; Damiani, F.; Davalli, S.; Donati, D.; Gallotti, C.; Petrone, M.; Rinaldi, M.; Riley, G.; Terreni, S.; Wood, M. Diaryl substituted pyrrolidinones and pyrrolones as 5-HT_{2C} inhibitors: Synthesis and biological evaluation. *Bioorg. Med. Chem. Lett.*, **2006**, *16*(15), 3906-3912.

544. Tautermann, C.S. GPCR structures in drug design, emerging opportunities with new structures. *Bioorg. Med. Chem. Lett.*, **2014**, *24*(17), 4073-4079.

545. Lenselink, E.B.; Beuming, T.; Sherman, W.; van Vlijmen, H.W.; IJzerman, A.P. Selecting an optimal number of binding site waters to improve virtual screening enrichments against the adenosine A_{2A} receptor. *J. Chem. Inf. Model.*, **2014**, *54*(6), 1737-1746.

546. Tautermann, C.S.; Seeliger, D.; Kriegl, J.M. What can we learn from molecular dynamics simulations for GPCR drug design? *Comput. Struct. Biotechnol. J.*, **2015**, *13*, 111-121.

547. Michino, M.; Abola, E.; Brooks, C.L.; Dixon, J.S.; Moult, J.; Stevens, R.C. Community-wide assessment of GPCR structure modelling and ligand docking: GPCR Dock 2008. *Nat. Rev. Drug Discov.*, **2009**, *8*(6), 455-463.

548. Piotto, S.; Biasi, L.D.; Fino, R.; Parisi, R.; Sessa, L.; Concilio, S. YADA: a novel tool for molecular docking simulations. *J. Comput. Aided Mol. Des.*, **2016**, *30*(9), 753-759.

549. Lie, M.A.; Thomsen, R.; Pedersen, C.N.; Schiøtt, B.; Christensen, M.H. Molecular docking with ligand attached water molecules. *J. Chem. Inf. Model.*, **2011**, *51*(4), 909-917.

550. Kim, M.; Cho, A.E. Incorporating QM and solvation into docking for applications to GPCR targets. *Phys. Chem. Chem. Phys.*, **2016**, *18*(40), 28281-28289.

551. Amadasi, A.; Spyrakis, F.; Cozzini, P.; Abraham, D.J.; Kellogg, G.E.; Mozzarelli, A. Mapping the energetics of water-protein and water-ligand interactions with the "natural" HINT forcefield: predictive tools for characterizing the roles of water in biomolecules. *J. Mol. Biol.*, **2006**, *358*(1), 289-309.

552. Verdonk, M.L.; Cole, J.C.; Taylor, R. SuperStar: a knowledge-based approach for identifying interaction sites in proteins. *J. Mol. Biol.*, **1999**, *289*(4), 1093-1108.

553. Michel, J.; Tirado-Rives, J.; Jorgensen, W.L. Prediction of the water content in protein binding sites. *J. Phys. Chem. B*, **2009**, *113*(40), 13337-13346.

554. Abel, R.; Young, T.; Farid, R.; Berne, B.J.; Friesner, R.A. Role of the active-site solvent in the thermodynamics of Factor Xa ligand binding, *J. Am. Chem. Soc.*, **2008**, *130*(9), 2817-2831.

555. Young, T.; Abel, R.; Kim, B.; Berne, B.J.; Friesner, R.A. Motifs for molecular recognition exploiting hydrophobic enclosure in protein–ligand binding, *Proc. Natl. Acad. Sci. U S A.*, **2007**, 104, 808-813.

556. Zheng, M.; Li, Y.; Xiong, B.; Jiang, H.; Shen, J. Water PMF for predicting the properties of water molecules in protein binding site. *J. Comput. Chem*., **2013**, *34*(7), 583-592.

557. Isberg, V.; Mordalski, S.; Munk, C.; Rataj, K.; Harpsøe, K.; Hauser, A.S.; Vroling, B.; Bojarski, A.J.; Vriend, G.; Gloriam, D.E. GPCRdb: an information system for G protein-coupled receptors. *Nucleic Acids Res*., **2016**, *44*, D356-D364.

558. Golovin, A.; Henrick, K. MSDmotif: exploring protein sites and motifs. *BMC Bioinformatics,* **2008**, 9, *312*. Available from: https://bmcbioinformatics.biomedcentral.com/articles/10.1186/1471-2105-9-312.